

DEVELOPMENT OF PENTABLOCK COPOLYMER BASED FORMULATIONS FOR
THE SUSTAINED DELIVERY OF PROTEIN THERAPEUTICS IN THE TREATMENT
OF POSTERIOR SEGMENT OCULAR DISEASES

A DISSERTATION IN
Pharmaceutical Sciences
and
Chemistry

Presented to the Faculty of University
of Missouri - Kansas City in partial fulfillment of
the requirements for the degree

DOCTOR OF PHILOSOPHY

by

SULABH P. PATEL

M.Sc., National Institute of Pharmaceutical Education and Research (NIPER), India, 2006

Kansas City, Missouri
2013

DEVELOPMENT OF PENTABLOCK COPOLYMER BASED FORMULATIONS FOR
THE SUSTAINED DELIVERY OF PROTEIN THERAPEUTICS IN THE TREATMENT
OF POSTERIOR SEGMENT OCULAR DISEASES

Sulabh P. Patel, Candidate for the Doctor of Philosophy degree,
University of Missouri-Kansas City, 2011

ABSTRACT

We have successfully synthesized pentablock (PB) copolymers comprised of various FDA approved polymer blocks such as polyethylene glycol (PEG), polycaprolactone (PCL), polylactic acid (PLA) and polyglycolic acid (PGA). PB copolymers with different composition, molecular weights and block arrangements were utilized to develop protein-embedded thermosensitive gels or nanoparticles (NPs) for sustained delivery in the treatment of posterior segment ocular diseases. In order to eliminate the burst release effect, we have studied PB composite formulation comprised of protein-encapsulated PB NPs dispersed in PB thermosensitive gel. The composite formulation eliminated burst release effect and exhibited nearly zero-order protein release for significantly longer durations. In this research work, we have utilized various model proteins (lysozyme, IgG-Fab, IgG, BSA, and catalase) and therapeutic proteins (octreotide, insulin and bevacizumab) to optimize the formulation.

We have synthesized various triblock (TB) (PCL-PEG-PCL, B-A-B) and PB (PLA-PCL-PEG-PCL-PLA (C-B-A-B-C) and PEG-PCL-PLA-PCL-PEG (A-B-C-B-A)) copolymers based thermosensitive gelling polymers. We have observed distinct effect of block arrangement and molecular weights of block copolymers on the sol-gel transition and on the kinematic viscosity of aqueous solutions. PB copolymers with A-B-C-B-A block arrangement exhibited significantly lower viscosity relative to TB copolymers or other types of PB copolymers (C-B-A-B-C). The difference in viscosity and sol-gel transition behavior has been

explained by two different processes of micellization for A-B-C-B-A and B-A-B, or C-B-A-B-C types of copolymers. Moreover, a PB copolymer based formulation sustained the release of IgG up to ~20 days, which is significantly longer relative to TB copolymers based formulations.

In order to sustain release for longer duration, we have synthesized various PB copolymers (PLA-PCL-PEG-PCL-PLA and PGA-PCL-PEG-PCL-PGA) with high molecular weight and utilized them for the fabrication of protein-encapsulated NPs. We observed a significant effect of the presence of PLA or PGA on entrapment efficiency (EE), drug loading (DL) and *in vitro* release behavior. This may be due to the fact that PB copolymers exhibited significantly reduced crystallinity relative to TB copolymers. In addition, we have successfully optimized NP preparation methods to achieve maximum possible DL. This achievement allowed the loading of a large amount of drug which can last for ~6 month in a limited injection volume (100 μ L). The optimized methods were successfully utilized to encapsulate a wide variety of peptides and proteins with molecular weights ranging from 1 - 237 kDa in PB NPs. PB NPs alone exhibited significant burst release in the first few days of release study. However, a composite formulation comprised of protein-encapsulated PB-NPs prepared with optimized method and optimized PB copolymers (PB copolymers for NPs and thermosensitive gel) exhibited protein release for significantly longer duration of time (~6 months) with nearly zero-order release rate.

We have evaluated the structural integrity of released protein at different time intervals by CD spectroscopy. Moreover, biological activity of bevacizumab was evaluated by cell proliferation and cell migration assays. Enzymatic activity of lysozyme and catalase were confirmed with their respective enzymatic assays. Our results indicated that proteins retained

their structural integrity and bioactivity during the preparation of formulation and also during the release process. *In vitro* cell culture studies such as cell viability, cytotoxicity and biocompatibility studies performed on various ocular cell lines confirmed the safety of PB copolymers for ocular applications. Further, we have performed *in vivo* ocular tolerability studies with optimized PB formulations which demonstrated no inflammation, retinal toxicity, change in intraocular pressure or cataract even after 16 week of exposure. Moreover, *in vivo* studies further revealed that PB copolymers based formulations were slowly degraded and dissolved in vitreous humor confirming biodegradability of polymers.

Our studies indicated that PB copolymer based composite formulation can serve as a platform technology for the development of sustained release therapy in the treatment of posterior segment ocular diseases such as wet age-related macular degeneration (wet-AMD), diabetic macular edema (DME) and diabetic retinopathy (DR). This technology has a scope beyond ocular treatments and can also be used for the treatment of other chronic diseases.

APPROVAL PAGE

The faculty listed below, appointed by the Dean of the School of Graduate Studies have examined a dissertation titled “Development of Pentablock Copolymer Based Formulations for the Sustained Delivery of Protein Therapeutics in the Treatment of Posterior Segment Ocular Diseases” presented by Sulabh P. Patel, candidate for the Doctor of Philosophy degree, and certify that in their opinion it is worthy of acceptance.

Supervisory Committee

Ashim K. Mitra, Ph.D., Committee Chair
Department of Pharmaceutical Sciences

Kun Cheng, Ph.D.
Department of Pharmaceutical Sciences

J. David Van Horn, Ph.D.
Department of Chemistry

Zhonghua Peng, Ph.D.
Department of Chemistry

Jacob Marszalek, Ph.D.
School of Education

CONTENTS

ABSTRACT	iii
LIST OF ILLUSTRATIONS	ix
LIST OF TABLES	xii
ACKNOWLEDGEMENTS	xiii
CHAPTERS	
1. LITERATURE REVIEW	1
Ocular barriers, routes of administration and their significance in drug delivery	1
Role of cell membrane transporters and melanin in drug ocular bioavailability	7
Various strategies for ocular drug delivery	8
Biodegradable polymers	33
2. INTRODUCTION	40
Statement of the problem	40
Hypothesis	41
Objectives	44
3. NOVEL THERMOSENSITIVE PENTABLOCK (PB) COPOLYMERS FOR SUSTAINED DELIVERY OF PROTEINS IN THE TREATMENT OF POSTERIOR SEGMENT DISEASES	45
Rationale	45
Materials and methods	47
Results and discussion	58
Conclusion	87
4. SUSTAINED DELIVERY OF PROTEINS EMPLOYING NOVEL PENTABLOCK COPOLYMER BASED NANOPARTICULULATE SYSTEM FOR THE TREATMENT OF POSTERIOR SEGMENT OCULAR DISEASES	88
Rationale	88
Materials and methods	89

Results and discussion	98
Conclusion	123
5. TAILOR-MADE PENTABLOCK COPOLYMER BASED COMPOSITE FORMULATION FOR SUSTAINED OCULAR DELIVERY OF PROTEIN THERAPEUTICS	125
Rationale	125
Materials and methods	126
Results and discussion	138
Conclusion	165
6. OPTIMIZATION OF NOVEL PENTABLOCK COPOLYMER BASED COMPOSITE FORMULATION FOR SUSTAINED DELIVERY OF PROTEIN THERAPEUTICS IN THE TREATMENT OF OCULAR DISEASES	166
Rationale	166
Materials and methods	167
Results and discussion	175
Conclusion	195
7. <i>IN VIVO</i> OCULAR TOLERABILITY STUDIES OF VARIOUS PENTABLOCK COPOLYMER BASED FORMULATIONS: DELIVERED TOPICALLY OR INTRAVITREALLY	197
Rationale	197
Materials and methods	198
Results and discussion	208
Conclusion	221
8. SUMMARY AND RECOMMENDATIONS.....	222
Summary	222
Recommendations.....	228
APPENDIX.....	231
LIST OF REFERENCES	235
VITA.....	249

LIST OF ILLUSTRATIONS

1.1: Anatomical sites for various routes of ocular drug delivery.	2
1.2: Corneal barriers	3
1.3: Blood retinal-barriers.....	6
1.4: Structure of biodegradable polymers.....	39
3.1a: Synthesis scheme for the TB-1, TB-2, TB-3, TB-4, TB-5, PB-1 and PB-2 copolymers	49
3.1b: Synthesis scheme for the PB-4 and PB-5 copolymers	50
3.2: FTIR spectrum of PB-4 (PEG ₅₅₀ -PCL ₅₅₀ -PLA ₁₁₀₀ -PCL ₅₅₀ -PEG ₅₅₀).....	61
3.3: ¹ H NMR of (a) TB-1 (PCL-PEG-PCL), (b) PB-1 (PLA-PCL-PEG-PCL-PLA) and (c) PB-4 (PEG-PCL-PLA-PCL-PEG).....	62
3.4: GPC chromatograms for (a) TB-1 (PCL-PEG-PCL), (b) PB-1 (PLA-PCL-PEG-PCL- PLA) and (c) PB-4 (PEG-PCL-PLA-PCL-PEG).....	63
3.5: XRD patterns of block copolymers.	64
3.6: Sol-gel transition curves of TB-1 and TB-2.	67
3.7: Sol-gel transition curves (a) PB-1/PB-2, (b) PB-4/PB-5, and (c) TB-2/PB-1.....	68
3.8: Sol-gel transition curves of PB-1 and PB-5.....	70
3.9: <i>In vitro</i> cytotoxicity assay (LDH) of various block copolymers at different concentrations were performed on (a) ARPE-19 and (b) RAW 264.7 cells.....	71
3.10: <i>In vitro</i> cell viability assay (MTS) of various block copolymers at different concentrations were performed on (a) ARPE-19 and (b) RAW 264.7 cells.....	72
3.11: <i>In vitro</i> release of (a) TNF- α , (b) IL-6 and (c) IL-1 β from RAW 264.7 cells upon exposure to various concentrations of block copolymers.	73
3.12: Effect of block copolymer composition on <i>in vitro</i> release of IgG from thermosensitive gels (20 wt%).	78
3.13: Effect of polymer concentrations (15, 20 and 25 wt%) on <i>in vitro</i> release of IgG from PB-1 thermosensitive gels.....	79
3.14: ¹ H-NMR of PB-1 and coumarin-6 in (a) CDCl ₃ and (b) D ₂ O, and PB-5 and coumarin-6 in (c) CDCl ₃ and (d) D ₂ O.....	81
3.15: Estimation of PB-1 copolymer micelles at various concentrations i.e., 0.1, 0.5, 2 and 5 wt%.	84
3.16: Possible micellar gelation schemes for B-A-B, C-B-A-B-C types of copolymers in water during the thermoreversible phase transition.	86
4.1: Synthesis scheme for TB-A, TB-B, PB-A, PB-B, PB-D and PB-E.	91
4.2: Synthesis scheme for PB-C and PB-F. Note: For synthesis of PB-C and PB-F.....	92
4.3: ¹ H-NMR of TB-B (PCL ₇₀₀₀ -PEG ₄₀₀₀ -PCL ₇₀₀₀).....	100
4.4: ¹ H-NMR of PB-A (PL(L)A ₂₀₀₀ -PCL ₅₀₀₀ -PEG ₄₀₀₀ -PCL ₅₀₀₀ -PL(L)A ₂₀₀₀).....	101
4.5: Gel permeation chromatogram of PB-A copolymer.....	102
4.6: XRD patterns of various TB and PB copolymers where (a) TB-A, PB-A, PB-B, and PB- C, (b) TB-B, PB-D, PB-E, and PB-F.	103

4.7: <i>In vitro</i> cytotoxicity (LDH) assay of various block copolymers at different concentrations were performed on (a) RAW 264.7 and (b) ARPE-19 cells.....	107
4.8: <i>In vitro</i> cell viability (MTS) assay of various block copolymers at different concentrations were performed on (a) RAW 264.7 and (b) ARPE-19 cells.....	108
4.9: <i>In vitro</i> biocompatibility of block copolymers were evaluated by estimating the levels of (a) TNF- α , (b) IL-6 and (c) IL-1 β in the supernatants of polymer treated RAW 264.7 cells.	109
4.10: <i>In vitro</i> release of IgG from NPs prepared with TB-A and TB-B block copolymers.	118
4.11: <i>In vitro</i> release of IgG from NPs prepared with TB-A, PB-A, PB-B, and PB-C block copolymers.....	119
4.12: <i>In vitro</i> release of IgG from NPs prepared with TB-B, PB-D, PB-E, and PB-F block copolymers.....	120
4.13: Effect of molecular weights of block copolymers on <i>in vitro</i> release of IgG (a) PB-A and PB-D NPs, (b) PB-B and PB-E NPs, and (c) PB-C and PB-F NPs.	121
4.14: CD spectrum of released IgG from PB-E NPs after 15 days.....	122
5.1: Synthesis scheme for PB-A (PGA-PCL-PEG-PCL-PGA) copolymer.....	128
5.2: Synthesis scheme for PB-B (PLA-PCL-PEG-PCL-PLA) copolymer.....	128
5.3: Synthesis scheme for PB-C (PEG-PCL-PLA-PCL-PEG) copolymer.....	129
5.4: ¹ H-NMR spectrum of PB-A copolymer in CDCl ₃	140
5.5: ¹ H-NMR spectrum of PB-B copolymer in CDCl ₃	141
5.6: ¹ H-NMR spectrum of PB-C copolymer in CDCl ₃	142
5.7: <i>In vitro</i> cytotoxicity assay (LDH) of PB-A and PB-B copolymers at the concentration of 10 mg/mL was performed on ARPE-19, SIRC, HCEC and RAW-264.7 cell lines.	144
5.8: <i>In vitro</i> cell viability assay (MTS) of PB-A and PB-B copolymers at the concentration of 10 mg/mL was performed on ARPE-19, SIRC, HCEC and RAW-264.7 cell lines.	145
5.9: <i>In vitro</i> biocompatibility of PB-A and PB-B copolymers was evaluated by estimating the levels of TNF- α , IL-6 and IL-1 β in the supernatants of polymer treated RAW 264.7 cells.	146
5.10: <i>In vitro</i> release of FITC-BSA from NPs prepared with PB-A and PB-B copolymers.	152
5.11: <i>In vitro</i> release of IgG from NPs prepared with PB-A and PB-B copolymers.....	153
5.12: <i>In vitro</i> release of FITC-BSA and IgG from PB-B NPs.....	154
5.13: <i>In vitro</i> release of IgG and bevacizumab from PB-B NPs	155
5.14: <i>In vitro</i> release of FITC-BSA from PB-B NPs and PB-B NPs suspended in PB-C gelling polymer	156
5.15: <i>In vitro</i> release of IgG from PB-B NPs and PB-B NPs suspended in PB-C gelling polymer (20 wt%).	157
5.16: Stability of released IgG confirmed by CD spectroscopy.	162
5.17: Cell proliferation assay performed on RF/6A cells to evaluate the biological activity of bevacizumab	163
5.18: Cell migration assay performed on RF/6A cells to evaluate the biological activity of bevacizumab	164
6.1b: Synthesis scheme for PB-C and PB-D (PGA-PCL-PEG-PCL-PGA).	169
6.1a: Synthesis scheme for PB-A and PB-B (PLA-PCL-PEG-PCL-PLA)	169
6.2: Synthesis scheme for PB-E (PEG-PCL-PLA-PCL-PEG).	170

6.3: ¹ H-NMR spectrum of PB-A copolymer in CDCl ₃	177
6.4: ¹ H-NMR spectrum of PB-D copolymer in CDCl ₃	178
6.5: ¹ H-NMR spectrum of PB-E copolymer in CDCl ₃	179
6.6: <i>In vitro</i> release of protein/peptide from PB-A NPs suspended in PB-E thermosensitive gel (20 wt%).	189
7.1: Preparation of low endotoxin PB NPs for ocular tolerability studies.	200
7.2: Representative images of rabbit eyes, 6 h post-topical application.	209
7.3: Mean +/-SD Cumulative Hackett-McDonald Irritation Scores.	213
7.4: Images of rabbit eyes taken after single intravitreal injection (100 μL) of PB thermosensitive gel, (a) day 1, (b) day 21, (c) day 42, (d) day 49, and (e) day 98.	214
7.5: Images of rabbit eyes taken after single intravitreal injection (100 μL) of PB NPs dispersed in PBS, (a) day 1, (b) day 21, (c) day 35, (d) day 42, and (e) day 77.	215
7.6: Images of rabbit eyes taken after single intravitreal injection (100 μL) of PB NPs dispersed in PB thermosensitive gel, (a) day 1, (b) day 21, (c) day 35, (d) day 42, and (e) day 77.	216
7.7: Intraocular pressure (IOP) estimated after single intravitreal injection.	217
7.8: Electroretinography performed after single intravitreal injection.	218

LIST OF TABLES

3.1: List of TB and PB copolymers studied.....	51
3.2: Coefficient of determination (R^2) for various kinetic models for <i>in vitro</i> release of IgG.	80
3.3: Viscosity of thermosensitive gelling solutions (15 wt%) at various temperatures.....	85
4.1: List of TB and PB copolymers studied.....	104
4.2: Characterization of NPs prepared TB-A and TB-B.....	112
4.3: Characterization of NPs prepared PB-A, PB-B and PB-C.	113
4.4: Characterization of NPs prepared PB-D, PB-E and PB-F.....	114
5.1: Characterization of PB copolymers.	143
5.2: Characterization of FITC-BSA and IgG-loaded NPs.	151
5.3: Coefficient of determination (R^2) for various kinetic models for <i>in vitro</i> release of FITC- BSA, IgG and bevacizumab.....	161
6.1: Characterization of polymers.....	180
6.2: Optimization of process parameters for the preparation of IgG-Fab-loaded PB NPs... ..	181
6.3: Encapsulation of various proteins with optimized methods A and B (PB-A).....	186
6.4: Encapsulation of various proteins with optimized methods A and B (PB-C).....	187
6.5: Encapsulation of various proteins with optimized methods A and B (PB-D).....	188
6.6: Coefficient of determination (R^2) for various kinetic models for <i>in vitro</i> release of octreotide, insulin, lysozyme, IgG-Fab, IgG and catalase.	192
6.7: Enzymatic activity of lysozyme estimated in the released samples and controls.	193
6.8: Enzymatic activity of catalase estimated in the released samples and controls.	194
7.1: Animals, housing and environmental conditions.	202
7.2: Animals assigned per group for topical tolerability study.....	204
7.3: Animals assigned per group for tolerability study of intravitreal injection.....	205
7.4: Mean cumulative Hackett-McDonald Ocular Irritation Scores after topical treatment.	210
7.5: Ocular histopathology of rabbit eyes after single intravitreal injection of various PB copolymer based formulations.....	219

ACKNOWLEDGEMENTS

It is with immense gratitude that I acknowledge exceptional guidance and support of my mentor Dr. Ashim K. Mitra. His constant motivation was extremely helpful in solving scientific challenges encountered throughout my graduate studies. I thank him for inspiring and believing in me which helped me to navigate through the rough waters of my graduate studies. It gives me great pleasure in acknowledging the support, and valuable critics of my dissertation supervisory committee members Drs. Kun Cheng, J. David Van Horn, Zhonghua Peng and Jacob Marszalek. I feel privileged to have such extraordinary researchers in my supervisory committee. I am greatly thankful to Dr. Dhananjay Pal for teaching me cell culture techniques and valuable scientific discussions which helped me to guide my research project. I am thankful to our collaborator Dr. Brian Gilger from North Carolina State University for performing *in vivo* tolerability studies of our PB copolymer based formulations. I am also thankful to Dr. Poonam, Dr. Grau and Dr. Weiss for their valuable suggestions. I would like to extend my appreciation to Mrs. Ranjana Mitra for her constant support, encouragement and timely help during my stay at UMKC.

I am greatly thankful to Ravi Vaishya, Varun Khurana and Mitan Gokulgandhi for standing beside me during the tough time of graduate study. I feel privileged to have such good friends. I am also thankful to Vibhuti Agrahari and Mary Joseph for helping me in my research experiments. I am thankful to Drs. Gyan Prakash Mishra and Viral Tamboli for their help in many experiments and scientific discussions. I thank my fellow lab mates Mitesh Patel, Megha Barot, Sujay Shah, Asha Patel, Animikh Ray, Ashwani Dutt Vadlapudi, and Kishore Cholkar for their timely help and creating such a cheerful environment in the lab throughout my studies.

My special thanks to Drs. Deep Kwatra, Sriram Gunda and Nanda Kishore Mandava for their valuable suggestions in my research project.

I sincerely thank Joyce Johnson and Sharon Self for their constant support in administrative assistance throughout my stay at UMKC. I appreciate support from Nancy Hoover and Connie Mahone from School of Graduate Studies. I am thankful to National Institute of Health and School of Graduate Studies for constant financial support. I would also express my sincere thanks to Dr. James B. Murowchick (School of Geological Sciences) and Dr. Natalya Shipulina (School of Biological Sciences, UMKC) for helping in XRD and CD spectroscopy.

I cannot find words to express my gratitude to my parents Pravin Patel and Ranjan Patel, my brother Tejas Patel and sister-in-law Dipali Patel for their invaluable sacrifices and love. I am greatly thankful to my beloved wife, Unnati for her selfless love, immense faith and moral support. Finally, I would thank to my spiritual Guru, Dhruv Vyas and the God Almighty for their mercy and grace.

CHAPTER 1

LITERATURE REVIEW

Development of controlled and sustained ophthalmic delivery systems still remains a major area for pharmaceutical research. It is even more relevant today because of the emergence of new and potent drugs, especially biological modifiers. Recent advances in the field of nanotechnology have led to the development of novel drug delivery systems for ocular complications.

Ocular barriers, routes of administration and their significance in drug delivery [1]

Various routes of administration have been explored for the local and targeted delivery of the therapeutics in the treatment of ocular diseases (Figure 1.1, anatomical locations for various routes of administration denoted in bold & italic). An understanding of various ocular barriers will be necessary to design novel drug delivery systems for the treatment of ocular diseases. Topical ophthalmic delivery systems are indicated for the treatment of anterior chamber diseases including glaucoma, allergic conjunctivitis, corneal epithelial keratitis, stromal keratitis and dry eye. For most topical administration, the sites of action are different anterior chamber tissues such as the layers of cornea, lacrimal glands, sclera, conjunctiva, iris and ciliary body. Topical formulations are also prescribed for the treatment of back of the eye diseases such as diabetic retinopathy (DR), bacterial endophthalmitis, age-related macular degeneration (AMD) and retinitis. However, the physical barriers imposed by various structural defensive mechanisms of the eye lead to poor absorption of the therapeutics after topical administration [2].

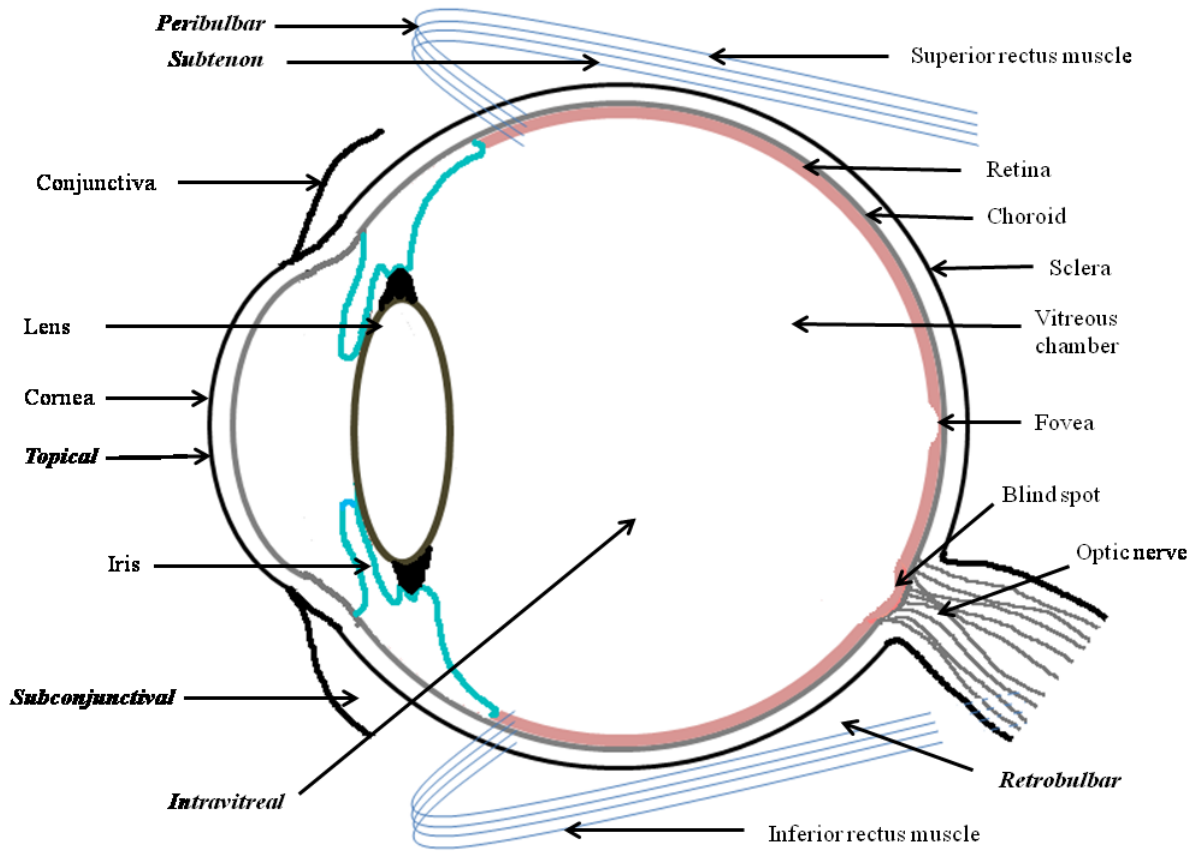


Figure 1.1: Anatomical sites for various routes of ocular drug delivery [1].

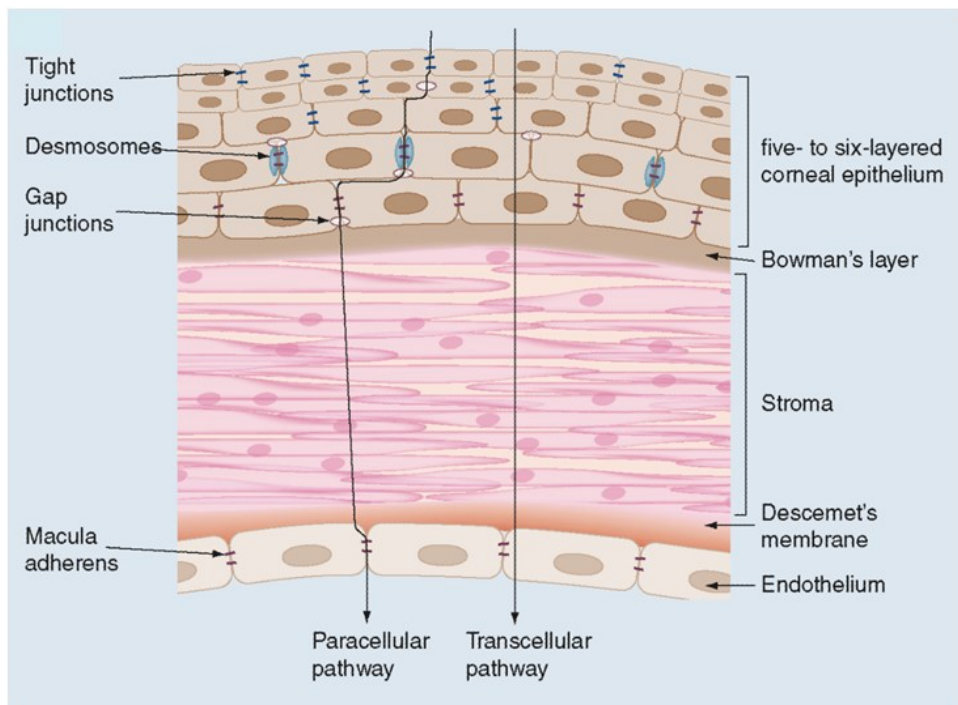


Figure 1.2: Corneal barriers [2]

The main limitations for conventional topical drug delivery are higher tear turnover rate and lower precorneal residence time, which lead to poor drug concentration or subtherapeutic levels in the anterior chamber, requiring frequent administration [3].

In addition, different layers of cornea, sclera and conjunctiva play a vital role in drug transport after topical administrations. The cornea, the outer most layer of the eye, can be divided into three distinct layers, epithelium, stroma, and endothelium (Figure 1.2). The corneal epithelial cells are highly lipoidal and are attached to each other by desmosomes and zonula occludens (tight junction complexes) [4, 5]. Due to their lipoidal nature, these cells act as a mechanical barrier for hydrophilic drugs. Moreover, the presence of tight junctions offers significant resistance to paracellular transport of various hydrophilic and large molecules. The corneal epithelium is followed by stroma, which comprises 90% of corneal thickness. Stroma is a highly hydrated lamellar arrangement of collagen fibers, and it acts as a static barrier for hydrophobic drugs. Corneal endothelial cells are layered between the aqueous humor and stroma. The tight junctions of these cells are leaky and facilitate the permeability of macromolecules between the stroma and aqueous humor [6].

Higher blood and lymphatic flow in conjunctiva eliminate a large fraction of the administered dose into systemic circulation and thus is considered as non-productive absorption. Moreover, tight junction complexes of the conjunctival epithelium prevent passive diffusion of hydrophilic drugs [7]. The sclera is a continuous layer, which originates from the limbus and extends posteriorly throughout the eye globe. It is a hydrophilic tissue composed of proteoglycans and collagen fibers. Scleral permeability of the therapeutics is inversely proportional to the hydrodynamic radius of the permeating molecules. For example, globular proteins were more permeable relative to dextrans with linear structures [8]. Furthermore,

permeability across the sclera is also affected by charge. A recent report suggests that permeability of anionic molecules is higher compared to cationic molecules, and it might be due to the interaction between positively charged molecules with the negatively charged proteoglycans [9].

Although intravitreal and periocular administrations are not patient compliant, these routes are employed to deliver therapeutics for the treatment of posterior segment diseases. The periocular route is relatively less invasive than the intravitreal route, which includes subtenon, subconjunctival, peribulbar and retrobulbar administrations (Figure 1.1). After periocular administrations, drug molecules can reach back of the eye by three different routes: systemic circulation through the choroid, transscleral pathway, and the anterior route (tear film, cornea, aqueous humor and vitreous humor) [10]. Subconjunctival administration can bypass conjunctival epithelium, which is the rate limiting factor for the absorption of hydrophilic drugs. However, many metabolic, static and dynamic barriers (conjunctival blood and lymphatic circulations) increase the elimination of the drug and eventually, reduce drug transport to the posterior section [11, 12]. Molecules, which escape the conjunctival vasculature, eventually reach to the photoreceptor cells and the retina *via* sclera and choroid. Permeability across the sclera is not a major constraint because it is highly dependent upon the molecular radius and not the hydrophobicity of drug molecule [13, 14]. However, choroidal blood circulation does act as a dynamic barrier for the drug permeability and eliminates a considerable amount of the dose. Nevertheless, the blood-retinal barrier (BRB) also plays a critical role for permeability of active molecules to the photoreceptor cells (Figure 1.3). Direct delivery of therapeutics to the vitreous humor can offer enormous advantage over the subconjunctival administration.

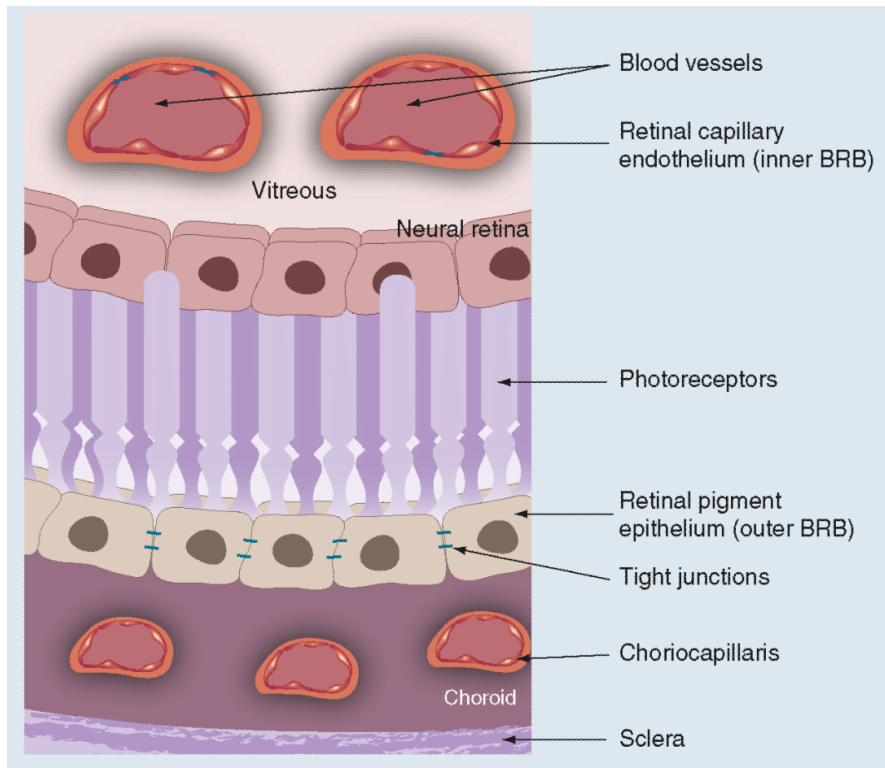


Figure 1.3: Blood retinal-barriers [2]

However, intravitreal injection has the least patient compliance and it also leads to non-uniform drug distribution in the vitreous humor. The vitreous allows rapid diffusion to small molecule, while it restricts the diffusion of macromolecules. Furthermore, pathophysiological conditions also have a significant effect on the distribution of therapeutics [15].

Role of cell membrane transporters and melanin in drug ocular bioavailability

The roles of transporters in ophthalmic drug delivery have been reviewed by many investigators [16-18]. Transporters play an important role in the ocular bioavailability of drug molecules. There are two types of transporters present on the ocular tissues: influx and efflux transporters. Out of these two transporters, the efflux transporter acts as a barrier for the drug absorption. Polyglycoprotein (P-gp), multi drug resistance protein (MRP) and breast cancer resistance protein (BCRP) have been identified on different ocular tissues and cell lines. In case of *in vitro* cell models, transporter protein expression pattern may vary according to its culture conditions and origin [19, 20]. P-gp has significant affinity for lipophilic drug molecules. It has been identified on conjunctiva [21, 22] and retinal pigment epithelium (RPE) [19, 23, 24]. However, recent reports indicate that functional expression of P-gp on human corneal epithelium may be absent or negligible [20, 25]. Out of nine isoforms of MRP, only three have been identified on various ocular tissues. Furthermore, presence of MRP1 has been reported on RPE [26]. The presence of BCRP on corneal epithelium cells has also been reported [27]. Freshly excised human corneal epithelial tissue showed the functional expression of MRP1, MRP5, and BCRP [20].

Melanin is located in various ocular tissues such as uvea, RPE, and choroid. It has a tendency to interact with lipophilic and basic drug molecules *via* van der Waals and electrostatic forces or by simple charge transfer [28, 29]. Binding of melanin to therapeutics

can significantly reduce the pharmacological activity [30]. In the anterior chamber, binding of drug molecules with melanin renders them unavailable for the receptor mediated uptake which eventually reduces ocular bioavailability [31] and necessitates the administration of larger dose [32]. Likewise, systemic or transscleral drug administration may be followed by interaction of drug molecule with melanin in RPE or choroid, which can reduce the fraction of molecules permeating to retina and vitreous humor [33, 34]. Higher binding of lipophilic drugs to the melanin was demonstrated in bovine choroid-Bruch's membrane [35].

A current challenge in ophthalmic drug delivery is to develop a tissue targeted delivery system, which can circumvent ocular barriers without altering ocular protective mechanisms. Colloidal or particulate drug delivery systems can evade many static, dynamic, and metabolic barriers. Moreover, they can offer the simplicity of a topical eye formulation and it can also be utilized for intraocular and periocular injections.

Various strategies for ocular drug delivery

Additives [36]

Several attempts have been made to improve drug availability into the anterior chamber either by utilizing enhancers to increase drug permeability across ocular tissues or by employing mucoadhesives to enhance precorneal residence time of the applied dose.

Viscosity enhancing polymers can be incorporated into ophthalmic formulations to improve residence time in the precorneal area and to increase absorption of the therapeutic agents into and across the cornea. Various polymers, such as hydroxypropylmethylcellulose (HPMC) [37], hyaluronic acid (HA) [38, 39], polyvinyl alcohol (PVA) [37], hydroxyethylcellulose [37], and methylcellulose [40] have been investigated to determine their potential in improving the bioavailability of therapeutic agents following topical applications.

Pluronics

Pluronics can significantly improve drug solubility and enhance the viscosity of topical formulations. Pluronic-F68 (15%) and Pluronic-F127 (10%) were more effective as an indomethacin solubilizer and viscosity enhancer relative to polyols and polysorbate 80 [41]. Moreover, Pluronic solutions were well tolerated on rabbit eyes than commercial formulation, Indocid-suspension. Poloxamer-407 [polyoxyethylene- polyoxypropylene block copolymer] was evaluated as a solubilizer for topical application of indomethacin [42]. This formulation has significantly elevated indomethacin levels in aqueous humor (AUC = ~21 h.µg/mL) relative to the marketed solution (AUC = ~8 h.µg/mL). In addition, anti-inflammatory studies performed on an immunogenic uveitis model demonstrated comparatively more rapid resolution of the symptoms. In another study, PVA and HPMC caused improvement in viscosity and stability of indomethacin topical ocular suspension [43]. Mucoadhesive eye drops of tolmetin (a pyrrole-acetic acid derivative) exhibited higher drug levels in aqueous humor in comparison to the aqueous solution, in both inflamed and uninflamed rabbit eyes [44].

A novel approach of a drug-embedded thermosensitive gel demonstrated some promising results for topical ophthalmic drug delivery. In a recently published study Gao, et al. have prepared and evaluated a dexamethasone-loaded polylactide-co-glycolide-PEG-polylactide-co-glycolide (PLGA-PEG-PLGA) thermosensitive gelling solution [45]. This formulation improved precorneal residence time and demonstrated 7-fold higher drug levels in aqueous humor ($C_{\max} = 125.2 \text{ mg/mL}$) relative to eye drops. This hydrogel system showed good biodegradability, sustained release, and ocular biocompatibility, indicating that the system is a safe candidate for sustained ophthalmic drug delivery. Many other *in situ* polymeric

gelling systems, such as chitosan [46], poloxamer [47], HPMC [48], PEG-PCL-PEG [49], poly N-isopropylacrylamide/chitosan [50], poloxamer/chitosan [51], pluronic F-127/chitosan [52], and poloxamer/carbopol [53] were explored for ocular applications.

Cyclodextrins

One of the strategies to enhance the ocular absorption of poorly soluble drugs is by increasing their aqueous solubility. Almost all NSAIDs and corticosteroids are highly lipophilic molecules, which exhibit very poor aqueous solubility, and therefore it is very challenging to formulate them in aqueous eye drops. Cyclodextrins have been commonly used to enhance the solubility of various hydrophobic drugs, owing to their excellent drug solubilizing property. Drug solubilizing property of cyclodextrins is highly dependent on their ability to form water soluble complexes with drug molecules. Such complexes interact with the membrane wherein, the hydrophobic drug molecules diffuse through the lipid membrane while the water soluble cyclodextrin molecules are retained in the aqueous tear fluid. It has been reported that the amount of cyclodextrin required to solubilize lipophilic drugs should be just enough (<15%) for improving drug penetration following topical administrations. A higher concentration of cyclodextrin retains the drug in the aqueous tear fluid, thereby decreasing its transcorneal penetration. The release rate of drug molecules from these complexes along with the partition of the drug into and then through the corneal and conjunctival epithelium determines the intraocular availability of the drug [54].

In a recently published manuscript Valls, et al. demonstrated improved solubility and a higher ocular bioavailability of diclofenac [55]. Six times higher transport of diclofenac across the corneal tissue was observed with β -CD/diclofenac complex treatment relative to free drug. Loftsson, et al. have examined the effects of various CDs (randomly methylated β -CD

(RM β CD) and 2-hydroxypropyl- β CD (HP β CD)) on ocular delivery of dexamethasone [56]. Results from *in vivo* ocular tissue distribution studies illustrated that both lipophilic RM β CD and hydrophilic HP β CD have improved dexamethasone levels in rabbit eyes. However, RM β CD delivered higher amounts of dexamethasone relative to other CDs.

The same investigators have recently published a patent, demonstrating the role of CDs (RM β CD and γ -cyclodextrin (γ -CD)) in the delivery of corticosteroids to various ocular tissues [57]. Nanoparticulate formulation of γ -CD-drug conjugates were able to deliver corticosteroids more efficiently to the back of the eye, contrary to the RM β CD drug solution, which causes localization of more drug into the anterior chamber of the rabbit eyes. Cyclooxygenase-2 (COX-2) inhibitors are also indicated in the treatment of ocular inflammations. However, poor aqueous solubility of these agents limits their topical application. In an attempt to improve ocular bioavailability, a nanoparticulate formulation of valdecoxib with HP β CD was evaluated [58]. As anticipated, levels of valdecoxib in the cornea and conjunctiva were significantly higher in NP-treated rabbit eyes relative to control.

In vivo ocular bioavailability of three different hydrocortisone (HC) formulations (1% HC solution with HP β CD, 1% HC solution with HP β CD along with sodium hyaluronate or carbopol 934P, and 1% HC suspension) was evaluated in New Zealand White rabbit [59]. Incorporation of HP β CD in formulation improved HC solubility and bioavailability in the cornea and aqueous humor by 75% and 55%, respectively, relative to aqueous suspension. Interestingly, inclusion of hyaluronate or carbopol in the HP β CD solution did not alter ocular bioavailability.

In clinical trials, topical delivery of the dexamethasone/HP β CD solution exhibited a significantly higher aqueous humor concentration (2.6-fold higher AUC) in human subjects

relative to suspension [60]. Currently, several CD containing formulations are marketed in Europe, such as Indocid (indomethacin with HP β CD) and Voltaren (diclofenac-Na with HP β CD), for the treatment of anterior chamber inflammations. It will not be surprising if CD containing ophthalmic topical formulations enter the US market in the near future.

Colloidal dosage forms for drug delivery to anterior segment of the eye

In the last decade, many novel strategies including liposomes, polymeric NPs, dendrimers, nanoemulsions, micelles, nanosuspensions, and combination approaches have been investigated for the development of sustained ocular drug delivery systems. These colloidal dosage forms offer numerous advantages over conventional dosage forms, such as higher drug solubility, enhanced bioavailability, improved physical and chemical stability, and sustained drug delivery. Furthermore, nanocarriers can lower toxicity and irritability concerns related to drug and/or formulation, and eventually these systems can improve *in vivo* performance and patient compliance. Such delivery systems can significantly bypass the blood-ocular barriers, overcome the efflux related issues of parent drugs, and reduce frequency of administration [61]. However, a clear understanding of the size, charge, and affinity of drug molecules towards various ocular tissues and pigments are crucial for the development of effective ocular formulations. For example, for transcorneal delivery, it is important to understand the structure and properties of each layer of the cornea. Corneal epithelium facilitates the transport of hydrophobic drugs, while the stroma acts as a barrier for hydrophobic drugs and allows only hydrophilic drugs to enter into the anterior chamber. Corneal mucosa is negatively charged, and therefore it increases the permeability of positively charged drugs and prolongs retention of positively charged nanocarriers [62]. Other than the transcorneal route, conjunctival and transscleral routes play a vital role for the treatment of

posterior segment diseases. Permeability of a drug molecule across the sclera depends upon various physicochemical properties such as hydrodynamic radius, molecular weight, surface charge, and hydrophilicity. Studies revealed that 200 nm particles could not cross the sclera, while 20 nm particles crossed the scleral tissue at very low extent [63, 64]. Similarly, the performance of nanocarriers is also affected by choroidal circulations (dynamic barrier: blood and lymphatic flow), surface modifications with endogenous molecules, size, and abundance of various enzymes particularly for biodegradable nanocarriers.

Liposomes

Research on liposomes has expanded considerably in the last thirty years. Liposomes are spherical biphasic vesicular system where the internal aqueous phase is surrounded by phospholipid bilayer membrane [65]. Hydrophilic drugs can be encapsulated in the inner aqueous core while the hydrophobic drugs tend to stay in the lipid bilayer [66]. Depending on the size, liposomes can be classified into small unilamellar vesicles (SUV) (10-100 nm), large unilamellar vesicles (LUV) (100-300 nm) and multilamellar vesicles (contains more than one bilayer). Liposomes can be formulated from sphingolipids, long chain fatty acids, cholesterol, glycolipids, membrane proteins, and non-toxic surfactants [67]. Therapeutic molecules such as proteins, nucleotides, small molecules, and even plasmids can be delivered with liposomes [68]. These delivery systems can be employed to control and sustain the release of therapeutic molecules, and more importantly, they can be used to protect the therapeutic agent from metabolic degradation [69]. Due to numerous advantages, liposomes have been extensively investigated in ophthalmic treatments.

Investigators have studied transcorneal permeation of neutral, anionic and cationic liposomes. Cationic liposomes interact more efficiently with negatively charged corneal

epithelial membrane relative to the anionic or neutral liposomes, and eventually provide higher drug (tropicamide, penicillin G and acetazolamide) transport across the cornea [70-72]. Along with small molecule drug delivery, liposomes have also been investigated as non-viral vectors for gene transfections [73] and as a carrier for the delivery of monoclonal antibodies [74]. Recently, a focal laser was employed to manage the release of drug and dyes from liposomes at the target site [75]. In the future, laser-targeted delivery system may be employed for the treatment of neovascular vessel occlusion, choroidal and retinal blood vessel stasis, angiography, and selective tumors.

Liposomes prepared with naturally derived phospholipids such as egg phosphatidyl ethanolamine or dioleoyl phosphatidyl ethanolamine (DOPE) are more suitable for the ophthalmic drug delivery purposes [76]. Liposomes have been successfully utilized for drug delivery to the anterior segment of the eye. The therapeutic efficiency of liposomes depends on various factors, including size and charge, encapsulation efficiency, retention and stability in conjunctival sac and ocular tissues and affinity towards corneal surface. The surface charge of liposomes plays a key role in determining their affinity towards the corneal surface. According to Felt, et al. negatively charged corneal surface has higher affinity towards positively charged liposomes. They also showed that the drug elimination due to lachrymal flow was reduced as the cationic liposomes increased the viscosity and interacted with the negatively charged mucus [77]. Liposomes-loaded with pilocarpine hydrochloride were prepared by Monem, et al. and researchers observed that neutral MLVs showed the most prolonged effect when compared to negatively charged MLVs and free drug [78]. Acyclovir (ACV) liposomes were formulated and evaluated for their *in vitro* permeation and *in vivo* absorption across the cornea in rabbits. Experiments showed that positively charged liposomes

formed a coating on the corneal surface. The morphology depicted that liposomes bound tightly to the corneal tissue and increased the residence time and thus improved the ACV absorption [79]. Ocular pharmacokinetics of ganciclovir (GCV) encapsulated in liposomes was studied in albino rats and compared with GCV solution. Transcorneal permeability of GCV liposomes was 3.9 fold higher when compared to GCV solution. The AUC of GCV in aqueous humor was found to be 1.7 fold higher in case of GCV liposomes. Ocular tissue distribution of GCV from liposomes demonstrated 2-10 times higher concentration in sclera, cornea, iris, lens and vitreous humor when compared to solution treated groups. These results suggest that liposomes can efficiently deliver GCV to the eye [80]. Ciprofloxacin-loaded liposomes suspended in hydrogels were formulated using two phospholipids, soya bean phosphatidyl choline and cholesterol. The encapsulation efficiency of drug was found to be $82 \pm 1\%$. Transcorneal permeation profiles of ciprofloxacin from 0.3% aqueous solution, 0.3% liposomal suspension and 0.3% liposomal hydrogels were studied for 6 h. The cumulative drug permeated across cornea was $201 \pm 9 \mu\text{g}$ with aqueous solution and the percentage permeation was 6.7%; while the cumulative amount permeated from liposomal suspension was $614 \pm 14 \mu\text{g}$ and percentage permeation was 20.4% and with liposomal hydrogel formulation, ciprofloxacin permeation was $918 \pm 25 \mu\text{g}$ and the percentage permeation was 30.6%. Investigators have observed that the liposomal suspension exhibit three-fold increase in permeation than aqueous solution [81]. This may be mainly attributed to the electrostatic interaction between positively charged liposomes and the negatively charged corneal membrane. The liposomes are well adsorbed onto the corneal surface and transfer their membrane associated drug directly into the corneal epithelial cell membranes, thereby enhancing drug transport across cornea [82]. Similarly, liposomes of ofloxacin and gatifloxacin

were prepared and studied for determining their efficiency in increasing the drug ocular bioavailability [83]. In case of ofloxacin liposomal hydrogel the permeation was seven fold higher than that of aqueous solution. Hence liposomal hydrogels can overcome all the precorneal barriers and ensures steady and prolonged transcorneal permeation of the drug.

Like other delivery systems, liposomal treatment is also associated with few drawbacks, such as possible toxicity and irritability [84-87]. Lipid components of the liposomes are believed to be a primary source of toxicity, while charge of the liposomes is a main reason for irritability. These constraints may restrict their chances for becoming popular ophthalmic dosage form of the future. Moreover, commercial success of liposomes is also limited because of the difficulties in sterilization and their relatively short shelf life.

Polymeric NPs

In order to address the problems of possible toxicity and irritability associated with liposomes, drug-loaded nanometer sized polymeric particles may be considered a viable alternative for the development of sustained release ophthalmic formulation. Nanoparticulate systems comprise of particles with less than one micron particle size in which therapeutically active agent is entrapped, absorbed, encapsulated, attached or adsorbed [67]. Aqueous or non-aqueous suspension of drug-loaded polymeric NPs can either be delivered as topical drops in the cul-de-sac or can be administered *via* transscleral, intravitreal or intraperitoneal routes. Development of sustained release biodegradable dosage form for intravitreal delivery may evade the limitation of frequent administration and it may also improve patient compliance. Polymeric NPs can sustain drug release by diffusion, dissolution, or mechanical disintegration and/or erosion of the polymer matrix [88]. NPs can circumvent the limitation of poor solubility of therapeutics. Moreover, the NP can also protect the drug (e.g. peptides and proteins) from

enzymatic degradation, and eventually, improves an ocular bioavailability. Thus, NPs are a better candidate for both posterior and anterior segment delivery.

Various biodegradable and non-biodegradable polymeric systems have been developed for sustained delivery of NSAIDs, such as ibuprofen, flurbiprofen, and indomethacin in the treatment of anterior chamber inflammations. In a recently published study, investigators have utilized Eudragit RS100 to prepare ibuprofen NPs for inhibition of an inflammatory response to surgical trauma [89]. Results from *in vivo* efficacy studies performed on the rabbit eye model demonstrated a significantly higher aqueous humor concentration than the control aqueous eye drop. Similar studies were performed with flurbiprofen as an active agent for the prevention of myosis induced by extracapsular cataract surgery [90]. A higher interaction of positively charged NPs (zeta potential +40–60 mV) with an anionic corneal surface was observed [91]. A higher precorneal retention achieved with controlled release formulation was noted to be a primary reason for improvement in flurbiprofen ocular bioavailability. Ocular applications of indomethacin are overshadowed by its poor availability. In an attempt to improve ocular bioavailability Calvo, et al. have examined three different colloidal carrier systems, that is, NPs, nanocapsules, and nanoemulsions [92]. Results of *ex vivo* transport studies across the excised rabbit cornea demonstrated higher indomethacin ocular bioavailability, due to the colloidal nature of the carrier system. Two different biodegradable polymers (PLGA and PCL) were utilized to formulate flurbiprofen-encapsulated NPs to improve ocular availability [55]. Significantly enhanced corneal transport of flurbiprofen was observed in case of a nanocarrier system relative to free drug. Moreover, PLGA NPs demonstrated ~2-fold higher transport of flurbiprofen compared with the PCL NPs. Subsequently, flurbiprofen-loaded PLGA NPs were prepared and evaluated by Vega, et al. [93]. Incorporation of Poloxamer 188 in NP preparation

has significantly improved stability of NPs. Moreover, topical instillation of NP formulation in the rabbit eyes, enhanced anti-inflammatory efficacy without any signs of irritation or toxicity to ocular tissues. Improved efficacy could be due to an improvement in the bioadhesive property of NPs.

Cyclosporin-A (CS-A)-loaded chitosan NPs were successfully prepared and evaluated for topical ocular applications [94]. Significantly positive zeta potential and a smaller particle size improved precorneal retention of NPs. *In vivo* studies have revealed that topical instillation of chitosan NPs can selectively increase CS-A levels in the cornea (2-fold higher) and in the conjunctiva (~4-fold higher) relative to topical eye drops of the chitosan solution or aqueous suspension of CS-A. Cholesterol-conjugated hydrophobically modified chitosan was utilized to prepare CS-A-encapsulated NPs [95]. Higher NP retention at the precorneal surface was confirmed by single photon emission computed tomography and scintillation counter measurement. In another study, the same research group has disclosed physical mixture of PLA/chitosan to prepare rapamycin-loaded NPs [96]. Incorporation of PLA significantly improved NP encapsulation efficiency (~13-fold) due to stronger hydrophobic interactions. *In vivo* studies were conducted in rabbits with topical dosing of rapamycin-loaded NPs, empty NPs, and no treatment. Post-treatment inflammation or blood vessel development was monitored. Results for treatment with rapamycin-loaded NPs demonstrated clear and transparent corneas. On the contrary, corneas, which received no treatment or empty NP treatment were found opaque with stromal edema and/or neovascularization, within first 10 days. In addition, the rapamycin suspension exhibited some degree of inhibitory effect on neovascularization.

Prednisolone is one of the most effective agents in a group of glucocorticoids, and it is marketed as ocular suspensions and drops. This product inhibits a wide variety of inflammatory responses, such as fibrin disposition, leukocyte migration, fibroblast proliferation, edema, capillary dilation, and capillary proliferation. Gatifloxacin and prednisolone were simultaneously incorporated in mucoadhesive polymer (HA)-coated Eudragit NPs (RS 100 and RL 100) in the treatment of bacterial keratitis [97]. Noticeably, improved ocular bioavailability (corneal and aqueous humor) for gatifloxacin was observed after topical instillation of NP suspension. However, investigators did not evaluate ocular tissue distribution of prednisolone.

Recently Alonso, et al. have patented CS-A and indomethacin-encapsulated PCL NPs for ocular drug delivery [98]. Specific ingredients such as chitosan and lecithin have provided positive charge to NPs and also improved stability of the formulation. Recently, Mitra and Mishra developed PB copolymer system with both NPs forming and thermosensitive gelling ability with changing the polymer block ratio [99]. These polymeric systems may be employed for treatment of chronic anterior ocular diseases.

Role of CD44 HA receptors, located on human corneal and conjunctival cells, in the uptake of hyaluronic acid-chitosan oligomer based NPs (HA-CSO NPs) have been studied. Results demonstrated that plasmid-loaded HA-CSO NPs undergo active transport mediated by CD44 HA receptors via caveolin-dependent endocytosis pathway [100]. Confocal studies demonstrated involvement of CD44 HA receptors mediated fluidic endocytosis, internalizing the plasmid-encapsulated HA-chitosan NPs [101]. Similarly Enriquez de Salamanca, et al. documented the contribution of active transport mechanism for internalization of chitosan NPs by human conjunctival epithelial cells [102]. Current research is focused on utilizing various transporters or receptors expressed on the cell surface for active targeting. Targeting specific

transporters or receptors with functionalized NPs may facilitate enhanced uptake into ocular tissues. Kompella, et al. studied the effect of surface functionalization on the uptake of NPs employing *ex vivo* bovine eye model [103]. NPs surface functionalized with deslorelin, a luteinizing hormone-releasing hormone agonist, or transferrin demonstrated 64% and 74% higher transport respectively, relative to non-functionalized NPs.

Nanosuspension

It is very difficult to formulate a poorly soluble drug in conventional ophthalmic dosage forms. Many approaches have been explored to enhance the solubility of such drugs to make them suitable for the preparation of ophthalmic formulations. A general approach for enhancing the solubility of drugs is micronization wherein the drug particle size is reduced to approximately 0.1 μm to 25 μm . However, this size range is not sufficient to increase the saturation solubility of the drug and hence its ocular bioavailability. Use of co-solvents can also improve drug solubility but they are not devoid of toxic effects. The most commonly used approach to trim down drug solubility issues is to formulate the drug into nanosuspension. Nanosuspension is a colloidal dispersion of nanosized particles. Nanosuspensions can be prepared by precipitation, pearl milling and high pressure homogenization techniques. Moreover, the solid state of the drug in nanosuspensions minimizes the problem of chemical stability of the drug as well as the physical stability of the formulation [104]. For ocular drug delivery, nanosuspension provides numerous advantages such as dose reduction, ease of eye drop formulation, increased bioadhesion and corneal penetration, reduced ocular irritation and enhanced bioavailability.

Nanosuspension is stabilized by other excipients, such as surfactants, viscosity enhancers, or charge modifiers. Topical delivery of 1% aqueous suspension and 1% oil

suspension in human subjects demonstrated higher levels of indomethacin in aqueous humor relative to oral delivery [105]. Notably, oil suspension exhibited higher aqueous humor levels (429 ng/mL) relative to aqueous suspension (198 ng/mL).

Glucocorticoids are widely prescribed in the treatment of ophthalmic inflammations. However, poor aqueous solubility poses a challenge to ophthalmic formulation development. In a recently published report Kassem, et al. have prepared and evaluated nanosuspension formulation of prednisolone, hydrocortisone, and dexamethasone for topical ocular delivery [106]. *In vivo* tissue distribution studies of the glucocorticoids nanosuspensions demonstrated significantly higher levels in anterior chamber tissues relative to solution and microcrystalline suspension of similar compounds. Moreover, investigators also reported a direct relationship between nanosuspension viscosity and ocular bioavailability. Recently, a randomized double-blind clinical study of Sophisen derivatives, 3A Ofteno (1.0% diclofenac sodium w/v), and Modusik-A Ofteno (0.1% CS-A w/v) were performed in 120 healthy volunteers [107]. Topical instillation of 3A Ofteno-diclofenac nanosuspension remained on the ocular surface for longer period with less annoying sensation and irritation. Also, Modusik-A Ofteno-CS-A nanosuspension caused significant improvement in the tear production from baseline 5 to 11 mm.

In a recent patent disclosure (WO 2006/062875) entitled, “Ophthalmic nanoparticulate formulation of a COX-2 selective inhibitor,” investigators have incorporated rofecoxib (COX-2 inhibitor) in the polystyrene nanoparticulate system for ophthalmic applications [108]. Formulation prepared with Poloxamer-407 (0.05% w/w) and HPMC remained physically stable, without any change in particle size up to 4 weeks. Drug levels in anterior chamber ocular tissues, such as the cornea (~6,610 ng·gram/tissue) and aqueous humor (~251

ng·gram/tissue) were significantly higher after topical instillation of nanosuspension. Readers are advised to read the patent for more detailed information of *in vivo* tissue distribution studies.

The efficiency of nanosuspensions in increasing the drug ocular bioavailability depends upon the intrinsic solubility of drugs in the lachrymal fluid, this intern is governed by the intrinsic dissolution rate of drugs in the lachrymal fluid which can vary due to constant inflow and outflow of lachrymal fluid. Nanosuspensions may therefore fail to give a consistent performance. However, nanosuspension formulation of drugs represents an ideal approach for ocular delivery of poorly soluble drug due to their inherent ability to increase a drug's saturation solubility [109].

Nanoemulsion

The only difference between conventional emulsion and nanoemulsion is the globule size of an internal phase. Nanoemulsion offers several advantages in ocular drug delivery, such as high capacity to dissolve both hydrophilic and lipophilic drugs, stability, improved bioavailability, and good spreadability [16]. In addition, surfactants used in formulating emulsions can also act as penetration enhancers, thereby improving drug permeability across the cornea. Emulsion based delivery of hydrophobic drugs has always remained a primary choice for the formulation researchers.

Chitosan, a cationic polymer, finds application in the field of ocular drug delivery due to its potential ability to enhance corneal drug permeability by opening tight junctions. It strongly interacts with negatively charged mucin and improves residence time on the precorneal surface. An indomethacin-embedded chitosan nanoemulsion was evaluated for its residence time and ability to deliver therapeutics into the anterior chamber of the eye [110].

Topical application of their nanoemulsion has significantly improved indomethacin levels in the cornea and aqueous humor of rabbit eyes relative to the indomethacin solution. Drug levels in the cornea and aqueous humor were about 12-fold higher for the nanoemulsion relative to solution-treated eyes.

A CS-A-loaded microemulsion, *in situ* electrolyte-triggered gelling system was developed by Gan, et al. [111] for the treatment of corneal allograft rejection. The microemulsion was dispersed in the Kelcogel (deacetylated gellan gum) solution, which provided the *in situ* gelling property when applied to the corneal surface. *In vivo* studies suggested that the microemulsion-Kelcogel system can generate ~3-fold higher levels of CS-A relative to CS-A microemulsion even at 32 h post-dosing. Moreover, concentration of CS-A in Kelco gel system treated corneas were maintained at therapeutic levels with no ocular irritation, even after 32 h. In another study, n-octenyl succinate starch was utilized to prepare the diclofenac solution and emulsion, and these formulations exhibit improved permeability across the excised porcine cornea compared to the commercial product Voltaren Ophtha [112]. An indomethacin nanoemulsion prepared with amphoteric surfactant (lauroamphodiacetate) improved corneal permeability by 3.8 times relative to a marketed product (Indocollyre) [113].

In a recently published patent, CS-A was successfully incorporated in a nanoemulsion, utilizing a positively charged polar lipid, such as stearylamine [114]. Mean droplet size of the formulation was within the range of 150-250 nm, with zeta potentials of 34-45 mV. Gan, et al. have recently patented a nanoemulsion-based *in situ* gelling system for topical ocular delivery of flurbiprofen [115]. A CS-A-loaded nanoemulsion (NOVA22007) containing cationic lipid formulation has just completed Phase III studies for dry eye [116]. The same emulsion was

applied for vernal keratoconjunctivitis treatment and this study has recently completed phase II/III studies [117].

Nanomicelles

Polymeric micelles are self-assembling colloidal systems comprised of block or graft amphiphilic copolymers and surface-active agents [118]. Development of ophthalmic drug delivery systems with micelles is very promising, particularly because of their advantages such as high thermodynamic and kinetic stability, ability to sustain the release, and the improvement of drug solubility and permeability across the ocular tissues [119]. Moreover, micelles can be functionalized with endogenous molecules for targeted ocular delivery. Normally, particle size of the micelles ranges from 5 to 50 nm [118].

Recently, a rapamycin and corticosteroid-loaded aqueous nanomicellar formulation was developed and patented (WO2010/144194) by Mitra, *et al.* [120]. Nanomicelles were prepared with 1 to 7% w/v of Vitamin E tocopherol PEG succinate (vitamin E TPGS, HLB-10) and 1 to 3% w/v of octoxynol-40 (HLB-13). Vitamin-E TPGS helped to increase the solubility of the poorly soluble drugs, while octoxynol-40 reduced ocular discomfort and also provided extra stability with higher optical clarity to the nanomicellar formulation. Investigators suggested that any buffer system with adjusted osmolality and physiological pH could be used to prepare an external aqueous phase. Rapamycin has very low aqueous solubility (2.6 µg/mL). However, after preparation of nanomicelles, its solubility improved to 2 mg/mL (~1000 fold). An average diameter of the nanomicelles was around 25 nm. Nanomicellar formulation of ¹⁴C rapamycin was instilled in rabbit eyes, and 60 min post-dosing ocular distribution of the drug was determined by liquid scintillation counter. Noticeably, a higher concentration of ¹⁴C rapamycin was observed in the choroid/retina (~360

ng/g), while very negligible radioactivity was found in the lens, aqueous humor and vitreous humor. Higher accumulations of rapamycin in the posterior segment of the eye was believed to be a result of the smaller mean diameter of nanomicelles. Optically clear and thermodynamically stable nanomicellar formulation could be a promising innovation for the non-invasive treatment of the posterior segment diseases.

In another disclosure (US 2009/0092665), Mitra and co-inventors developed mixed micellar formulation of calcineurin inhibitors (voclosporin) and mTOR inhibitors for ophthalmic applications [121]. Various concentrations of Vitamin-E TPGS and octoxynol-40 were used to prepare nanomicelles. Dilution studies were performed to evaluate the stability of voclosporin-loaded mixed micelles (0.2 wt%), and micellar stability was confirmed up to a 20 fold dilution in saline. In addition, results have demonstrated that micelles dissociated at around 44 °C and the formulation was re-stabilized well within 8 min. Moreover, formulation remained stable in LDPE, polypropylene and polyvinylchloride containers at room temperature for 48 h. The particle size of the voclosporin-loaded (0.2 wt%) nanomicelles was between 13-33 nm. *In vivo* ocular tissue distribution studies were performed in two groups (single dose and 7 days repeat dose) of rabbits after topical application of mixed micellar formulation-loaded with ¹⁴C-radio labeled voclosporin. Almost 1.5-2.5 fold higher C_{max} were observed in all ocular tissues (cornea, aqueous humor, sclera, upper eyelid, lower eyelid, retina/choroid, lacrimal gland, optic nerve and lower bulbar conjunctiva) of a group with 7 days repeated dosing over to the single dose group. No signs or serious symptoms of irritation were observed in any rabbits after a tolerability and tissue irritability study. According to the results discussed in this disclosure, nanomicellar formulation seems to be very promising in the treatment of anterior and/or posterior segment ocular diseases including AMD and DME.

Results discussed in these patent applications explained that the nanomicellar drug delivery systems can effectively change the course of ocular treatment.

Cubosomes

Novel dexamethasone-embedded self-assembled liquid crystalline particles (cubosomes) were developed and investigated for precorneal retention and ocular tissue distribution [122]. The apparent permeability coefficient of dexamethasone, delivered in cubosomes was 3.5–4.5 times higher than dexamethasone eye drops. In addition, precorneal retention of cubosomes was significantly longer than carbopol gel or solution. *In vivo* microdialysis studies were performed to evaluate pharmacokinetics of dexamethasone in aqueous humor. Delivery of cubosomes exhibited 1.8-fold and 8-fold higher AUC 0/240min of dexamethasone in aqueous humor relative to eye drops and suspension, respectively. Moreover, tissue integrity and corneal structure indicated good biocompatibility with the cubosome formulation.

Ocular implants and inserts

Intraocular implants have been studied in order to control and sustain the drug delivery in the treatment of proliferative vitreoretinopathy (PVR), cytomegalovirus (CMV) retinitis, glaucoma, endophthalmitis, and posterior capsule opacification. Understanding of physicochemical properties of the active compound and release kinetics helps to design specific ocular implantable drug delivery systems. Ocular implants can be classified in two categories according to their *in vivo* degradability i.e., non-biodegradable implants and biodegradable implants.

Non-biodegradable ocular implants

Since the early in 70s, non-biodegradable implants have offered the advantages of controlled and sustained release of active drugs with minimal host responses. Nowadays, new non-biodegradable polymers (e.g., polyvinyl alcohol (PVA), ethylene vinyl acetate (EVA), and polysulfone capillary fiber (PCF)) have been designed to ensure sustained release for longer period of time with higher biocompatibility [123]. Intraocular drug release kinetics is controlled by the rate of erosion and spontaneous degradation of these polymers. Diffusion of fluid (water) inside the polymer structure dissolves the drug pellet and generates a saturated drug solution inside the implant. Saturated drug solution diffuses out from the implant and provides nearly zero-order drug release [124]. Lack of initial burst release makes non-biodegradable implants superior to implants constructed from biodegradable polymers. Complications such as retinal detachment, endophthalmitis, vitreous hemorrhage, formation of tenacious epiretinal membranes, and cystoids macular edema have been observed with the use of non-biodegradable polymeric devices [125]. Moreover, implantation of this device requires surgical treatment and necessitates surgery to remove the empty device.

Sanborn and colleagues have employed non-biodegradable implants for the ocular delivery of ganciclovir in the treatment of CMV retinitis [126]. These implants were reservoir type devices, composed of drug and coating polymers such as PVA and EVA. PVA is a permeable polymer, which acts as a framework and controls release of ganciclovir. In contrast, EVA acts as an impermeable polymer, which limits the practical surface area of the device and hence, sustains drug release. Implication of both polymers in structure design enables zero-order controlled drug release.

Vitrasert, a commercially available implant of ganciclovir, is relatively large and requires 4-5 mm of sclerotomy at pars plana for implantation [127]. Moreover, the device is made from non-biodegradable polymers and, needs to be removed after 5-8 months for the implantation of another device, or because of unwanted complications such as retinal detachment related to the implant, or severe inflammation. Almost 12% of eye complications (endophthalmitis, retinal detachment, cystoids macular edema, formation of tenacious epiretinal membranes and vitreous hemorrhage) have been observed after implantation of these devices.

To overcome these problems, a betamethasone-loaded intrascleral implant (4 mm in diameter, 1 mm in thickness and 4 mg in weight) composed of PVA and EVA has been developed and evaluated [128]. Results demonstrated that the disc was able to maintain therapeutic levels of betamethasone up to 4 weeks without an adverse burst release of drug. No substantial adverse reactions were observed after histological and electroretinographical evaluations. Intrascleral implantation does not require perforation of the eye wall, hence this system may reduce complications associated with other implanted devices.

The FDA has approved fluocinolone-loaded Retisert in April 2005 in the treatment of chronic non-infectious uveitis [127]. A total of 36 eyes with non-infectious posterior uveitis, which had an average of 2.5 episodes of recurrence annually, were treated with these implants. After implantation of fluocinolone-loaded implants, no recurrence was observed up to two years [129]. Pearson, et al. have prepared Cs-A-loaded PVA-EVA device for the controlled intravitreal delivery of Cs-A [130]. A 500 ng/mL of Cs-A concentrations was observed for more than 6 months in rabbit and cynomolgus monkey eyes. However, complications such as opacity of lens were observed in the implanted rabbit eyes. A PVA-EVA device loaded with

both Cs-A and dexamethasone was prepared, and examined in the treatment of PVR and uveitis [131].

Biodegradable ocular implants

Biodegradable polymers generate non-toxic degradation products after *in vivo* enzymatic degradation that can easily eliminate from the body without any side effects. Hence, biodegradable implants are not required to be removed after implantation. It is more difficult to achieve optimal drug release through biodegradable implants when compared to the reservoir type of non-biodegradable implants. The main two categories of biodegradable implants are monolithic and binding types. Monolithic types of implants are made by solidifying the homogenous physical mixture of the drug and polymer. The procedure to produce this kind of implant involves heating of drug, and hence thermolabile drugs such as proteins, polypeptides or nucleic acids are difficult to incorporate in monolithic implants. However, binding type of implants have showed suitability for the delivery of biologically active molecules. Biologically active molecules make chemical bond or a polyion complex with polymers, which finally undergoes enzymatic degradation and gets released from the polymer matrix. Biodegradable polymers can be made into sheets, plugs, rods, pellets and discs, and can be implanted into intrascleral or peribulbar, anterior chamber, vitreous cavity, or through the pars plana [132]. An undesirable final burst release is the major drawback of the controlled release system composed of biodegradable polymers.

Scleral implants of ganciclovir were successfully made using various blends of PLA (DL isomer) and evaluated in the treatment of CMV retinitis in pigmented rabbit eyes. Implants made up from physical mixture of 80% of PLA (70 kDa) and 20% of PLA (5 kDa) were able to maintain therapeutic levels of ganciclovir up to 6 months without any significant burst

release [133]. Fluorouracil-loaded biodegradable intravitreal implants were prepared from PLGA and evaluated in the treatment of tractional retinal detachment due to PVR [134]. The sustained therapeutic concentration of drug was observed to be above 0.3 $\mu\text{g/mL}$ up to 21 days however, 89% of the rabbit eyes were suffered retinal detachment after treatment. Zhou, et al. have investigated multiple drug delivery through implant in the treatment of PVR [135]. Three cylindrical parts (triamcinolone, human recombinant tissue plasminogen activator (tPA) and 5-fluorouridine) containing PLGA implant (0.8 mm in diameter, 7 mm long) have been prepared and evaluated. This implant exhibited release of 5-fluorouridine and triamcinolone at the maximal rate of 1 $\mu\text{g/day}$ over 4 weeks and 10 - 190 $\mu\text{g/day}$ over 2 weeks, respectively. Moreover, the portion of PLGA coated tPA started release after 2 days at the rate of 0.2 - 0.5 $\mu\text{g/day}$ for 2 weeks, which may minimize the risk of post-operative bleeding. These types of implants unwrap the feasibility of co-delivery of three different drugs or drugs with different release profiles.

Xie, et al. have examined heparin incorporated PLGA implants (HPI) in the treatment of posterior capsular opacification (PCO) [136]. Heparin levels in blood and aqueous humor were investigated after subconjunctival implantation of HPI, posterior chamber implantation of HPI and instillation of 5% topical heparin drops. Implantation of heparin delivery systems in posterior chamber demonstrated significantly higher heparin levels in aqueous humor for longer period of time (12 weeks). A proline analog (*cis*-4-hydroxyproline (CHP)), inhibits collagen secretion in proliferative vitreoretinopathy (PVR). Yasukawa and colleagues have incorporated CHP in different blends of PLGA (65/35 and 50/50) for the sustained delivery to rabbit eyes [137]. The PLGA 65/35 implants have decreased the incidence of PVR from 89%

to 56% but the PLGA 50/50 implant did not show any significant effect. On the other side, the application of both implants together revealed synergistic inhibition of PVR.

Natural polymers such as gelatin, collagen and alginates have also been studied for the preparation of ocular implants. Koelwel, et al. have prepared and investigated epidermal growth factor (EGF) incorporated alginate inserts in 18 test volunteers in the treatment of keratoconjunctivitis sicca (KCS) [138]. Alginate inserts with higher amount of guluronic acid (G block) were able to sustain the release of EGF for much longer period of time. Dried gelatin hydrogel prepared by cross-linking of acidic gelatin was soaked in basic fibroblast growth factor (bFGF) solution with different concentrations and implanted into rabbit corneal pocket [139]. The inserts with 50 ng or more doses exhibited dose dependent corneal angiogenesis started from day 3 to day 4, while inserts with 20 ng or below were devoid of this side effect.

Moreover, effective sustained delivery of antimetabolic [140, 141], antifungal [142], immunosuppressive agents [143] and steroids [144, 145] have been studied using biodegradable ocular implants. Hence, the employment of implants for the ocular delivery of small molecules (hydrophilic and hydrophobic) and macromolecules is a viable approach.

Microneedles

The concept of microneedles was proposed in early 1970s but practically this method not demonstrated until 1990s when the microelectronic industries provided tools to fabricate such small devices. Application of an array of microneedles creates large transport pathways, larger than the molecular dimensions, and thus facilitates the transport of macromolecules (peptides such as insulin, desmopressin and human growth factors), supramolecular complexes, NPs, microparticles and liposomes [146]. Although micro-scale holes in the skin are safer than intraocular injections, safety studies are needed to be performed. Microneedle

based drug delivery is widely studied in transdermal applications, but recently, several studies have been performed to evaluate its application in ocular drug delivery. Mainly, two approaches have been studied for the ocular application of microneedles, solid coated microneedles [147] and hollow microneedles [148]. In the first approach, Jiang, et al. have coated microneedle with five different model drugs (sulforhodamine, sodium fluorescein, bovine serum albumin (BSA), plasmid DNA, and pilocarpine) for intrascleral and intracorneal application to evaluate different model drugs with different physicochemical properties [147]. Microneedles coated with sulforhodamine and BSA demonstrated excellent penetration into human cadaveric sclera and rapid dissolution of coated model drugs. Moreover, intracorneal delivery of sodium fluorescein exhibited higher *in vivo* levels when compared to the levels achieved after topical application of same dose. The same study using pilocarpine in rabbit eyes has also revealed some promising results.

Moreover, researchers have evaluated the applicability of hollow microneedles for the delivery of solutions containing soluble molecules, NPs, and microparticles into sclera in a minimally invasive manner [148]. The results described successful intrascleral delivery of solutions and fluorescence tagged NPs with insignificant effects of scleral thickness and infusion pressure. However, investigators have reported that the presence of scleral glycosaminoglycans and collagen fibers are the rate limiting factors for the microneedle based intrascleral microparticles delivery.

These studies exhibited the versatility of microneedles' applications in terms of drug selection (coated microneedles) as well as formulation delivery tool (hollow microneedles). Moreover, these targeted delivery systems are less invasive, less painful and more patient compliant.

Biodegradable polymers [149]

Biodegradable polymers have numerous applications in the field of ocular drug delivery and can be classified as natural or synthetic. Applications of PGA as suture material in the late 1960 provided an impetus for the design and development of novel synthetic biodegradable polymers. Synthetic biodegradable polymers can be tailored in various compositions and molecular weights. The molecular weight or composition regulates the degradation of polymer where the main weight loss takes place due to chain cleavage. Many researchers have investigated several types of biodegradable polymers and studied their applicability for the development sustained ocular formulations. Structures of various biodegradable polymers are depicted in Figure 1.4.

Polyalkylcyanoacrylates (PACA)

Polyalkylcyanoacrylates (PACA) belong to a class of acrylate polymers synthesized from alkylcyanoacrylic monomers through anionic polymerization. The faster degradation rate of PACA was attributed to the unique instability of a carbon-carbon sigma bond and presence of electron withdrawing neighboring groups. It has shown remarkable applicability as surgical glue and skin adhesive. PACA was also explored for the development of NPs. The PACA degradation rate varies from hours to days depends on the length of alkyl side chain. For example, PACA having shorter alkyl chain length such as polymethylcyanoacrylate degrades in few hours whereas higher alkyl chain length derivatives such as octyl and isobutyl cyanoacrylates degrade slowly. NPs composed of PACA are advantageous in terms of fabrication and application in drug delivery [150].

Polyanhydrides

Numerous investigations have elucidated the role of polyanhydrides (POA) for ocular drug delivery applications. These polymers exhibit faster degradation and limited mechanical strength, which make them an ideal candidate for fabrication of sustained release devices. Low molecular weight polyanhydrides were synthesized through dehydrative coupling and dehydrochlorination whereas melt polycondensation polymerization was employed for synthesis of high molecular weight polymers. The degradation rate of polyanhydrides can be easily modulated by changing the polymer composition and depends on the crystallinity and hydrophilicity of the final polymer. These polymers undergo surface erosion and generate monomeric acids that are non-toxic. Homo-polyanhydrides have limited application in controlled drug delivery due to their crystalline nature. In contrast, copolymers such as poly((carboxyphenoxy)propane–sebacic acid (PCPP-SA) demonstrated controlled degradation rates [151]. This polymer was approved by the FDA for human applications for the delivery of carmustine in the treatment of brain cancer [152]. Other approaches based on aromatic comonomers composed of hydrophobic aliphatic linear fatty acids were also investigated for drug delivery applications [153].

Polyesters

Polyesters are biodegradable polymers having short aliphatic, ester-linked backbones. These classes of polymers are generally produced by either ring-opening or condensation polymerization. Ring-opening polymerization is preferred over condensation reaction to produce high molecular weight polyesters. Homo- or co-polymers of cyclic lactones and anhydrides having narrow molecular weight distribution can be produced via ring-opening polymerization. The molecular weight of the final polymer can be controlled by varying the

ratio of monomers. The molecular weight of the polyesters regulates the hydrolytic cleavage that follows bulk erosion kinetics to produce metabolic products which are eliminated through normal metabolic pathways [154]. The hydrolytic degradation rate of the polymers can be altered by varying the molecular weight, crystallinity and structure of the polymeric chain. Among polyesters, poly- α -hydroxyesters are the most broadly investigated class of polymers for ocular drug delivery applications; this includes PGA, PLA and their copolymers.

Polycaprolactone (PCL)

PCL is a semicrystalline polymer synthesized by ring-opening polymerization of ϵ -caprolactone. It has a glass transition temperature of $-60\text{ }^{\circ}\text{C}$ and a melting temperature in the range of 59 to $64\text{ }^{\circ}\text{C}$. PCL was investigated for long term delivery due to higher permeability to many drugs, excellent biocompatibility and extremely slow hydrolytic cleavage of polyester backbone. The PCL based Capronor[®] implant was developed for controlled delivery of levonorgestrel. It has a low tensile strength of 23 MPa and an extremely high elongation factors, more than 700% . Numerous investigations were attempted to improve the slower degradation of PCL. Copolymers of ϵ -caprolactone with lactide or glycolide exhibits remarkably better degradation profile.

Polyglycolide (PGA)

PGA is a relatively hydrophilic polymer compared to other polyesters with high crystallinity and low solubility in organic solvents. The low solubility in organic solvent is attributed to its higher tensile modulus. It has a high melting point of $225\text{ }^{\circ}\text{C}$ and glass transition temperature of $36\text{ }^{\circ}\text{C}$. It has a comparatively faster degradation rate than other polyesters and generates glycine upon degradation, which eventually eliminates through the citric acid cycle. Major losses in the mechanical strength of PGA usually take place in one to two months and

it completely degrades *in vivo* within six to twelve months. PGA was initially explored for developing sutures because of their fiber-forming properties and excellent mechanical strength. However, it has limited role in ocular drug delivery due to its faster degradation rate and higher crystallinity. PGA implants can be easily fabricated by widely applicable processing techniques such as solvent casting, compression and extrusion techniques. Processing technique utilized for the production of implant regulates the degradation properties of implant [155].

Poly(lactic acid) (PLA)

PLA is comparatively more hydrophobic than PGA due to the presence of an additional methyl group. It is chiral in nature because of the structure of lactic acid and commonly exists in three isomeric forms the D (-), L (+) and racemic (D, L) lactide. The crystalline nature of PLA depends upon the isomeric forms and molecular weight of the polymer. PLA (L) is crystalline in nature and hydrolyzed through normal metabolic pathway due to presence of naturally occurring isomer (L-lactide). It has a melting point of 175 °C and glass transition temperature of 60 to 65 °C. It also possesses a good tensile strength of 50-70 MPa and high modulus of 4.8 GPa. On the other hand, PLA (DL) is amorphous in nature due to presence of the racemic mixture. It has glass transition temperature of 55 to 60 °C and comparatively faster degradation rate than PLLA. All isomeric forms of PLA follow bulk erosion kinetics and generate lactic acid upon hydrolytic cleavage [116]. Researchers have often utilized PLA for ocular drug delivery applications.

Poly (lactide-co-glycolide) (PLGA)

Poly (lactide-co-glycolide), commonly known as PLGA is obtained by the copolymerization of lactide and glycolide. This copolymer is hydrolytically less stable than

the homopolymers, PLA or PGA. Extensive research on a full range of these copolymers suggests their implication in drug delivery. These copolymers are divided into two main compositions, comprised of lactide and glycolide. PLGA follows bulk erosion kinetics, and its degradation depends on molecular weight and lactide to glycolide ratio. As the ratio of glycolide in copolymer decreases, the hydrolytic degradation rate decreases. The intermediate PLGA, i.e. 50:50, hydrolyses faster than PLGA 75:25 and PLGA 85:15. PLGA copolymers are FDA approved for human applications because of the excellent biocompatibility and controlled degradation profiles [117]. PLGA is negatively charged and thus has a non-mucoadhesive nature.

Polyorthoesters

Polyorthoesters (POE) are hydrophobic polymers composed of a hydrolytically unstable polyester linkage. However, they exhibit slower degradation due to surface erosion. This degradation characteristic is ideal for designing sustained release devices. In this polymer the degradation profile can be easily adjusted by employing different diols for polymerization [156]. The POE group is hydrolytically unstable in acidic conditions and requires basic additives to inhibit autocatalysis. The first generation of POE was developed by the ALZA Corporation. It was synthesized by the transesterification reaction of diol with diethoxy tetrahydrofuran [157]. Degradation profile of POE II can be easily altered by incorporation of acidic additives such as adipic acid. POE III upon hydrolysis generates diol and pentaerythriol dipropionate, which subsequently generate propionic acid and pentaerythriol. This class of polymers is biocompatible and follows pH dependent degradation behavior. They do not require organic solvents for the incorporation of drugs due to their semisolid nature. However, there are difficulties in scale up processes that limit their application in drug delivery.

Modification of second generation polyester (POE II) with smaller lactic or glycolic acid chains led to the development of POE IV. This polymer upon hydrolysis liberates acids which further promotes the polymer degradation. The physical form and degradation rate of the polymer can be easily varied by changing diols and acid segment respectively. POE IV has demonstrated good biocompatibility for controlled delivery applications [158].

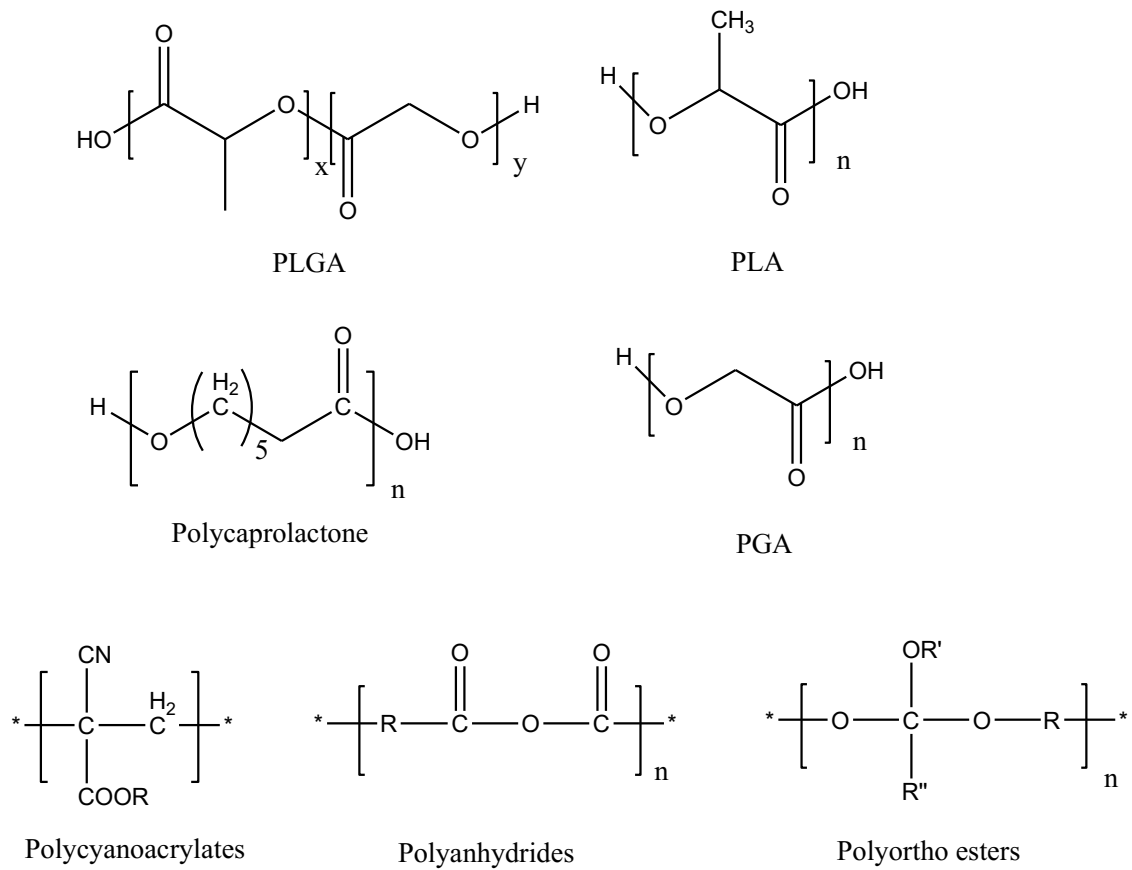


Figure 1.4: Structure of biodegradable polymers

CHAPTER 2

INTRODUCTION

Statement of the problem

The retinal pigment epithelium (RPE), macular region, choriocapillaries and Bruch's membrane are the primary target sites of vision threatening diseases such as dry and wet AMD, proliferative vitreoretinopathy, DR and DME [159]. Out of all these diseases, wet AMD is believed to be a major cause for severe central vision loss or legal blindness in the individuals 65 years or older [160]. Elevated levels of vascular endothelial growth factor (VEGF) are reported in choroidal neovascularization (CNV), and it is a primary reason for the development of wet AMD. Occurrence of CNV is followed by leakage of fluid and blood into the subretinal space and subsequent scar formation, which eventually leads to irreversible vision loss [161]. Therefore, anti-VEGF antibodies such as bevacizumab and ranibizumab are recommended in the treatment of wet AMD [162]. Bevacizumab (149 kDa) is a full-length recombinant humanized murine monoclonal antibody (rhum-anti-VEGF antibody) specific to all isoforms of VEGF [163]. It specifically binds to the extracellular VEGF and blocks the angiogenic action of VEGF. At a dose of 1 mg or 1.25 mg [164], it has shown reduction in the macular thickness, reduction in angiogenic leakage, and improvement in visual acuity of neovascular AMD patients [165, 166]. Ranibizumab is a 48 kDa Fab-fragment of a humanized murine anti-VEGF antibody active against all isomers of VEGF. It is one-third the size of bevacizumab and use the same molecular mechanism to block the VEGF [167]. Due to short half-life, current anti-VEGF therapy with bevacizumab or ranibizumab requires frequent intravitreal injection to maintain therapeutic levels at retina/choroid. However, treatment with frequent intravitreal

administrations is associated with many potential complications like endophthalmitis, retinal detachment, retinal hemorrhage, and patient non-compliance [168].

Therefore, there is a need to develop a novel formulation for the sustained delivery of macromolecules (e.g., antibodies). Sustained delivery systems such as NPs may offer an advantage of higher residence time for macromolecules at the site of absorption. Drug encapsulation within NPs (1-1000 nm) can be achieved with most commonly used biodegradable and biocompatible polymers such as PLA, PCL, and PLGA. However, *in vivo* degradation of PLA and PLGA NPs produces high molar masses of lactic acid and glycolic acid, which reduces the pH in microenvironment. This pH change leads to the higher hydrolytic degradation of protein therapeutics, and also causes tissue irritation and toxicity [169]. In addition, rapid degradation of PGA or PLGA based formulation results in significantly higher burst release followed by faster rate of release [170, 171]. On the other hand, the rate of degradation for PLA or PCL based copolymers are very slow. Poor degradation of PCL based formulation leads to accumulation of formulation (without drug) in limited vitreous space, which is highly unacceptable.

Hypothesis

There is a need to develop novel polymeric system which can sustain the release of macromolecules and also improves the stability of the same. Therefore, preparation of novel biodegradable PB copolymers, and their applications for the development of macromolecules-loaded NPs and thermosensitive gel have been proposed in this research protocol. Various macromolecules such as catalase (237 kDa), IgG (150 kDa), IgG-Fab (48 kDa), bovine serum albumin (BSA) (66 kDa), lysozyme (14.7 kDa), insulin (5.8 kDa), octreotide (1 kDa), and bevacizumab (149 kDa) loaded formulations have been investigated in this research work.

The PB copolymers are comprised of FDA approved polymer blocks such as PEG, PCL and a small molar mass of PLA/PGA. Tailoring of the molecular weight or interplay of the sequence of blocks can provide different hydrophilic or hydrophobic polymers. The presence of PEG in the PB copolymers will allow improving the physical stability of NP formulation. In addition, it will also help to enhance the stability of peptide/protein molecules by avoiding the direct interaction between hydrophobic segments of polymers with peptide/protein. PEG will also decrease the direct contact of protein therapeutics with the organic solvents during the NP preparation. PCL is the second important block of PB copolymers. In corporation of highly crystalline PCL block in the backbone of PB copolymers will significantly improve DL and drug EE of PB NPs. Furthermore, slower degradation of PCL blocks will sustain the drug release for significant period of time. PB copolymers are also composed of small molar mass of PLA/PGA. Incorporation of PLA/PGA in PB copolymers significantly reduces crystallinity of PCL which eventually accelerates hydrolytic degradation of PCL. Alteration of polymer degradation rate will shift the drug release kinetics from diffusion controlled to degradation controlled. Hence, by these structural modifications in PB copolymers, nearly zero-order drug release can be easily achieved. The second important reason behind designing of PB copolymer is to minimize the amount of lactic acid produced upon *in vivo* degradation. It is anticipated that reduction of the PLA molar mass in PB copolymers will improve the stability of encapsulated protein molecules, and it will also reduce possible tissue irritation and toxicity.

This novel approach will provide the entire range of polymers with different hydrophilicity-hydrophobicity index. This enormous advantage will allow us to select a unique composition of polymer which will be best suited for a respective therapeutic agent. Furthermore, reduction in the molecular weight and/or change in the polymer block

arrangement will allow us to prepare PB copolymer with totally different and unique physicochemical property i.e., temperature sensitivity. These new compositions will be water soluble at room temperature but upon increase in temperature, they will transform to solid hydrogel.

Catalase (237 kDa), IgG (150 kDa), IgG-Fab (48 kDa), BSA (66 kDa), lysozyme (14.7 kDa), insulin (5.8 kDa), and octreotide (1 kDa) will be used as model proteins for the optimization of formulation components and processes. PB copolymers will be utilized for the preparation of NPs and thermosensitive gel. Many investigators have reported significant burst release of therapeutic agents (peptides/proteins) when delivered from NPs or hydrogel systems [170, 171]. This problem may be eliminated by introducing dual approach or composite formulations, in which drug-loaded NPs are suspended in thermosensitive gel. This composite approach may minimize the burst release effect and provide nearly zero-order drug release by offering longer drug diffusion pathway across the system.

Subconjunctival/intravitreal administration of such a novel formulation may result in a prolong duration of action (approximately 6 months) and thereby eliminate the need for repeated administration. It is anticipated that this formulation will provide higher patient compliance with reduced side effects. This approach may act as a platform for ocular delivery of other therapeutic macromolecules such as siRNA, aptamers, peptides and large proteins. Therefore, the broad objective of this research is to develop novel PB copolymer based sustained delivery systems of various peptide/protein therapeutics for the treatment of posterior segment diseases.

Objectives

Objectives of this research are as follow,

- 1) To synthesize and characterize various triblock (TB) and PB copolymers for the preparation of thermosensitive hydrogels. In addition, the effects of various parameters including molecular weight, arrangement of blocks and hydrophobicity on sol-gel transition, viscosity and *in vitro* drug release will be investigated. The possible mechanism of sol-gel transition will also be evaluated.
- 2) To synthesize and characterize various TB and PB copolymers for the preparation of IgG-loaded PB NPs. The effect of molecular weight, hydrophobicity and isomerism on EE, loading and *in vitro* release of IgG will be investigated.
- 3) To synthesize and characterize various PB copolymers for the preparation of protein-encapsulated NPs. More importantly, the effect of hydrophobicity of PB copolymer on the encapsulation of different proteins (IgG, BSA and Bevacizumab) will be investigated. The effect of size and hydrodynamic diameter of protein on various formulation parameters will also be studied. The stability of released protein will be investigated by chemical and biological assays. Approaches to composite formulations (NP suspended in thermosensitive gel) to achieve zero order drug release will be investigated.
- 4) In order to achieve maximum DL and zero-order drug release, various formulation process parameters including addition of NaCl will be optimized.
- 5) *In vitro* and *in vivo* polymer tolerability studies will be performed.

CHAPTER 3

NOVEL THERMOSENSITIVE PENTABLOCK (PB) COPOLYMERS FOR
SUSTAINED DELIVERY OF PROTEINS IN THE TREATMENT OF POSTERIOR
SEGMENT DISEASES

Rationale

Bevacizumab, a chimeric anti-VEGF antibody (149 kDa) approved for treatment of colon cancer is being used off-label for the treatment of ocular neovascularization. Intravitreal injection of bevacizumab has caused reduction in macular thickness, angiogenic leakage and improvement of visual acuity in neovascular AMD patients [165, 166]. However, due to the chronic nature of ocular diseases and shorter intravitreal half-life of this anti-VEGF antibody, frequent intravitreal injections are indicated to maintain therapeutic activity in the retina and choroid. Frequent administrations are inconvenient and cause potential complications such as endophthalmitis, retinal detachment, retinal hemorrhage, and more importantly, patient non-compliance [172-174]. Since the wide application of protein therapeutics in many treatments including ophthalmology, tumor biology and immunology, pharmaceutical scientists are more focused towards the development of novel delivery strategies utilizing current therapeutics rather than on development of new drugs. Development of sustained release formulations of protein therapeutics can reduce the frequency of intravitreal injections and eventually eliminate potential complications. This approach may lower cost of treatment and improve patient compliance.

Recently, various gel forming polymers, sensitive to external environmental stimuli such as pH, temperature, electric field and ionic concentrations have been investigated as sustained delivery systems [175]. In particular, temperature sensitive biodegradable polymers

composed of hydrophilic and hydrophobic blocks have drawn more attention. Injectable thermosensitive hydrogel remains in solution phase during injection and as soon as it is exposed to body temperature, it immediately phase transforms into a solid hydrogel polymer matrix. The hydrogel matrix protects protein therapeutics from enzymatic degradation and provides sustained release for a longer period of time, eliminating repeated monthly injections. Various biodegradable copolymers composed of hydrophobic polymer blocks including PCL, PLA, polyglycolide (PGA) and PLGA, and hydrophilic polymer blocks, in particular PEG, have been investigated for their thermosensitive behavior [176-178]. Adjustment of the hydrophilic-hydrophobic balance in the block copolymer backbone allows manipulation of the sol-gel transition curve.

Many researchers have synthesized and investigated thermosensitive TB copolymers (A-B-A or B-A-B) composed of PLA/PCL/PLGA blocks (A) and PEG block (B) for their applicability in the development of sustained delivery formulations [176, 179]. However, applicability of PCL based TB copolymers (A-B-A or B-A-B) as thermosensitive gels is not very suitable due to their poor biodegradability and faster drug release [180]. Slow degradation of PCL is attributed to its highly crystalline nature [181]. Degradation of PLGA/PLA/PGA produces lactic acid and glycolic acid, and significantly reduces pH in the microenvironment and hence triggers the degradation of protein therapeutics [182]. Moreover, PLGA also induces structural changes in protein molecules by the process of acylation [182, 183]. Therefore, an alternative development of novel polymeric system which reduces the molar mass of lactic acid/glycolic acid upon degradation becomes pivotal. It is also crucial to establish coordination between degradation profile and drug release profile. To date, very limited studies utilizing

thermosensitive hydrogels have been established for the treatment of posterior segment neovascular diseases.

In the present study, we have synthesized and evaluated various novel PB copolymer based thermosensitive biodegradable hydrogels. PB copolymers are composed of FDA approved polymer blocks including PEG, PCL and PLA. This study has addressed four important aspects ocular sustained release formulation i.e., synthesis and structural characterization of PCL-PEG-PCL, PLA-PCL-PEG-PCL-PLA, and PEG-PCL-PLA-PCL-PEG block copolymers, the effect of molecular weight and block arrangements of polymers on sol-gel transition behavior, the *in vitro* cytotoxicity/biocompatibility and the *in vitro* release of IgG (a model full length antibody similar to bevacizumab, 150 kDa). Moreover, a possible gelation mechanism of PB copolymers has been hypothesized and supportive studies are discussed.

Materials and methods

Materials

PEG (1000, 1500, 2000 and 4000), monomethoxy PEG (550), L-lactide, ϵ -caprolactone, stannous octoate, coumarin-6 and lipopolysaccharide were procured from Sigma-Aldrich (St. Louis). Hexamethylene diisocyanate (HMDI) and Micro-BCATM were obtained from Fisher scientific. Mouse TNF- α , IL-6 and IL-1 β (Ready-Set-Go) ELISA kits were purchased from eBioscience Inc. Lactate dehydrogenase estimation kit and CellTiter 96[®] AQueous non-radioactive cell proliferation assay (MTS) kit were obtained from Takara Bio Inc. and Promega Corp., respectively. All other reagents utilized in this study were of analytical grade.

Methods

Synthesis of TB copolymers with B-A-B (PCL-PEG-PCL) and PB copolymers with C-B-A-B-C (PLA-PCL-PEG-PCL-PLA) block arrangements

The PCL-PEG-PCL TB copolymers were synthesized by ring-opening bulk copolymerization of ϵ -caprolactone [176]. PEG was utilized as macroinitiator and stannous octoate as a catalyst. Briefly, before polymerization, PEG (1, 1.5, 2 and 4 kDa) were vacuum dried for 4 h. A predetermined amount of PEG (4.0 g) and ϵ -caprolactone (8.0 g) were added in the round bottom flask. The polymer melt was degassed under vacuum for 30 min at 130 °C. The flask was then purged with nitrogen gas, followed by addition of stannous octoate (0.5 wt%). The reaction was carried out for 24 h at 130 °C. The resulting polymer was then dissolved in dichloromethane and precipitated by addition of cold diethyl ether. Precipitate was centrifuged and vacuum-dried to remove residual solvents. Purified polymers were stored at -20 °C. A schematic synthesis scheme is presented in Figure 3.1a.

Synthesis of PB copolymers with C-B-A-B-C (PLA-PCL-PEG-PCL-PLA) block arrangements

TB copolymer (PCL₁₂₅₀-PEG₁₅₀₀-PCL₁₂₅₀, TB-5) was synthesized as per method described in earlier section for preparation of PB copolymers A (PB-1), B (PB-2) and C (PB-3) (Table 3.1). To synthesize PB copolymers, predetermined amount of TB-5 and L-lactide were added in a round bottom flask and degassed under vacuum for 30 min at 130 °C. The flask was then purged with nitrogen gas and followed by addition of stannous octoate (0.5 wt%). The reaction was carried out at 130 °C for 24 h. The resulting polymers were purified and stored in a similar manner as described earlier.

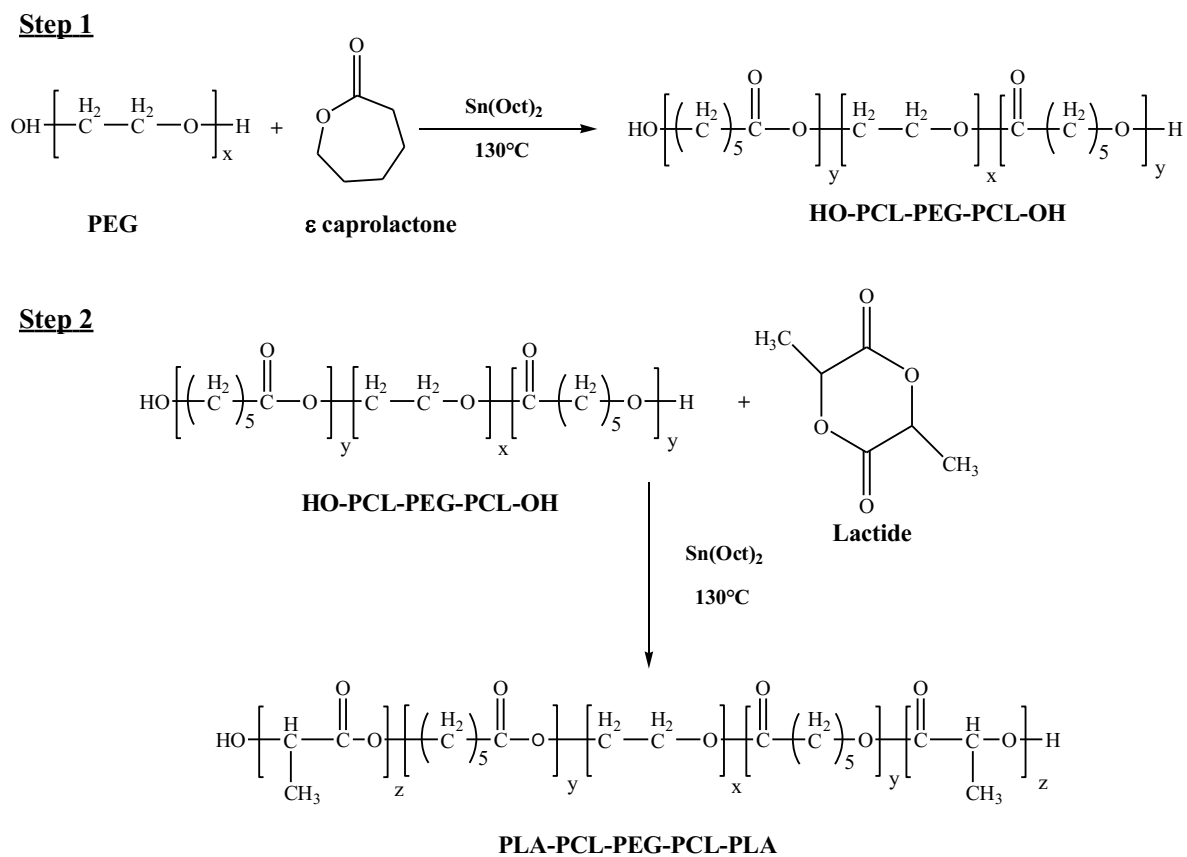
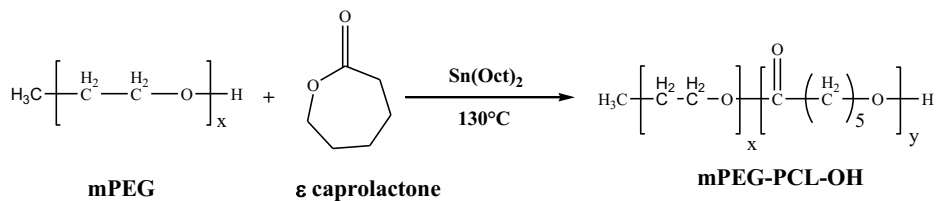


Figure 3.1a: Synthesis scheme for the TB-1, TB-2, TB-3, TB-4, TB-5, PB-1 and PB-2 copolymers

Step 1



Step 2

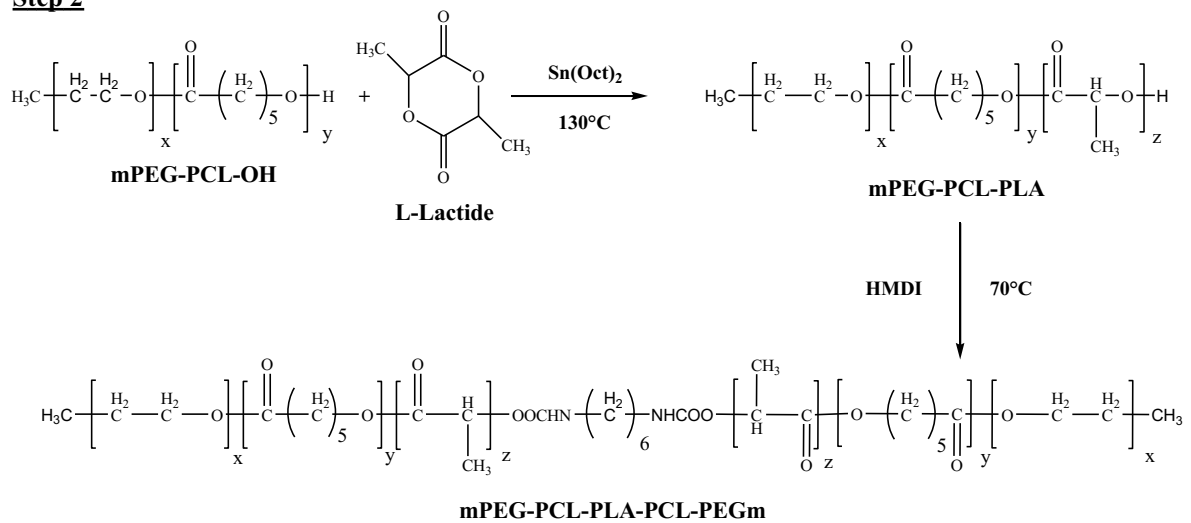


Figure 3.1b: Synthesis scheme for the PB-4 and PB-5 copolymers

Table 3.1: List of TB and PB copolymers studied

Code	Structure	PLA/PCL/PEG	Total M_n^a (theoretical)	Total M_n^b (calculated)	Total M_n^c (calculated)	M_w^c (GPC)	PDI ^c	Solubility in water
TB-1	PCL ₁₀₀₀ -PEG ₁₀₀₀ -PCL ₁₀₀₀	0/2/1	3000	3050	3430	4720	1.37	Soluble
TB-2	PCL ₁₅₀₀ -PEG ₁₅₀₀ -PCL ₁₅₀₀	0/2/1	4500	4580	4900	6760	1.38	Soluble
PB-1	PLA ₂₅₀ -PCL ₁₂₅₀ -PEG ₁₅₀₀ -PCL ₁₂₅₀ -PLA ₂₅₀	0.33/1.67/1	4500	4520	4750	6640	1.40	Soluble
PB-2	PLA ₅₀₀ -PCL ₁₂₅₀ -PEG ₁₅₀₀ -PCL ₁₂₅₀ -PLA ₅₀₀	0.67/1.67/1	5000	4980	5250	6900	1.32	Soluble
PB-4	PEG ₅₅₀ -PCL ₅₅₀ -PLA ₁₁₀₀ -PCL ₅₅₀ -PEG ₅₅₀	1/1/1	3300	3220	4270	6290	1.47	Soluble
PB-5	PEG ₅₅₀ -PCL ₈₂₅ -PLA ₅₅₀ -PCL ₈₂₅ -PEG ₅₅₀	0.5/1.5/1	3300	3270	4330	6100	1.41	Soluble
TB-3	PCL ₂₀₀₀ -PEG ₂₀₀₀ -PCL ₂₀₀₀	0/2/1	6000	5870	-	-	-	Insoluble
TB-4	PCL ₄₀₀₀ -PEG ₄₀₀₀ -PCL ₄₀₀₀	0/2/1	12000	11850	-	-	-	Insoluble
PB-3	PLA ₇₅₀ -PCL ₁₂₅₀ -PEG ₁₅₀₀ -PCL ₁₂₅₀ -PLA ₇₅₀	1/1.67/1	5500	5330	-	-	-	Insoluble

a: Theoretical value, calculated according to the feed ratio.

b: Calculated from ¹H-NMR.

c: Determined by GPC analysis.

Synthesis of PB copolymers with A-B-C-B-A (PEG-PCL-PLA-PCL-PEG) block arrangements

PB copolymers, PB-4 and PB-5 were synthesized by ring-opening copolymerization where mPEG (550) was utilized as macroinitiator and stannous octoate (0.5 wt%) as a catalyst [176]. Firstly, TB copolymers, mPEG-PCL-PLA were synthesized by ring-opening copolymerization in a manner described earlier. The resulting TB copolymers were coupled utilizing hexamethylene diisocyanate (HMDI) as a linker to prepare PEG-PCL-PLA-PCL-PEG PB copolymers. Coupling reaction was carried out at 70 °C for 8 h. Polymers were purified by cold ether precipitation and stored at -20 °C. A brief synthetic scheme is depicted in Figure 3.1b.

Characterization of PB copolymers

FTIR analysis

Fourier transform infrared spectroscopy (FTIR) spectra were recorded with a Perkin Elmer SpectrumOne infrared spectrophotometer at a resolution of 4 cm⁻¹ with scan number of 16. FTIR scan was carried out in a range of 4000-650 cm⁻¹. The resulting IR spectra were analyzed with spectrum-v5.3.1 software.

¹H-NMR analysis

Purity, molecular structure and molecular weight (Mn) of the block copolymers were estimated utilizing a Varian 400-MHz NMR spectrometer. NMR spectra were recorded by dissolving block copolymers in CDCl₃.

Gel Permeation Chromatography (GPC) analysis

Molecular weights (Mn and Mw) and polydispersity of polymers were examined by GPC analysis. Briefly, 5 mg of polymer was dissolved in 1.5 mL of tetrahydrofuran (THF).

Polymer samples were separated on a Styragel HR-3 column maintained at 35 °C. THF at the rate of 1 mL/min was utilized as eluting solvent. Samples were analyzed by refractive index detector (Shimadzu).

X-ray diffraction (XRD) analysis

Physical states of all the synthesized polymers were determined by XRD analysis. TB and PB copolymers were analyzed at room temperature by MiniFlex automated X-ray diffractometer (Rigaku, The Woodlands, Texas, USA) equipped with Ni-filtered Cu- α radiation (30 kV and 15 mA). The diffraction angle ranged from 5 to 45° using a 1° per min increment. Jade 8+ (Material Data, Inc, Livermore, CA) was employed to process the diffraction patterns.

Sol-Gel transition

The sol (flow)-gel (no flow) transition of block copolymers was examined by following a previously published protocol with minor modifications [184]. Briefly, block copolymers ranging from 15-30 wt% were dissolved in distilled deionized water followed by 12 h incubation at 4 °C. After equilibration, 1 mL of aqueous polymeric solution was transferred in 4 mL glass vial and placed in water bath. The temperature of water bath was raised gradually from 10 to 60 °C at an increment of 1 °C. Vials were kept for 5 min at each temperature. The gel formation was observed visually by inverting the tubes. A physical state with no fluidity for 1 min was considered as gel phase. The temperature at which solution transforms to gel phase was considered as critical gelling temperature (CGT) and the temperature where a polymer starts to precipitate (phase separation) was described as critical precipitation temperature (CPT).

Cytotoxicity

Cell culture

Human retinal pigment epithelial cell line (ARPE-19) were cultured and maintained according to a protocol provided by ATCC. In brief, ARPE-19 cells were cultured in Dubelcco's modified Eagle medium (DMEM)/F-12 containing 10% heat-inactivated fetal bovine serum (FBS), sodium bicarbonate (2 mM), HEPES (15 mM), streptomycin (100 mg/L) and penicillin (100 U/L). Mouse macrophage (RAW-264.7) cells were procured from ATCC. RAW-264.7 cells were cultured and maintained in DMEM supplemented with 10% FBS, streptomycin (100 mg/L) and penicillin (100 U/L). Both cell lines were maintained in humidified atmosphere at 37 °C and 5% CO₂.

Lactate Dehydrogenase (LDH) assay

In order to evaluate cytotoxicity of polymeric materials, various concentrations of block copolymers were exposed to the ARPE-19 cells or RAW-264.7 cells at density of 1.0 x 10⁴ per well. Cells were incubated at 37 °C and 5% CO₂ in humidified atmosphere for 48 h. After incubation, levels of LDH in cell supernatant were estimated by LDH detection kit. Samples were analyzed at 450 nm by 96-well plate reader. The amount of released LDH is directly proportional to the cytotoxicity of the polymers. In this study, more than 10% of LDH release was considered as cytotoxic. LDH release (%) was calculated according to the following equation,

$$LDH\ release(\%) = \frac{Abs.\ of\ Sample - Abs.\ of\ negative\ control}{Abs.\ of\ positive\ control - Abs.\ of\ negative\ control} * 100 \quad \dots Eq. 3.1$$

MTS assay

MTS assay was performed according to a previously published protocol with minor modifications [185]. Briefly, ARPE-19 and RAW-264.7 cells at a density of 1.0×10^4 cells per well were seeded in 96-well plate. Cells were incubated for 24 h at 37 °C and 5% CO₂ in humidified atmosphere. After incubation, the culture medium was replaced with fresh medium containing various concentrations of block copolymers. Cells were further incubated for 48 h. At the end of incubation period, culture medium was substituted with 100µL of serum free medium containing 20 µL of MTS solution. Cells were then incubated for 4 h at 37 °C and 5% CO₂. After 4 h, absorbance of each well was estimated at 450 nm by 96-well plate reader. Polymer concentrations which exhibited more than 90% cell viability were considered as non-toxic. Percent cell viability was estimated by following equation.

$$\text{Cell viability (\%)} = \frac{\text{Abs. of Sample} - \text{Abs. of negative control}}{\text{Abs. of positive control} - \text{Abs. of negative control}} * 100 \quad \dots \text{Eq. 3.2}$$

Biocompatibility

RAW-264.7 cells were cultured and maintained according to a protocol described in previous section. In order to evaluate *in vitro* biocompatibility of gelling polymers, a previously published protocol was followed with minor modifications [185]. Briefly, 5.0×10^4 cells were seeded per well of 48-well plates and incubated for 24 h. After incubation, the cell culture medium was replaced with fresh medium containing various concentrations of block copolymers. After 24 h of incubation at 37 °C and 5% CO₂, the supernatant of each well was analyzed by ELISA for quantitative estimation of various cytokines (TNF- α , IL-6 and IL-1 β). ELISA was performed according to the manufacturer's protocol. Calibration curves for TNF-

α , IL-6 and IL-1 β were prepared in the range of 10-750 pg/mL, 5-500 pg/mL and 10-500 pg/mL, respectively.

In vitro drug release studies

For *in vitro* release experiments, 0.5 wt% of IgG was added to 10 mL vials containing 500 μ L of 20 wt% aqueous block copolymer solutions. Solutions were gently mixed at 4 $^{\circ}$ C until IgG was dissolved. Vials were incubated at 37 $^{\circ}$ C for 30 min followed by addition of 5 mL 0.01M phosphate buffer saline (PBS, pH 7.4). Throughout the release period, vials were kept in a water bath maintained at 37 $^{\circ}$ C and 60 rpm. At predetermined time intervals, 1 mL of release sample was collected and replaced with fresh PBS (pre-incubated at 37 $^{\circ}$ C). The amount of released IgG was estimated by Micro BCATM total protein assay kit. To understand the effect of polymer concentration on IgG release, a similar experiment was performed utilizing 15 wt% and 25 wt% aqueous solutions of PB-1 copolymer.

Release kinetics

In order to investigate release mechanisms, release data were fitted in various kinetic models including the Korsmeyer-Peppas, Higuchi, Hixon-Crowell, first-order and zero-order.

Korsmeyer-Peppas equation

$$\frac{M_t}{M_{\infty}} = kt^n \quad \dots \text{Eq. 3.3}$$

k is the kinetic constant and n is the diffusion exponent describes release mechanism. M_t and M_{∞} represent the cumulative IgG release at time t and at the equilibrium, respectively.

Higuchi equation

$$Q_t = Kt^{1/2} \quad \dots \text{Eq. 3.4}$$

K denotes the Higuchi rate kinetic constant, Q_t is the amount of released IgG at time t, and t is time in hours.

Hixon-Crowell equation

$$C_0^{1/3} - C_t^{1/3} = kt \quad \dots \text{Eq. 3.5}$$

C_0 and C_t represents the initial amount and remaining amount of IgG in gel, respectively. k is the constant incorporating surface-volume relation and t is time in hours.

First order equation

$$\text{Log}C = \text{Log}C_0 - \frac{Kt}{2.303} \quad \dots \text{Eq. 3.6}$$

K denotes the first order rate constant, C_0 is the initial IgG concentration and t represents time in hours.

Zero order equation

$$C = K_0t \quad \dots \text{Eq. 3.7}$$

K_0 is the zero-order rate constant and t is time in hours.

¹H-NMR for coumarin-6-loaded gel

Five mg of PB-1 copolymer was dissolved in either CDCl_3 or D_2O followed by addition of 0.5 mg of coumarin-6 a (hydrophobic dye). Samples containing both polymer and hydrophobic dye were subjected to ¹H-NMR analysis. A similar study was performed utilizing PB-5 copolymer.

Micelle size analysis

Aqueous solutions of PB-1 copolymer were subjected to micelle size analysis at room temperature utilizing a particle size analyzer (ZetasizerNano ZS, Malvern Instruments Ltd, Worcestershire, UK). PB-1 copolymer concentrations ranging from 0.1 to 5 wt% were investigated without any further dilution.

Viscosity measurements

Rheological properties of 15 wt% aqueous solution of block copolymers were estimated with an Ubbelohde capillary viscometer at temperatures ranging from 5 ± 1 °C to 25 ± 1 °C. Temperature of the viscometer was maintained with a temperature controlled water bath. Viscosity values are represented as an average of triplicates (kinematic viscosity, cP \pm standard deviation).

Results and discussion

Synthesis and characterization of block copolymers

FTIR spectrum of PB-4 is reported in Figure 3.2. Absorption band at 1725 cm^{-1} and multiple bands ranging $1000\text{-}1300\text{ cm}^{-1}$ established the presence of ester linkages in PB copolymer. C-H stretching bands at 2936 and 2865 cm^{-1} depicted presence of PCL blocks. Absorption band at 1534 cm^{-1} (N-H banding) and 3344 cm^{-1} (N-H stretching) exhibited the formation of urethane group in PB-4 copolymer.

$^1\text{H-NMR}$ was employed to characterize PCL-PEG-PCL, PLA-PCL-PEG-PCL-PLA and PEG-PCL-PLA-PCL-PEG copolymers. Figure 3.3 depicts the $^1\text{H-NMR}$ spectra of TB-1, PB-1 and PB-4 block copolymers in deuterated chloroform. As described in Figures 3.3a, 3.2b and 3.2c, characteristic $^1\text{H-NMR}$ peaks were observed at 1.40, 1.65, 2.30 and 4.06 ppm

corresponding to the methylene protons of $-(\text{CH}_2)_3-$, $-\text{OCO}-\text{CH}_2-$, and $-\text{CH}_2\text{OOC}-$ of PCL units, respectively. A sharp peak at 3.65 ppm was attributed to the methylene protons ($-\text{CH}_2\text{CH}_2\text{O}-$) of PEG. Typical signals (Figures 3.3b and 3.3c) at 1.50 ($-\text{CH}_3$) and 5.17 ($-\text{CH}-$) ppm were assigned for PLA blocks. Whereas, a peak (Figure 3.3c) at 3.38 ppm was denoted to terminal methyl of ($-\text{OCH}_3-$) of PEG.

The [EO]-[CL]-[LA] molar ratios of final products were calculated from integration of PEG signal at 3.65 ppm, PCL signal at 2.30 ppm and PLA signal at 5.17 ppm. In case of PB-4 copolymer, the PEG signal at 3.38 ppm was applied for the calculation of molar ratio.

The molecular weight (M_w and M_n) and polydispersity of polymers were determined by GPC. Typical GPC curves of TB-1, PB-1 and PB-4 are shown in Figure 3.4. A single peak for each polymer was observed describing unimodal distribution of molecular weight and absence of any other homopolymer block such as PEG, PCL or PLA. Moreover, molecular weights of block copolymers were very close to feed ratio. Polydispersity (PD) was also below 1.47, describing a narrow distribution of molecular weights. $^1\text{H-NMR}$ and GPC were applied to calculate molecular weight of block copolymers (Table 3.1). As summarized in Table 3.1, experimental values were consistent with theoretical values derived from feed ratios. Hence for simplicity, theoretical values are mentioned in the following text.

In order to evaluate crystallinity and phase composition, all the block copolymers were analyzed for XRD patterns (Figure 3.5). Two sharp peaks were observed at $2\theta = 21.5^\circ$ and 23.9° which belong to PCL blocks. No peaks for PEG or PLA were observed. Interestingly, only TB-1, TB-2, PB-1 and PB-2 exhibited crystalline peaks of PCL, whereas PB-4 and PB-5 were devoid of any such peaks. XRD patterns of TB-1 and TB-2 indicated that PCL blocks retained a semi-crystalline structure even after covalent conjugation with PEG blocks.

Interestingly, conjugation of PLA blocks at the terminals of TB copolymers exhibited significant reduction in crystalline peak indicating semi-crystalline structures of PB-1 and PB-2. However, PB-4 and PB-5 were devoid of any crystalline peak suggesting amorphous nature of copolymers with A-B-C-B-A block arrangements. Thus, crystallinity of polymer can be easily controlled by the arrangement of polymer blocks in structural backbone. Moreover, previously published reports suggest that decrease in crystallinity significantly enhanced degradation of block polymer [181]. Hence, it is anticipated that PB-4 and PB-5 might cause faster rate of degradation relative to TB-1, TB-2, PB-1 and PB-2 copolymers.

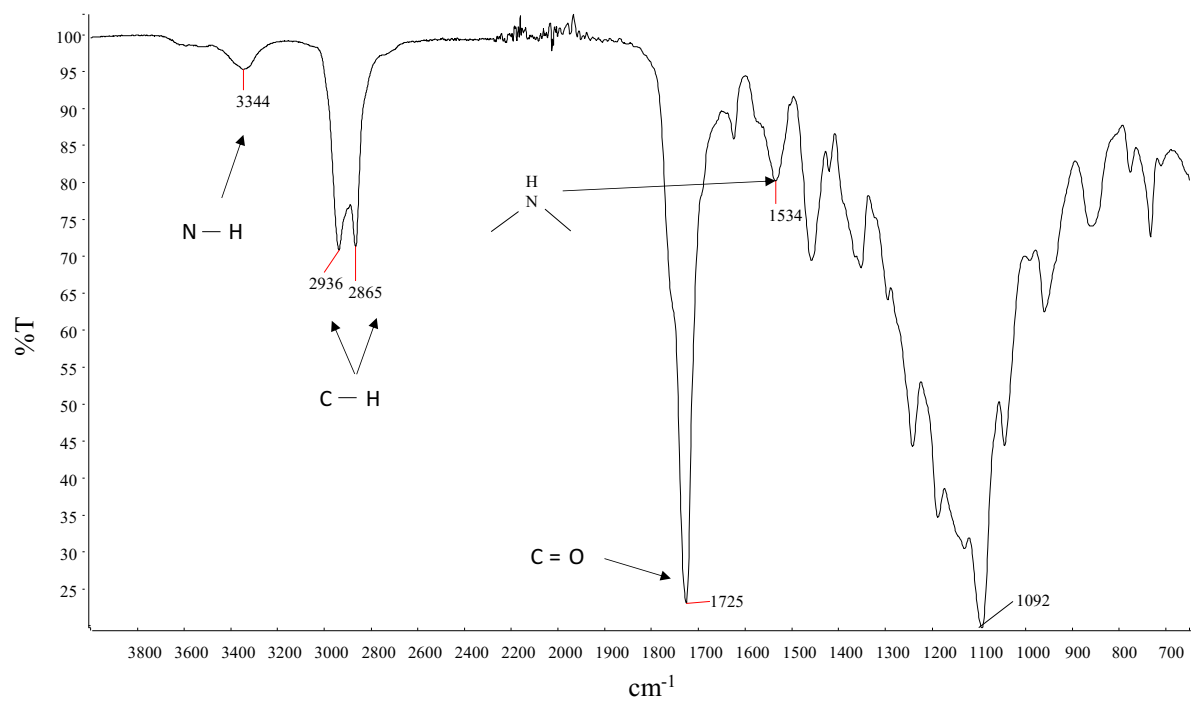


Figure 3.2: FTIR spectrum of PB-4 (PEG₅₅₀-PCL₅₅₀-PLA₁₁₀₀-PCL₅₅₀-PEG₅₅₀).

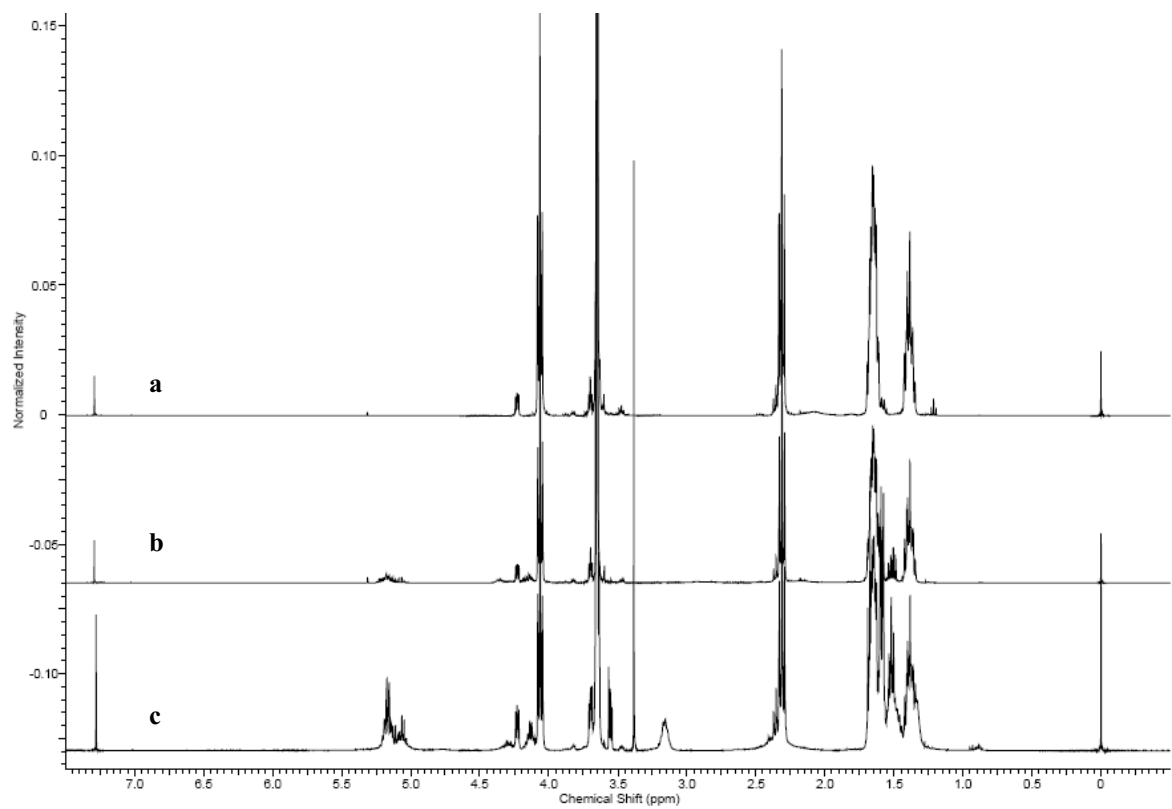


Figure 3.3: ^1H NMR of (a) TB-1 (PCL-PEG-PCL), (b) PB-1 (PLA-PCL-PEG-PCL-PLA) and (c) PB-4 (PEG-PCL-PLA-PCL-PEG).

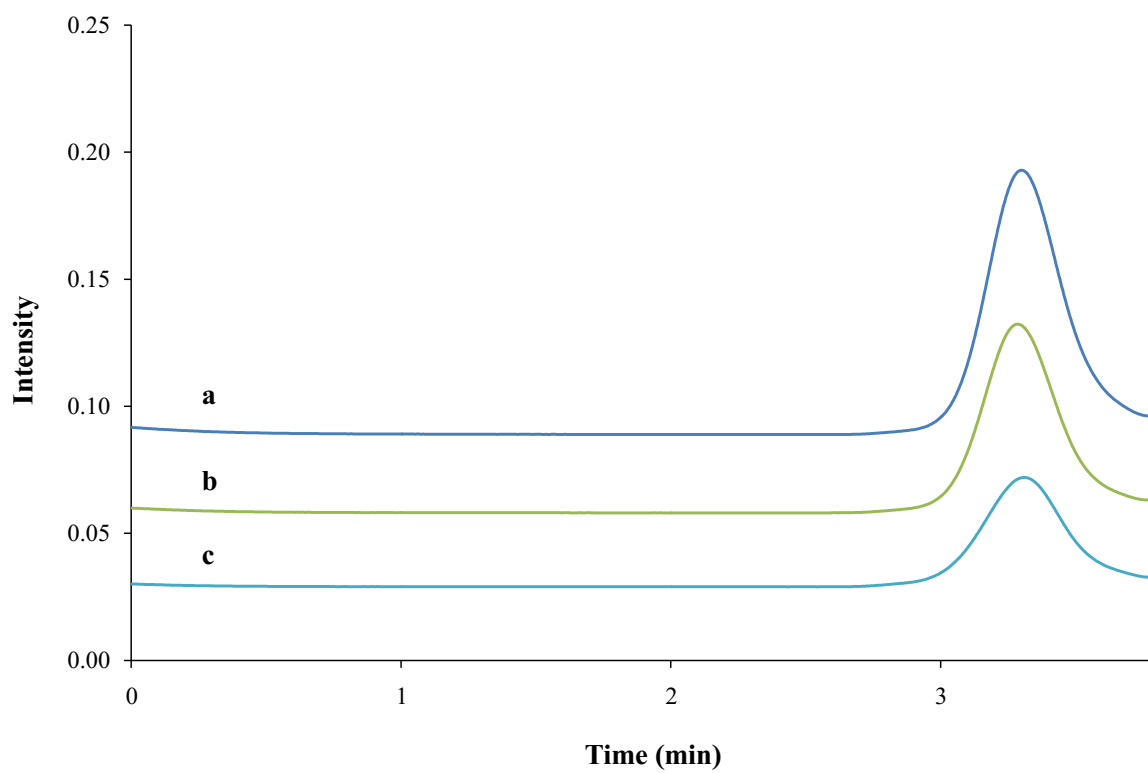


Figure 3.4: GPC chromatograms for **(a)** TB-1 (PCL-PEG-PCL), **(b)** PB-1 (PLA-PCL-PEG-PCL-PLA) and **(c)** PB-4 (PEG-PCL-PLA-PCL-PEG).

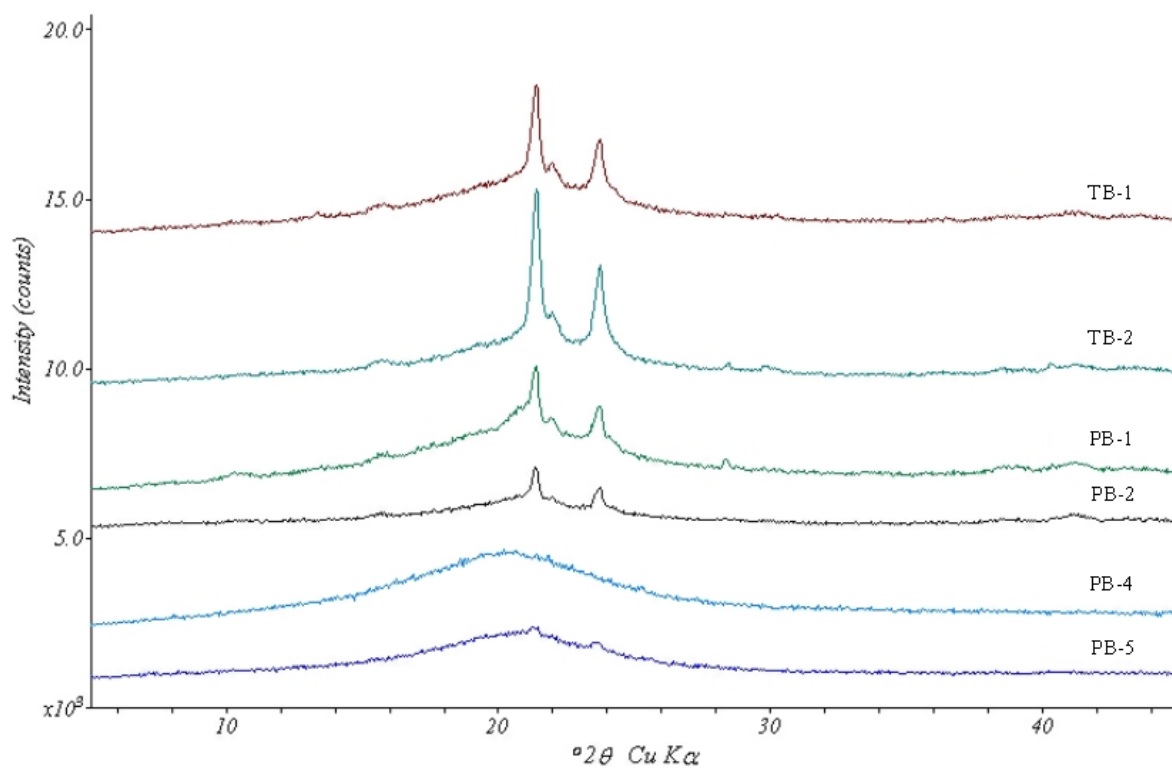


Figure 3.5: XRD patterns of block copolymers.

Sol-gel transition

The block copolymers reported in this study are amphiphilic in nature containing hydrophilic block (PEG) and hydrophobic block(s) (PCL and/or PLA). In the case of TB copolymers (TB-1 and TB-2), increased total molecular weight, but keeping molecular weight ratio constant i.e., PCL/PEG (2:1), did not alter their thermosensitive behavior. However, further increase in molecular weights (TB-3 and TB-4) with the same hydrophobic-hydrophilic block ratio (2:1) reduced aqueous solubility. This may be attributed to longer PCL chains, which may significantly enhance intermolecular and intramolecular hydrophobic interactions of polymer and outweigh the ability of PEG to solubilize polymer. PB-1 and PB-2 copolymers are easily soluble in water and exhibit sol-gel transition behavior. However, the increase in hydrophobicity by increasing molecular weight of PLA chain (PB-3) exhibited poor aqueous solubility, which might be due to limitation of PEG to solubilize polymer. For all block copolymers, an increase in aqueous polymer concentration from 15 to 30 wt% significantly shifted CGT to lower and CPT to higher values.

Effect of molecular weight of block copolymer

In order to understand the effect of molecular weight of the block copolymers, sol-gel transition curves of TB-1 and TB-2 were compared (Figure 3.6). With an increase in total molecular weight of block copolymers from 3000 (TB-1) to 4500 (TB-2), CGT decreased whereas the CPT increased to higher values. The temperature range for the gel region or area between CGT and CPT at any given concentration was also significantly enhanced. A similar trend was observed for PB-1 and PB-2 polymers, where molecular weight of PLA was raised in PB-2.

Effect of hydrophobicity of block copolymer

Hydrophobicity of block copolymers can be increased by enhancing the molecular weight of the whole while keeping the molecular weight of PEG constant (PB-1 and PB-2) or by substituting the molecular weight of PLA by PCL (TB-2 and PB-1, PB-4 and PB-5). PB-2 has larger chains of PLA relative to PB-1 copolymer suggesting a greater hydrophobicity of PB-2 copolymer. It is important to note that a PLA block is less hydrophobic relative to a PCL block of similar molecular weight. Therefore, TB-2 and PB-5 are more hydrophobic compared to PB-1 and PB-4, respectively. Sol-gel transition curves of PB-1 and PB-2 (Figure 3.7a), PB-4 and PB-5 (Figure 3.7b), and TB-2 and PB-1 (Figure 3.7c) were compared to understand the effect of hydrophobicity on the sol-gel behavior of block copolymers. As described in Figure 3.7a, increased hydrophobicity of PB-2 has significantly reduced the CGT and shifted the value of CPT to higher temperature. A similar behavior was observed when the sol-gel transition curves of PB-4/PB-5, and TB-2/PB-1 were compared.

Higher hydrophobicity polymers may enhance intramolecular and intermolecular hydrophobic interactions even at lower temperatures compared to hydrophilic copolymers which lead to lower CGT. Additionally, these hydrophobic interactions allow for a more rigid gel matrix and hence delay polymer precipitation at higher temperature (CPT).

Effect of block arrangement

In order to understand the effect of block arrangement on thermogelling behavior, sol-gel transition curves of PB-1 (C-B-A-B-C) and PB-5 (A-B-C-B-A) were compared (Figure 3.8). Interestingly, CGT and CPT for PB-1 copolymer were significantly lower than PB-5 copolymer at any respective concentration. This behavior may be attributed to the different mechanism of gelation of these block copolymers.

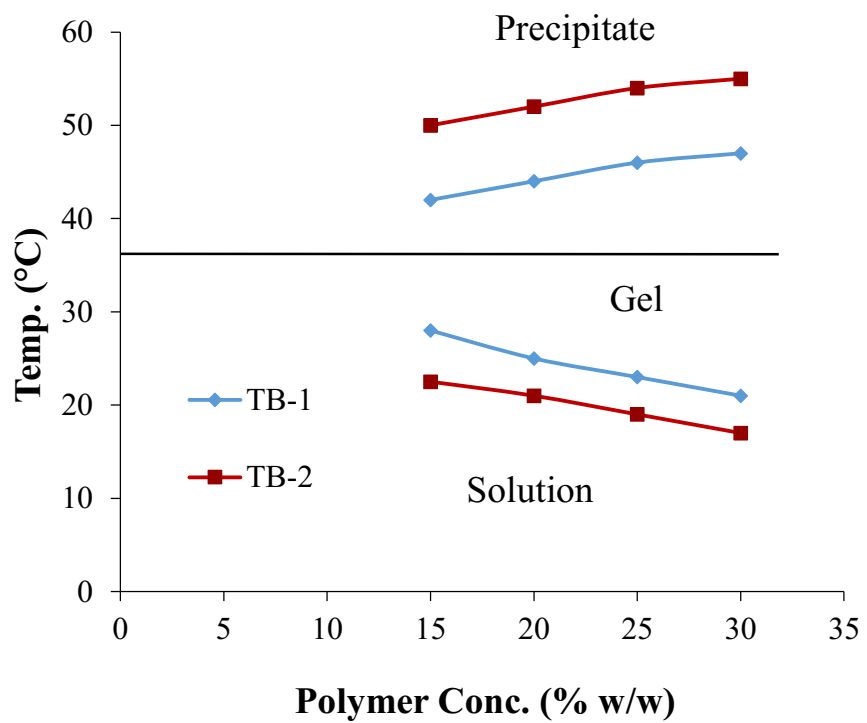


Figure 3.6: Sol-gel transition curves of TB-1 and TB-2.

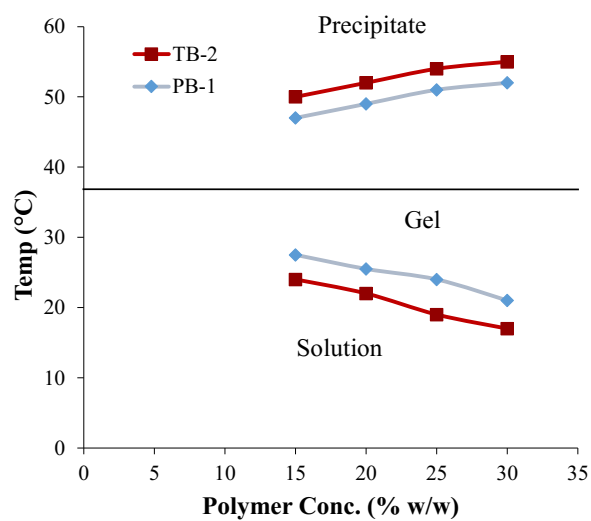
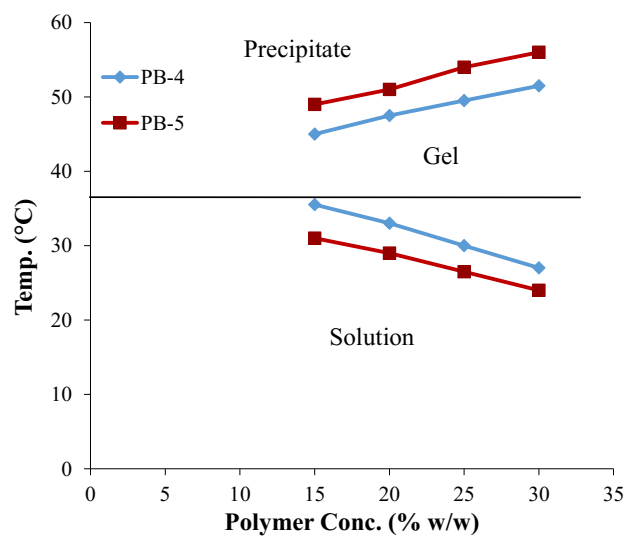
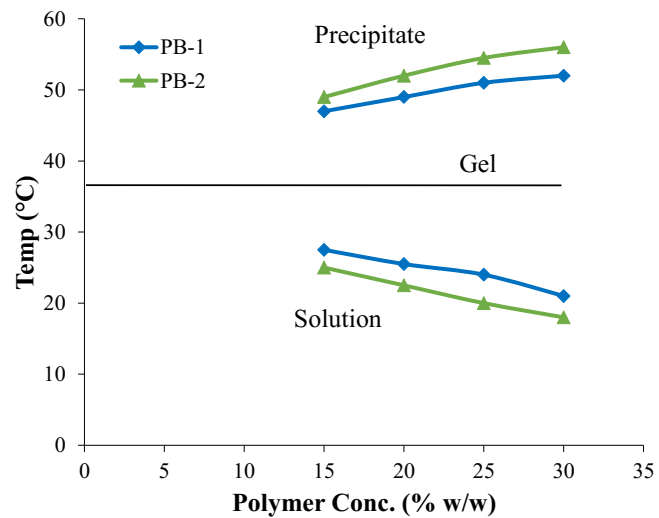


Figure 3.7: Sol-gel transition curves (a) PB-1/PB-2, (b) PB-4/PB-5, and (c) TB-2/PB-1.

Effects of total molecular weight, arrangement of blocks and hydrophobicity of PB copolymers on sol-gel transition behavior are in agreement with previously published reports of PLGA-PEG-PLGA [186] and PEG-PLGA-PEG [187] copolymer hydrogels.

In vitro cytotoxicity

To study the compatibility between polymer and biological system (*in vitro* cell culture model), various concentrations of block copolymers were exposed to ARPE-19 and RAW-264.7 cells for 48 h. LDH is the cytosolic enzyme, which is secreted into the cell supernatant following membrane damage. Concentration of released LDH provides a direct estimation of polymer toxicity. Results (Figures 3.9a and 3.9b) indicate less than 10% of LDH release at any given concentration for both the cell types. The results were not significantly different than negative controls, i.e., cells without treatment.

Results observed in LDH assay were further confirmed by employing the MTS cell viability study. In order to study metabolic response, ARPE-19 and RAW-264.7 cells were incubated with various concentrations of block copolymers. Results indicated in Figures 3.10a and 3.9b demonstrate that more than 90% of cells are viable after 48 h of polymer exposure. No significant difference in cell viability is observed relative to negative control. Results obtained from LDH and MTS assay indicated negligible toxicity suggesting excellent safety profile of block copolymers for back of the eye applications.

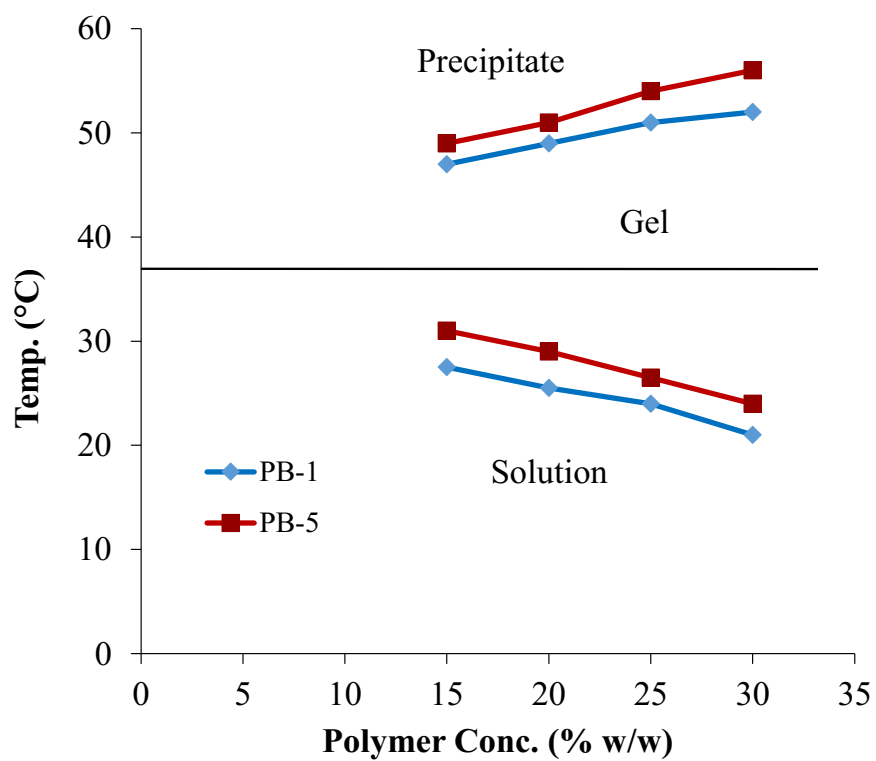


Figure 3.8: Sol-gel transition curves of PB-1 and PB-5.

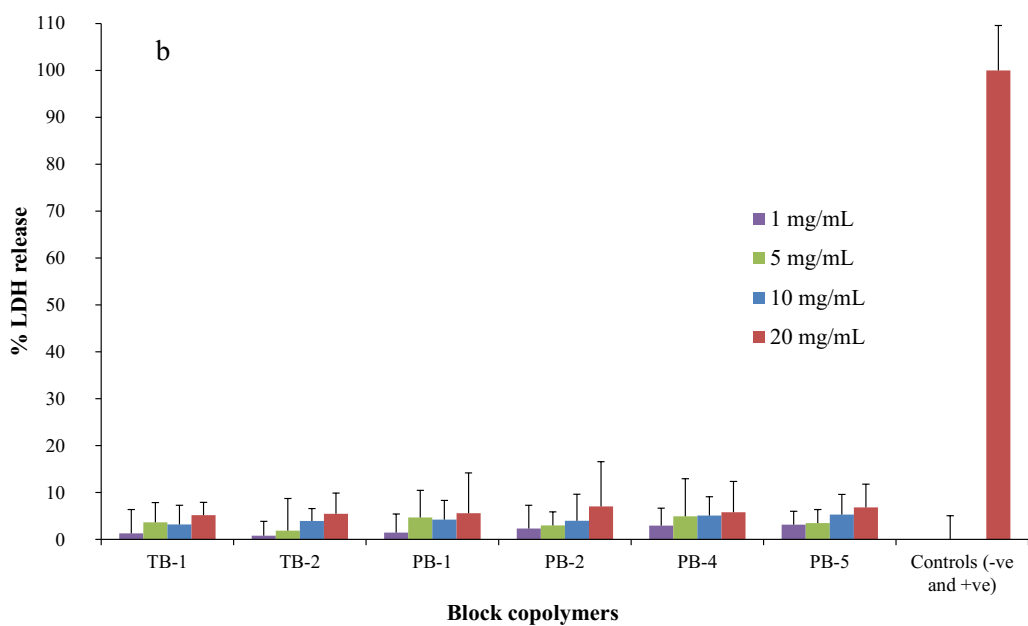
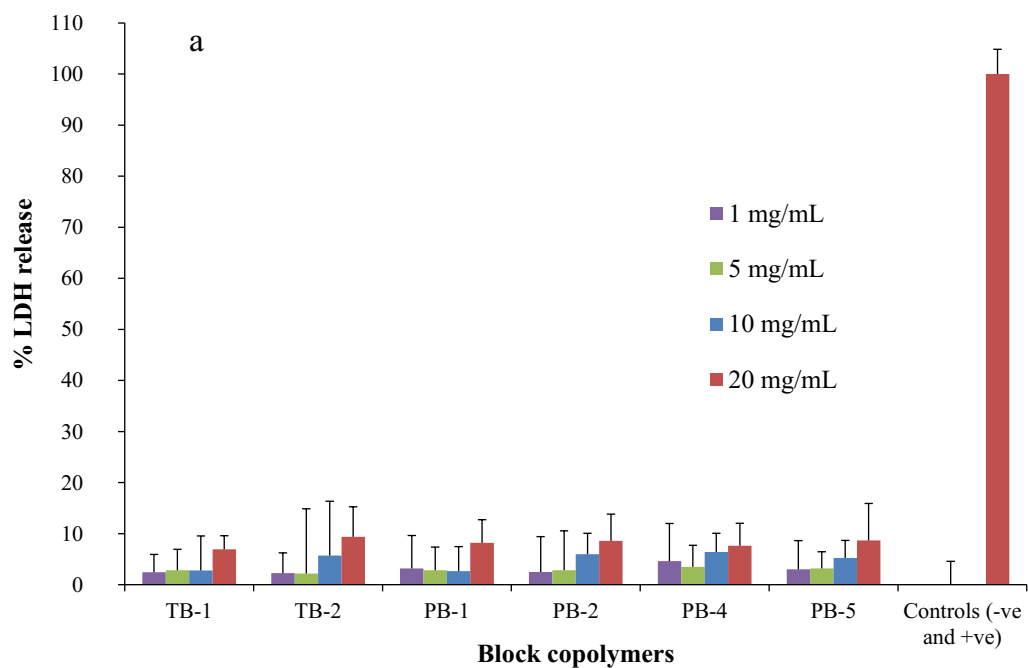


Figure 3.9: *In vitro* cytotoxicity assay (LDH) of various block copolymers at different concentrations were performed on (a) ARPE-19 and (b) RAW 264.7 cells.

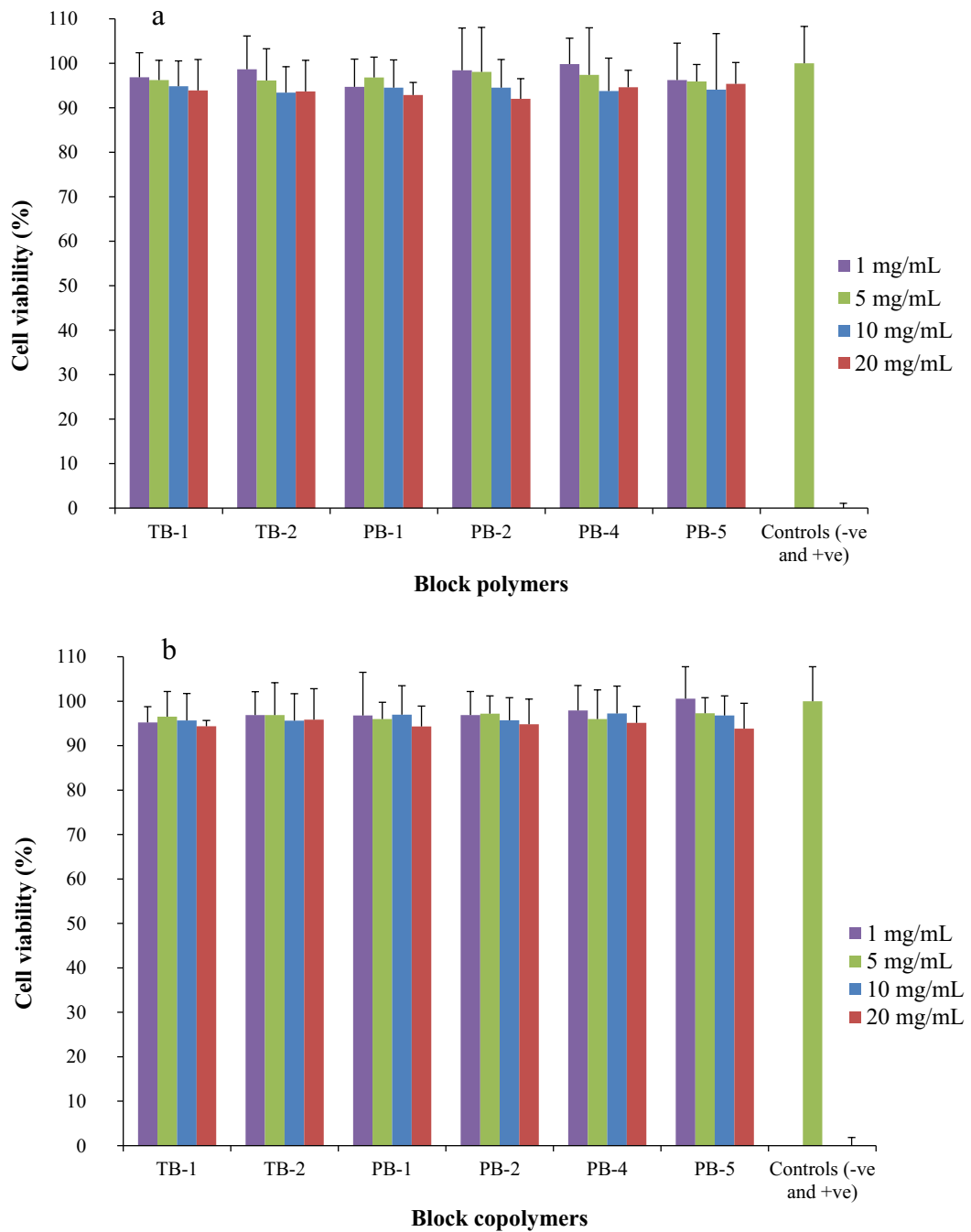


Figure 3.10: *In vitro* cell viability assay (MTS) of various block copolymers at different concentrations were performed on (a) ARPE-19 and (b) RAW 264.7 cells.

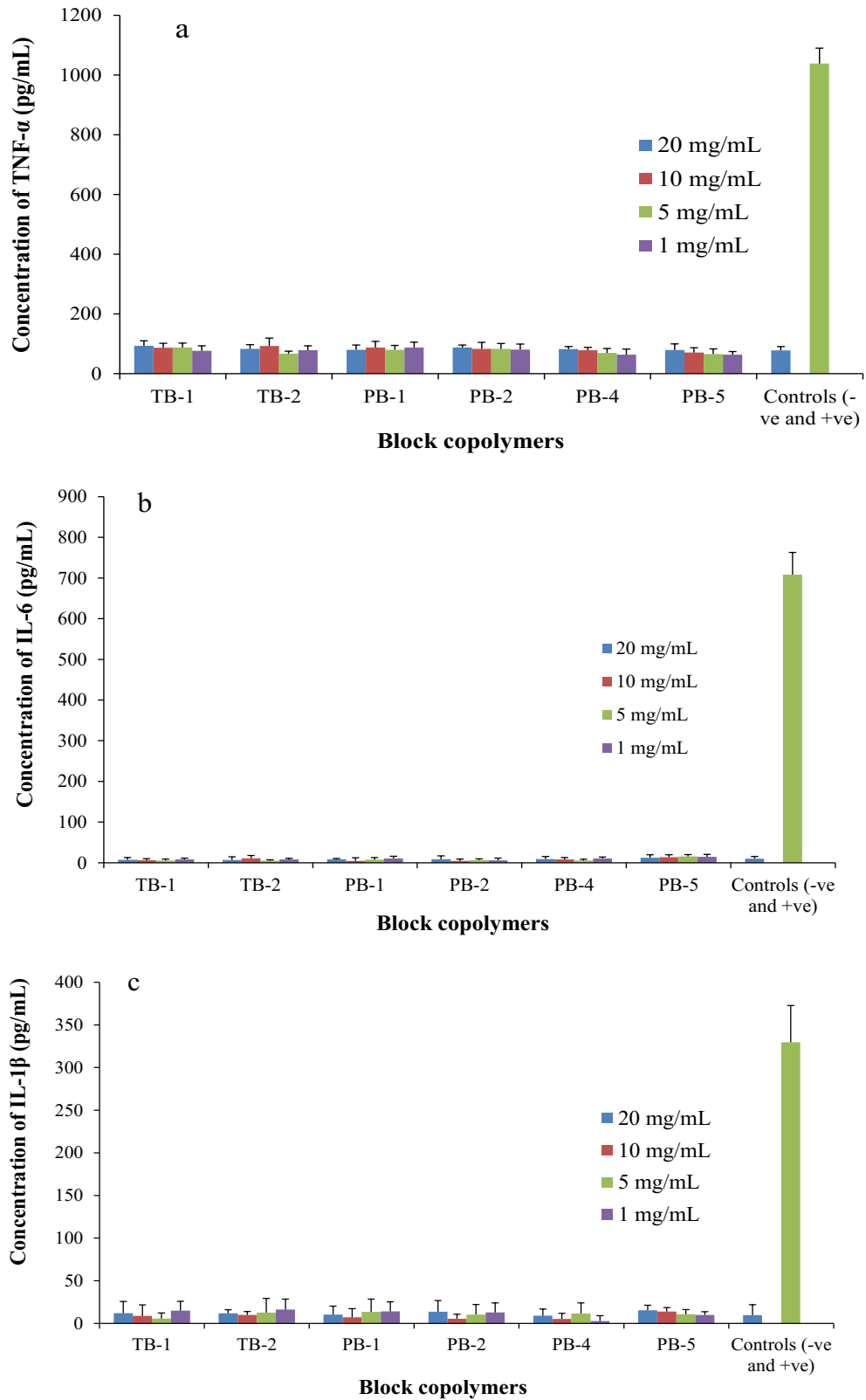


Figure 3.11: *In vitro* release of (a) TNF- α , (b) IL-6 and (c) IL-1 β from RAW 264.7 cells upon exposure to various concentrations of block copolymers.

In vitro biocompatibility study

Estimation of inflammatory mediators such as TNF- α , IL-6 and IL-1 β secreted in cell supernatant is a good measure to confirm biocompatibility of block copolymers. These cytokines were estimated in the supernatant of RAW-264.7 cells after 24 h of polymer exposure. Levels of cytokine were estimated by sandwich ELISA method according to manufacturer's protocol. Our results (Figures 3.11a, 3.11b, and 3.11c) indicate that at 20 mg/mL polymer concentration, release of cytokines was negligible with no significant difference to negative control. Negligible release of TNF- α , IL-6 and IL-1 β suggest excellent biocompatibility of PB copolymers with low toxicity.

In vitro release study

IgG was selected as a model protein to evaluate the suitability of block copolymers as controlled release delivery systems for ocular indications. *In vitro* release studies were performed by dissolving IgG in 20 wt% aqueous solution of respective block copolymers. To estimate the concentration of IgG, release samples were analyzed by Micro BCATM. *In vitro* release behavior of IgG from various thermosensitive gels is compared in Figure 3.12. Release of IgG was noticeably affected by the chemical composition of block copolymers. TB copolymers (TB-1 and TB-2) exhibited significantly higher burst release (~40-45% of initial dose) relative to PB copolymers (PB-1, PB-2, PB-4 and PB-5) which showed burst release between ~24-31% of initial dose. Moreover, release of IgG from PB copolymer based thermosensitive gels were sustained for more than 20 days, whereas TB copolymers prolonged the release for only ~12-14 days. Partial replacement of PCL with PLA block significantly reduces the crystallinity (XRD data, Figure 3.5) and hydrophobicity of copolymers. This

reduction in hydrophobicity of PB copolymers may have increased the affinity with IgG resulting in prolonged release of IgG from PB copolymers relative to TB copolymers.

In addition, the effect of polymer concentration on the rate of IgG release was also studied. As depicted in Figure 3.13, 25 wt% of PB-1 copolymer solution exhibited 74.92% of IgG release within 20 days, whereas 20 wt% and 15 wt% gel showed 85.32% and 96.23% of IgG release during the same time period. It appears that an increase in polymer concentration from 15 wt% to 25 wt% significantly retards drug release rate, indicating direct relationship of polymer concentration on drug release. At higher polymer concentration, the gels may form compact structures with a smaller porosity in the gel matrix relative to lower polymer concentration. This structural change may lower the diffusion of IgG across gel matrix resulting in lower initial burst release and prolonged duration of release.

Release kinetics

In vitro release data were fitted to zero and first order, Korsmeyer-Peppas, Higuchi and Hixson-Crowell models to delineate kinetics of IgG release (Table 3.2). The Korsmeyer-Peppas model was found to be the best fit model based on R^2 value. The diffusion exponent, n , ranged from 0.272 - 0.386 for all gelling polymers. The n -values below 0.43 indicates a diffusion controlled mechanism of IgG release.

¹H-NMR of Coumarin-6-loaded polymer solutions

In order to understand the process of polymer solubilization and behavior of sol-gel transition, ¹H-NMR of PB-1 copolymer was carried out in CDCl₃ (Figure 3.14a) and D₂O (Figure 3.14b) spiked with coumarin-6. Coumarin-6 is insoluble in water however aqueous solubility is significantly enhanced in the presence of PB-1 copolymer, which may be due to

micellization. A sample containing PB-1 copolymer and coumarin-6 in CDCl_3 exhibited sharp peaks representing various protons of PEG, PCL, PLA and coumarin-6. Interestingly, a sample containing PB-1 copolymer and coumarin-6 in D_2O was devoid of signals of coumarin-6 suggesting that coumarin-6 is inside the micellar core. Broad peaks observed at 3.65 ppm and 2.30 ppm were attributed to the protons of PEG ($-\text{CH}_2-\text{CH}_2-$) and PCL ($-\text{OCO}-\text{CH}_2-$), respectively. Proton peaks for PLA and coumarin-6 were absent. Exactly, similar behavior was also observed with the sample containing PB-5 copolymer and coumarin-6 simultaneously dissolved in CDCl_3 (Figure 3.14c) or D_2O (Figure 3.14d). NMR analysis carried out in CDCl_3 exhibited sharp peaks for all the protons indicating free movement of polymer chains and coumarin-6 in organic solvent. However, NMR spectra carried out in D_2O exhibited very few broad peaks representing PEG and PCL blocks only. These results suggest that coumarin-6 was located in the core of the micelles along with PCL and PLA blocks. Hence, we were able to see very weak NMR signals for PCL blocks due to the restricted molecular movement, and no signals for PLA and coumarin-6. Strong peak of PEG in D_2O was observed indicating that the location of PEG is in the corona of the micelles. Results from this study suggest that PB copolymers are solubilized in water via micellization process where core is composed of PCL-PLA and shell is of PEG.

Micelle size analysis

Micelle size and its distribution of PB-1 copolymer were evaluated in water by DLS at room temperature as a function of concentration (Figure 3.15). As the aqueous concentration of polymer was raised from 0.1 wt% to 5 wt%, two peaks (22 nm and 150 nm) were continuously shifted toward higher particle size. Moreover, a broader size distribution with the increase of polymer concentration was observed. Interestingly, at 5 wt% polymer

concentration, emergence of a third peak with very large micelle size ($\sim 5 \mu\text{m}$) was also revealed. Increase in particle size and polydispersity as a function of concentration clearly indicate the involvement of a micellar aggregation mechanism.

Viscosity measurement

Table 3.3 describes the kinematic viscosity of 15 wt% aqueous gelling solutions of different block copolymers at various temperatures ranging from 5 to 25 °C. Kinematic viscosities of polymer solutions accelerated with rise in temperature. Interestingly, at any given temperature, an increase in molecular weight of the block copolymers exhibited higher viscosity (TB-1 and TB-2 or PB-1 and PB-2).

Also, the viscosities of TB-2 and PB-5 (hydrophobic polymers) were considerably higher relative to PB-1 and PB-4 (hydrophilic polymers), respectively. we speculate that the hydrophobic interactions exerted by PCL or PCL-PLA blocks with large molecular weight and hydrophobic copolymers are significantly stronger at any given temperature relative to small molecular weight and hydrophilic copolymers, respectively. Subsequently, this phenomenon may have elevated the viscosity of aqueous solutions. In addition, as temperature of the solution rises, these hydrophobic interactions also begin to dominate which eventually improve the viscosity of aqueous polymer solution. Interestingly, polymer structure (arrangement of blocks) also exhibited a noticeable effect on viscosity. Hence, kinematic viscosity of PB-1 solution was significantly higher compared to PB-5 aqueous solution.

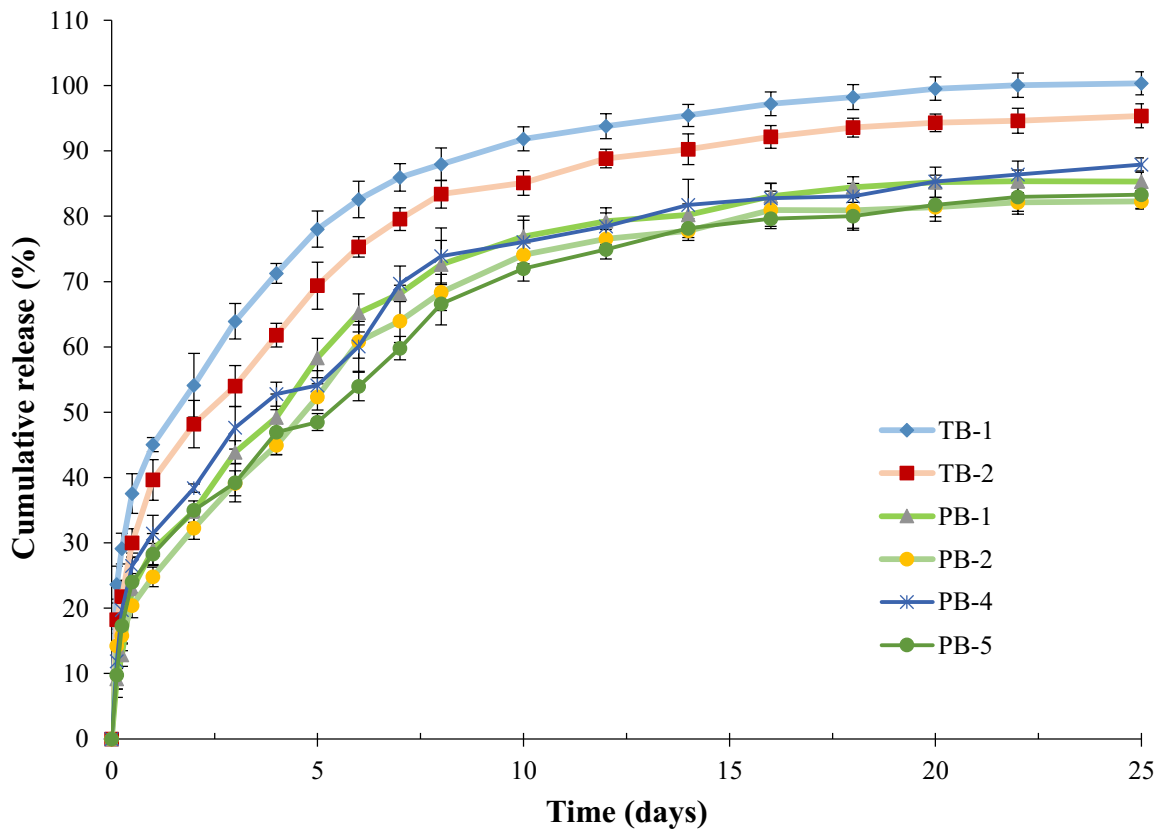


Figure 3.12: Effect of block copolymer composition on *in vitro* release of IgG from thermosensitive gels (20 wt%).

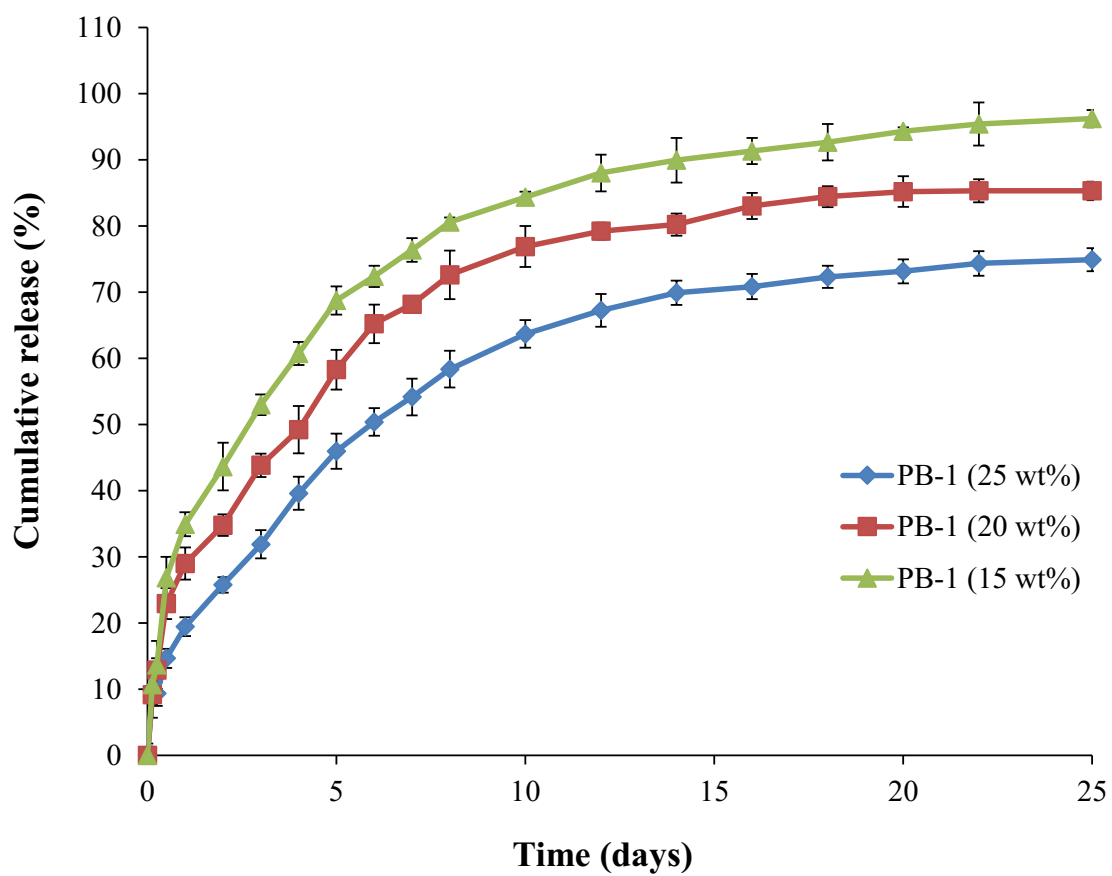


Figure 3.13: Effect of polymer concentrations (15, 20 and 25 wt%) on *in vitro* release of IgG from PB-1 thermosensitive gels.

Table 3.2: Coefficient of determination (R^2) for various kinetic models for *in vitro* release of IgG.

Block copolymers	Korsmeyer-Peppas		Higuchi	Hixson-Crowell	First-Order	Zero-Order	Best fit model
	R^2	N	R^2	R^2	R^2	R^2	
TB-1	0.995	0.272	0.959	0.904	0.945	0.822	Korsmeyer-Peppas
TB-2	0.992	0.347	0.984	0.965	0.947	0.864	Korsmeyer-Peppas
PB-1	0.997	0.386	0.985	0.954	0.967	0.891	Korsmeyer-Peppas
PB-2	0.997	0.344	0.991	0.981	0.981	0.934	Korsmeyer-Peppas
PB-4	0.989	0.296	0.970	0.957	0.973	0.871	Korsmeyer-Peppas
PB-5	0.988	0.293	0.979	0.943	0.979	0.859	Korsmeyer-Peppas

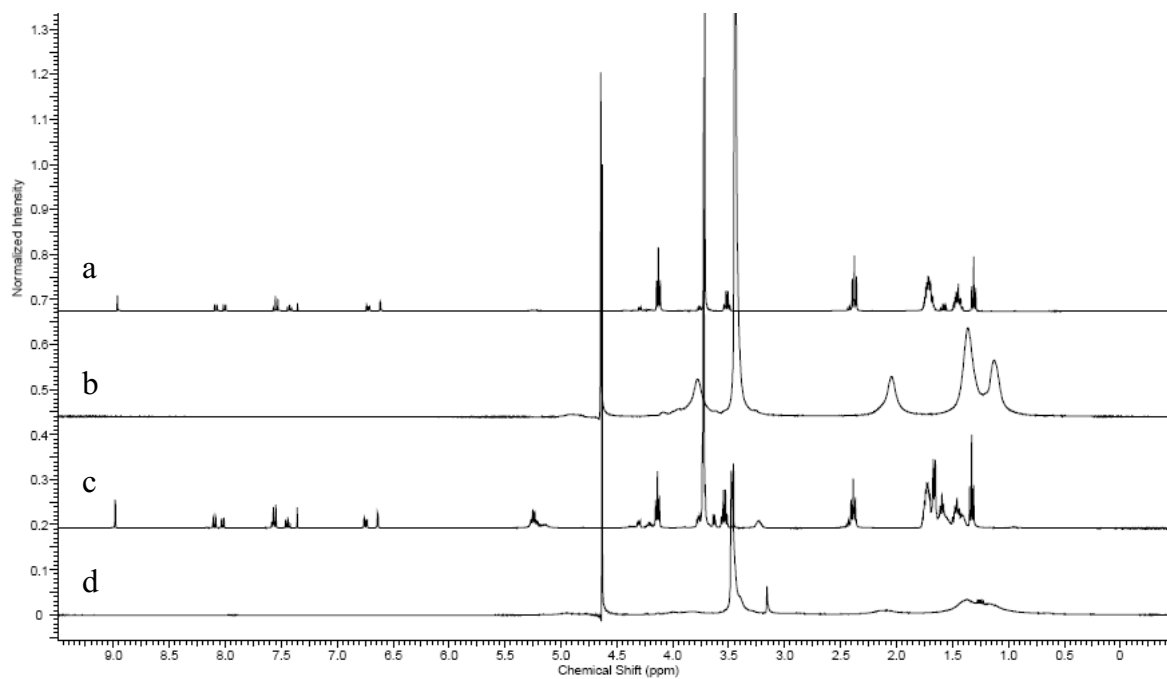


Figure 3.14: ¹H-NMR of PB-1 and coumarin-6 in (a) CDCl₃ and (b) D₂O, and PB-5 and coumarin-6 in (c) CDCl₃ and (d) D₂O.

Hypothesis for gelation mechanisms

From the observed results of $^1\text{H-NMR}$, viscosity and micelle size analysis, we propose two different mechanisms of sol-gel transition for different types of block copolymers related to, (i) the hydrophobic segments at the terminals (B-A-B (TB-1 and TB-2) or C-B-A-B-C (PB-1 and PB-2)) and (ii) the hydrophilic segments at the termini (A-B-C-B-A (PB-4 and PB-5)). According to our hypothesis, both types of copolymers can be dissolved via micellization where the core is composed of hydrophobic segments and shell is made up of hydrophilic segments. Therefore, as described in Figure 3.16, interaction of PEG with water molecules dominated at low temperature (4 °C) allowing the polymer to solubilize (Figure 3.16a). In contrast, elevation in temperature causes polymer aggregation and initiates the process of micellization. Therefore, it is possible to solubilize a hydrophobic dye (coumarin-6) in an aqueous solution of PB-1 copolymers. B-A-B or C-B-A-B-C copolymers possess hydrophobic termini and hence behave differently in aqueous solution relative to A-B-C-B-A types of copolymers. In the case of B-A-B or C-B-A-B-C copolymers, during micellization polymer molecules can serve as intermicellar bridges, where the hydrophobic ends of the polymer are diffused in the core of different micelles (Figure 3.16b). With a rise in temperature (up to CGT), progression of intermicellar bridges may initiate micellar aggregation and eventually enhance the viscosity of solution. Therefore, we have observed significant enhancement in viscosity of each block copolymer solution as a function of temperature (Table 3.3). Moreover, the numbers of intermicellar bridges are also proportional to the concentration of block copolymers at any given temperature. Micellar aggregation and larger micelle size were observed with an increase in polymer concentration (Figure 3.15). At CGT, intermicellar bridges and micellar aggregation may be sufficient enough to form the opaque hydrogel (Figure 3.16c). Further heating of the heterogeneous opaque gel results in polymer

precipitation. This may be due to strong hydrophobic interactions between PCL or PCL-PLA chains that can significantly overcome weaker hydrophilic interactions (hydrogen bonds) between PEG and water. This phenomenon may eventually dehydrate the PCL or PCL-PLA core leading to collapse of hydrogel structure (Figure 3.16d).

A-B-C-B-A (PB-4 and PB-5) types of copolymers may also be solubilized by micellization. However, in case of A-B-C-B-A types of copolymers, micellar arrangements may lack intermicellar bridges. Therefore, such copolymers demonstrated lower viscosity relative to B-A-B or C-B-A-B-C types of copolymers at any given temperature. At CGT, A-B-C-B-A copolymers may aggregate in compact micellar structure resulting in the opaque hydrogel. Further heating of the gelling solution (above CPT) may lead to dominate hydrophobic interactions causing dehydrated micelle cores which eventually result in polymer precipitation.

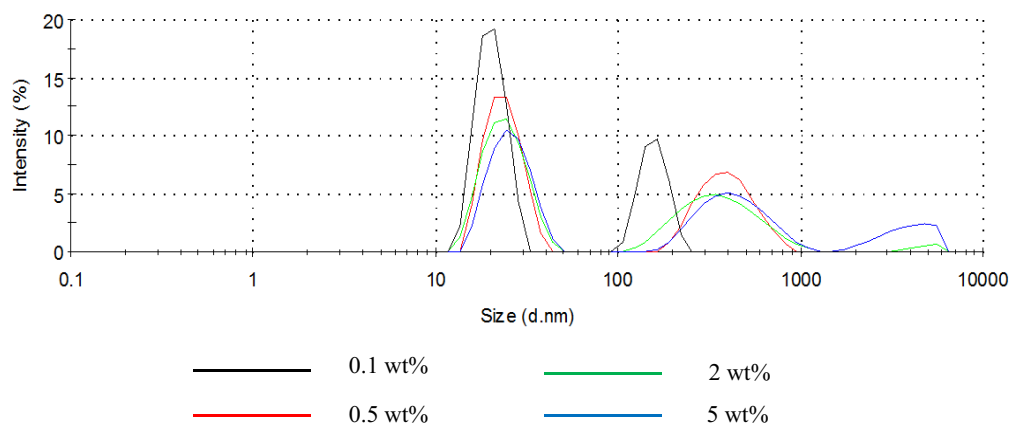


Figure 3.15: Estimation of PB-1 copolymer micelles at various concentrations i.e., 0.1, 0.5, 2 and 5 wt%.

Table 3.3: Viscosity of thermosensitive gelling solutions (15 wt%) at various temperatures.

Block copolymers	Viscosity (cp) at various temperature				
	5°C	10°C	15°C	20°C	25°C
TB-1	2.45 ± 0.07	2.75 ± 0.02	3.30 ± 0.07	3.76 ± 0.12	-
TB-2	3.31 ± 0.11	3.95 ± 0.09	4.39 ± 0.06	5.30 ± 0.07	-
PB-1	2.85 ± 0.05	3.02 ± 0.09	3.40 ± 0.04	3.95 ± 0.02	-
PB-2	3.56 ± 0.05	4.02 ± 0.14	4.60 ± 0.02	5.85 ± 0.08	-
PB-4	1.92 ± 0.03	2.16 ± 0.05	2.53 ± 0.08	2.76 ± 0.04	3.16 ± 0.12
PB-5	2.07 ± 0.08	2.22 ± 0.06	2.63 ± 0.05	2.97 ± 0.08	3.38 ± 0.11

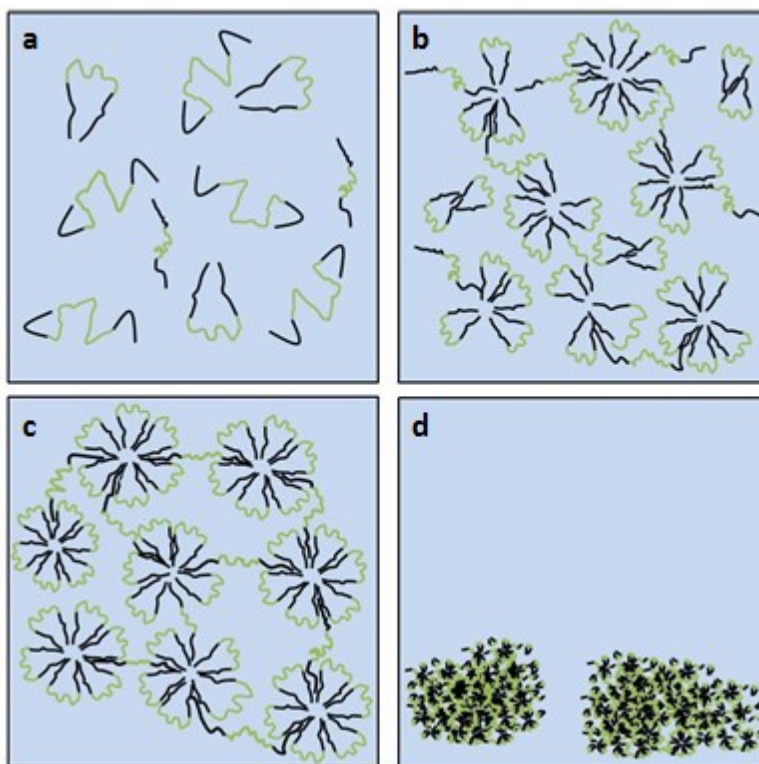


Figure 3.16: Possible micellar gelation schemes for B-A-B, C-B-A-B-C types of copolymers in water during the thermoreversible phase transition. (a) 4 °C, solution phase, (b) 25 °C, polymer solution is clear but polymer self-assembles to form micelles, (c) 37 °C, formation of intermicellar bridges resulting in gel formation, and (d) 50 °C, dehydration of PCL segments to water phase resulting in precipitation.

Conclusion

Compositions of PCL-PEG-PCL (B-A-B), PLA-PCL-PEG-PCL-PLA (C-B-A-B-C) and PEG-PCL-PLA-PCL-PEG (A-B-C-B-A) block copolymers were successfully synthesized and evaluated for their utility as an injectable *in situ* hydrogel forming depot for controlled ocular protein delivery. PB copolymers exhibit significantly reduced crystallinity. It is anticipated that biodegradability of these novel copolymers is significantly improved relative to TB copolymers. PB copolymers with A-B-C-B-A block arrangements are easy to handle at room temperature. Cell viability and biocompatibility studies confirmed that PB copolymers may be considered safe biomaterials for ocular delivery. More importantly, PB copolymers also exhibit significant sustained release of IgG relative to TB copolymers. These outcomes clearly suggest that a PB copolymer based controlled drug delivery system may serve as a promising platform for back of the eye complications.

CHAPTER 4

SUSTAINED DELIVERY OF PROTEINS EMPLOYING NOVEL PENTABLOCK COPOLYMER BASED NANOPARTICULATE SYSTEM FOR THE TREATMENT OF POSTERIOR SEGMENT OCULAR DISEASES

Rationale

A considerable amount of research has been carried out for the development of peptide- or protein-encapsulated, sustained delivery formulations for the treatment of posterior segment diseases such as wet AMD and DR. However, physical and chemical instability, and rapid enzymatic degradation of protein therapeutics are few of the many challenges encountered by formulation scientists during the development of controlled release formulation. To date, biodegradable micro- and nanoparticles (NPs) are proven to be the most promising carrier systems that provide peptide/protein asylum against catalytic enzymes, allowing improvement in their biological half-lives.

Among all biomaterials, biodegradable polymers such as PLA [188], PCL-PEG-PCL [189], and PLGA [190] have been extensively investigated for the development of peptide- or protein-encapsulated NPs. It is widely reported that protein/peptide can undergo a loss of biological activity during formulation, storage and/or release [191-194]. Presence of hydrophobic/hydrophilic interface [195], reduction in pH during polymer degradation [196], and polymer degradation product-induced acylation processes [183, 197] are potential sources of irreversible aggregation or inactivation of therapeutic proteins inside the PLA, PLGA, PCL-PLA-PCL and PLA-PEG-PLA based delivery systems. It is imperative to note that any change in protein/peptide structure, either physically or chemically, may cause toxicity or immunogenicity and inactivity (loss of pharmacological effect). The consecutive response to

antibody directs safety concerns and thus restricts efficacy of subsequent applications [198]. Therefore, there is an urgent need to develop a biodegradable sustained-release system, which does not compromise protein stability during release. In addition, sustained release of therapeutic agents for longer durations can eliminate repeated intravitreal injections.

PB copolymers with thermosensitive properties, studied in chapter 3 exhibited sustained release of IgG up to only ~15-20 days. Sustained release for lower duration and significantly higher burst release exhibited by thermosensitive gels are unfavorable. Hence in this study, we have investigated PB copolymers with block arrangements of PLA-PCL-PEG-PCL-PLA and PGA-PCL-PEG-PCL-PGA for the development of protein-loaded NPs which can sustain drug release for significantly longer duration of time (~60 days). We have synthesized and characterized PB copolymer variants to investigate effects of molecular weight, isomerism and polymer composition on various parameters such as entrapment efficiency, drug loading, and *in vitro* drug release profiling. Human immunoglobulin G (IgG, 150 kDa), a full length antibody was utilized as model protein which is very similar to bevacizumab.

Materials and methods

Materials

PEG (4 kDa), stannous octoate, ϵ -caprolactone, polyvinylalcohol (PVA), lipopolysaccharide were procured from Sigma-Aldarich (St. Louis, MO; USA). L-lactide and D,L-lactide were purchased from Acros organics (Morris Plains, NJ; USA). Micro-BCATM was obtained from Fisher Scientific. Mouse TNF- α , IL-6 and IL-1 β (Ready-Set-Go) ELISA kits were purchased from eBioscience Inc. Lactate dehydrogenase estimation kit and CellTiter 96[®] AQ_{ueous} non-radioactive cell proliferation assay (MTS) kit were obtained from Takara Bio

Inc. and Promega Corp., respectively. All other reagents utilized in this study were of analytical grade. ARPE-19 and RAW-264.7 cells were procured from the American type culture collection (ATCC).

Methods

Synthesis of TB and PB copolymers

The TB and PB copolymers were synthesized by ring-opening bulk copolymerization [176]. In brief, PCL-PEG-PCL copolymers were synthesized by copolymerization of ϵ -caprolactone on the hydroxyl ends of PEG (4 kDa). In this reaction, PEG was utilized as macroinitiator and stannous octoate (0.5 wt%) as a catalyst. To synthesize PCL-PEG-PCL, a pre-determined amount of PEG was vacuum-dried for 4 h followed by addition of ϵ -caprolactone and catalyst. Reaction was carried out in a closed vessel under nitrogen, at 130 °C for 36 h. The reaction mixture was solubilized in DCM followed by precipitation in ice-cold diethyl ether. The precipitated polymer was vacuum-dried to remove residual solvent and characterized to evaluate the reaction yield. The structure and molecular weight of TB copolymers were confirmed by ¹H-NMR and GPC.

In order to prepare PB copolymers, a predetermined amount of TB copolymer was utilized as macroinitiator and stannous octoate (0.5 wt%) as catalyst. For the synthesis of PB-A and PB-D, L-lactide was polymerized on the hydroxyl ends of TB copolymer. Similarly, PB-B/PB-E, and PB-C/PB-F were synthesized by polymerizing D,L-lactide and glycolide, respectively. For the synthesis of PB-A, PB-B, PB-D and PB-E, the reaction was carried out at 130 °C for 36 h. However, to synthesis of PB-C and PB-F, reaction was performed at 200 °C for 24 h.

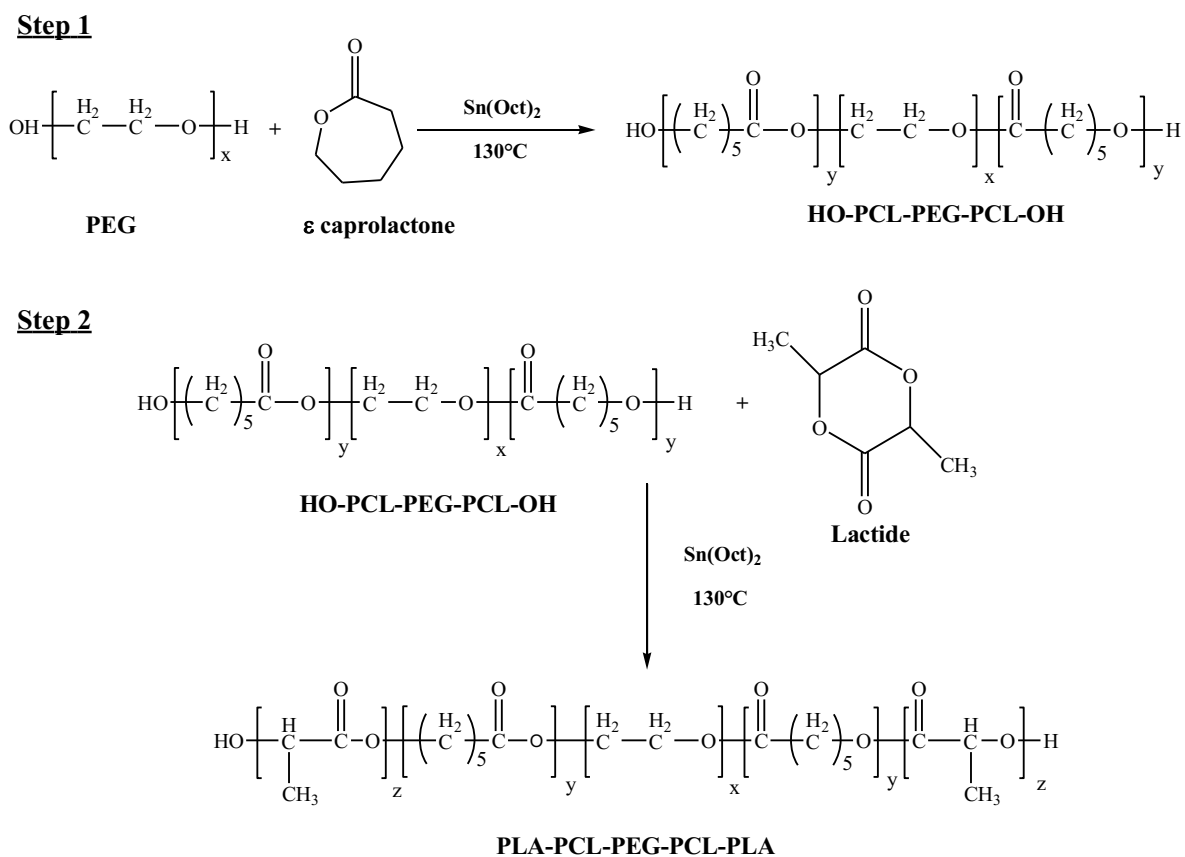


Figure 4.1: Synthesis scheme for TB-A, TB-B, PB-A, PB-B, PB-D and PB-E.

Step 2

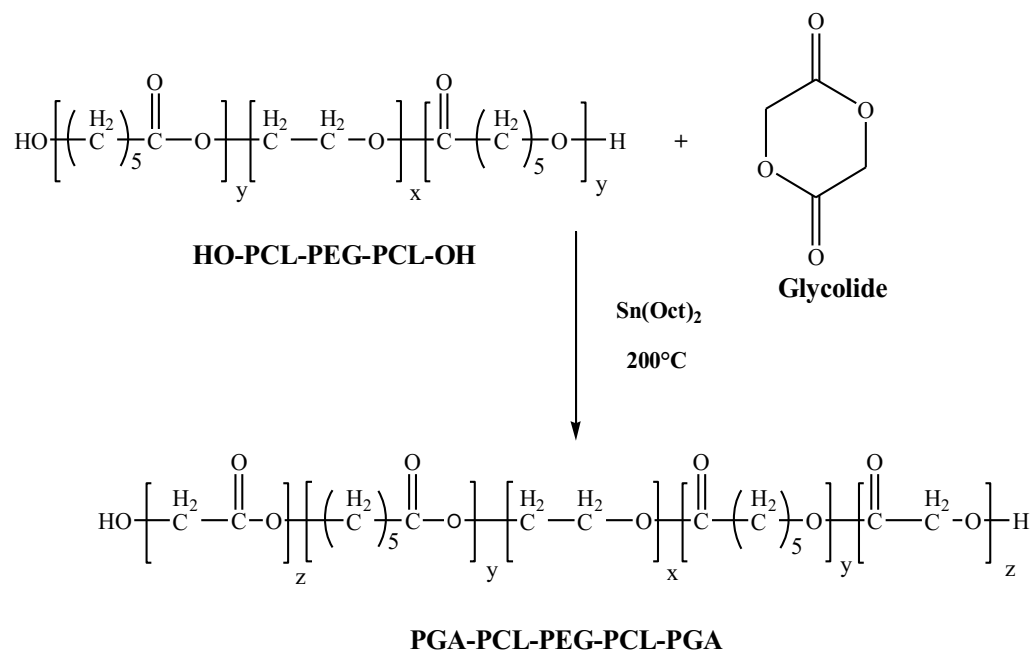


Figure 4.2: Synthesis scheme for PB-C and PB-F. Note: For synthesis of PB-C and PB-F step 1 was similar as described in Figure 4.1.

In order to remove catalyst and unreacted monomers, the reaction mixture was dissolved in DCM and precipitated by addition of ice-cold diethyl ether. Polymers were vacuum-dried and characterized for their structure and polydispersity by employing $^1\text{H-NMR}$ and GPC as analytical techniques. Purified polymers were stored at $-20\text{ }^\circ\text{C}$ until further use. Reaction scheme for the synthesis of TB-A, TB-B, PB-A, PB-B, PB-D and PB-E are described in Figure 4.1 whereas for the synthesis of PB-C/PB-F are described in Figure 4.2.

Characterization of polymers

Polymers were characterized for purity, molecular weight and polydispersity by $^1\text{H-NMR}$ and GPC. Polymers were further evaluated by powder XRD to examine their crystalline nature.

$^1\text{H-NMR}$

To perform $^1\text{H-NMR}$ spectroscopy, polymeric material was dissolved in CDCl_3 and analyzed on a Varian-400 MHz NMR spectrometer. Purity and molecular weight (M_n) of the polymers were confirmed from the $^1\text{H-NMR}$ spectrum.

GPC

To further confirm purity, molecular weight and polydispersity, polymeric samples were analyzed via GPC equipped with refractive index detector (Waters 410). Briefly, 5 mg of polymeric material was dissolved in tetrahydrofuran (THF). THF was utilized as eluting solvent at the flow rate of 1 mL/min whereas separation was carried out on Styragel HR-3 column. Polystyrene samples with narrow molecular weight distribution were utilized as standards.

X-ray diffraction (XRD) analysis of copolymers

Samples were analyzed for diffraction patterns to understand the effects of polymer composition (TB vs PB), molecular weight, and block types (P(L)LA, P(DL)LA and PGA) on the crystallinity of copolymers. MiniFlex automated X-ray diffractometer (Rigaku, The Woodlands, Texas) with Ni-filtered Cu- α radiation (30 kV and 15 mA) was employed to study the diffraction patterns. XRD analysis was carried out at room temperature.

In vitro cytotoxicity studies

Cell culture

RAW-264.7 cells were cultured and maintained in Dubelcco's modified Eagle medium (DMEM) supplemented with 10% FBS, 100 mg/L of streptomycin and 100 U/L of penicillin. Human retinal pigment epithelial cells (ARPE-19) were cultured and maintained according to the protocol reported from our lab [199]. In brief, ARPE-19 cells were cultured in DMEM/F-12 medium containing 10% heat-inactivated fetal bovine serum (FBS), 29 mM of sodium bicarbonate, 15 mM of HEPES, 100 mg/L of streptomycin and 100 U/L of penicillin. Both cell lines were maintained in humidified atmosphere at 37 °C and 5% CO₂.

Lactate Dehydrogenase (LDH) assay

The cytotoxicity of block copolymers were evaluated according to previously published protocol with minor modifications [200]. Briefly, different concentrations (1-20 mg/mL) of TB and PB copolymers were prepared in acetonitrile (ACN). A 100 μ L of solutions was aliquoted in each well of 96-well cell culture plates. In order to evaporate ACN and to sterilize block copolymers, cell culture plates were exposed overnight under UV light (laminar flow). Once the ACN is evaporated, 1.0×10^4 of RAW 264.7 cells were seeded in each well and incubated for 48 h at 37 °C and 5% CO₂ in humidified atmosphere. Followed by

appropriate incubation, cell supernatant were analyzed for the levels of LDH by LDH detection kit. LDH assay was performed according to the supplier's protocol. Samples were analyzed at 450 nm by 96-well plate reader. Amount of released LDH is directly proportional to cytotoxicity of the polymers. In this study, more than 10% of LDH release was considered as cytotoxic. To evaluate toxicity of block copolymers on retinal cell line, the similar experiment was performed with ARPE-19 cells. LDH release (%) was calculated by employing following equation,

$$LDH\ release(\%) = \frac{Abs.\ of\ Sample - Abs.\ of\ negative\ control}{Abs.\ of\ positive\ control - Abs.\ of\ negative\ control} * 100 \quad \dots\ Eq.\ 4.1$$

MTS assay

In order to confirm safety of PB copolymers, *in vitro* cell viability (MTS) assay was performed. MTS assay was carried out according to previously published protocol with minor modifications [185]. Different concentrations of block copolymer solutions were prepared, aliquoted and sterilized according the procedure mentioned in previous section. After sterilization, RAW-264.7 cells at the density of 1.0×10^4 cells per well were seeded in 96-well plate. Cells were incubated for 48 h at 37 °C and 5% CO₂ in humidified atmosphere. After incubation, cell culture medium was replaced with 100 μL of serum free medium containing 20 μL of MTS solution. Cells were further incubated at 37 °C and 5% CO₂ for 4 h. Absorbance of each well was determined at 450 nm. Polymer concentrations at which more than 90% of cell viability was observed, were considered as non-toxic. Percent cell viability was estimated by following equation. The similar experiment was repeated with ARPE-19 cells.

$$Cell\ viability(\%) = \frac{Abs.\ of\ Sample - Abs.\ of\ negative\ control}{Abs.\ of\ positive\ control - Abs.\ of\ negative\ control} * 100 \quad \dots\ Eq.\ 4.2$$

In vitro biocompatibility studies

As described in previous section, different concentrations (1-20 mg/mL) of block copolymer solutions were prepared in acetonitrile. A 200 μ L aliquot of polymer solution was added in each well of 48-well cell culture plate. These plates were incubated overnight under UV light (laminar flow) for sterilization as well as for evaporation of ACN. After sterilization, RAW-264.7 cells were plated at the cell density of 5.0×10^4 per well. Cells were exposed to polymer for 48 h at 37 °C and 5% CO₂. After incubation, cell supernatant was analyzed for the quantification of three different cytokines, i.e., TNF- α , IL-6 and IL-1 β . Levels of cytokines were estimated by ELISA method. ELISA was performed according to the manufacturer's instruction. Calibration curves for TNF- α , IL-6 and IL-1 β were prepared in the range of 10-750 pg/mL, 5-500 pg/mL and 10-500 pg/mL, respectively.

Preparation of NPs

NPs were prepared by W₁/O/W₂ double emulsion solvent evaporation method according to previously published protocol with minor modifications [201]. Briefly, predetermined amount of IgG was dissolved in water (1 mL) containing 50 μ L of Tween-80 (W₁ phase) and 100 mg of respective block copolymer was dissolved in 4 mL of dichloromethane (DCM) comprising 50 μ L of Span-20 (organic phase). W₁/O primary emulsion was prepared by drop-wise addition of W₁ phase in organic phase under constant sonication for 1 min at 4 W output. Immediately after sonication, W₁/O primary emulsion was added (drop-wise) in 20 mL of 2% PVA solution (W₂) and sonication was applied for 4 min at 5 W output. W₁/O/W₂ double emulsion was stirred for 30 min at room temperature followed by evaporation of DCM under vacuum. The resulting NPs were centrifuged at 20000 rpm for 30 min at 4 °C followed by two washing cycles with distilled deionized water. NPs were freeze-

dried in 5% mannitol solution and stored at -20 °C until further characterization. NPs were prepared utilizing three different drug to polymer ratios i.e., 1:10, 1:15 and 1:20. Freeze-dried NPs were characterized for particle size, EE, DL and *in vitro* drug release behavior.

Characterization of NPs

Particle size

NPs (1 mg/mL) were suspended in DDW and subjected to particle size analysis. Particle size was evaluated at room temperature and 90° scattering angle utilizing Zeta sizer (Zetasizer Nano ZS, Malvern Instruments Ltd, Worcestershire, UK). All the samples were analyzed in triplicate and average particle size were reported in ± SD.

Entrapment efficiency (EE %) and drug loading (DL %)

IgG-loaded freeze-dried NPs were examined for the estimation of DL and EE. EE was calculated by analyzing supernatants (collected during NP preparation) with Micro BCA™ protein estimation kit. To evaluate DL, 2 mg equivalent drug-encapsulated NPs were dissolved in 200 µL of DMSO. The resulting solution was subjected for protein estimation via UV absorbance spectroscopy. A standard curve of IgG ranging from 31.25 to 2000 µg/mL was prepared in DMSO. EE (%) and DL (%) were estimated according to the following equations.

EE (%) was calculated with eq. 4.3

$$\%EE = \left(1 - \frac{\text{Amount of drug in supernatant}}{\text{Total amount of drug}}\right) * 100 \quad \dots\text{Eq. 4.3}$$

DL (%) was calculated by eq. 4.4.

$$\%DL = \left(\frac{\text{Amount of drug in nanoparticles}}{\text{Total amount of drug and polymer}}\right) * 100 \quad \dots\text{Eq. 4.4}$$

In vitro release studies

For *in vitro* drug release studies, 1 mg protein equivalent IgG-encapsulated NPs were dispersed in 1 mL of 0.1 M phosphate buffer saline (pH - 7.4). The NPs suspension was incubated in water bath maintained at 37 °C. In order to collect release samples, at pre-determined time intervals NPs suspension were centrifuged at 13000 rpm for 30 min and 4 °C. A 200 µL of clear supernatant was withdrawn for protein estimation and replaced with same volume of 0.1 M PBS. NPs were then resuspended and release was continued at 37 °C. *In vitro* release experiments were repeated in triplicates and mean value \pm SD was expressed as cumulative % drug released with time.

Stability estimation of IgG

Secondary structure analysis by circular dichroism (CD) spectroscopy

To confirm the stability of secondary structure of released IgG, CD spectroscopy was employed as an analytical technique. CD analysis was performed using Jasco 720 spectropolarimeter at 25 °C. CD spectra were recorded at scanning speed of 5 nm/min between the range of 200 to 250 nm utilizing 1 cm cell, and 1 nm band width. CD measurements were described as molar ellipticity $[\theta]$. A CD spectrum of PBS was used as blank.

Results and discussion

In this study, we have prepared novel PB copolymers which are composed of FDA approved polymer blocks such as PEG, PCL, and PLA/PGA. Each block plays an important role such as presence of PEG helps to improve stability of NPs by reducing NP aggregation, and also prevents phagocytosis by macrophages resulting in improved half-life. PCL is a slowly degrading, semi-crystalline polymer which improves protein loading in NPs and also sustains drug release for longer duration of time. Such a slow degradation is also not

advantageous particularly for intravitreal injections. It is very important for formulation scientists to synchronize polymer degradation profile with the drug release profile in order to avoid accumulation of empty formulation in the limited space of the vitreous cavity. Previous reports suggest that poor degradation of PCL is attributed to its crystalline nature, hence reduction in the crystallinity of PCL may improve its hydrolytic and enzymatic degradation [202]. According to Huang, et al. conjugation of PLA/PGA to PCL chains can significantly reduce its crystallinity resulting in faster degradation of PCL [203].

Synthesis and characterization of various TB and PB copolymers

TB and PB copolymers were successfully synthesized by ring-opening bulk copolymerization of ϵ -caprolactone, and L-lactide/D,L-lactide/glycolide. In the first step, TB copolymers (PCL-PEG-PCL) with different molecular ratios of PEG/PCL were synthesized utilizing PEG (4kDa) as macroinitiator and stannous octoate as catalyst. Purified TB copolymers were used as macroinitiator for the synthesis of PB copolymers. Purity and molecular weight (M_n) of block copolymers were confirmed by $^1\text{H-NMR}$ spectroscopy. As described in Figure 4.3, typical $^1\text{H-NMR}$ characteristic peaks of PCL units were observed at 1.40, 1.65, 2.30 and 4.06 ppm representing methylene protons of $-(\text{CH}_2)_3-$, $-\text{OCO-CH}_2-$, and $-\text{CH}_2\text{OOC-}$, respectively. A sharp proton peak observed at 3.65 ppm was attributed to methylene protons ($-\text{CH}_2\text{CH}_2\text{O-}$) of PEG.

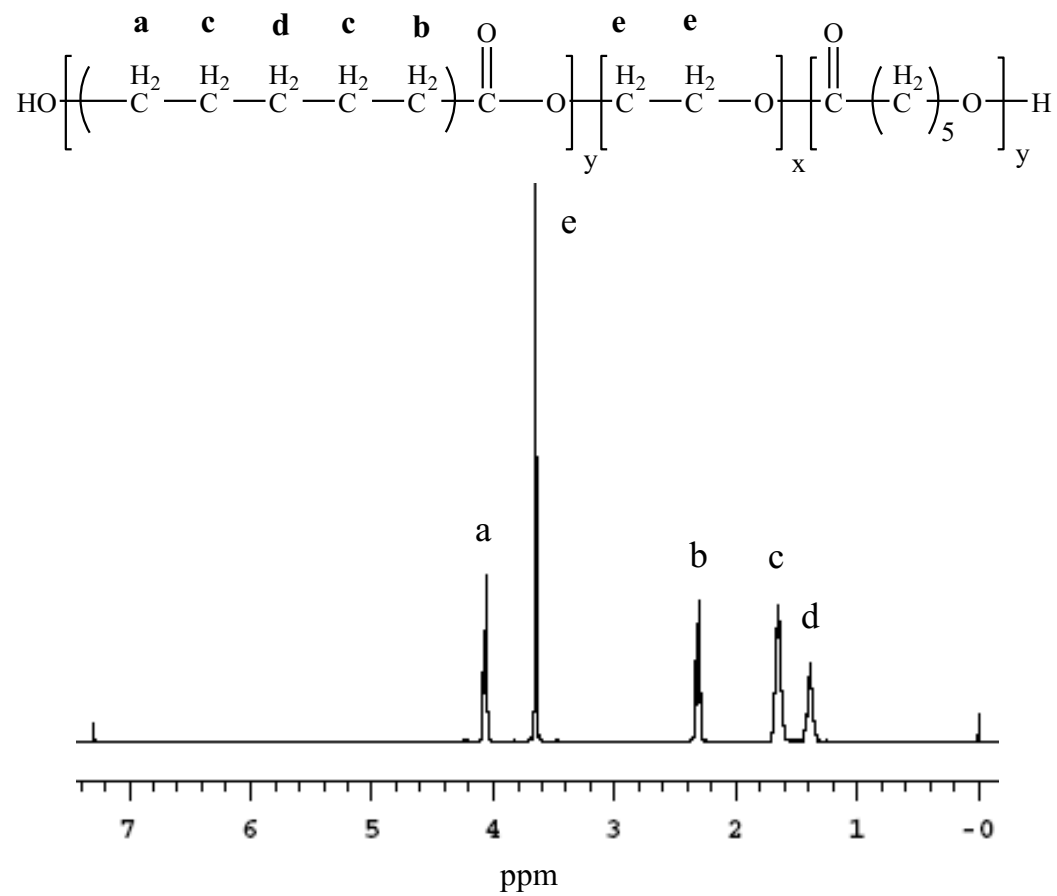


Figure 4.3: $^1\text{H-NMR}$ of TB-B (PCL₇₀₀₀-PEG₄₀₀₀-PCL₇₀₀₀).

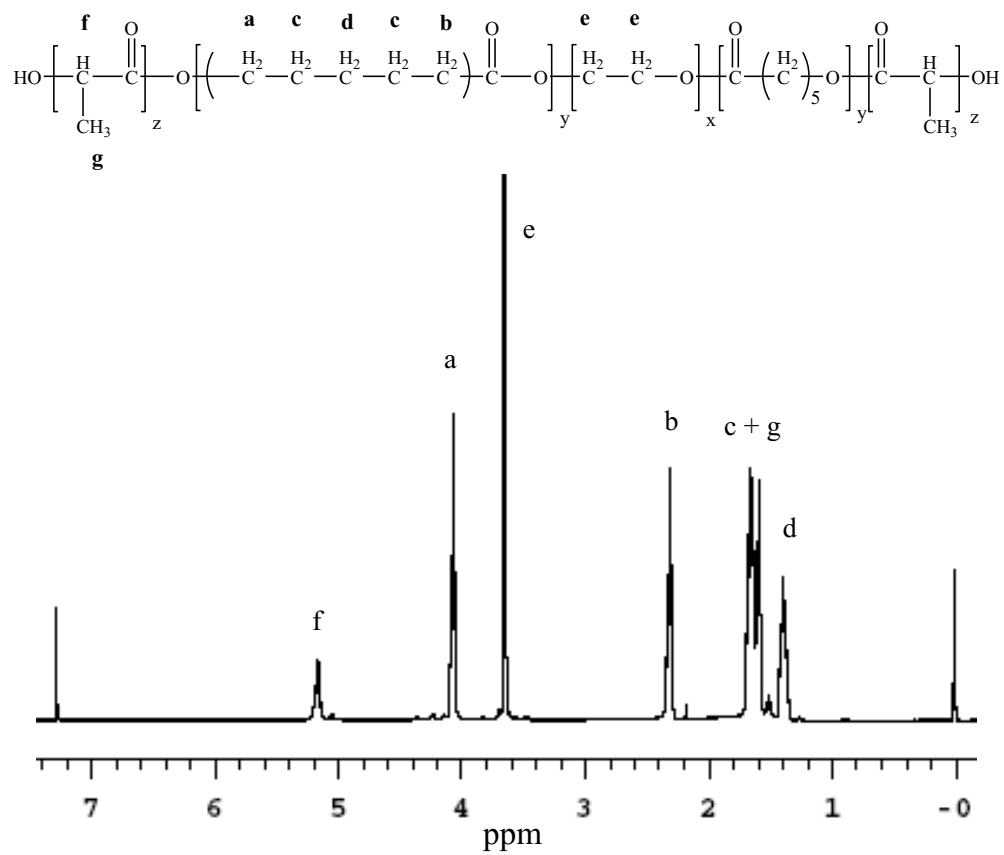


Figure 4.4: ¹H-NMR of PB-A (PL(L)A₂₀₀₀-PCL₅₀₀₀-PEG₄₀₀₀-PCL₅₀₀₀-PL(L)A₂₀₀₀).

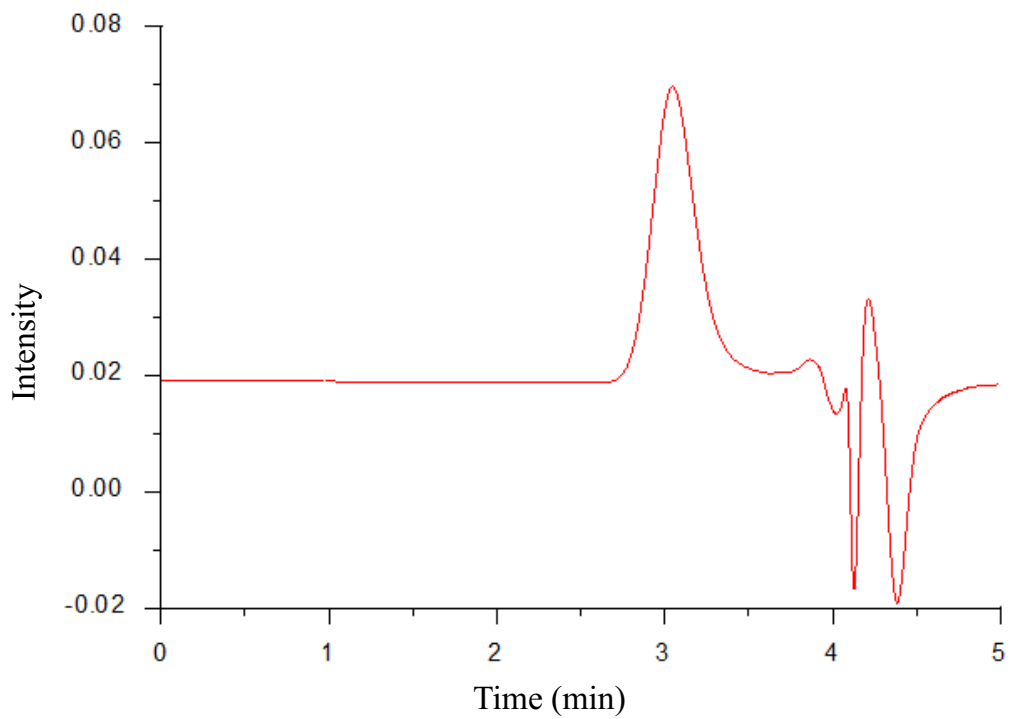


Figure 4.5: Gel permeation chromatogram of PB-A copolymer.

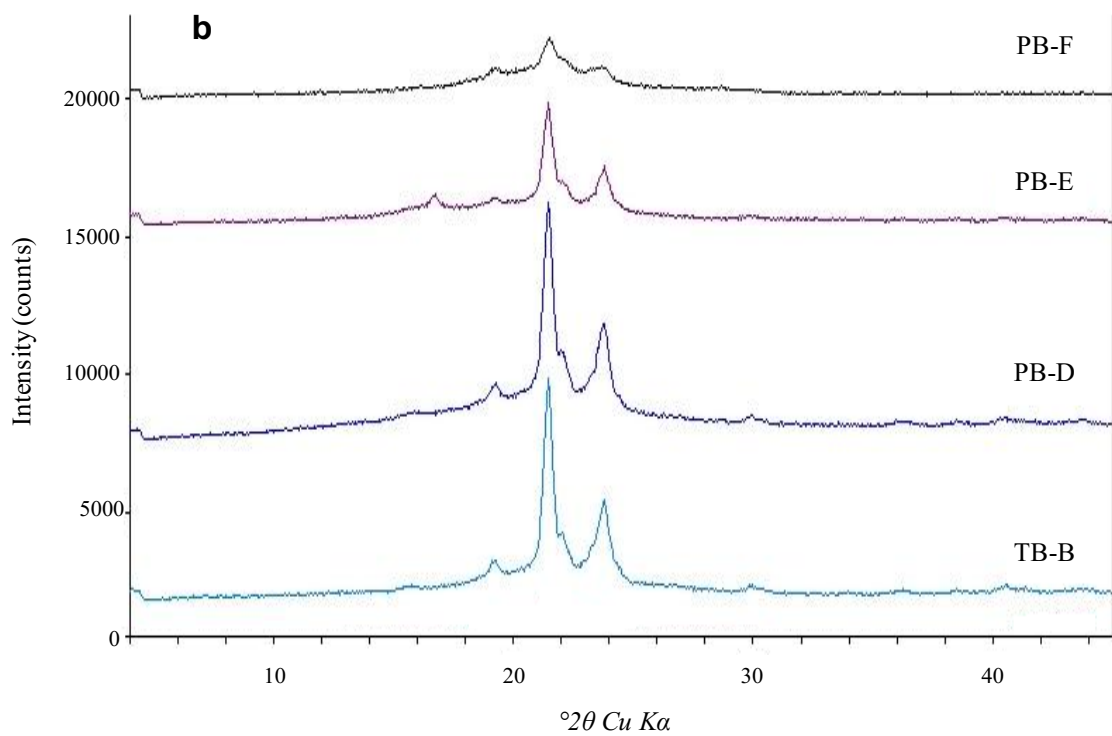
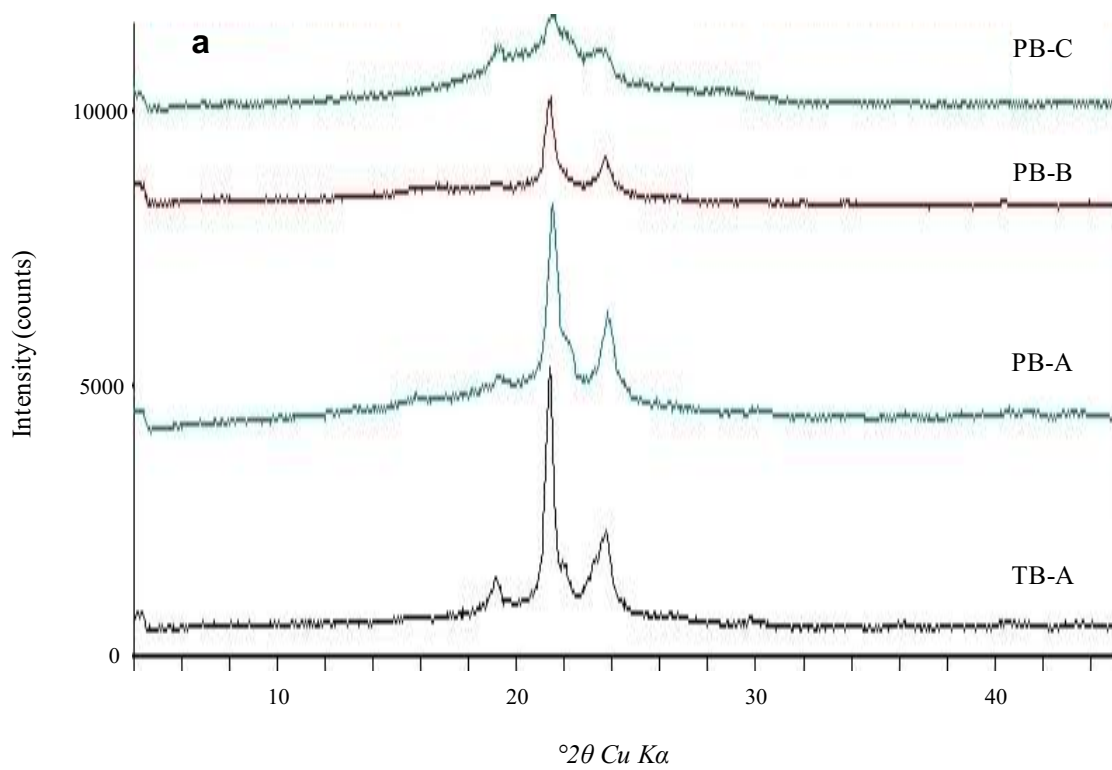


Figure 4.6: XRD patterns of various TB and PB copolymers where (a) TB-A, PB-A, PB-B, and PB-C, (b) TB-B, PB-D, PB-E, and PB-F.

Table 4.1: List of TB and PB copolymers studied

Code	Structures	PLA/PCL/PEG or PGA/PCL/PEG	Total Mn^a (theoretical)	Total Mn^b (calculated)	Total Mn^c (calculated)	Mw^c (GPC)	PD ^c
TB-A	PCL ₅₀₀₀ -PEG ₄₀₀₀ -PCL ₅₀₀₀	2.5/1	14000	13350	10990	14520	1.32
TB-B	PCL ₇₀₀₀ -PEG ₄₀₀₀ -PCL ₇₀₀₀	3.5/1	18000	16650	14560	18800	1.29
PB-A	PL(L)A ₂₀₀₀ -PCL ₅₀₀₀ -PEG ₄₀₀₀ -PCL ₅₀₀₀ -PL(L)A ₂₀₀₀	1/2.5/1	18000	16950	14990	20800	1.39
PB-B	PL(DL)A ₂₀₀₀ -PCL ₅₀₀₀ -PEG ₄₀₀₀ -PCL ₅₀₀₀ -PL(DL)A ₂₀₀₀	1/2.5/1	18000	16880	13810	19560	1.42
PB-C	PGA ₂₀₀₀ -PCL ₅₀₀₀ -PEG ₄₀₀₀ -PCL ₅₀₀₀ -PGA ₂₀₀₀	1/2.5/1	18000	17210	13450	19210	1.43
PB-D	PL(L)A ₃₀₀₀ -PCL ₇₀₀₀ -PEG ₄₀₀₀ -PCL ₇₀₀₀ -PL(L)A ₃₀₀₀	1.5/3.5/1	24000	21350	17640	23830	1.35
PB-E	PL(DL)A ₃₀₀₀ -PCL ₇₀₀₀ -PEG ₄₀₀₀ -PCL ₇₀₀₀ -PL(DL)A ₃₀₀₀	1.5/3.5/1	24000	21330	18210	24940	1.37
PB-F	PGA ₃₀₀₀ -PCL ₇₀₀₀ -PEG ₄₀₀₀ -PCL ₇₀₀₀ -PGA ₃₀₀₀	1.5/3.5/1	24000	21290	16180	23210	1.43

- a. Theoretical value, calculated according to the feed ratio
b. Calculated from ¹H-NMR results
c. Determined by GPC analysis

¹H-NMR spectra of PB copolymers with PLA as terminals (PB-A, PB-B, PB-D and PB-E) exhibited two additional peaks at 1.50 (-CH₃) and 5.17 (-CH-) ppm (Figure 4.4). However, PB-C and PB-E exhibited cluster of singlets between 4.6 to 4.9 ppm representing methylene protons (-CH₂-) of PGA units (data not shown). The [EO]-[CL]-[LA] molar ratio of the final products were calculated from the integration values of PEG signal at 3.65 ppm, PCL signal at 2.30 ppm and PLA signal at 5.17 ppm. In case of PB-C and PB-F copolymers, proton signals between 4.6 to 4.9 ppm were utilized for the calculation of molar ratio.

In order to confirm the molecular weight and purity, all the block copolymers were further analyzed by GPC. Block copolymers exhibited a monodistributed molecular weight and absence of any other homopolymers such as PEG, PCL, PLA or PGA. A typical GPC chromatogram of PB-A copolymer is depicted in Figure 4.5. Moreover, calculated molecular weights were very close to the feed ratio, and polydispersity of block copolymers were well below 1.45 indicating narrow distribution of molecular weights. Table 4.1 represents theoretical molecular weights, calculated molecular weights (¹H-NMR and GPC) and polydispersity. The Mn values obtained from ¹H-NMR were noticeably higher relative to the Mn values observed from GPC analysis. This observation may attributed to the difference in hydrodynamic diameter of block copolymers relative to parent homopolymers. As reported in Table 4.1, observed molecular weights were very similar to theoretical molecular weights. For the ease, in the following text, theoretical molecular weights will be mentioned instead of calculated molecular weights.

Reports published elsewhere described that covalent conjugation between PLA and PCL, significantly reduces the crystallinity of PCL [176, 204-207]. However, effects of various isomers of PLA (L or D,L) and also an effect of PGA on the crystallinity of PCL-PEG-PCL

tri-block copolymers are not reported, yet. Hence, we have analyzed TB and PB copolymers for their XRD patterns. PLA with D,L-lactide has amorphous structure whereas PLA with L-lactide is a semi-crystalline [202]. Both polymers may act differently to reduce the crystallinity of PCL. This may have direct effect on various formulation parameters such as EE, DL and *in vitro* release. Moreover, we have also evaluated the effect of PGA to reduce the crystallinity of PCL-PEG-PCL TB copolymers.

Figure 4.6 describes the XRD patterns of various TB and PB copolymers. As reported in Figure 4.6a, TB-A exhibited two strong characteristic crystalline peaks of PCL blocks at diffraction angles (2θ) of 21.5° and 23.8° . L-lactide containing PB copolymer (PB-A) exhibited reduced intensity of PCL peaks, which suggest that conjugation of PLA (L-lactide) has significantly diminished the crystallinity of TB-A. Noticeably, conjugation of D,L-lactide has further reduced the crystalline peaks of PCL blocks. These results may be attributed to the fact that PLA with L-lactide is more crystalline than PLA with D,L-lactide. Moreover, PLA with D,L-lactide have a random arrangement of L and D-lactide in their polymer chain which does not allow systemic arrangement of polymer chains, resulting in reduced crystallinity. Surprisingly, PB-C demonstrated amorphous structure suggesting that conjugation of PGA at the termini of TB-A have totally eliminated crystallinity of PCL. To further confirm this behavior, we have evaluated the solid states of TB-B, PB-D, PB-E and PB-F by XRD. Results described in Figure 4.6b demonstrated similar pattern, where PB-F with PGA a block was amorphous in nature. PLA with L-lactide reduced peak intensity of PCL up to some extent, while PLA with D,L-lactide has significantly diminished crystalline peaks.

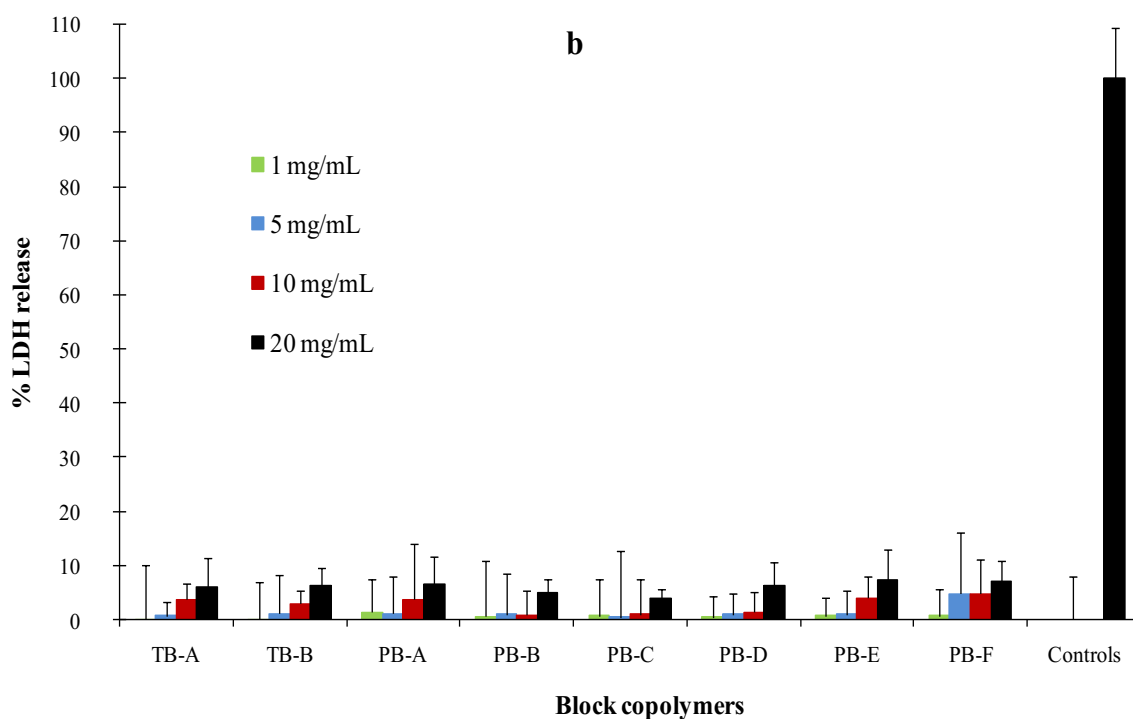
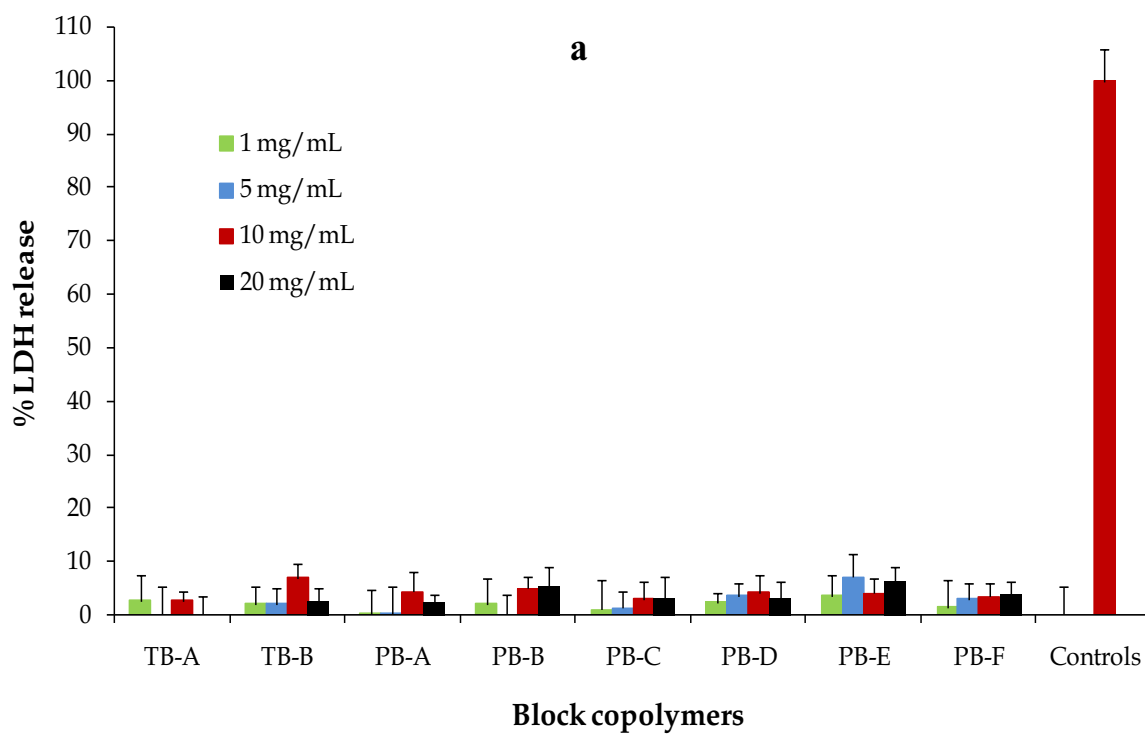


Figure 4.7: *In vitro* cytotoxicity (LDH) assay of various block copolymers at different concentrations were performed on (a) RAW 264.7 and (b) ARPE-19 cells.

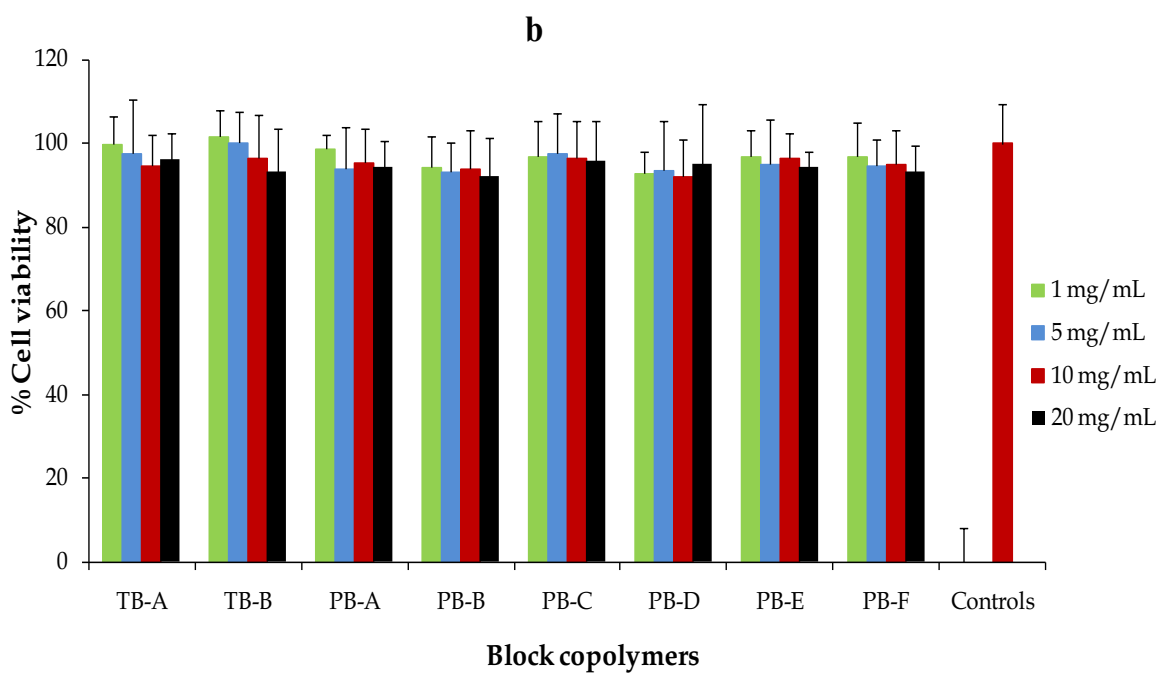
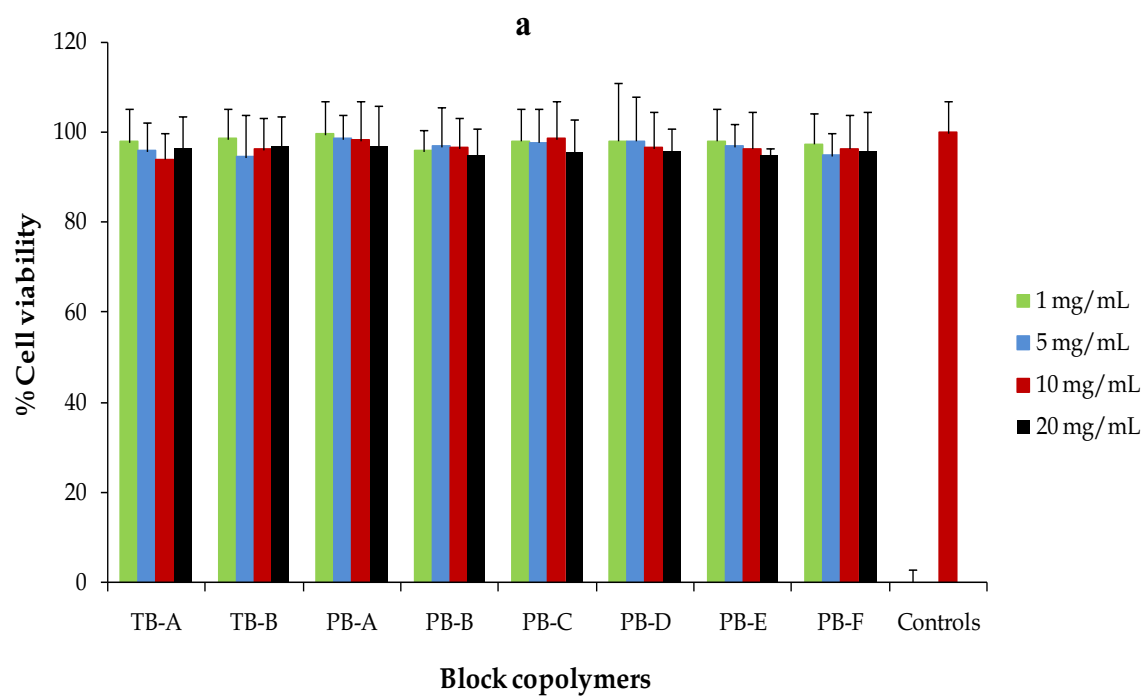


Figure 4.8: *In vitro* cell viability (MTS) assay of various block copolymers at different concentrations were performed on (a) RAW 264.7 and (b) ARPE-19 cells.

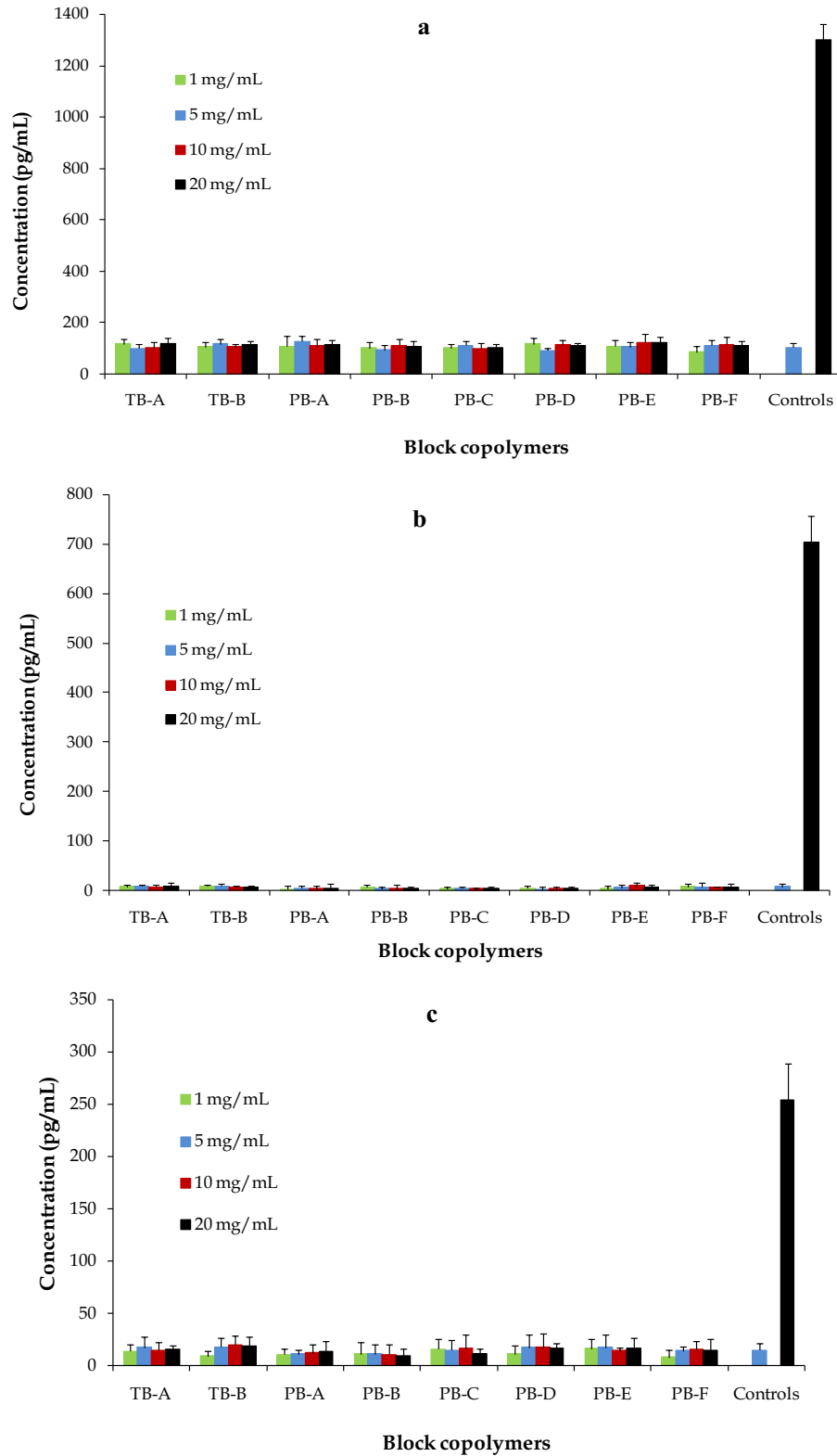


Figure 4.9: *In vitro* biocompatibility of block copolymers were evaluated by estimating the levels of (a) TNF- α , (b) IL-6 and (c) IL-1 β in the supernatants of polymer treated RAW 264.7 cells.

In vitro cytotoxicity studies

LDH assay

Lactate dehydrogenase (LDH) is the cytosolic enzyme, secreted in the culture medium upon the rupture of cell membrane. As the cell membrane is the potential site for polymer-cell interaction, measuring the amount of LDH release has been the preferred way to estimate the membrane damage and hence the cytotoxicity of polymer. As described in Figure 4.7a (RAW-264.7 cells) and Figure 4.7b (ARPE-19), LDH release upon the exposure of block copolymers were less than 10% at any given concentrations and also comparable with negative control indicating negligible or no toxicity.

MTS assay

In order to confirm the results observed in cytotoxicity (LDH assay) studies, the safety of block copolymers were further evaluated by MTS assay. Block copolymers exhibited more than 90% cell viability upon exposure to various concentrations ranging from 1-20 mg/mL (Figures 4.8a and 4.8b). Moreover, results were comparable to the negative control indicating no toxicity of PB copolymers. Results observed in LDH and MTS assays clearly indicated that block copolymers are very safe for the intravitreal applications.

In vitro biocompatibility studies

It is also important to confirm that newly synthesized PB copolymers are not producing inflammatory responses upon intravitreal administration. *In vitro* assessment for release of cytokines upon exposure to polymer is a quick, cost effective and reliable technique to examine biocompatibility of polymers. RAW-264.7 cells, is a well-established *in vitro* cell culture model to study inflammatory responses of polymers intended for human applications. Results described in Figures 4.9a, 4.9b and 4.9c have demonstrated negligible release of TNF α , IL-6

and IL-1 β upon 24 h exposure to different concentrations of block copolymers ranging from 1-20 mg/mL. Release of any cytokines was not significantly different to their respective negative controls indicating excellent biocompatibility of block copolymers for ocular applications.

Characterization of NPs

Particle size

IgG-loaded TB and PB NPs were prepared by the W₁/O/W₂ double emulsion solvent evaporation method. As described in Tables 4.2, 4.3 and 4.4, the size of NPs were between 285 nm to 330 nm. We did not observe any significant effect of polymer composition on the particle size. Moreover, in order to understand the effect of drug to polymer ratio on particle size, we have prepared NPs with three distinct drug to polymer ratios i.e., 1:10, 1:15 and 1:20. Interestingly, a change in drug to polymer ratio did not exhibit any noticeable effect on particle size. These results suggest that particle size is highly influenced by process parameters and not by polymer:drug ratio.

Entrapment efficiency (EE) and drug loading (DL)

EE and DL are influenced by many parameters including copolymer composition (isomerism, molecular weight and polymer structure) and volumes of various phases (W₁, O and W₂). To understand the effect of copolymer compositions on DL and EE, we kept volumes of W₁, O and W₂ phases constant. In addition, we have also studied the effect of drug to polymer ratio on DL and EE. As described in Table 4.2, at respective drug to polymer ratios, TB-B NPs exhibited significantly higher DL and EE relative to TB-A NPs. PB-D, PB-E and PB-F (Table 4.3) with significantly higher molecular weight relative to PB-A, PB-B and PB-C (Table 4.4), respectively exhibited improved EE and DL.

Table 4.2: Characterization of NPs prepared TB-A and TB-B.

Structure	Drug/polymer ratio	Entrapment efficiency (%)	Loading (%)	Particle size(nm)
TB-A	1:10	27.3 ± 2.2	3.6 ± 0.3	330 ± 20
	1:15	28.2 ± 2.0	2.3 ± 0.1	320 ± 30
	1:20	29.8 ± 1.9	2.0 ± 0.2	310 ± 30
TB-B	1:10	34.7 ± 3.2 *	4.1 ± 0.3 *	320 ± 20
	1:15	33.7 ± 2.4 *	2.7 ± 0.2 *	300 ± 20
	1:20	35.7 ± 2.8 *	2.6 ± 0.2 *	300 ± 20

*significantly different than respective ratios of TB-A NPs

Table 4.3: Characterization of NPs prepared PB-A, PB-B and PB-C.

Structure	Drug/polymer ratio	Entrapment efficiency (%)	Loading (%)	Particle size(nm)
PB-A	1:10	46.8 ± 2.4 *	5.2 ± 0.3 *	320 ± 10
	1:15	49.6 ± 3.1 *	3.8 ± 0.3 *	300 ± 20
	1:20	47.7 ± 2.2 *	3.1 ± 0.2 *	300 ± 20
PB-B	1:10	51.5 ± 2.7 *	5.5 ± 0.4 *	300 ± 10
	1:15	50.4 ± 4.1 *	4.2 ± 0.4 *	290 ± 20
	1:20	53.5 ± 4.3 *	3.6 ± 0.3 *	290 ± 20
PB-C	1:10	39.7 ± 3.6	4.3 ± 0.5	310 ± 20
	1:15	41.5 ± 4.2	3.2 ± 0.2	300 ± 20
	1:20	40.3 ± 3.1	2.8 ± 0.1	290 ± 10

*significantly different than respective ratios of PB-C NPs

Table 4.4: Characterization of NPs prepared PB-D, PB-E and PB-F.

Structure	Drug/polymer ratio	Entrapment efficiency (%)	Loading (%)	Particle size(nm)
PB-D	1:10	61.1 ± 4.2 *	5.7 ± 0.9 *	310 ± 20
	1:15	61.8 ± 3.7 *	4.9 ± 0.3 *	300 ± 20
	1:20	62.7 ± 4.0 *	3.8 ± 0.1 *	290 ± 10
PB-E	1:10	63.2 ± 2.2 *	5.8 ± 0.4 *	300 ± 20
	1:15	64.9 ± 3.6 *	5.0 ± 0.3 *	300 ± 10
	1:20	65.8 ± 3.8 *	4.3 ± 0.2 *	290 ± 10
PB-F	1:10	51.0 ± 3.0	5.0 ± 0.1	320 ± 30
	1:15	52.4 ± 3.1	4.2 ± 0.2	310 ± 20
	1:20	54.1 ± 3.7	3.2 ± 0.3	290 ± 20

*significantly different than respective ratios of PB-F NPs

It is important to note that higher molecular weights of block copolymers acquire longer polymer chain with significantly higher hydrophobicity relative to lower molecular weight block copolymers. Additionally, during the step of solvent evaporation, high hydrophobicity (PB-D, PB-E and PB-F) may allow faster polymer precipitation to form NPs preventing diffusion of IgG in the external aqueous (W_2) phase.

Interestingly, we have also observed significantly higher entrapment and loading efficiency in PLA based PB copolymers (PB-A, PB-B, PB-D and PB-E) relative to PGA based PB copolymers (PB-C and PB-F). These results may be attributed to the fact that PLA is more hydrophobic compare to PGA, hence its copolymers were also hydrophobic than that of PGA based copolymers. Due to higher hydrophilicity, PB-C and PB-F copolymers may have higher interaction with W_1 and W_2 phase which may allow IgG to escape from W_1 to W_2 phase (during NP preparation) resulting in lower EE and DL. In contrast, PLA based PB copolymers may have inhibited or reduced the diffusion of IgG from W_1 to W_2 phase ensuring improved DL and EE.

In vitro release studies

In vitro drug release studies were performed to understand the effects of isomerism (P(L)LA vs P(D,L)LA), molecular weight and polymer composition. IgG-loaded NPs with drug to polymer ratio of 1:10 were utilized for release study for all polymer compositions. *In vitro* release profiles of IgG from TB-A and TB-B NPs are compared in Figure 4.10. Both NPs demonstrated bi-phasic release profile i.e., initial burst release phase followed by a phase of sustained release. Noticeably, TB-A NPs exhibited significantly higher burst release (~64%) relative to TB-B NPs (~55%). In later stage, TB-A NPs displayed ~95% of IgG release in first 15 days whereas TB-B NPs released ~87% of IgG during the duration.

To evaluate the release of IgG from TB and PB NPs, and also to compare the effect of PGA and PLA based copolymers, we have compared release profiles of IgG from PB-A, PB-B, PB-C and TB-A NPs (Figure 4.11). Our results demonstrated that TB-A NPs exhibited significantly higher burst release (~64%) than any of the PB NPs (~41-49%). Moreover, PB NPs prolonged the IgG release for more than 27 days, whereas TB-A NPs sustained it for only 15 days. In addition, we have observed a noticeable effect of polymer structure on the burst release as well as on the duration of release. Surprisingly, burst release observed for PB-C (~49%) and PB-A (~48%) NPs were significantly higher compared to PB-B (~41%). PB-C NPs released ~93% of IgG over the period of 27 days, whereas PB-A (~91%) and PB-B (~90%) NPs prolonged the release up to 31 and 35 days, respectively.

As described earlier, PGA based PB-C copolymer is relatively hydrophilic compared to the PLA based PB-A and PB-B copolymers. It is anticipated that PB-C NPs may have higher affinity for protein molecules, hence these NPs may have higher amount of surface adsorbed drug. Moreover, being hydrophilic, PB-C NPs may become easily hydrated and allow easy diffusion of water molecules in to the polymer matrix. Both the larger amount of surface adsorbed drug and higher affinity towards water may simultaneously contribute to the higher burst release and shorter sustained release period. We have also studied the effect of isomerism on drug release by comparing the release profiles of PB-A and PB-B copolymers. PB-A copolymers exhibited higher burst release with shorter sustained release phase relative to PB-B copolymers. As observed in XRD studies, PB-A copolymer is more crystalline than PB-B copolymer. In other words, polymer chains in PB-A NPs maybe in more ordered arrangement than in the PB-B NPs. Due to the ordered arrangements, during the preparation of NPs, the highly crystalline materials may form channels. Numbers and length of channels in PB-A NPs

might be higher than that of PB-B NPs. Water molecules may easily diffuse into the NPs via these channels facilitating the release of IgG. This phenomenon may also have contributed to the higher burst release and faster rate of release of IgG from PB-A NPs relative to PB-B NPs.

In order to support this reasoning, we have studied three more PB NPs i.e., PB-D, PB-E and PB-F. As described in Figure 4.12, PB-F exhibited ~92% of IgG release within 52 days with the burst release of ~43%. PB-D and PB-E demonstrated ~84% and ~87% of IgG release over the period of 55 and 59 days, respectively. However, all the PB NPs exhibited enhanced sustained release and a lower burst release compared to TB-B NPs. These results clearly indicated that PB-D, PB-E and PB-F NPs followed a similar trend to PB-A, PB-B and PB-C NPs.

To understand the effect of molecular weight on burst release as well as duration of release, we compared release profiles of PB-A and PB-D NPs (Figure 4.13a), PB-B and PB-E NPs (Figure 4.13b), and PB-C and PB-F NPs (Figure 4.13c). As discussed earlier, an increase in molecular weight of hydrophobic segments (PCL-PLA) also enhances hydrophobicity and polymer chain length. Hydrophobic copolymers may have less affinity with water and hence restrict the hydration of NPs. This may have resulted in less diffusion of water in NPs leading to the prolonged release of IgG. Moreover, longer chain length of polymers may have increased the mesh-like structure and reduced the effective porosity of NPs resulting in longer path for diffusion of IgG from NPs. In addition, reports published elsewhere suggest that with larger molecular weights, there is a slower rate of polymer degradation [208]. Therefore, PB-D, PB-E and PB-F may also degrade more slowly compared to PB-A, PB-B and PB-C, respectively, resulting in a slower rate of IgG release.

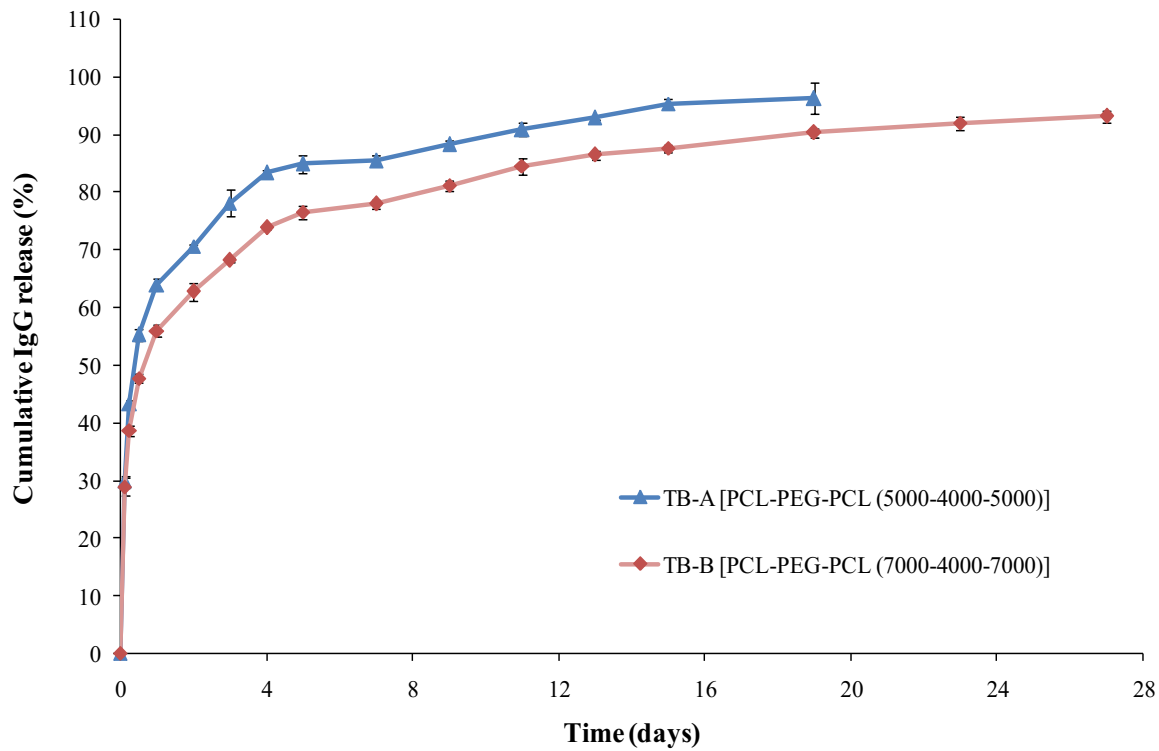


Figure 4.10: *In vitro* release of IgG from NPs prepared with TB-A and TB-B block copolymers.

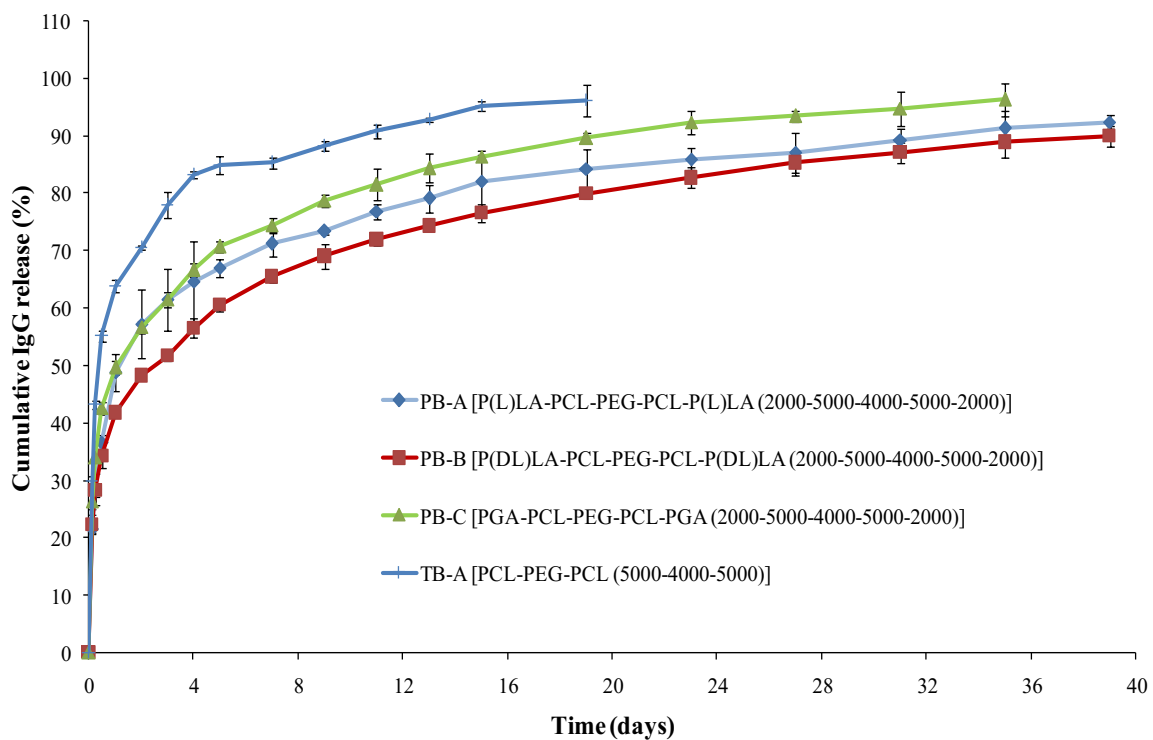


Figure 4.11: *In vitro* release of IgG from NPs prepared with TB-A, PB-A, PB-B, and PB-C block copolymers.

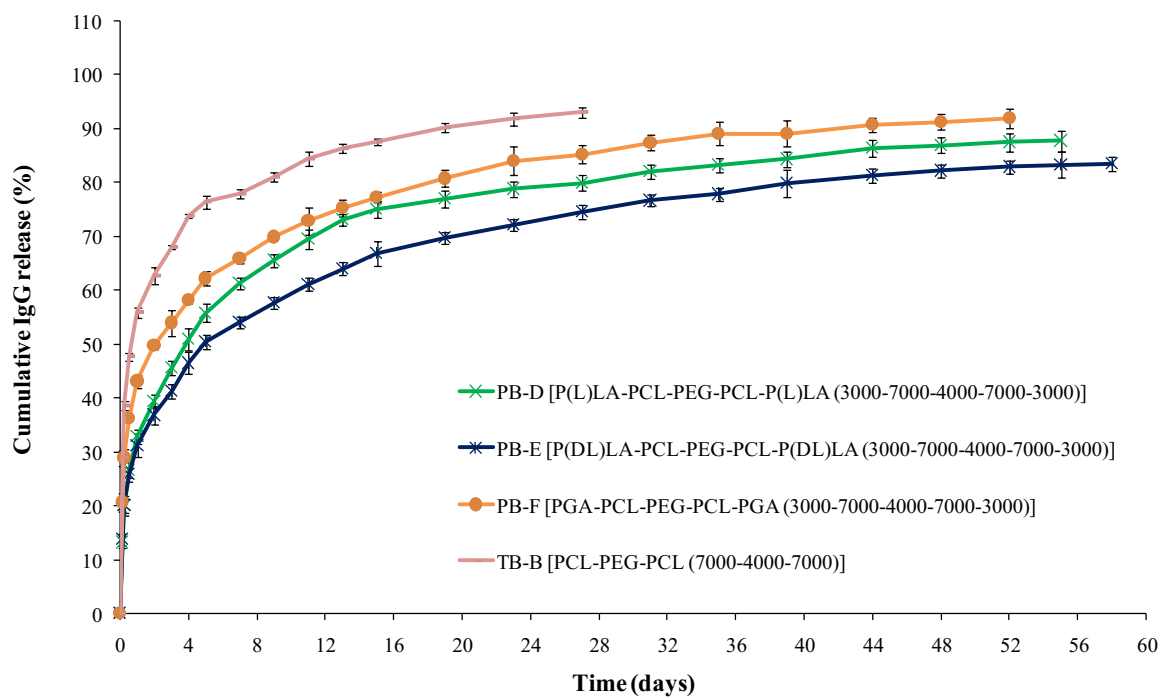


Figure 4.12: *In vitro* release of IgG from NPs prepared with TB-B, PB-D, PB-E, and PB-F block copolymers.

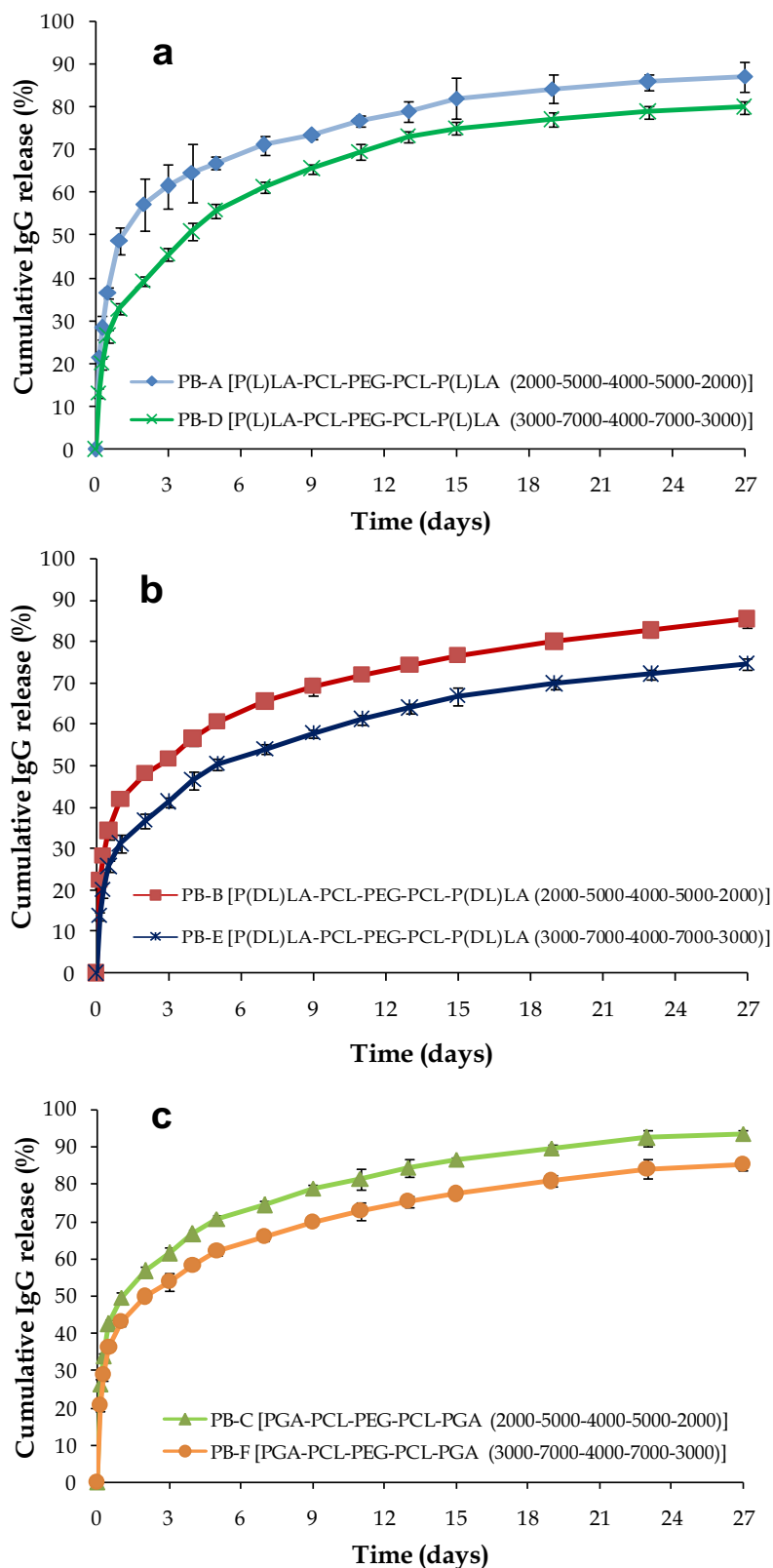


Figure 4.13: Effect of molecular weights of block copolymers on *in vitro* release of IgG (a) PB-A and PB-D NPs, (b) PB-B and PB-E NPs, and (c) PB-C and PB-F NPs.

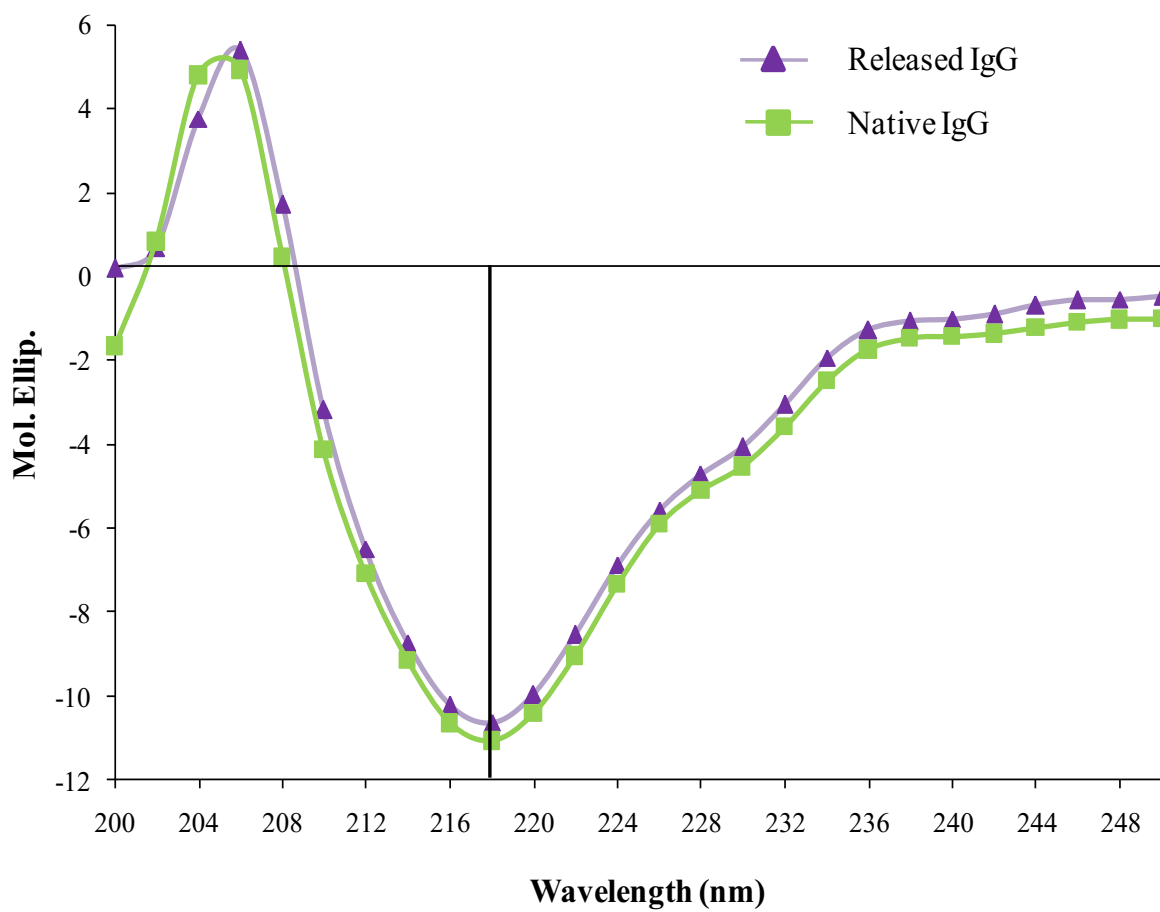


Figure 4.14: CD spectrum of released IgG from PB-E NPs after 15 days.

Secondary structure stability estimation of IgG

It is very important for protein therapeutics to maintain their structural conformation to exert pharmacological actions. CD spectroscopy is a very sensitive analytical technique utilized for the estimation of secondary, and to some extent tertiary, structures of proteins. The method provides α -helix and β -sheet conformational information and also able to detect minor changes in protein conformation. Therefore, we have employed CD spectroscopy to study the conformational stability of released IgG and compared it with the CD spectrum of native IgG. Results reported in Figure 4.14 exhibited λ minima of released IgG at 218 nm which is similar to the λ minima of native IgG. Moreover, the entire spectrum of released IgG ranging from 200 nm to 250 nm was identical to native IgG suggesting retention of conformation of IgG during the NPs preparation and even after the release from NPs. Previous reports suggest that PLA and/or PGA based copolymer produce large molar mass of lactic acid and/or glycolic acid [183, 197]. These degradation products can stimulate hydrolytic degradation of protein therapeutics. The retention of protein stability in PB NPs may be attributed to lower molar masses of PLA or PGA blocks which produce lower amounts of lactic or glycolic acid, reducing the possibility of protein degradation.

Conclusion

We have successfully synthesized and characterized novel PB copolymers with different block ratios of PEG/PCL/PLA or PEG/PCL/PGA. These PB copolymers were studied for the development of protein-loaded NPs in the treatment of posterior segment diseases such as wet AMD and DR. Our results demonstrated that crystallinity of PB copolymers can be easily modulated by changing the ratios of PLA/PCL or PGA/PCL blocks and also by utilizing different isomers of PLA (L or D,L). Moreover, results exhibited that molecular weight,

crystallinity and copolymer composition have significant effects on EE, DL and *in vitro* release kinetics. PB copolymers composed of PLA with D,L-lactide exhibited higher EE and slower release relative to PB copolymers comprising PLA (L-lactide) or PGA. The stability of released IgG was established by CD spectroscopy. In addition, cytotoxicity, cell viability and *in vitro* inflammatory studies confirmed that PB copolymers are excellent biomaterials for the development of protein-loaded, sustained delivery formulations for the treatment of posterior segment ocular diseases.

CHAPTER 5

TAILOR-MADE PENTABLOCK COPOLYMER BASED COMPOSITE FORMULATION FOR SUSTAINED OCULAR DELIVERY OF PROTEIN THERAPEUTICS

Rationale

Various biodegradable polymeric NP formulations have been extensively investigated for controlled delivery of protein therapeutics. Biodegradable polymers such as PCL, PLA, PGA and PEG have been comprehensively studied for the preparation of protein-encapsulated NPs. Current challenges in the development of protein-encapsulated NPs are to ensure protein stability during the NP preparation and drug release. In addition, the second major problem with any NP formulation is higher burst release (initial rapid drug release phase).

The objective of this research is to synthesize and evaluate novel tailor-made PB copolymers for the controlled and non-invasive delivery of macromolecules in the treatment of posterior segment diseases. We have synthesized three PB copolymers by sequential ring-opening polymerization either for the preparation of protein-loaded NPs (two PB copolymers) or thermosensitive gel (one PB copolymer). Different ratios and molecular weights of each block (PGA, PEG, PLA and PCL) were selected for synthesis to optimize the release profile of FITC-BSA, IgG and bevacizumab from NPs. We have hypothesized that release of protein therapeutics from NPs is affected by their hydrodynamic diameter. Therefore, in this study we have examined effect of hydrodynamic diameter of proteins on EE and *in vitro* drug release. We have characterized NPs for particle size, polydispersity, EE, DL and *in vitro* release studies.

As described earlier, PB thermosensitive gel (chapter 3) and PB NPs (chapter 4) exhibited significantly higher burst release and relatively shorter duration of sustained release. In many of the cases, burst release (~25-45%) can exhibit dose dependent toxicity. Moreover,

loss of ~25-45% of dose in first two days can significantly reduce the duration of release. So in order to eliminate burst release phase and to achieve continuous zero-order drug release, we have prepared and characterized a novel composite formulation comprised of protein-loaded NPs suspended thermosensitive gelling solution. A composite formulation also offers an additional advantage to eliminate any possibility of floater effect which may arise during the intravitreal injection of NPs alone. Stability of released protein was also confirmed by CD spectroscopy and *in vitro* biological assays.

Materials and methods

Materials

PEG (1 kDa and 4 kDa), methoxy-PEG (550 Da), stannous octoate, ϵ -caprolactone, poly (vinyl alcohol) (PVA), lipopolysaccharide were procured from Sigma-Aldarich (St. Louis, MO; USA). L-lactide and hexamethylene diisocyanate (HMDI) were purchased from Acros organics (Morris Plains, NJ; USA). Micro-BCATM was obtained from Fisher scientific. Mouse TNF- α , IL-6 and IL-1 β (Ready-Set-Go) ELISA kits were purchased from eBioscience Inc. Lactate dehydrogenase estimation kit and CellTiter 96[®] AQueous non-radioactive cell proliferation assay (MTS) kit were obtained from Takara Bio Inc. and Promega Corp., respectively. All other reagents utilized in this study were of analytical grade.

Methods

Synthesis of PB copolymers

Novel PB copolymers, PGA-PCL-PEG-PCL-PGA (PB-A), PLA-PCL-PEG-PCL-PLA (PB-B) and PEG-PCL-PLA-PCL-PEG (PB-C) were synthesized by ring-opening bulk polymerization method [176]. PB copolymers for the preparation of NPs i.e., PB-A and PB-B were synthesized in two steps by sequential ring-opening polymerization. PEG (1 kDa and 4

kDa) was utilized as macroinitiator and stannous octoate as a catalyst. In the first step, TB copolymer PCL-PEG-PCL (Figure 5.1, step 1) was synthesized by polymerization of ϵ -caprolactone on two open hydroxyl ends of PEG. In brief, PEG was dissolved in anhydrous toluene followed by distillation to remove residual moisture. ϵ -caprolactone and stannous octoate (0.5% w/w) were added to anhydrous PEG and temperature was raised to 130 °C. After 24 h, reaction mixture was dissolved in methylene chloride followed by precipitation in cold petroleum ether. The precipitated polymer was filtered and dried for 24 h under vacuum at room temperature. In the second step, the PCL-PEG-PCL TB copolymer was reacted with glycolide and L-lactide to prepare the PB-A (Figure 5.1, step 2) and PB-B (Figure 5.2) copolymers, respectively. The TB copolymer and glycolide/L-lactide were added in round bottom flask and temperature was raised to 130 °C under inert atmosphere. To this, stannous octoate (0.5% w/w) was added and reaction was allowed to run for 24 h. PB copolymer was purified by cold ether precipitation method described in the first step. The polymer was dried under vacuum and stored at -20 °C until further use.

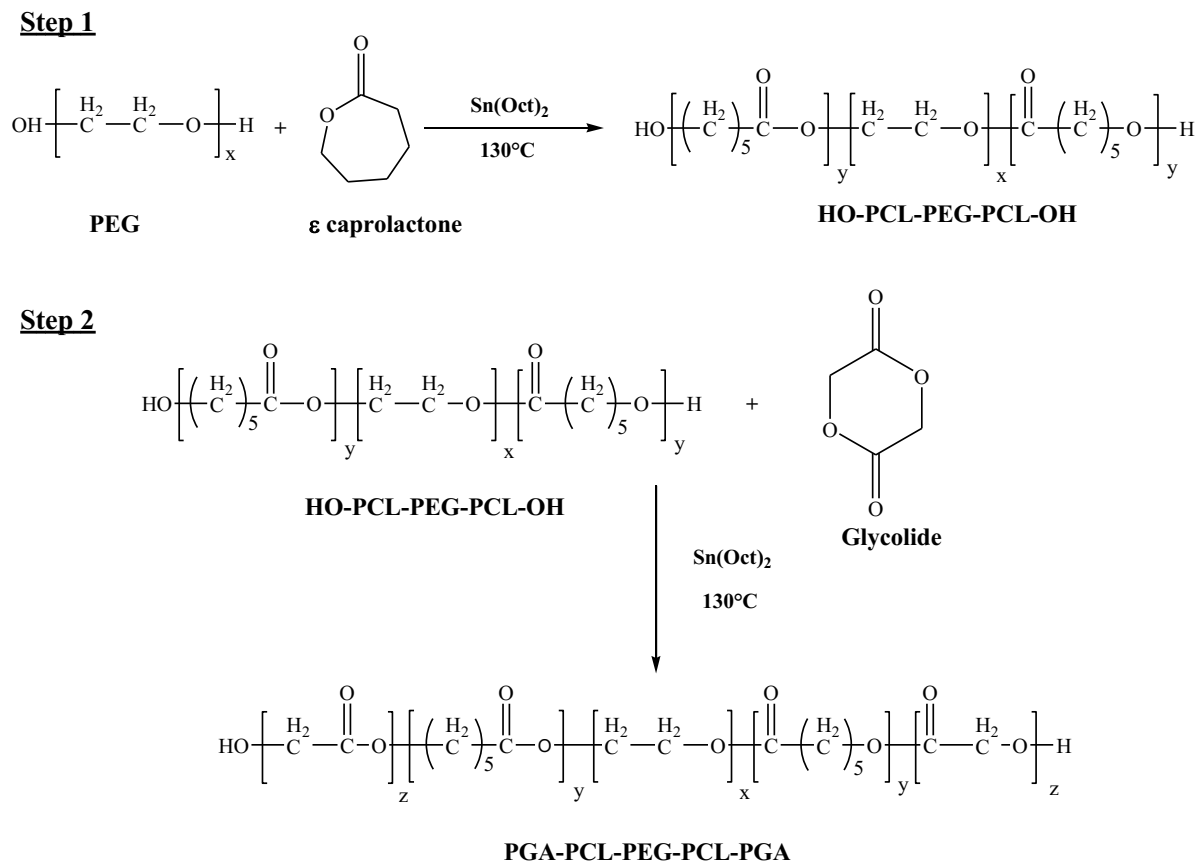


Figure 5.1: Synthesis scheme for PB-A (PGA-PCL-PEG-PCL-PGA) copolymer.

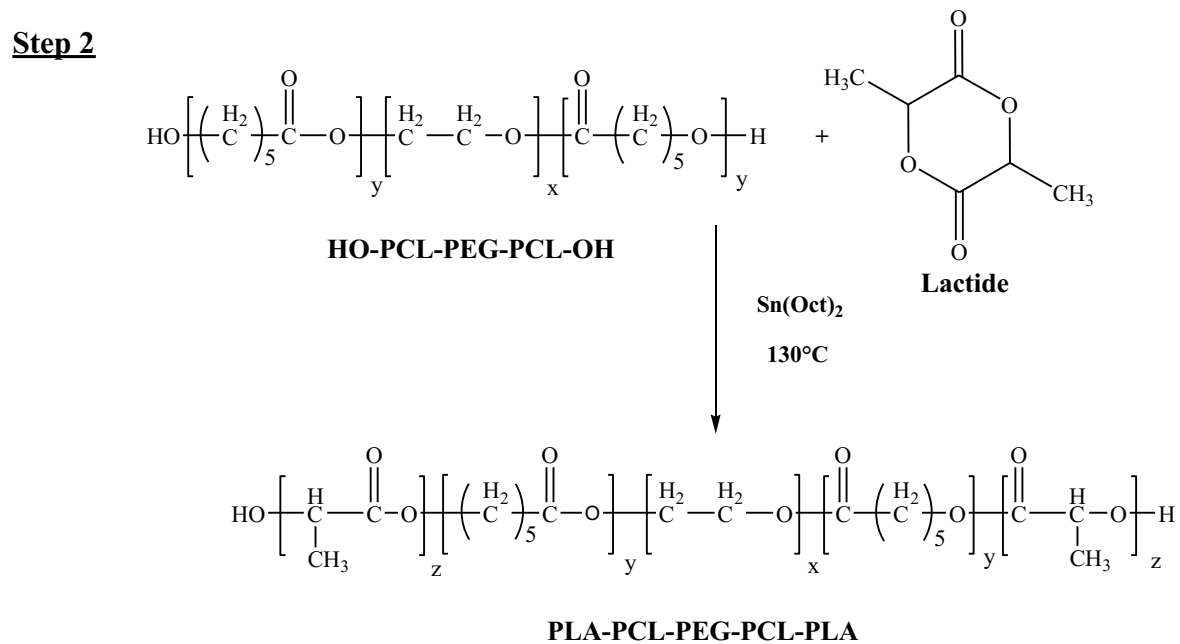
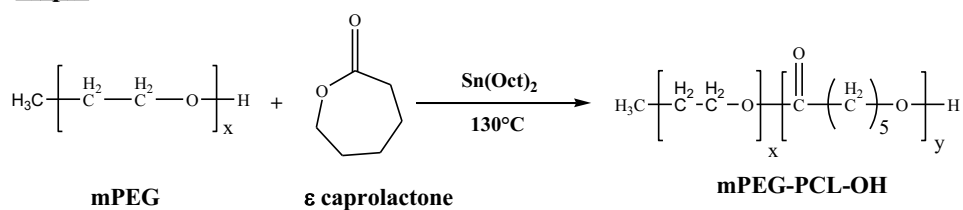


Figure 5.2: Synthesis scheme for PB-B (PLA-PCL-PEG-PCL-PLA) copolymer.

Step 1



Step 2

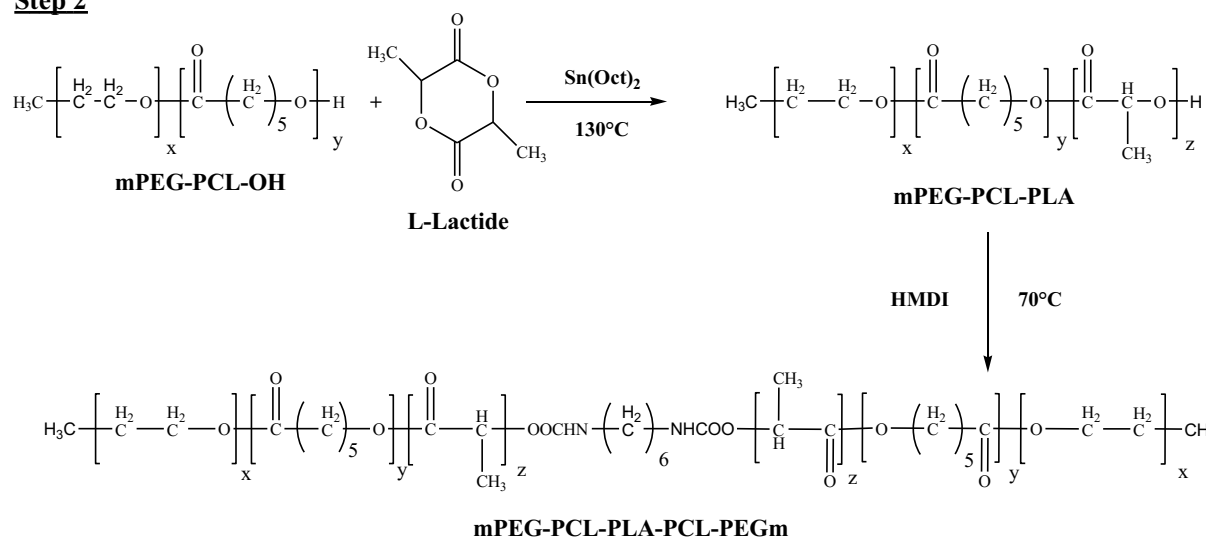


Figure 5.3: Synthesis scheme for PB-C (PEG-PCL-PLA-PCL-PEG) copolymer.

For the synthesis of thermosensitive gelling polymer, TB copolymer (mPEG-PCL-PLA) was synthesized by ring-opening bulk copolymerization as described above (Figure 5.3). Firstly, ϵ -caprolactone was polymerized at the hydroxyl terminal of mPEG (550 Da) followed by polymerization of L-lactide. Resulting TB copolymers were coupled utilizing HMDI as a linker. Coupling reaction was carried out at 70 °C for 8 h. Polymers were purified by cold ether precipitation followed by drying under vacuum and stored at -20 °C.

Characterization of polymers

The resulting polymers were characterized for molecular weight and purity by ^1H NMR spectroscopy and gel permeation chromatography (GPC).

^1H -NMR analysis

To perform ^1H -NMR spectroscopy, polymeric materials were dissolved in CDCl_3 and spectra were recorded with Varian-400 NMR instrument. Purity and molecular weight (M_n) were calculated from the ^1H -NMR spectra.

GPC analysis

Purity, molecular weights and polydispersity of PB copolymers were further confirmed by GPC analysis. Polymeric samples were analyzed with refractive index detector (Waters 410). Briefly, samples were prepared by dissolving 5 mg of polymeric material in tetrahydrofuran (THF) whereas THF was utilized as eluting agent at the flow rate of 1 mL/min. Separation was carried out on Styragel HR-3 column and polystyrene samples with narrow molecular weight distribution were utilized as standards.

In vitro cytotoxicity studies

Cell culture

Human retinal pigment epithelial cells (ARPE-19) were cultured and maintained according to the previously published protocol from our lab [199]. In brief, cells were cultured in Dubelcco's modified Eagle medium (DMEM)/F-12 medium containing 10% fetal bovine serum (FBS), 15 mM of HEPES, 29 mM of sodium bicarbonate, 100 U/L of penicillin and 100 mg/L of streptomycin. A mouse macrophage cell line, RAW-264.7 was procured from ATCC. RAW-264.7 cells were cultured and maintained in DMEM supplemented with 10% FBS, 100 U/L of penicillin and 100 mg/L of streptomycin. The Statens Seruminstitut rabbit corneal (SIRC) cell line was purchased from ATCC at passage 400 and used between passages 410 - 425. During the study and maintenance period cells were supplemented with cell culture media composed of MEM containing 10% FBS, lactalbumin, HEPES, sodium bicarbonate, 100 U/L of penicillin and 100 mg/L of streptomycin. Human conjunctival epithelial cells (HCEC) were maintained in cell culture flask containing MEM Earle's BSS medium supplemented by 10% FBS, 100 U/L of penicillin, 100 mg/L of streptomycin, 29 mM of sodium bicarbonate, and 2 mM L-glutamine. Choroid-retinal endothelial cells (RF/6A cells) were procured from ATCC. Briefly, cells were cultured and maintained in cell culture medium composed of RPMI-1640 comprising 10% FBS, 100 U/L of penicillin and 100 mg/L of streptomycin [209]. All five cell lines were maintained in humidified atmosphere at 37 °C and 5% CO₂.

Lactate Dehydrogenase (LDH) assay

Previously published protocol with minor modification was employed to evaluate the cytotoxicity of PB copolymers [210]. Briefly, 10 mg/mL of PB copolymers (PB-A and PB-B) were dissolved in ACN and 100 µL of these solutions were aliquoted in each well of 96-well

cell culture plates. Plates were exposed overnight under UV light (laminar flow) for the sterilization of polymer and evaporation of ACN. ARPE-19 cells at the density of 1.0×10^4 were seeded in each well and incubated at 37 °C, 5% CO₂ in humidified atmosphere for 48 h. After completion of incubation period, cell supernatant were analyzed for the quantification of LDH. According to supplier's protocol, levels of LDH were analyzed utilizing a LDH detection kit. Absorbance of each well was estimated at 450 nm by 96-well plate reader. More than 10% of LDH release was considered as cytotoxic. To evaluate the cytotoxicity of block copolymers on conjunctiva, cornea and macrophages, the similar experiment was performed with HCEC, SIRC and RAW-264.7 cells. LDH release (%) was calculated with following equation,

$$LDH\text{release}(\%) = \frac{\text{Abs. of Sample} - \text{Abs. of negative control}}{\text{Abs. of positive control} - \text{Abs. of negative control}} * 100 \quad \dots \text{Eq. 5.1}$$

MTS assay

Safety of PB copolymers was further established by performing *in vitro* cell viability assay (MTS assay) [211]. MTS assay was performed according to previously reported protocol with minor changes. As described earlier, PB copolymer solutions at the concentration of 10 mg/mL were prepared, aliquoted and sterilized. After sterilization, ARPE-19 cells were seeded in each well of 96-well plate at the cell density of 1.0×10^4 , and incubated at 37 °C and 5% CO₂ in humidified atmosphere for 48 h. At the end of incubation period, cell culture medium was aspirated and cells were incubated for 4 h (37 °C and 5% CO₂) in presence of 100 µL of serum free medium containing 20 µL of MTS solution. Absorbance of each well was estimated at 450 nm. The similar experiment was repeated with other ocular and macrophage cell line such as HCEC, SIRC and RAW-264.7 cells. Percent cell viability was calculated by the following equation.

$$\text{Cellviability}(\%) = \frac{\text{Abs. of Sample} - \text{Abs. of negative control}}{\text{Abs. of positive control} - \text{Abs. of negative control}} * 100 \quad \dots \text{Eq. 5.2}$$

In this study, PB copolymers which exhibited more than 90% of cell viability were considered non-toxic for ocular applications.

In vitro biocompatibility studies

PB copolymers were dissolved in ACN at the concentration of 10 mg/mL and 200 μ L of these solutions were aliquoted in each well of 48-well cell culture plates. Cell culture plates were incubated overnight under UV lights (laminar flow) for the evaporation of ACN and sterilization of resulting polymer film. After sterilization, RAW-264.7 cells (5.0×10^4) were seeded in each well of cell culture plate and incubated for 24 h at 37 °C and 5% CO₂. After 24 h, cell supernatants were analyzed for the presence of cytokines such as TNF- α , IL-6 and IL-1 β . Lipopolysaccharide (LPS) was utilized as positive control whereas cells without treatment were considered as negative control. Levels of cytokines were quantified by ELISA method which was performed according to supplier's instructions. Standard calibration curves for TNF- α , IL-6 and IL-1 β were prepared in the range of 10-750 pg/mL, 5-500 pg/mL and 10-500 pg/mL, respectively.

Preparation of NPs

IgG-loaded PB NPs were prepared by W₁/O/W₂ double emulsion solvent evaporation method [212]. Briefly, predetermined quantity of IgG (10 mg) was dissolved in 0.1 M phosphate buffer saline (PBS, pH 7.4) (1 mL) containing 50 μ L of Tween-80 (W₁ phase). In order to prepare organic phase, 100 mg of respective PB copolymers were solubilized in 4 mL of dichloromethane (DCM) with 50 μ L of Span-20 (organic phase). Primary emulsion (W₁/O) was prepared by drop-wise addition of W₁ phase in organic phase under constant sonication.

Sonication was applied with probe-sonicator for 1 min at 4 W output. To avoid excessive heating and subsequent degradation of protein, the preparation of emulsion was carried out in ice-bath. Resulting W₁/O primary emulsion was then added drop-wise in 20 mL of 2% polyvinyl alcohol (PVA) solution (W₂ phase) under constant sonication for 4 min at 5 W output. Double emulsion (W₁/O/W₂) was stirred at room temperature for 30 min followed by evaporation of DCM under low pressure. Once the DCM was evaporated, NPs were centrifuged for 30 min at 20000 rpm and 4 °C followed by two washing cycles with distilled deionized water (DDW). Finally, IgG-loaded NPs were freeze-dried in presence of 5% mannitol (cryoprotectant) and stored at -20 °C until further use. NPs were prepared with two PB copolymers i.e., PB-A and PB-B. The similar protocol was utilized to prepare FITC-BSA and bevacizumab-loaded NPs. Freeze-dried NPs were evaluated for particle size, EE (%), DL (%) and *in vitro* drug release behavior.

Characterization of NPs

Particle size and polydispersity

Freeze-dried NPs were dispersed in DDW (1 mg/mL) and analyzed for their size and its distribution. Particle size was evaluated by particle size analyzer (Zetasizer Nano ZS, Malvern Instruments Ltd, Worcestershire, UK) at 90° scattering angle. All the NP samples were analyzed in triplicate.

Entrapment efficiency (EE) and drug loading (DL)

Protein-encapsulated freeze-dried NPs were evaluated for the estimation of EE and DL. EE of the NPs was estimated by quantifying the amount of protein in the supernatants which were obtained during the NP preparation. Micro BCA™ protein estimation kit was employed for the quantification of total protein. In order to evaluate DL, 2 mg equivalent protein-loaded

NPs were dissolved in 200 μ L of dimethyl sulfoxide (DMSO). Resulting solutions were analyzed by UV absorbance spectroscopy. Standard curve of respective proteins (IgG, FITC-BSA and bevacizumab) ranging from 31.25 to 2000 μ g/mL were prepared in DMSO. Following equations were utilized for the calculation of EE (%) and DL (%).

$$EE (\%) = \left(1 - \frac{\text{Amount of drug in supernatant}}{\text{Total amount of drug}}\right) * 100 \quad \dots \text{Eq. 5.3}$$

$$DL (\%) = \left(\frac{\text{Amount of drug in nanoparticles}}{\text{Total amount of drug and polymer}}\right) * 100 \quad \dots \text{Eq. 5.4}$$

In vitro release studies

IgG-loaded NPs were further characterized for their ability to sustain drug release. In order to perform *in vitro* drug release studies, 1 mg of IgG equivalent freeze-dried NPs were suspended in 1 mL of PBS (pH 7.4). Resulting NPs suspension was then incubated in water bath equilibrated at 37 $^{\circ}$ C. At predefined time intervals, NPs were centrifuged at 13000 rpm for 30 min. A 200 μ L of supernatant was collected and replaced with the same volume of PBS. NPs were then resuspended and release study was continued at 37 $^{\circ}$ C. In a second set of *in vitro* release studies, 1 mg drug equivalent IgG-NPs were suspended in 500 μ L of aqueous solution of thermosensitive gelling polymer (PB-C) (20 wt%). Resulting suspension was incubated in 10 mL vial at 37 $^{\circ}$ C for 30 min. Once gel was solidified, 5 mL of PBS (preincubated at 37 $^{\circ}$ C) was slowly added. At predetermined time intervals, 1 mL of clear supernatant was collected and replaced with same volume of fresh PBS (preincubated at 37 $^{\circ}$ C). Release samples were analyzed by Micro BCATM for total protein content. Micro BCATM was performed according to supplier's instructions. FITC-BSA and bevacizumab-loaded NPs were also evaluated for their *in vitro* release behavior. Release samples of FITC-BSA were

analyzed by fluorescence spectroscopy, where excitation and emission wavelengths were 490 nm and 525 nm, respectively. *In vitro* release experiments were performed in triplicates and expressed as cumulative drug released (%) with time.

Release kinetics

In order to investigate release mechanisms, release data were fitted to various kinetic models described below,

Korsmeyer-Peppas equation

$$\frac{M_t}{M_\infty} = kt^n \quad \dots\text{Eq. 5.5}$$

k is the kinetic constant and n is the diffusion exponent describes release mechanism. M_t and M_∞ represent the cumulative protein release at time t and at the equilibrium, respectively.

Higuchi equation

$$Q_t = Kt^{1/2} \quad \dots\text{Eq. 5.6}$$

K denotes the Higuchi rate kinetic constant, Q_t is the amount of released protein at time t, and t is time in hours.

Hixon-Crowell equation

$$C_0^{1/3} - C_t^{1/3} = kt \quad \dots\text{Eq. 5.7}$$

C_0 and C_t represents the initial amount and remaining amount of protein in formulation, respectively. k is the constant incorporating surface-volume relation and t is time in hours.

First-order equation

$$\text{Log}C = \text{Log}C_0 - \frac{Kt}{2.303} \quad \dots\text{Eq. 5.8}$$

K denotes the first-order rate constant, C_0 is the initial protein concentration and t represents time in hours.

Zero-order equation

$$C = K_0t \quad \dots\text{Eq. 5.9}$$

K_0 is the zero-order rate constant and t is time in hours.

Stability estimation of IgG

Released IgG was analyzed by CD spectroscopy for the estimation of secondary structure. CD analysis was carried at room temperature with Jasco 720 spectropolarimeter. CD spectra were recorded between the wavelengths of 200 to 250 nm at scanning speed of 5 nm/min utilizing 1 cm cell. CD measurements were reported as molar ellipticity $[\theta]$. CD spectrum of PBS was utilized as blank.

Stability estimation of bevacizumab by in vitro biological assays

Cell proliferation assay

A cell proliferation assay was performed according previously published protocols with minor modifications [213-215]. Concentrations of live cells were quantified by MTS assay, which was performed according to manufacturer's instructions. Briefly, cells were seeded at the density of 5×10^3 cells/well of 96-well cell culture plate. After 24 h of incubation, cells were serum-starved overnight followed by addition of serum free medium containing 100 ng/mL of VEGF and 0.25 mg/mL of released bevacizumab (test samples) or 0.25 mg/mL of native bevacizumab. Cells without VEGF or bevacizumab were considered as negative control or cells exposed only to VEGF (100 ng/mL) as positive control. Cells were further incubated for 24 h at 37 °C and 5% CO₂. After completion of treatment, cells were exposed to 100 μ L of

serum free medium containing 20 μ L of MTS solution and incubated for 4 h. The absorbance was recorded at 450 nm using a microplate reader.

Cell migration assay

A cell migration assay was performed as described elsewhere with few modifications [216]. RF/6A cells were starved overnight (by exposing to serum free medium), trypsinized and suspended in serum free medium containing 0.25 mg/mL of bevacizumab (native or released from NPs). The 5×10^3 cells were seeded in upper chamber of Transwell (8.0 μ m pore size, 10 mm diameter; Corning Inc.), pre-incubated with cell culture medium. VEGF (100 ng/mL) was placed into the lower chamber and the cells were incubated for 24 h at 37 °C and 5% CO₂. Non-migrated cells were removed from upper chamber by cotton swab and concentration of migrated cells was estimated by AlamarBlue[®] assay. AlamarBlue[®] assay was performed according to supplier's protocol. Moreover, for visual evidence, migrated cells were also stained with methylene blue and images were taken with Leica DMI3000B inverted microscope (Germany). Each experiment was repeated three times.

Results and discussion

Synthesis and characterization of PB copolymers

PB copolymers (PB-A and PB-B) were successfully synthesized by ring-opening bulk copolymerization of ϵ -caprolactone, and L-lactide/glycolide. Firstly, TB copolymers (PCL-PEG-PCL) were synthesized, purified and characterized. Purified TB copolymers were then utilized for the synthesis of respective PB copolymers i.e., PB-A (PGA-PCL-PEG-PCL-PGA) and PB-B (PLA-PCL-PEG-PCL-PLA). Purity and molecular weights (Mn) of PB copolymers were calculated by ¹H-NMR spectroscopy. As described in Figures 5.4 and 5.5, typical ¹H-NMR signals of PCL blocks were observed at 1.40, 1.65, 2.30 and 4.06 ppm depicting

methylene protons of $-(\text{CH}_2)_3-$, $-\text{OCO}-\text{CH}_2-$, and $-\text{CH}_2\text{OOC}-$, respectively. PB-A exhibited cluster of singlets between 4.6 to 4.9 ppm representing methylene protons ($-\text{CH}_2-$) of PGA units. PB copolymer with PLA units as terminals (PB-B) demonstrated two additional peaks at 1.50 ($-\text{CH}_3$) and 5.17 ($-\text{CH}-$) ppm. Molar ratios of PB-A and PB-B were calculated from the integration values of PEG (3.65 ppm), PCL (2.30 ppm), and PLA (5.17 ppm) or PGA (4.6-4.9 ppm). $^1\text{H-NMR}$ spectra of PB-C depicted in (Figure 5.6) demonstrated typical proton signals of PEG, PCL and PLA. An additional peak at 3.38 ppm was denoted to terminal methyl of ($-\text{OCH}_3-$) of PEG, which was utilized for the molecular weight (M_n) calculation of PB-C copolymer. As depicted in Table 5.1, observed molecular weights (M_n) of PB-A, PB-B and PB-C were very similar to theoretical molecular weights. For the ease, in the following text, theoretical molecular weights are mentioned instead of calculated molecular weights (M_n).

In vitro cytotoxicity studies

In order to investigate compatibility of PB polymeric materials with biological system (ocular cell lines), 10 mg/mL concentration of PB-A and PB-B were exposed to ARPE-19, SIRC, HCEC and RAW-264.7 cells for 48 h. LDH is a cytoplasmic enzyme, secreted in cell culture medium following cell-membrane damage. Estimation of the concentration of LDH in the cell supernatant provides a direct estimation of PB copolymer toxicity. Less than 10% of LDH release was observed after 48 h of exposure period indicating negligible toxicity for any of the ocular cell lines (Figure 5.7). Noticeably, results were comparable with the respective negative controls.

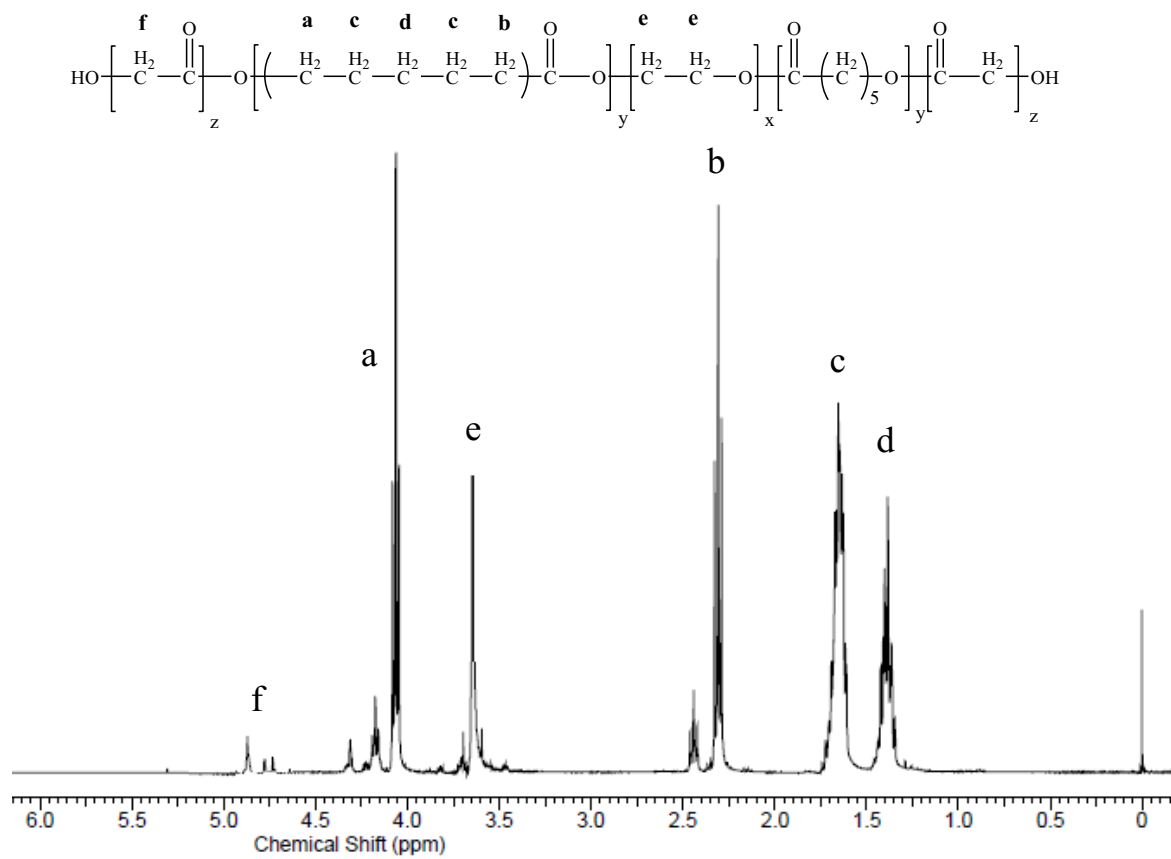


Figure 5.4: ^1H -NMR spectrum of PB-A copolymer in CDCl_3 .

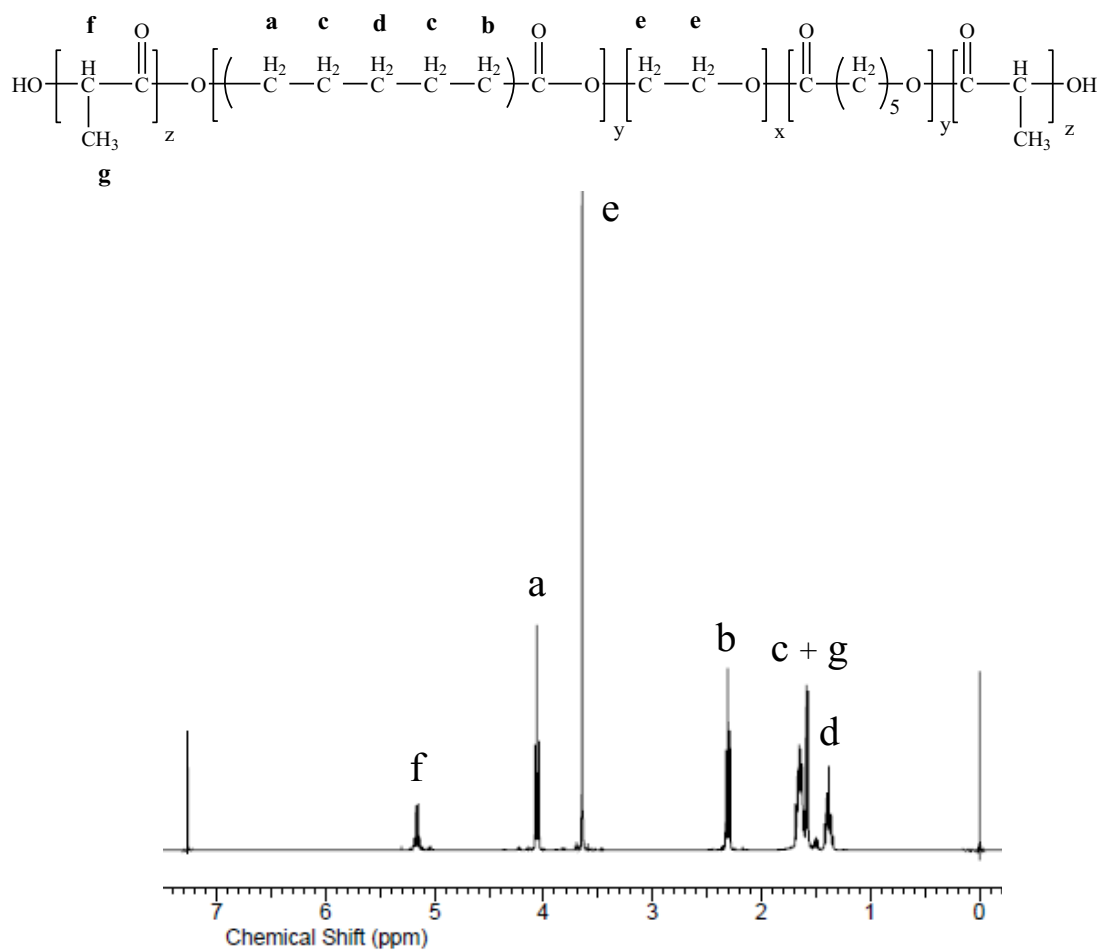


Figure 5.5: $^1\text{H-NMR}$ spectrum of PB-B copolymer in CDCl_3 .

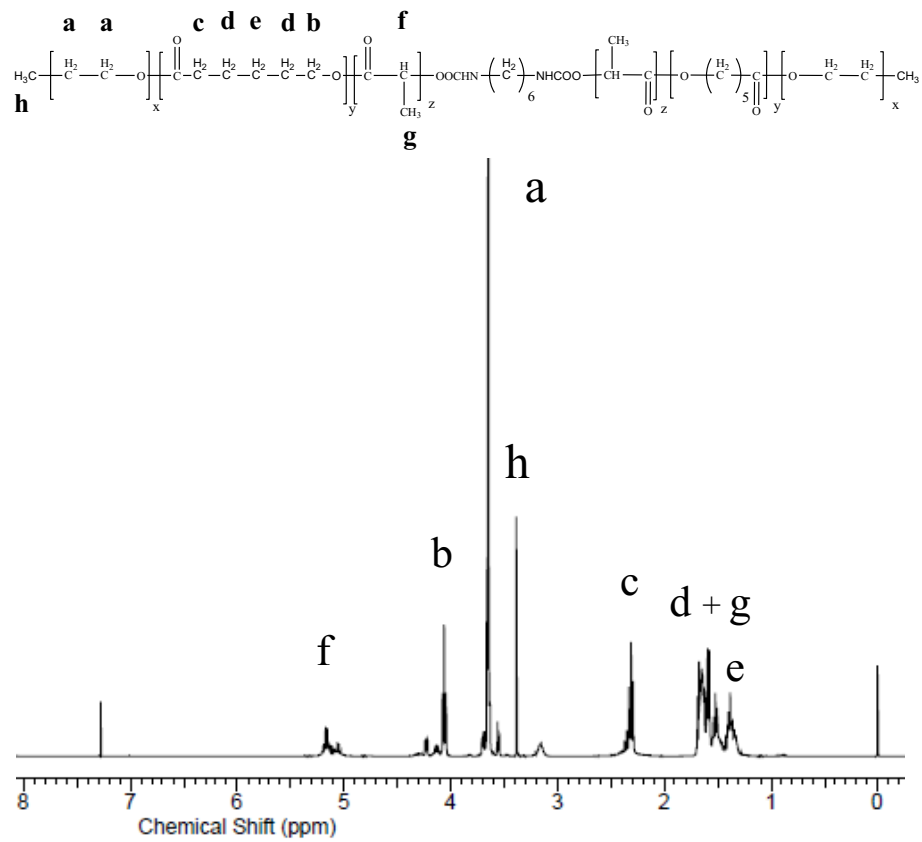


Figure 5.6: ¹H-NMR spectrum of PB-C copolymer in CDCl₃.

Table 5.1: Characterization of PB copolymers.

Code	Structure	PGA/PCL/PEG or PLA/PCL/PEG	Total M_n^a (theoretical)	Total M_n^b (calculated)	Total M_n^c (calculated)	M_w^c (GPC)	PDI ^c
PB-A	PGA ₃₀₀ -PCL ₇₅₀₀ -PEG ₁₀₀₀ -PCL ₇₅₀₀ -PGA ₃₀₀	0.6/15/1	16600	15710	13780	18640	1.35
PB-B	PLA ₃₄₅₀ -PCL ₅₇₀₀ -PEG ₄₀₀₀ -PCL ₅₇₀₀ -PLA ₃₄₅₀	1.73/2.85/1	22300	21030	19160	26980	1.41
PB-C	PEG ₅₅₀ -PCL ₈₂₅ -PLA ₅₅₀ -PCL ₈₂₅ -PEG ₅₅₀	0.5/1.5/1	3300	2910	4230	6040	1.43

- a. Theoretical value, calculated according to the feed ratio
b. Calculated from ¹H-NMR results
c. Determined by GPC analysis

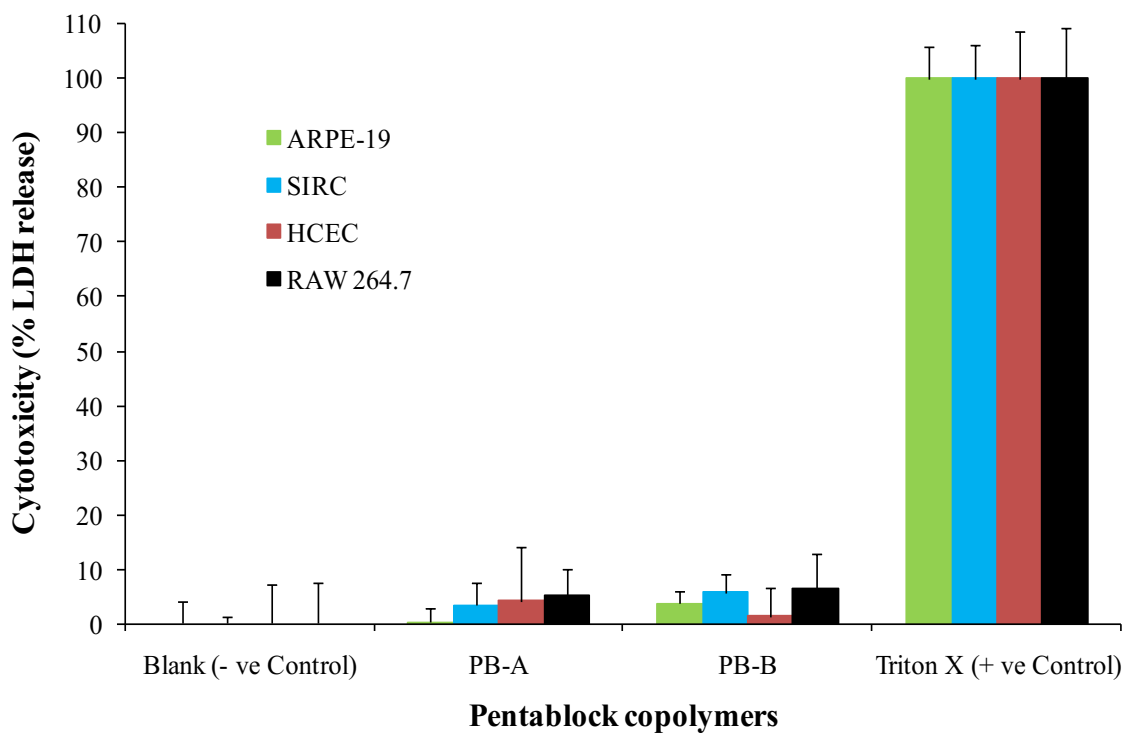


Figure 5.7: *In vitro* cytotoxicity assay (LDH) of PB-A and PB-B copolymers at the concentration of 10 mg/mL was performed on ARPE-19, SIRC, HCEC and RAW-264.7 cell lines.

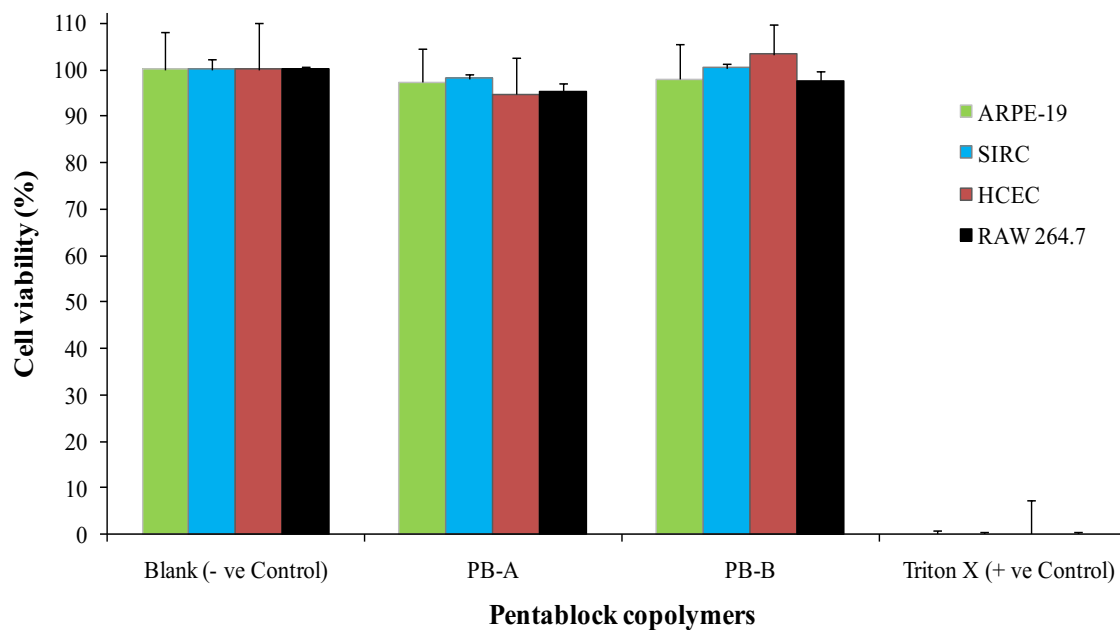


Figure 5.8: *In vitro* cell viability assay (MTS) of PB-A and PB-B copolymers at the concentration of 10 mg/mL was performed on ARPE-19, SIRC, HCEC and RAW-264.7 cell lines.

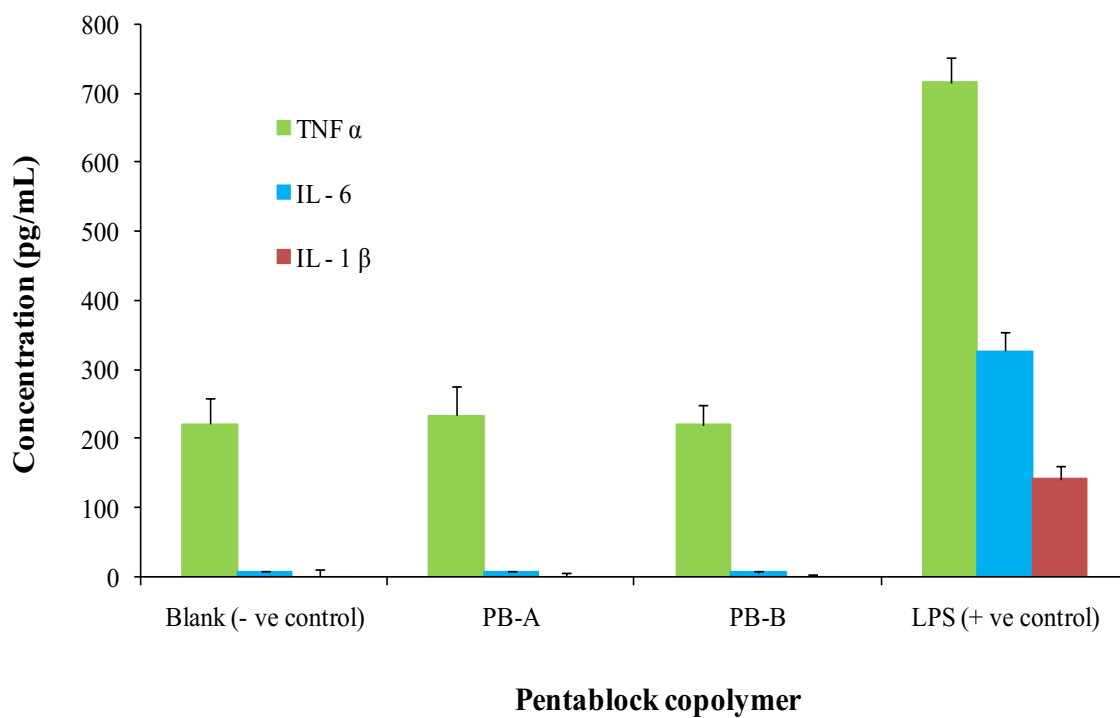


Figure 5.9: *In vitro* biocompatibility of PB-A and PB-B copolymers was evaluated by estimating the levels of TNF- α , IL-6 and IL-1 β in the supernatants of polymer treated RAW 264.7 cells.

To further confirm the results observed for LDH assays, MTS cell viability studies were performed utilizing the similar protocol. In MTS assay, only metabolically active cells convert tetrazolium compound to formazan. Hence, the concentrations of formazan products provide a direct estimation of cell viability. Results described in Figure 5.8 demonstrated more than 90% cell viability (for all the cell lines) after 48 h exposure to polymer materials suggesting excellent safety profile of block copolymers for the ocular applications. No significant difference in cell viability was observed relative to negative control.

In vitro biocompatibility studies

Many investigators have utilized *in vitro* cell culture model (RAW-264.7) for the estimation of biocompatibility of polymeric materials intended for human applications. In this experiment we have estimated concentration of various cytokines such as TNF- α , IL-6 and IL-1 β secreted in cell supernatant following 24 h exposure to PB-A and PB-B copolymers. Samples were analyzed via sandwich ELISA method provided by manufacturer. Results depicted in Figure 5.9 indicate significant release of TNF- α (~200 pg/mL) in both groups i.e., PB-A and PB-B. However, these values are comparable to negative control (cells without treatment) with no significant difference. Similarly, negligible release of IL-6 and IL-1 β were observed suggesting outstanding safety profile of PB copolymers.

Characterization of NPs

Particle size and polydispersity

IgG, FITC-BSA and bevacizumab-encapsulated PB NPs were prepared by W₁/O/W₂ double emulsion solvent evaporation method. NPs prepared from PB copolymers were ranging from 320-355 nm (Table 5.2). Moreover, we have observed unimodal size distribution with very narrow polydispersity (0.273-0.305). We did not observe any significant effect of polymer

composition (PB-A/PB-B) or type of protein molecule (IgG/BSA/bevacizumab) on particle size. These results suggest that hydrodynamic diameter of protein therapeutics or polymer composition has little or no effect on particle size or its distribution.

Entrapment efficiency (EE) and drug loading (DL)

EE and DL are significantly influenced by various parameters including copolymer composition (hydrophobicity of polymer) and volumes of various phases (W_1 , O and W_2). In order to understand the effect of hydrophobicity of copolymers on EE and DL, we have prepared and evaluated IgG and FITC-BSA-loaded NPs with PB-A and PB-B. It is important to note that PB-A copolymer comprising PGA (hydrophilic block) is relatively hydrophilic copolymer than PB-B copolymer comprising PLA (hydrophobic block). As described in Table 5.2, encapsulation of IgG or FITC-BSA in PB-A NPs were ~40% and ~35%, respectively. However, PB-B NPs exhibited significantly higher encapsulation for IgG (~70%) and FITC-BSA (~69%) relative to PB-A NPs. This may attributed to the fact that during the preparation of NPs (solvent evaporation), high hydrophobicity may allow faster precipitation of PB-B copolymer to form NPs preventing diffusion of IgG/FITC-BSA from W_1 phase to external aqueous (W_2) phase. This phenomenon possibly ensured higher EE of protein therapeutics in PB-B NPs. Due to higher hydrophilicity, PB-A copolymer may remain hydrated with W_1 and W_2 phase (during NPs preparation) allowing escape of IgG/FITC-BSA in external phase resulting poor EE. However, we did not observe any effect of hydrodynamic diameter of IgG or FITC-BSA on EE or DL. It may possible that both the proteins are too large (≥ 66 kDa) to show any significant effect of hydrodynamic diameter on EE or DL. Bevacizumab-loaded PB-B NPs exhibited ~67% of EE and ~6% of DL, very similar to IgG-loaded PB-B NPs (Table 5.2) suggested that bevacizumab may behaved very similar to IgG during NP preparation.

In vitro release studies

In order to evaluate the effect of polymer hydrophobicity, release of FITC-BSA and IgG from PB-A and PB-B NPs were evaluated. As described in Figure 5.10, both NPs (PB-A and PB-B) demonstrated biphasic release profile i.e., initial burst release followed by sustained release. PB-A NPs exhibited significantly higher burst release (~56%) of FITC-BSA relative to PB-B NPs (~48%). In a second phase of release, PB-B NPs sustained release of BSA for ~36 days whereas PB-A NPs prolonged the release for only ~27 days. Similarly, effects of polymer hydrophobicity were observed with IgG-encapsulated NPs where PB-B NPs displayed prolonged release (~44 days) than PB-A NPs (~30 days) (Figure 5.11). As described earlier, PGA based PB-A copolymer is hydrophilic than the PLA based PB-B copolymer. Therefore, it is anticipated that PB-A NPs possibly have higher affinity for the protein molecules which may allow higher amount of surface adsorbed drug. Moreover, being hydrophilic, PB-A NPs may get easily hydrated and allow easy diffusion of water molecules through the polymer matrix. Both, higher amount of surface adsorbed proteins and higher affinity towards water molecules may have simultaneously contributed to the higher burst release and shorter duration of release period.

We have hypothesized that hydrodynamic diameter of protein therapeutics has significant effect on drug release pattern. In order to confirm that we have compared *in vitro* release profiles of FITC-BSA (66 kDa) and IgG (150 kDa) (Figure 5.12) from PB-B NPs. Results clearly indicated significantly higher burst release and shorter release duration for FITC-BSA relative to IgG from their respective NPs. It may be attributed to the fact that FITC-BSA has smaller hydrodynamic diameter compared to IgG which may lead to faster diffusion through the polymer matrix of NPs. To further confirm this hypothesis, we have compared *in*

in vitro release profile of IgG and bevacizumab (149 kDa) from their respective PB-B NPs. Results reported in Figure 5.13 described no significant difference between the release profile of IgG and bevacizumab. This may be due to the fact that IgG and bevacizumab are full length antibodies with similar hydrophilicity and molecular weight (hydrodynamic diameter). Hence, both protein molecules might behave alike during NPs preparation and also during release study. These results indicate that there is a little or no effect of the type of protein (IgG or bevacizumab) on drug release pattern but there is a significant effect of hydrodynamic diameter (FITC-BSA or IgG).

Protein therapeutics possess very high specificity hence require very low dose to assert their therapeutic action. Any nanoparticulate or microparticulate system have certain amount of surface adsorbed drug, which releases within first 24 h giving burst effect. Being very potent by nature, burst release of protein therapeutics may produce serious side effects. Therefore, pharmaceutical scientists are focused to develop a formulation which can eliminate burst effect and offer zero-order drug release throughout a release period. In order to achieve zero-order drug release profile, we have suspended protein-encapsulated PB-B NPs in an aqueous solution of thermosensitive gelling polymer (PB-C). Thermosensitive gelling solution was composed of 20 wt% PB-C copolymer in DDW. Aqueous solution of PB-C copolymer remains liquid at room temperature or below and immediately transforms to hydrogel at body temperature (sol-gel transition curve is not shown).

Table 5.2: Characterization of FITC-BSA and IgG-loaded NPs.

Proteins	Polymers	Entrapment efficiency (%)	Loading (%)	Particle size (nm)	Polydispersity
FITC-BSA	PB-A	35.0 ± 3.7	5.0 ± 0.4	350 ± 30	0.286
	PB-B	69.5 ± 6.2	5.4 ± 0.5	320 ± 20	0.280
IgG	PB-A	40.5 ± 3.5	6.3 ± 0.3	370 ± 10	0.305
	PB-B	70.1 ± 4.1	6.1 ± 0.3	350 ± 10	0.273
Bevacizumab	PB-B	67.3 ± 3.3	6.1 ± 0.2	340 ± 20	0.246

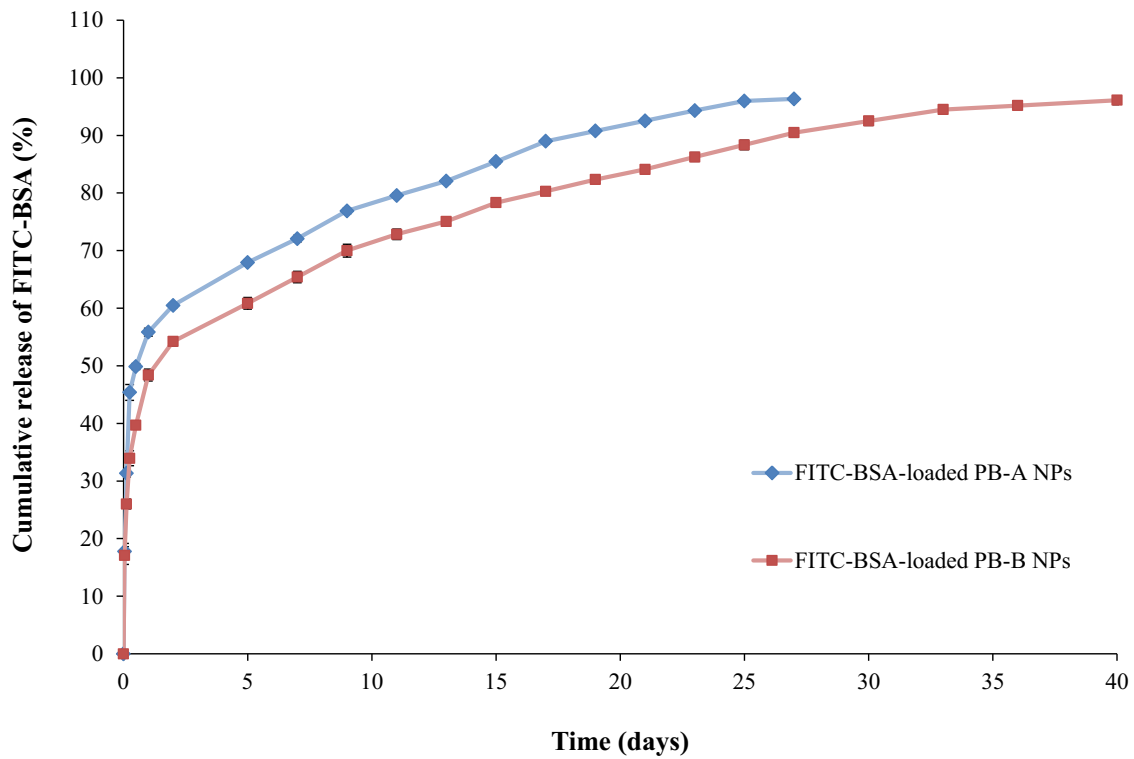


Figure 5.10: *In vitro* release of FITC-BSA from NPs prepared with PB-A and PB-B copolymers.

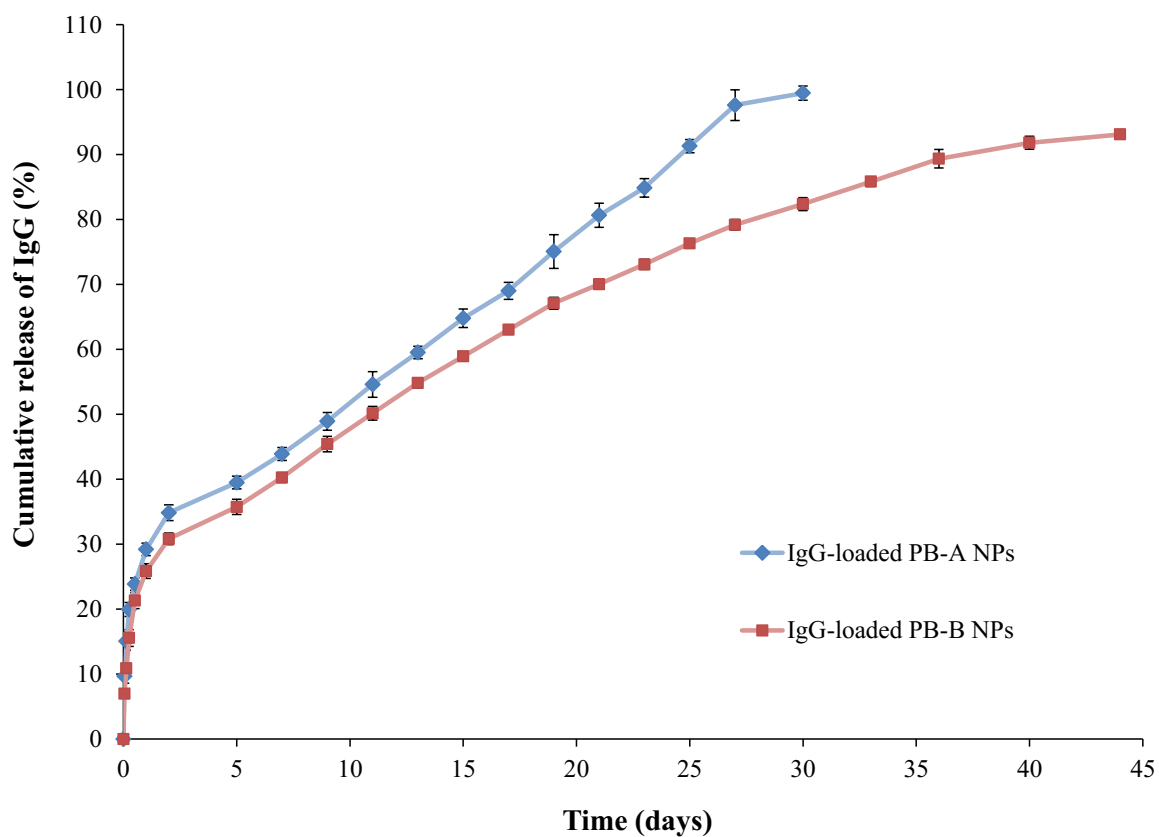


Figure 5.11: *In vitro* release of IgG from NPs prepared with PB-A and PB-B copolymers.

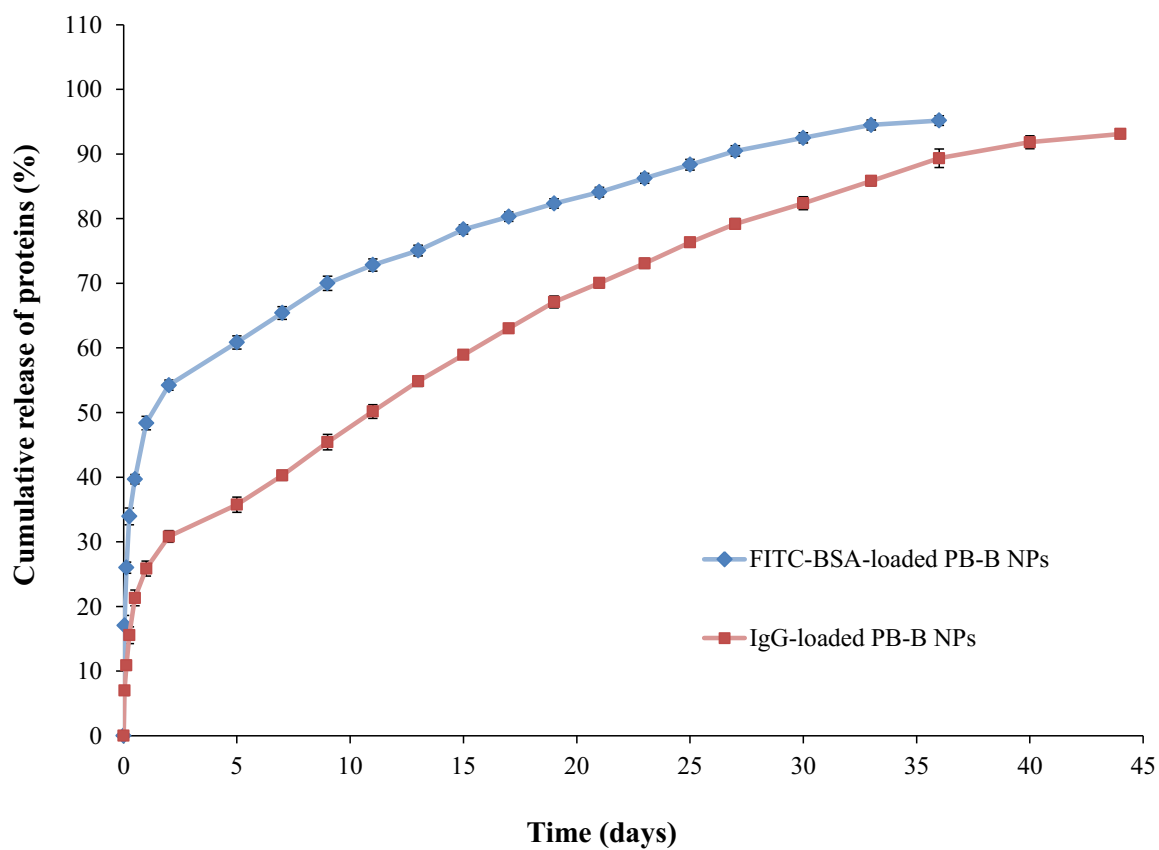


Figure 5.12: *In vitro* release of FITC-BSA and IgG from PB-B NPs

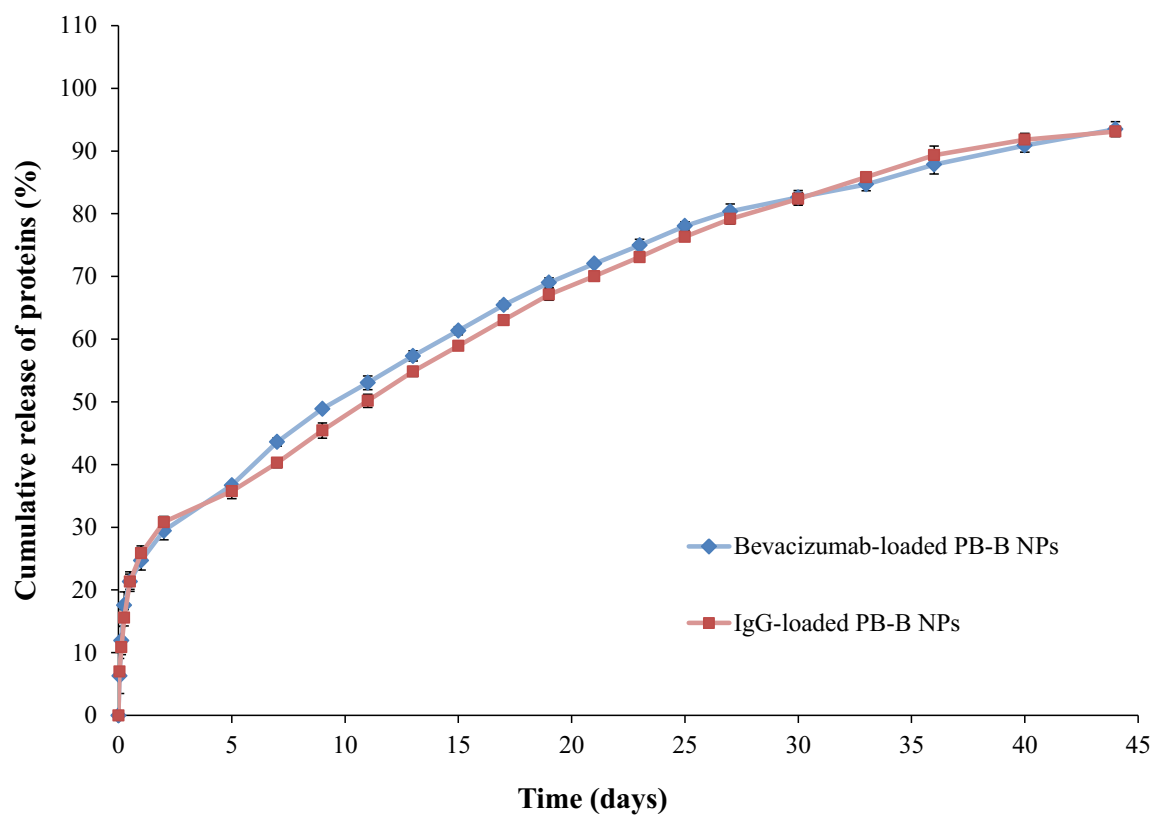


Figure 5.13: *In vitro* release of IgG and bevacizumab from PB-B NPs

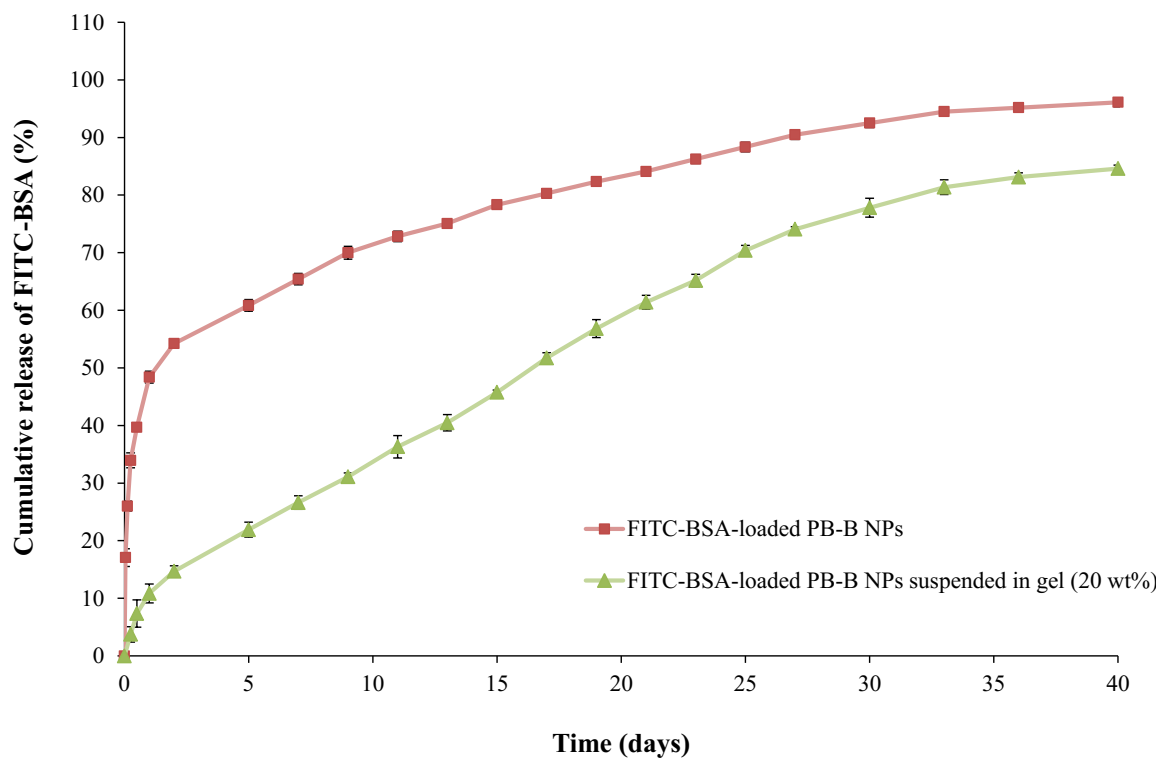


Figure 5.14: *In vitro* release of FITC-BSA from PB-B NPs and PB-B NPs suspended in PB-C gelling polymer

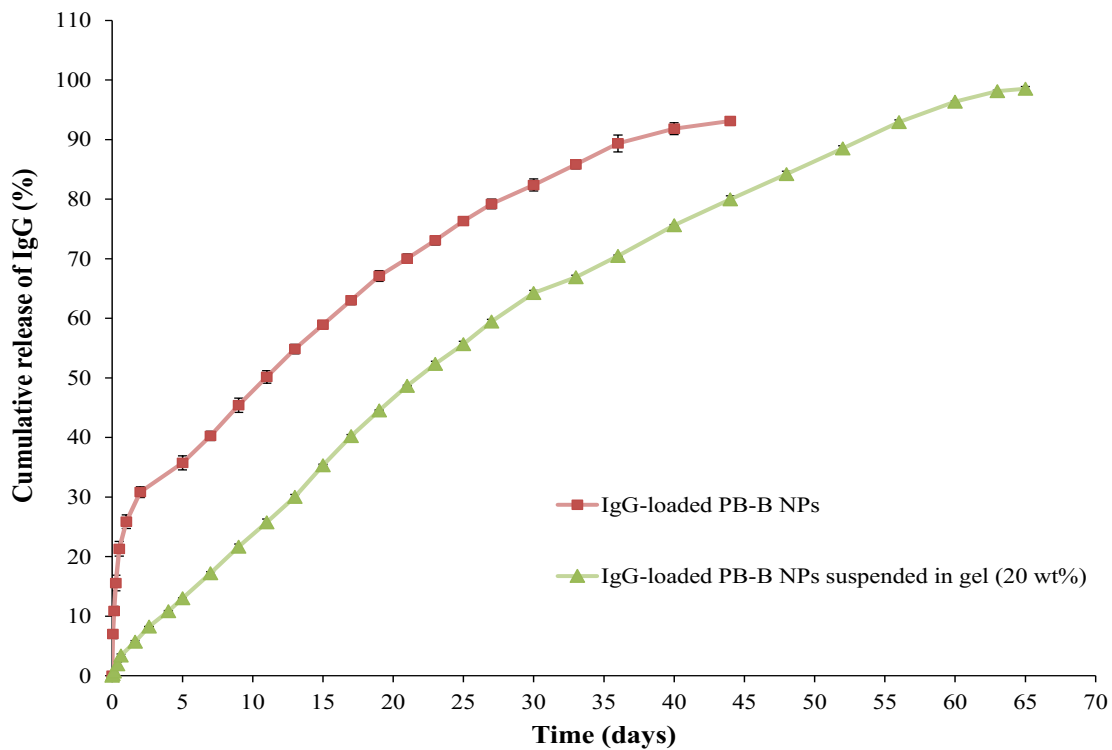


Figure 5.15: *In vitro* release of IgG from PB-B NPs and PB-B NPs suspended in PB-C gelling polymer (20 wt%).

Protein-loaded NPs were suspended in 20 wt% gelling solution and exposed to 37 °C which immediately transformed to solid hydrogel entrapping NPs throughout the polymer matrix. These composite formulations comprised of protein-loaded PB-B NPs (FITC-BSA and IgG) suspended in thermosensitive gel were evaluated for their release behavior. As described in Figure 5.14, burst release of FITC-BSA from composite formulation was negligible (~10%) relative to burst release observed from PB-B NPs (~48%) alone. In addition, release of FITC-BSA was prolonged for ~40 days. The similar behavior was observed for a composite formulation comprising IgG-loaded PB-B NPs suspended in 20 wt% thermosensitive gelling solution (Figure 5.15). Composite formulation of IgG exhibited negligible burst release followed zero-order release up to ~60 days. This behavior may be due to the fact that when the NPs were suspended into the gel matrix, gel matrix might serve as an additional diffusion barrier for the surface adsorbed drug. The gel matrix might deter the dumping of surface adsorbed dose eliminating burst effect which eventually provided nearly zero-order drug release throughout the release period.

Release kinetics

In order to evaluate drug release mechanism, we have fitted *in vitro* drug release data in five different release kinetic models i.e., Korsmeyer-Peppas, Higuchi, Hixon-Crowell, zero-order and first-order. Results showed in Table 5.3, indicated that Korsmeyer-Peppas was the best fit model for all the formulations with R^2 values ranging between 0.977-0.997. Moreover, n values in Korsmeyer-Peppas model for release of FITC-BSA, IgG and bevacizumab from PB-B NPs were below 0.43 indicating diffusion controlled release. Interestingly, n values for composite formulation of FITC-BSA (0.549) and IgG (0.818) (NPs suspended in thermosensitive gel) were between 0.43-0.89 suggesting anomalous diffusion. In other words,

release of protein therapeutics from composite formulation is controlled by diffusion as well as degradation of polymer.

Stability of secondary structure of IgG confirmed by CD spectroscopy

It is obvious that protein therapeutics need to maintain their three dimensional structure to exert pharmacological action. CD spectroscopy is a sensitive and robust analytical technique exploited for the investigation of secondary and at some extent tertiary conformation of proteins. It is sensitive enough to detect minor conformational changes in α -helix and β -sheets of the protein. Therefore, we have utilized this technique to confirm the conformational stability of released IgG and compared with CD spectrum of native IgG (Figure 5.16). CD spectrum of released IgG demonstrated λ minima of 218 nm similar to the native IgG. In addition, the CD spectra of native IgG and released IgG ranging from 200 nm to 250 nm were identical to each other indicating retention of structural conformation during NP preparation.

Cell proliferation assay

A cell proliferation assay was performed as described previously [215]. RF/6A cells proliferated rapidly in presence of VEGF (100 ng/mL, +ve control) whereas its proliferation was inhibited in absence of VEGF indicating sensitivity of endothelial cells toward growth factor particularly, VEGF (Figure 5.17). Native bevacizumab (standard group) has strongly inhibited the VEGF-induced cell proliferation at the concentration of 0.25 mg/mL. The similar level of inhibition was observed when released (released from NPs) bevacizumab (test/sample group) was exposed for 24h to VEGF treated cells. Moreover, inhibitory effects of released and native bevacizumab were not significantly different than -ve control.

Cell migration assay

Chemo-attractant property of VEGF stimulates RF/6A cell migration of across a porous membrane toward a VEGF stimulus. Biological activity of released bevacizumab was further evaluated by VEGF-induced cell migration assay. As described in Figure 5.18, a test/sample group (released bevacizumab) exhibited significant inhibition of cell migration across the transwell membrane relative to VEGF group (+ve control). Results showed that this inhibitory effect was not significantly different than -ve control or a standard group (cells treated with native bevacizumab). For the visual evidence, migrated cells were stained with methylene blue and images were taken. Data depicted in Figure 5.18b also supported the results described earlier.

Data observed in cell proliferation and cell migration assays clearly pointed out that bevacizumab has retained its biological activity during the process of NP preparation. Previous reports suggest that PLA and/or PGA based copolymer produce large molar mass of lactic acid and/or glycolic acid [183, 197]. These degradation products stimulate hydrolytic degradation of protein therapeutics. Retention of protein stability (IgG and bevacizumab) in PB NPs may attributed to lower molar mass of PLA or PGA blocks which produce very low amounts of lactic acid or glycolic acid, eliminating or reducing protein degradation.

Table 5.3: Coefficient of determination (R^2) for various kinetic models for *in vitro* release of FITC-BSA, IgG and bevacizumab.

Block copolymers	Korsmeyer-Peppas		Higuchi	Hixson-Crowell	First-Order	Zero-Order	Best fit model
	R^2	n	R^2	R^2	R^2	R^2	
FITC-BSA PB-B NPs	0.989	0.327	0.945	0.905	0.984	0.783	Korsmeyer-Peppas
IgG NPs PB-B NPs	0.982	0.334	0.979	0.979	0.959	0.898	Korsmeyer-Peppas
Bevacizumab PB-B NPs	0.977	0.344	0.969	0.961	0.959	0.881	Korsmeyer-Peppas
FITC-BSA PB-B NPs suspended in gel	0.992	0.549	0.978	0.959	0.982	0.851	Korsmeyer-Peppas
IgG PB-B NPs suspended in gel	0.997	0.818	0.971	0.996	0.987	0.994	Korsmeyer-Peppas

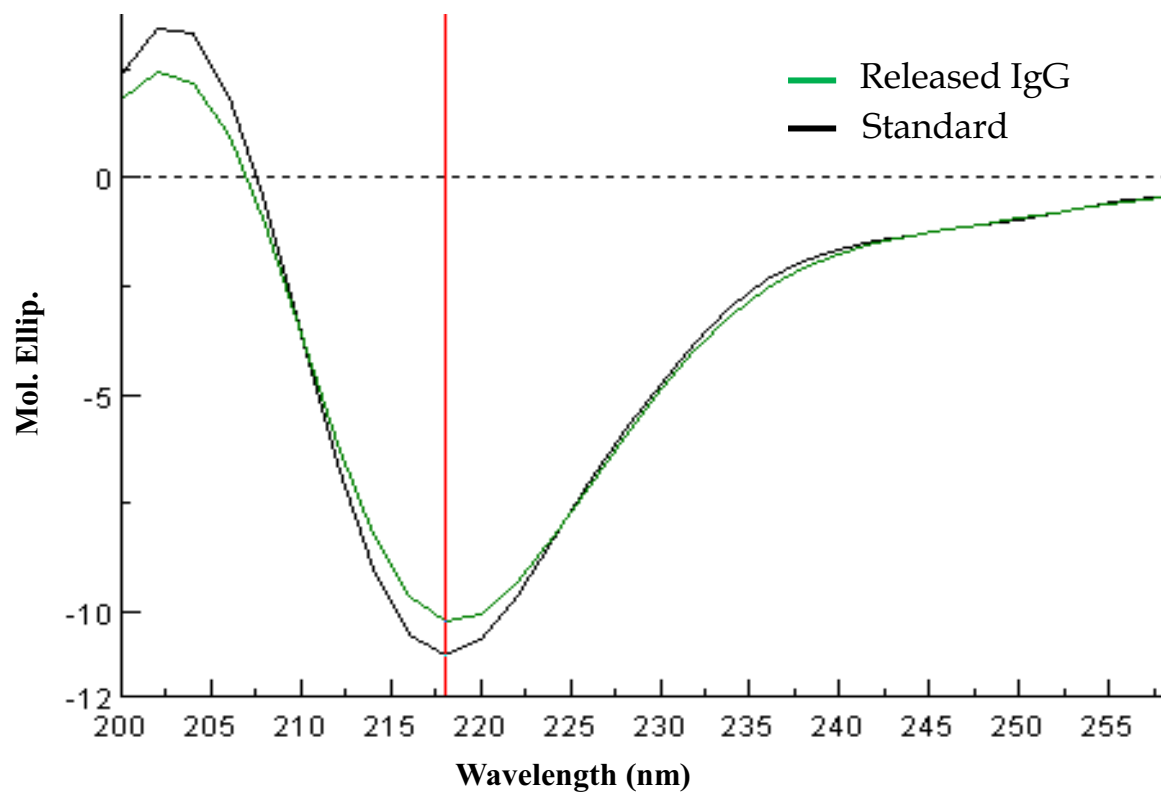


Figure 5.16: Stability of released IgG confirmed by CD spectroscopy.

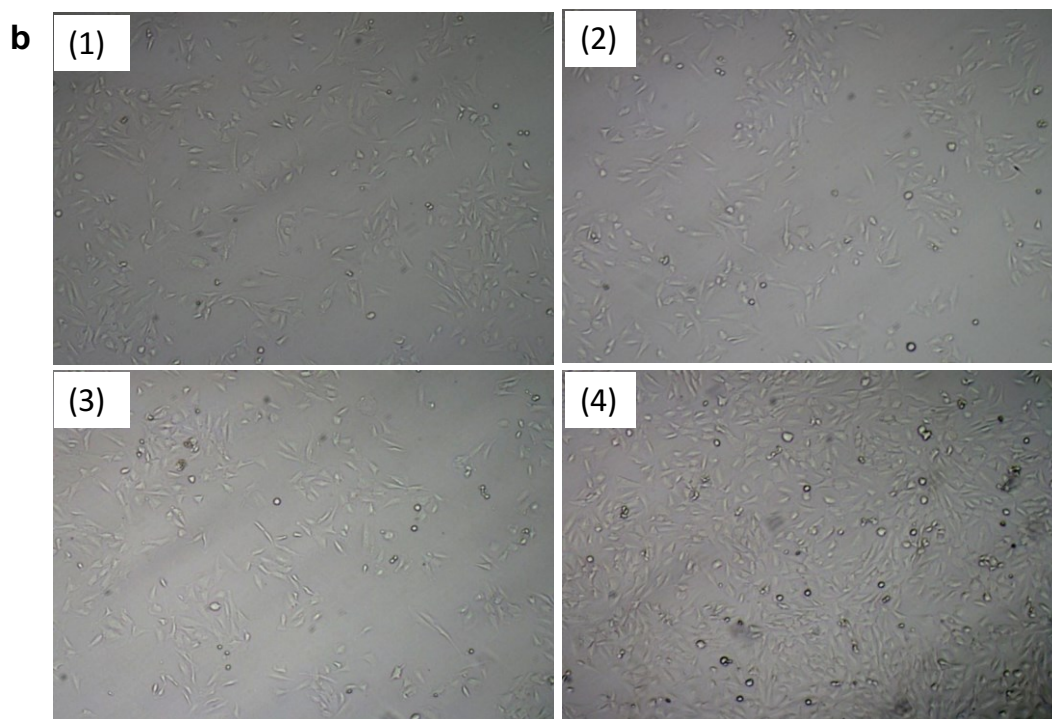
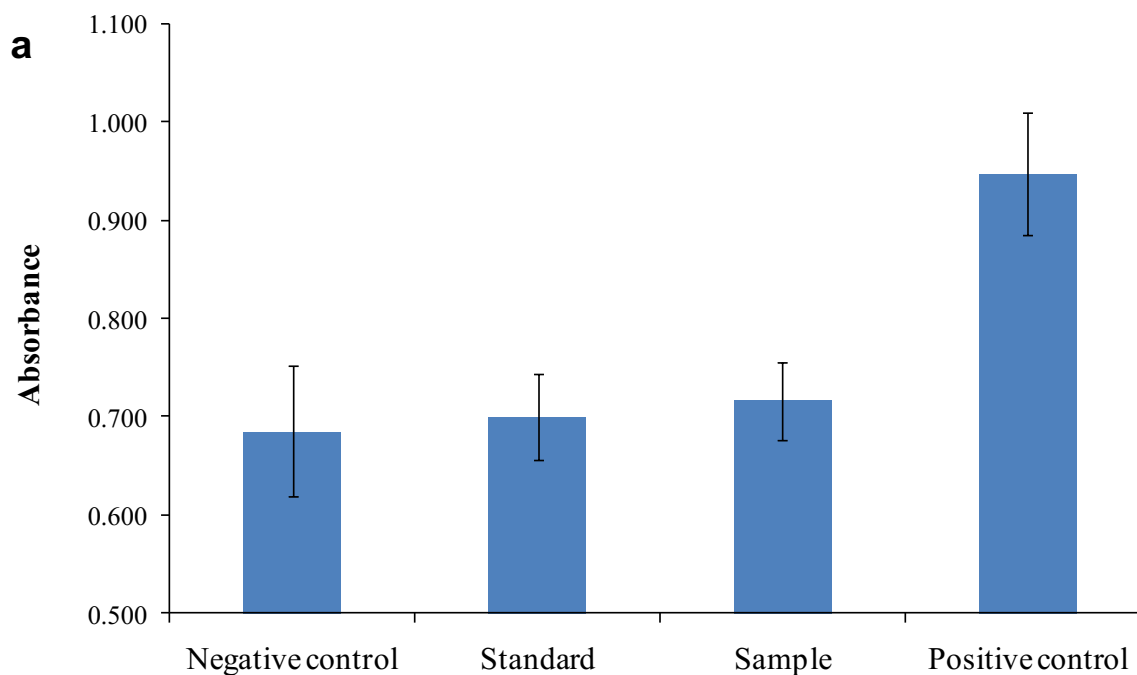


Figure 5.17: Cell proliferation assay performed on RF/6A cells to evaluate the biological activity of bevacizumab (a) absorbance produced by live cells (b) images of live cells where (1) negative control (untreated cells), (2) standard (cells exposed to 100 ng/mL of VEGF and 0.25 mg/mL of bevacizumab), (3) sample (cells exposed to 100 ng/mL of VEGF and 0.25 mg/mL of released bevacizumab), and (4) positive control (cell exposed to 100 ng/mL VEGF).

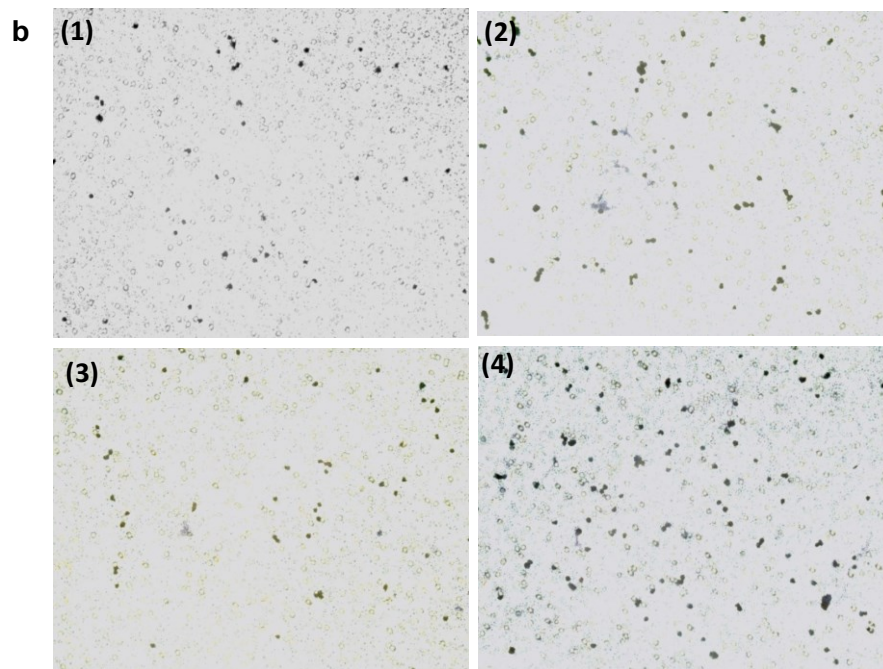
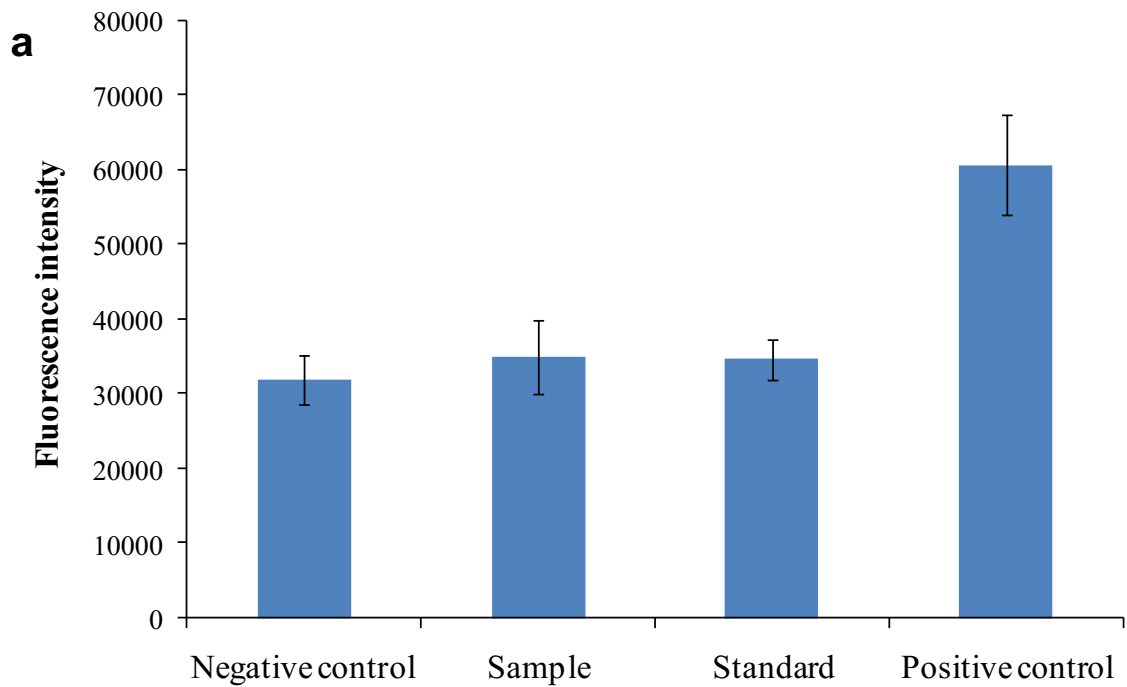


Figure 5.18: Cell migration assay performed on RF/6A cells to evaluate the biological activity of bevacizumab (a) fluorescence intensity indicating number of migrated cells (b) images of migrated cells stained by methylene blue where (1) negative control (untreated cells), (2) standard (cells exposed to 100 ng/mL of VEGF and 0.25 mg/mL of bevacizumab), (3) sample (cells exposed to 100 ng/mL of VEGF and 0.25 mg/mL of released bevacizumab), and (4) positive control (cell exposed to 100 ng/mL VEGF).

Conclusion

We have successfully synthesized and characterized novel PB copolymers for the preparation of NPs and thermosensitive gel. In order to eliminate burst release phase, a novel composite formulation comprised of protein-loaded PB NPs suspended in a PB thermosensitive gel was successfully formulated and evaluated. FITC-BSA and IgG-encapsulated NPs suspended in thermosensitive gel demonstrated continuous zero-order release, avoiding the possibility of dose dependent toxicity that may occur due to an initial burst release. Moreover, CD spectroscopy demonstrated the retention of structural conformation of released IgG. Bevacizumab-loaded NPs demonstrated similar patterns of burst release and sustained release as of IgG-embedded NPs. *In vitro* cell proliferation and cell migration assay confirmed retention of biological activity of the bevacizumab. This approach can act as a platform for the ocular delivery of therapeutic macromolecules, and can minimize the side effects associated with frequent intravitreal injections.

CHAPTER 6
OPTIMIZATION OF NOVEL PENTABLOCK COPOLYMER BASED COMPOSITE
FORMULATION FOR SUSTAINED DELIVERY OF PROTEIN THERAPEUTICS IN
THE TREATMENT OF OCULAR DISEASES

Rationale

The ideal formulation for the intravitreal delivery should possess following characteristics, (a) high drug loading in small volume ($\leq 100 \mu\text{L}$) that lasts up to 6 months or more, (b) provide constant release (zero-order release) throughout the release period without any burst effect, (c) easy to administered such as injectable system and not implants, (d) ensure stability of protein/peptide, (e) biodegradable and biocompatible, and (f) the time required for biodegradation of formulation should not be more than 1.5 times the release period.

Many researchers are investigating protein-encapsulated NPs for the sustained delivery in the treatment of back of the eye diseases. It is easy to achieve high drug loading in NPs for hydrophobic therapeutic agents. In contrast, it is very difficult to achieve high drug loading of protein therapeutics (hydrophilic agents). One more limitation for intravitreal injection is small injection volume ($\leq 100 \mu\text{L}$). Therefore, one of the important challenges is to develop a formulation which can carry large amount of dose in limited injection volume and provide constant release up to 6 months or more.

In order to address mentioned issues, we have synthesized novel biodegradable and biocompatible PB copolymers composed of PEG, PCL, and PLA/PGA. In this section, we study the effects of various formulation parameters on EE, DL and *in vitro* release profile. In order to incorporate a large amount of protein therapeutic in small volume of formulation, we have optimized NP preparation methods to attain maximum possible DL. To achieve constant

(zero-order) release, we have utilized a novel concept of composite formulation (discussed in chapter 5) where protein/peptide-loaded PB NPs were suspended in a PB thermosensitive gel. Moreover, the optimized methods for NP preparation were also applied to encapsulate proteins or peptides with different molecular weights ranging from 1-237 kDa. Biological activity of released proteins or peptides was also determined utilizing enzymatic activity assays.

Materials and methods

Materials

PEG (2 kDa and 4 kDa), methoxy-PEG (550 Da), ϵ -caprolactone, poly (vinyl alcohol) (PVA), stannous octoate, lysozyme from chicken egg white and *Micrococcus luteus* were procured from Sigma-Aldarich (St. Louis, MO; USA). Hexamethylene diisocyanate (HMDI), glycolide and L-lactide were obtained from Acros organics (Morris Plains, NJ; USA). Catalase was purchased from Worthington Biochemical Corp. IgG-Fab and IgG were purchased from Athens research technology Inc., and Lee Biosolutions, respectively. Octreotide and insulin were procured from China Peptides Co. ltd. and MP Biomedicals LLC., respectively. Micro-BCATM and catalase colorimetric assay kits were obtained from Fisher Scientific and Arbor Assays Inc., respectively. All other reagents utilized in this study were of analytical grade.

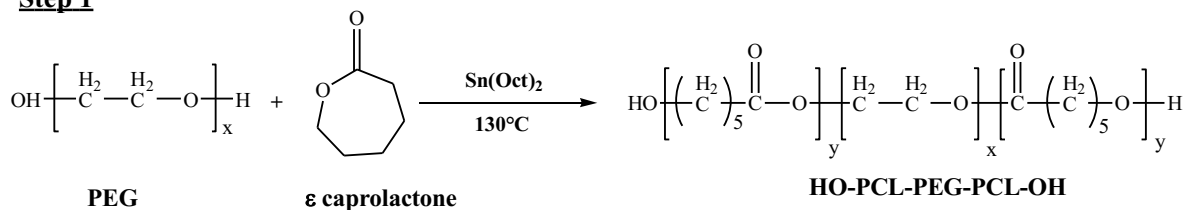
Methods

Synthesis of PB copolymers

Novel PB copolymers, PLA-PCL-PEG-PCL-PLA (PB-A/PB-B), PGA-PCL-PEG-PCL-PGA (PB-C/PB-D), and PEG-PCL-PLA-PCL-PEG (PB-E) were synthesized by ring-opening bulk copolymerization [217]. Briefly, ϵ -caprolactone was polymerized on two open hydroxyl ends of PEG (2 kDa or 4 kDa) utilizing stannous octoate as catalyst (0.5% w/w). The reaction was carried out for 24 h at 130 °C in inert environment. TB (TB) copolymer (PCL-

PEG-PCL) was purified by dissolving in dichloromethane (DCM) followed by cold-ether precipitation. Purified TB copolymer was then utilized for the preparation of PB copolymer. Predetermined quantities of TB copolymer and L-lactide (PB-A/PB-B) or glycolide (PB-C/PB-D) were added in round bottom flask. Stannous octoate (0.5% w/w) was added in reaction mixture as a catalyst. Reaction for the synthesis of PB-A/PB-B were carried out at 130 °C for 24 h whereas for PB-C/PB-D at 200 °C for 24 h. At the end, reaction mixture was purified for PB copolymers as described earlier. Purified PB copolymers were vacuum-dried and stored at -20 °C until further characterization. PB copolymer with thermosensitive properties (PB-E) was synthesized, purified and characterized according to previously published protocol with minor modifications [217]. For the synthesis of PB-E, TB copolymer (mPEG-PCL-PLA) was synthesized by ring-opening bulk copolymerization. Firstly, ϵ -caprolactone was polymerized at the hydroxyl terminal of mPEG (550 Da) followed by polymerization of L-lactide. Resulting TB copolymers were coupled with HMDI as a linker. Coupling reaction was carried out for 8 h at 70 °C. Resulting polymer was purified by cold-ether precipitation followed by drying under vacuum. Reaction schemes for the synthesis of PB copolymers are depicted in Figures 6.1 and 6.2.

Step 1



Step 2

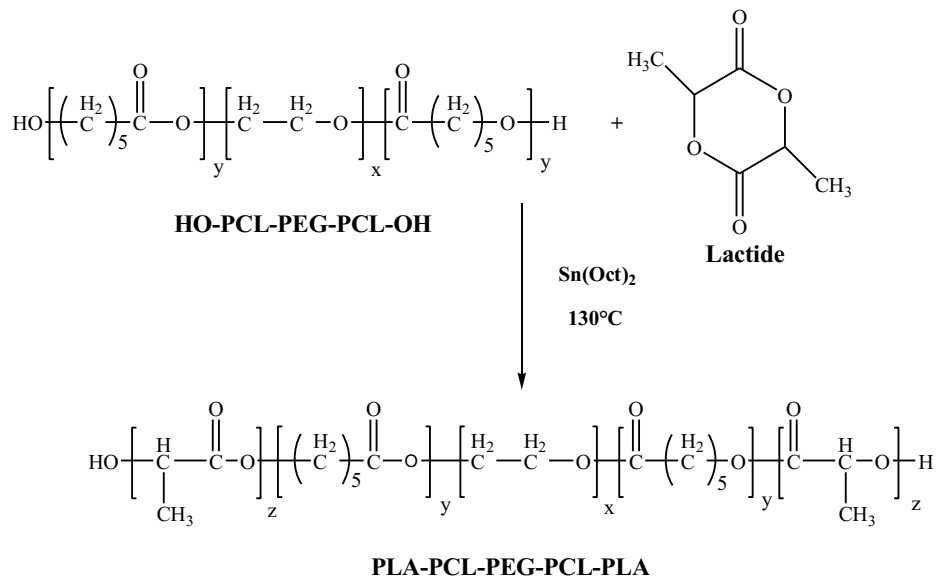


Figure 6.1a: Synthesis scheme for PB-A and PB-B (PLA-PCL-PEG-PCL-PLA)

Step 2

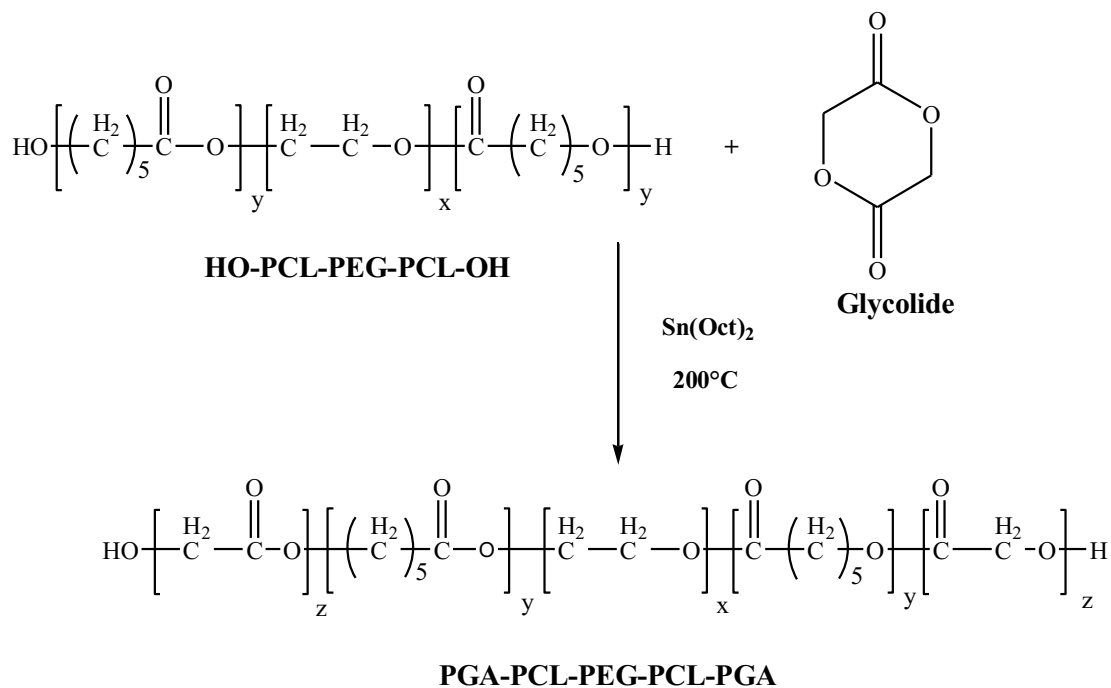
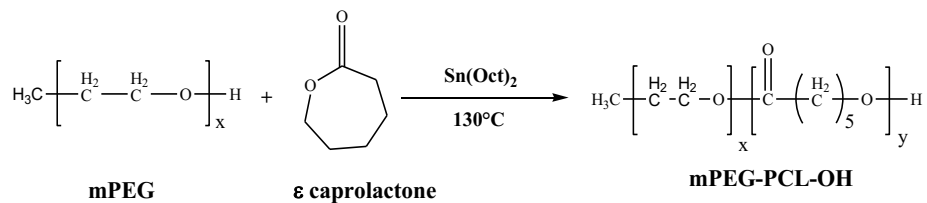


Figure 6.1b: Synthesis scheme for PB-C and PB-D (PGA-PCL-PEG-PCL-PGA).

Step 1



Step 2

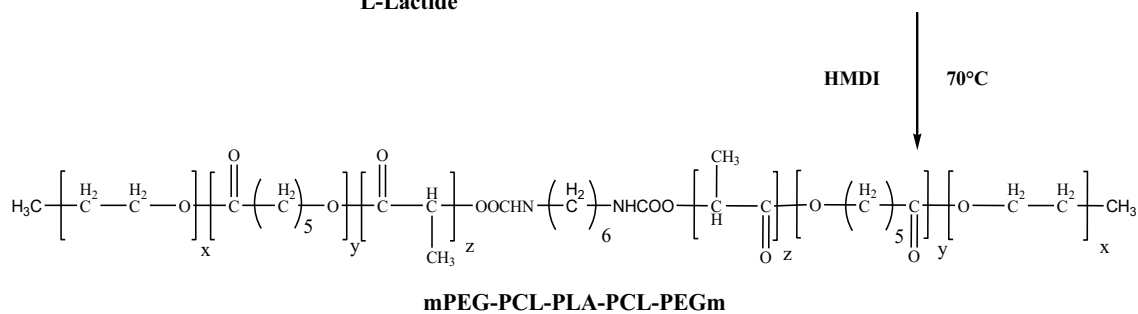
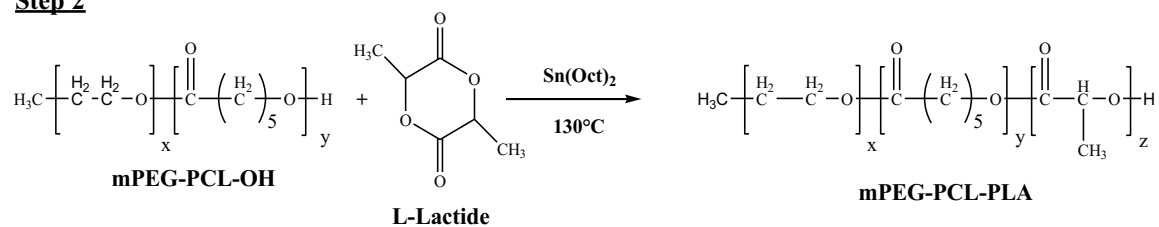


Figure 6.2: Synthesis scheme for PB-E (PEG-PCL-PLA-PCL-PEG).

Characterization of polymers

PB copolymers were characterized for their molecular weight and purity by $^1\text{H-NMR}$ spectroscopy and gel permeation chromatography (GPC).

$^1\text{H-NMR}$

Polymeric materials (5 mg) were dissolved in 600 μL of CDCl_3 and were analyzed on Varian-400 MHz NMR instrument. Molecular weight (M_n) and purity of the polymers were evaluated from the $^1\text{H-NMR}$ spectrum.

GPC

Molecular weights (M_n and M_w), purity and polydispersity (PD) were further evaluated by Ecosec HLC 8320 gel permeation chromatograph connected with differential refractometer. Briefly, 5 mg of polymeric materials were dissolved in tetrahydrofuran (THF) and separated on Styragel HR-3 column. THF was used as eluting solvent and polystyrene samples with narrow molecular weight distribution were utilized as standards.

Preparation of thermosensitive gelling solution

To prepare 20 wt% aqueous gelling solution, 200 mg of PB-E copolymer was dissolved in 800 mg of phosphate buffer saline (PBS, pH 7.4) by keeping overnight at 4 $^\circ\text{C}$. Sol-gel behavior of aqueous solution was confirmed by vial inverting method reported earlier [179]. Aqueous solution was exposed to 37 $^\circ\text{C}$ for 5 min followed by inversion of vial for 1 min, state of no flow was considered as hydrogel.

Preparation of NPs

Protein/peptide-loaded PB-NPs were prepared by $W_1/O/W_2$ double emulsion solvent evaporation method [201]. Briefly, a peptide or protein aqueous solution (W_1 phase) was

emulsified in organic phase (dichloromethane (DCM) comprising PB copolymers) using probe sonication to form W₁/O primary emulsion. The primary emulsion was further emulsified in aqueous phase containing 2% polyvinyl alcohol (PVA) using probe sonication to prepare W₁/O/W₂ double emulsion. Resulting emulsion was diluted with 2% PVA (W₃) under continuous stirring. DCM of organic phase was then evaporated under vacuum using rotavap to obtain NPs. NPs were separated by ultracentrifugation at 20,000 rpm for 30 min (4 °C). Particles were washed twice with distilled deionized water (DDW), and centrifuged to remove traces of PVA and untrapped peptide/protein. Purified NPs were freeze-dried with mannitol (5% w/v) and stored at -20 °C until further use. Freeze-dried NPs were evaluated for EE, DL and *in vitro* drug release behavior. Process parameters such as phase volume ratio, drug/polymer ratio, and types of polymer were optimized to achieve higher DL. The detailed process parameters are reported in Table 6.2.

Characterization of NPs

Entrapment efficiency (EE) and drug loading (DL)

Protein/peptide-encapsulated freeze-dried NPs were evaluated for the estimation of EE and DL. Amount of untrapped protein/peptide in supernatant was determined by micro BCA™ protein assay kit following manufacturer's protocol. Standard curve of respective proteins/peptides (octreotide, insulin, lysozyme, IgG-Fab, IgG and catalase) were prepared in the range of 3-200 µg/mL. Following equations were utilized for the calculation of EE (%) and DL (%).

EE (%) was calculated with eq. 6.1

$$EE (\%) = \left(1 - \frac{\text{Amount of drug in supernatant}}{\text{Total amount of drug}}\right) * 100 \quad \dots \text{Eq. 6.1}$$

DL (%) was calculated by eq. 6.2

$$DL (\%) = \left(\frac{\text{Amount of drug in nanoparticles}}{\text{Total amount of drug and polymer}} \right) * 100 \quad \dots \text{Eq. 6.2}$$

In vitro release studies

Protein/peptide-loaded freeze-dried NPs were characterized for their release behavior. To perform *in vitro* drug release from composite formulation, precalculated amount of NPs were suspended in 100 μL of PB-E thermosensitive gelling solution (20 wt%) maintained at 4 $^{\circ}\text{C}$. Resulting PB NP suspension was then incubated at 37 $^{\circ}\text{C}$ for 30 min followed by slow addition of 1 mL of PBS (pH 7.4) preincubated at 37 $^{\circ}\text{C}$. At predefined time intervals, 200 μL of clear supernatant was collected and replaced with fresh PBS (37 $^{\circ}\text{C}$). Release samples were evaluated for protein content by Micro BCATM total protein assay which was performed according to supplier's instructions. Release experiments were carried out in triplicates and depicted as cumulative drug release (%) against time. Biological activity of lysozyme and catalase were confirmed by their enzymatic assays.

Release kinetics

In order to investigate release mechanisms, release data were fitted to various kinetic models i.e., Korsmeyer-Peppas ($M_t/M_{\infty} = kt^n$), Higuchi ($Q_t = Kt^{1/2}$), Hixon-Crowell ($C_0^{1/3} - C_t^{1/3} = kt$), First-order ($\text{Log}C = \text{Log}C_0 - Kt/2.303$), and Zero-order ($C = K_0t$). Based on the R^2 value, best fit model was identified. Diffusion exponent (n) of Korsmeyer-Peppas equation was utilized to understand the mechanism of release.

Stability evaluation of lysozyme and catalase

Estimation of enzymatic activity of lysozyme

Enzymatic activity of lysozyme in the released samples was estimated by comparing with freshly prepared lysozyme solutions and/or controlled samples. Controls were comprised of lysozyme solution incubated at 37 °C in PBS (pH 7.4) which kept parallel to the *in vitro* release study from composite formulation. In order to determine enzymatic activity of lysozyme, a stock solution of *Micrococcus luteus* (0.01% w/v) was prepared with phosphate buffer (66 mM, pH 6.15) and diluted to achieve absorbance between 0.2 - 0.6 at 450 nm. A 100 µL of samples, standards or controls were mixed with 2.5 mL of *Micrococcus luteus* suspension. A rate of deceleration of absorbance at 450 nm was determined over a period of 4 min at room temperature. Data was plotted for absorbance against time and slope was utilized for the quantification of lysozyme in enzyme unit (EU). The units of lysozyme (active) per milligram of protein were calculated from the following equations [218].

$$\text{Units of lysozyme in one mL sample} = \frac{(\Delta A_{450 \text{ nm/min Test}} - \Delta A_{450 \text{ nm/min Blank}})(df)}{(0.001)(0.1)} \dots \text{Eq. 6.3}$$

$$\frac{\text{Units of lysozyme}}{\text{mg of sample}} = \frac{\text{Units of lysozyme/mL of sample}}{\text{mg of lysozyme/mL of sample}} \dots \text{Eq. 6.4}$$

Where, 0.001 was obtained from the definition of lysozyme as one unit of enzyme is able to produce $\Delta A_{450\text{nm}}$ of 0.001 per minute at pH 6.15 and 25 °C utilizing *Micrococcus luteus* suspension, 0.1 represent the volume of release samples, standards or controls and df depicts dilution factor. Biological activity observed for release samples were compared with the respective controls of the same time points.

Estimation of enzymatic activity of catalase

Enzymatic activity of catalase was estimated for *in vitro* release samples. Control samples with known concentration of catalase were prepared in PBS (pH 7.4) and exposed at 37 °C along with *in vitro* release samples. Control, test and standard samples were analyzed for catalase activity with catalase colorimetric assay kit. Assay was performed according to supplier's protocol. Briefly, standards with known concentrations were prepared in assay buffer. A 25 µL of standard, control or sample was added in 96-well plate containing 25 µL of hydrogen peroxide solution. The resulting mixture was then incubated for 30 min at room temperature. After incubation, 25 µL of colorimetric detection reagent was added in each well followed by addition of 25 µL horseradish peroxidase (HRP) reagent. Plate was incubated for 15 min at room temperature and then analyzed by UV spectrophotometer at 570 nm. According to catalase activity assay, reduction in the absorbance is directly proportional to the catalase activity.

Results and discussion

Synthesis and characterization of PB copolymers

PB copolymers designed for the preparation of NPs and thermosensitive gel were successfully synthesized by ring-opening bulk copolymerization. Firstly, TB copolymers (PCL-PEG-PCL or mPEG-PCL-PLA) were synthesized, purified and characterized. Resulting TB copolymers were utilized for the preparation of PB copolymers i.e., PB-A/PB-B (PLA-PCL-PEG-PCL-PLA), PB-C/PB-D (PGA-PCL-PEG-PCL-PGA) and PB-E (PEG-PCL-PLA-PCL-PEG). Molecular weights (M_n) and purity of the PB copolymers were examined by $^1\text{H-NMR}$ spectroscopy. As depicted in Figures 6.3, 6.4 and 6.5, PCL blocks exhibited typical $^1\text{H-NMR}$ peaks at 1.40, 1.65, 2.30 and 4.06 ppm attributed to methylene protons of $-(\text{CH}_2)_3-$, -

OCO-CH₂-, and -CH₂OOC-, respectively. PB-A, PB-B and PB-E, L-lactide containing PB copolymers demonstrated two ¹H-NMR peaks at 5.17 and 1.50 ppm representing -CH- and -CH₃- groups. Similarly, PB-C and PB-D copolymers comprised of glycolic acid exhibited series of singlets between 4.6 to 4.9 ppm explaining methylene protons of PGA block. ¹H-NMR of PB-E copolymer exhibited an additional peak at 3.38 ppm which was denoted to terminal methyl of (-OCH₃-) of PEG. Molecular weight of PB copolymers were calculated from the integration values of ¹H-NMR peaks of individual blocks [EO]/[CL]/[LA] or [EO]/[CL]/[GA]. Moreover, absence of any additional peaks in ¹H-NMR spectrum confirmed the purity of PB copolymers. Molecular weight calculated from ¹H-NMR is reported in Table 6.1.

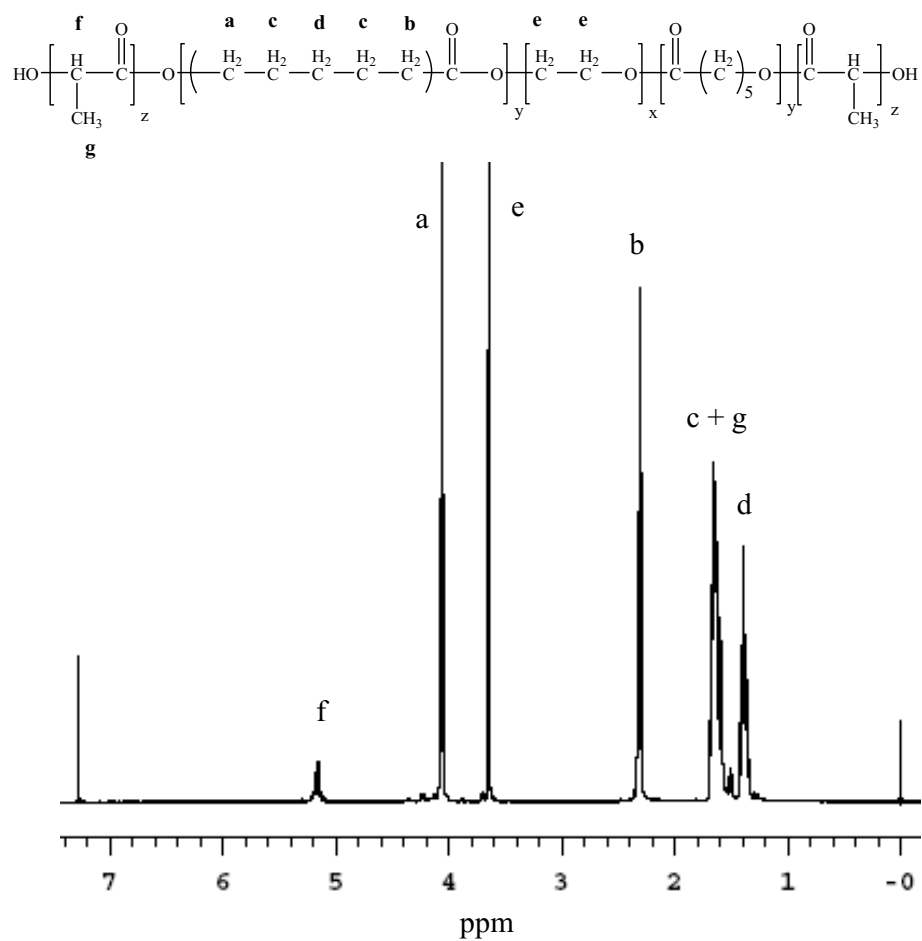


Figure 6.3: $^1\text{H-NMR}$ spectrum of PB-A copolymer in CDCl_3 .

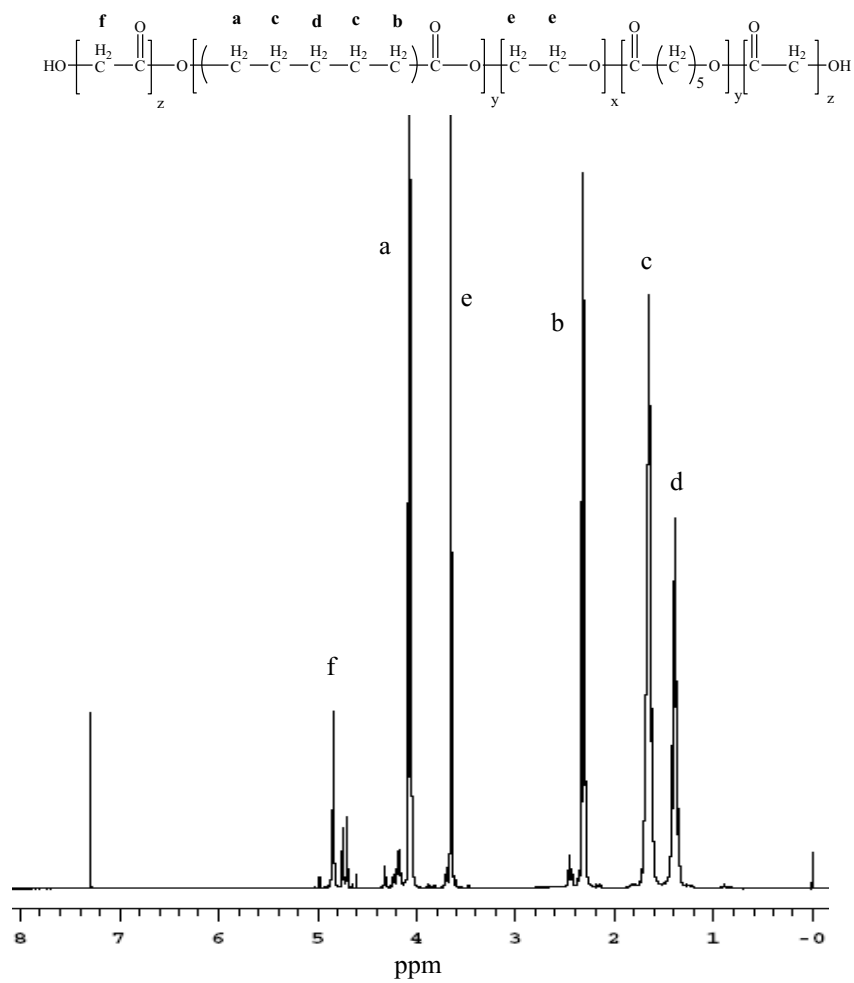


Figure 6.4: ^1H -NMR spectrum of PB-D copolymer in CDCl_3 .

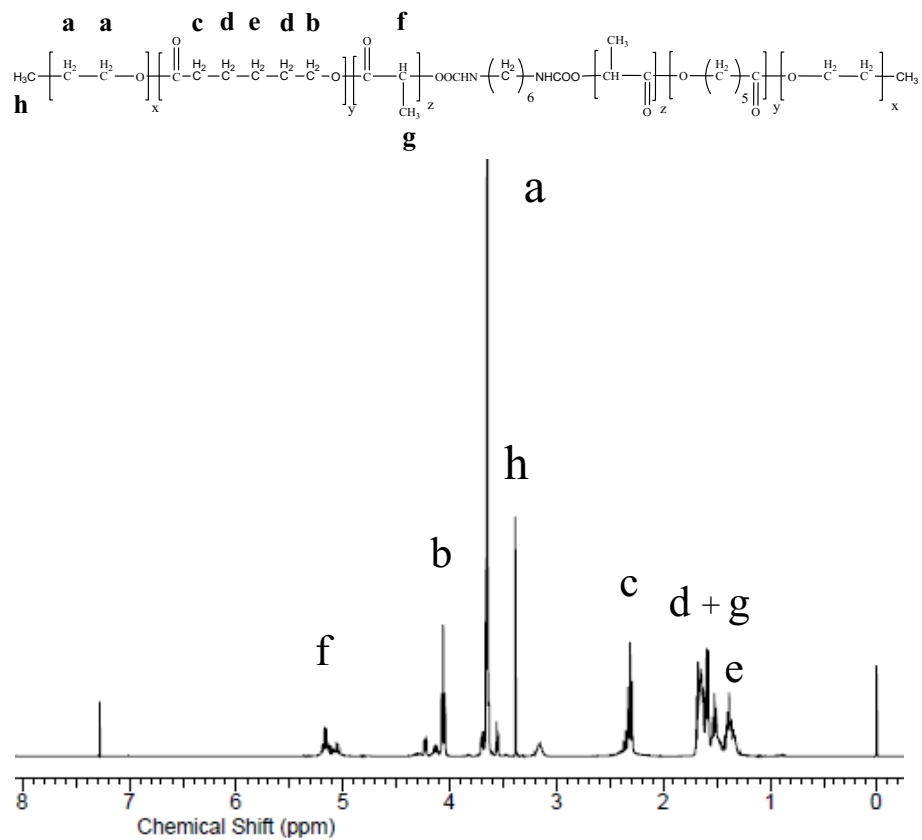


Figure 6.5: $^1\text{H-NMR}$ spectrum of PB-E copolymer in CDCl_3 .

Table 6.1: Characterization of polymers.

Code	Structure	PLA/PCL/PEG or PGA/PCL/PEG	Total M_n^a (theoretical)	Total M_n^b (calculated)	Total M_n^c (calculated)	M_w^c (GPC)	PDI ^c
PB-A	PLA ₃₀₀₀ -PCL ₇₀₀₀ -PEG ₂₀₀₀ -PCL ₇₀₀₀ -PLA ₃₀₀₀	3/7/1	22000	20780	17250	24020	1.39
PB-B	PLA ₃₀₀₀ -PCL ₇₀₀₀ -PEG ₄₀₀₀ -PCL ₇₀₀₀ -PLA ₃₀₀₀	1.5/3.5/1	24000	21350	17640	23830	1.35
PB-C	PGA ₃₀₀₀ -PCL ₇₀₀₀ -PEG ₄₀₀₀ -PCL ₇₀₀₀ -PGA ₃₀₀₀	1.5/3.5/1	24000	21290	16180	23210	1.43
PB-D	PGA ₃₀₀₀ -PCL ₇₀₀₀ -PEG ₂₀₀₀ -PCL ₇₀₀₀ -PGA ₃₀₀₀	3/7/1	22000	20120	17030	24190	1.42
PB-E	PEG ₅₅₀ -PCL ₈₂₅ -PLA ₅₅₀ -PCL ₈₂₅ -PEG ₅₅₀	0.5/1.5/1	3300	3280	4330	6100	1.41

a. Theoretical value, calculated according to the feed ratio

b. Calculated from ¹H-NMR results

c. Determined by GPC analysis

Table 6.2: Optimization of process parameters for the preparation of IgG-Fab-loaded PB NPs.

Batch #	Process parameters									EE (%)	Drug loading (%)
	Polymer types	Polymer (mg)	IgG-Fab (mg)	Volume of W ₁ (mL)	Volume of organic phase (mL)	Volume of W ₂ (mL) ^a	Volume of W ₃ (mL) ^b	Sonication time W ₁ /O	Sonication time W ₁ /O/W ₂		
Batch 1	PB-A	100	10	1	4	20	-	45 Sec (4 Output)	3 min (7 Output)	54.0 ± 1.8	5.6 ± 0.2
Batch 2	PB-B	100	10	1	4	20	-	45 Sec (4 Output)	3 min (7 Output)	45.7 ± 2.7	5.0 ± 0.3
Batch 3	PB-A	100	10	1 + 1% NaCl	4	20 + 10% NaCl	-	45 Sec (4 Output)	3 min (7 Output)	54.8 ± 2.3	6.7 ± 0.2
Batch 4	PB-B	100	10	1 + 1% NaCl	4	20 + 10% NaCl	-	45 Sec (4 Output)	3 min (7 Output)	49.5 ± 1.3	5.9 ± 0.2
Batch 5	PB-A	10	2.5	0.25	1	8.8	-	30 Sec (1 Output)	45 Sec (2 Output)	25.9 ± 2.3	6.4 ± 1.0
Batch 6	PB-A	10	2.5	0.25	1	2	3	30 Sec (1 Output)	45 Sec (2 Output)	45.2 ± 1.6	11.7 ± 1.3
Batch 7 (Method A)	PB-A	10	2.5	0.167	0.667	1.333	3.667	30 Sec (1 Output)	45 Sec (2 Output)	69.6 ± 9.0	15.6 ± 2.0
Batch 8 (Method B)	PB-A	10	2.5	0.1	0.4	0.8	4.2	30 Sec (1 Output)	45 Sec (2 Output)	73.2 ± 0.2	15.5 ± 0.1

a. W₂ phase was comprised of 2% PVA

b. W₃ phase was comprised of 2% PVA

Purity, molecular weight (Mn and Mw) and polydispersity were further evaluated by GPC. As described in Table 6.1, polydispersity of all the polymers were below 1.45 suggesting narrow distribution of molecular weights. Molecular weights obtained for GPC analysis were very close to the feed ratio. Moreover, block copolymers depicted a single peak in GPC chromatogram (data not shown) indicating monodistribution of molecular weight and absence of any homopolymers such as PLA, PGA, PCL and PEG. The Mn values obtained from GPC analysis were noticeably smaller than Mn values observed from ¹H-NMR spectroscopy. This result was attributed to the difference in hydrodynamic diameter of block copolymers relative to parent homopolymers [219]. Calculated molecular weights were very similar to the theoretical molecular weights obtained from feed ratio. Hence, in the following text theoretical molecular weights are mentioned instead of calculated molecular weights.

Preparation and characterization of NPs

PB NPs were successfully prepared with double emulsion solvent evaporation method (W₁/O/W₂). We have attempted to optimize NP preparation method to achieve maximum possible DL. In this section we have studied the effect of polymer hydrophobicity, salt (NaCl), drug to polymer ratio, concentration and phase volumes, and types of protein/peptide on EE and DL.

Entrapment efficiency (EE) and Drug loading (DL)

IgG-Fab-loaded NPs were prepared utilizing two PB copolymers (PB-A and PB-B) to determine the effect of polymer type or hydrophobicity on DL where PB-A copolymer is more hydrophobic than PB-B copolymer. As represented in Table 6.2, EE and DL for PB-A copolymers (Batch 1) were ~54% and 5.62%, respectively whereas PB-B copolymer (Batch 2) exhibited ~46% of EE and 4.99% of DL. NPs composed of PB-A copolymer demonstrated

higher DL relative to PB-B NPs, which may be attributed to relatively high hydrophobicity of PB-A copolymer. During solvent evaporation, high hydrophobicity may allow faster polymer precipitation to form NPs preventing diffusion of IgG-Fab in external aqueous (W_2) phase.

Reports published elsewhere suggested significant effect of NaCl on EE and DL in nanoparticulate system [220]. As described in Batches 3 and 4, incorporation of NaCl in W_1 (1%) and W_2 (10%) phase exhibited higher EE and loading of IgG-Fab in both PB-A (EE = ~55% and DL = 6.68%) and PB-B (EE = ~49% and DL = 5.88%) NPs relative to the respective PB NPs prepared without NaCl. An important prerequisite for higher DL is separation of droplets during emulsification process where organic phase act as a diffusion barrier between the W_1 and W_2 phase. Higher concentration of drug in W_1 phase may enhance osmotic pressure in the internal phase which facilitates diffusion of water from external (W_2) phase. Process of diffusion may result in thinning of organic phase and eventually in lower EE and DL. Addition of salt in external phase may helped to balance osmotic pressure between W_1 and W_2 phases which resulted in lower diffusion of external phase and higher DL. However, addition of salt did not exhibit significant effect on IgG-Fab loading. This may be due to the colligative characteristic of osmotic pressure, hence, this effect may enhance the loading of lower molecular weight drug drastically relative to higher molecular weight proteins. Based on these results, PB-A copolymer was utilized for further optimization of NP preparation.

In order to study the effect of drug to polymer ratio, PB-A NPs with two different drug/polymer ratios (1/10 and 1/4) were prepared and evaluated. Results depicted in Batch 5 suggest that as drug/polymer ratio was increased from 1/10 to 1/4, EE was significantly reduced which is in accordance to the previously published results [221]. This might have resulted from the fact that in case of 1/10 (drug/polymer) ratio, more polymer (10 mg) was

available to entrap 1 mg of IgG-Fab relative to a ratio of 1/4 (drug/polymer). Despite the high drug/polymer ratio with Batch 5, there was no significant difference observed in DL compared to earlier PB-A NPs (Batch 1). The poor DL could be attributed to high volume of external aqueous (W_2) phase. Hence, in further preparation the drug/polymer ratio was kept constant at 1/4 and effect of external phase (W_2) volume was evaluated. For instance, in Batch 6 total external phase (W_2) volume was lowered to 5 mL. In addition, double emulsion was prepared with only 2 mL of external aqueous (W_2) phase to reduce partition of protein in water (W_2 phase). The resulting multiple emulsion was stabilized by dilution with 3 ml of 2% PVA (W_3 phase). Interestingly, 11.7% of DL was observed with Batch 6 which was significantly higher compared to all earlier batches. Reduction in external phase volume has significantly improved EE relative to Batch 5.

Based on results from Batch 6, it can be inferred that reduction in external phase (W_2) volume along with high drug/polymer ratio have significant effect on DL. Hence, volumes of all the phases were further reduced while keeping the volume ratio constant. It was hypothesized that the lower volume of W_2 would diminish partition of protein in aqueous phase improving loading efficiency. In addition, a reduction in organic phase volume would increase polymer concentration that may lead to faster polymer precipitation and NP formation. A DL of 15.61% was observed with NPs in Batch 7 as expected with improved EE (~70%). However, further reduction in volumes (Batch 8) did not result in any improvement of DL (15.47%) or EE (~73%). Optimized process parameters utilized for the preparation of Batch 7 and Batch 8 were denoted as method-A and method-B, respectively.

Process parameters optimized in Batches 7 and 8 for the preparation of IgG-Fab-loaded PB-A NPs were utilized to encapsulate various protein/peptide molecules with different

molecular weights such as octreotide (1 kDa), insulin (5.8 kDa), lysozyme (14.7 kDa), IgG (150 kDa) and catalase (237 kDa). As reported in Table 6.3, the size (molecular weight) of protein or peptide have significant effect on DL and EE. Interestingly, peptides or proteins with lower molecular weight i.e., <15 kDa behaved very similarly and exhibited similar EE (35-38%) and DL (8.2-8.8%) when prepared with either method A or B. Likewise higher molecular weight proteins (≥ 48 kDa) demonstrated similar EE (69.5-78.5%) and DL (15-16.5%) when prepared with optimized methods A and B. Moreover, no significant difference of EE and DL were observed for insulin, lysozyme, IgG-Fab and catalase-loaded PB-A NPs prepared with method A relative to method B. Surprisingly, octreotide (Batch 14) and IgG (Batch 17) loaded PB-A NPs prepared with method B demonstrated lower EE and DL relative to NPs formulated with method A. These results clearly suggest that protein or peptide molecules of certain hydrodynamic diameter or molecular weight behave similarly during a process of NP preparation.

W₁/O/W₂ methods optimized earlier with PB-A copolymer (Batches 7 and 8) were further utilized for the preparation of NPs with PB-C and PB-D copolymers. As shown in Table 6.4, mean DL of IgG-Fab in PB-C NPs was 10.49 and 12.49% (Batches 19 and 22). However, loading of IgG-Fab with PB-D copolymer (Table 6.5) was 17.19 and 16.34% (Batches 25 and 28), which was significantly higher relative to PB-C copolymer. The higher loading efficiency may be due to the hydrophobic nature of PB-D copolymer. A similar trend in DL was observed for IgG-loaded NPs. There was a small increase in DL with PB-D (Batches 26 and 29) copolymer compare to PB-C copolymer (Batches 20 and 23).

Table 6.3: Encapsulation of various proteins with optimized methods A and B (PB-A).

Method	Batch #	Protein	EE (%)	Loading (%)
Method A	Batch 9	Octreotide (1 kDa)	35.8 ± 3.6	8.2 ± 0.8
	Batch 10	Insulin (5.8 kDa)	38.4 ± 0.8	8.8 ± 0.2
	Batch 11	Lysozyme (14.7 kDa)	37.6 ± 1.7	8.6 ± 0.4
	Batch 7	IgG-Fab (48 kDa)	69.6 ± 9.0	15.6 ± 2.0
	Batch 12	IgG (149 kDa)	74.6 ± 1.3	15.7 ± 0.2
	Batch 13	Catalase (237 kDa)	78.6 ± 0.8	16.4 ± 0.1
Method B	Batch 14	Octreotide (1 kDa)	26.9 ± 1.6	6.3 ± 0.3
	Batch 15	Insulin (5.8 kDa)	36.4 ± 2.3	8.3 ± 0.5
	Batch 16	Lysozyme (14.7 kDa)	38.4 ± 2.4	8.8 ± 0.5
	Batch 8	IgG-Fab (48 kDa)	73.2 ± 0.2	15.5 ± 0.1
	Batch 17	IgG (149 kDa)	54.6 ± 2.6	12.0 ± 0.5
	Batch 18	Catalase (237 kDa)	76.9 ± 0.6	16.1 ± 0.1

Table 6.4: Encapsulation of various proteins with optimized methods A and B (PB-C).

Method	Batch #	Protein	EE (%)	Loading (%)
Method A	Batch 19	IgG-Fab (48 kDa)	46.9 ± 0.8	10.5 ± 0.2
	Batch 20	IgG (149 kDa)	72.0 ± 0.7	15.3 ± 0.1
	Batch 21	Catalase (237 kDa)	75.8 ± 1.2	15.9 ± 0.2
Method B	Batch 22	IgG-Fab (48 kDa)	57.2 ± 8.5	12.5 ± 1.6
	Batch 23	IgG (149 kDa)	68.5 ± 1.4	14.6 ± 0.3
	Batch 24	Catalase (237 kDa)	72.1 ± 0.7	15.3 ± 0.1

Table 6.5: Encapsulation of various proteins with optimized methods A and B (PB-D).

Method	Batch #	Protein	EE (%)	Loading (%)
Method A	Batch 25	IgG-Fab (48 kDa)	83.1 ± 1.4	17.2 ± 0.3
	Batch 26	IgG (149 kDa)	85.3 ± 0.4	17.6 ± 0.1
	Batch 27	Catalase (237 kDa)	72.9 ± 1.2	15.4 ± 0.2
Method B	Batch 28	IgG-Fab (48 kDa)	78.1 ± 0.4	16.3 ± 0.1
	Batch 29	IgG (149 kDa)	81.8 ± 0.6	17.0 ± 0.1
	Batch 30	Catalase (237 kDa)	76.9 ± 1.2	16.1 ± 0.2

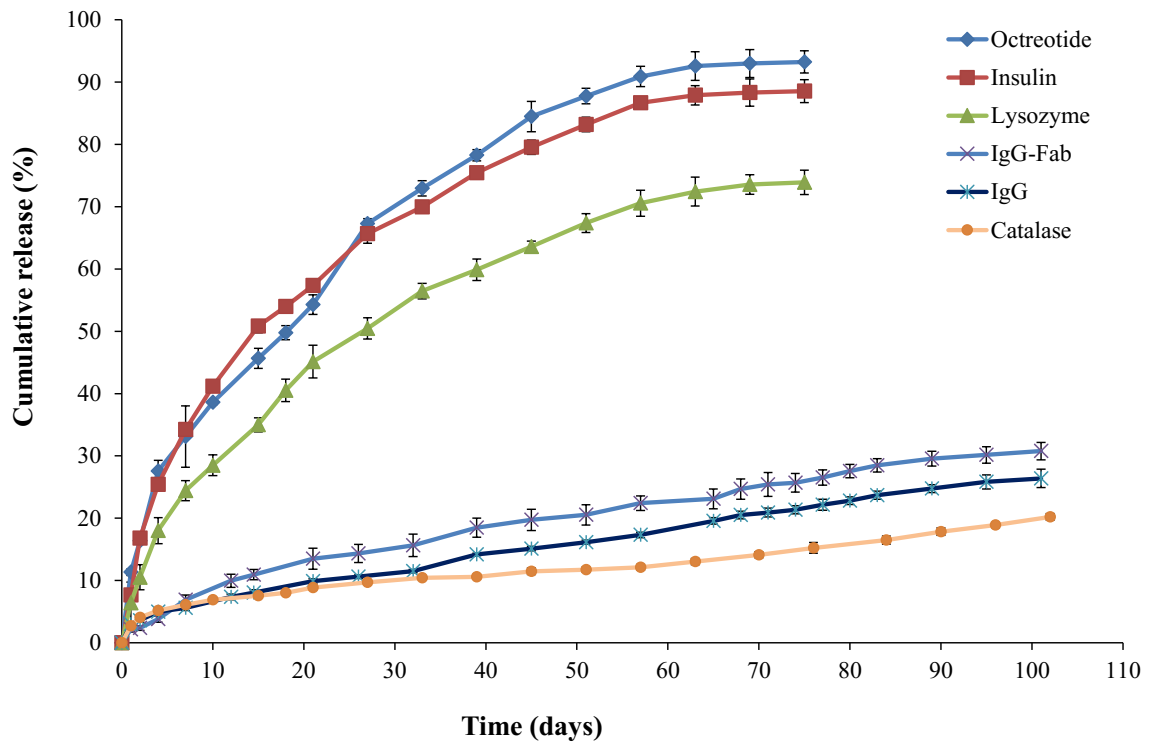


Figure 6.6: *In vitro* release of protein/peptide from PB-A NPs suspended in PB-E thermosensitive gel (20 wt%).

With catalase, a 237 kDa protein, DL efficiency remained relatively similar for both PB-C (Batches 21 and 24) and PB-D NPs (Batches 27 and 30) prepared by either method.

Overall, as the molecular weight of protein was enhanced from 48 kDa to 237 kDa, the difference in DL for PB-C and PB-D was diminished. This may be due to the reduced diffusivity of protein with large molecular weight.

In vitro release studies

In order to study the release behavior of various proteins, we have performed *in vitro* release studies from a composite formulation comprised of PB-A NPs suspended in thermosensitive gel (20 wt%). Figure 6.6 describes *in vitro* release profiles of octreotide, insulin, lysozyme, IgG-Fab, IgG and catalase from a composite formulation. All the release profiles depicted negligible or no burst release phase. It may be due the presence of thermosensitive gel which may act as additional diffusion layer for the NP-surface adsorbed protein. Interestingly, we have observed significantly rapid release of octreotide (~93% in 63 days) from composite formulation relative to the release of lysozyme (~72% in 63 days). It can be explained due to the fact that octreotide has smaller hydrodynamic radius than lysozyme that may have facilitated rapid diffusion of octreotide from composite formulation. The similar trend was observed when we compared the release profiles of lysozyme and IgG-Fab (~24% in 65 days). These results clearly suggest that the hydrodynamic radius of protein molecules plays a crucial role in defining of their release profiles from composite formulations.

However, we have not observed any significant difference between the release profile of octreotide and insulin (~89% in 63 days). It may possible that the difference in molecular weights between octreotide and insulin were not sufficient enough to exert any difference of diffusivity through formulation that led to the similar release profiles. This fact may be true

with smaller molecular weight proteins. There were no noticeable difference between the release profiles of IgG-Fab, IgG (~20% in 65 days) and catalase (~13% in 63 days) from PB-A NPs suspended in thermosensitive gel. It may possible that IgG-Fab, IgG and catalase have much less diffusivity through the polymer matrix (due to large molecular weight), thus their release was mainly controlled by polymer degradation. As published in previous reports, degradation of PCL is very slow [204-207, 217], so it was anticipated that PB copolymers composed of PCL blocks may also degrade very slowly. Due to the slower degradation of PB copolymers, release of IgG-Fab, IgG and catalase may be sustained for significantly longer durations.

Release kinetics

In vitro release data were fitted to zero and first order, Korsmeyer-Peppas, Higuchi and Hixson-Crowell models to delineate the kinetics of IgG release (Table 6.6). The Korsmeyer-Peppas model had the best fit based on R² value. The diffusion exponent, n value ranged from 0.513-0.642 for the tested composite formulations. The n-values between 0.43-0.89 indicate anomalous transport (diffusion and degradation controlled) mechanism of protein release.

Enzymatic activity of lysozyme and catalase

Specific enzymatic activity of lysozyme is reported in Table 6.7. Lysozyme activity of freshly prepared solution was found to be 61.4 ± 3.8 (U/mg of protein) $\times 10^3$. As described in the Table 6.7, enzymatic activity estimated for released samples were relatively higher than the respective controls. PB copolymers are composed of PEG, a hydrophilic block.

Table 6.6: Coefficient of determination (R^2) for various kinetic models for *in vitro* release of octreotide, insulin, lysozyme, IgG-Fab, IgG and catalase.

Block copolymers	Korsmeyer-Peppas		Higuchi	Hixson-Crowell	First-Order	Zero-Order	Best fit model
	R^2	n	R^2	R^2	R^2	R^2	
Octreotide	0.990	0.513	0.983	0.988	0.989	0.949	Korsmeyer-Peppas
Insulin	0.996	0.523	0.988	0.977	0.987	0.901	Korsmeyer-Peppas
Lysozyme	0.994	0.616	0.9926	0.967	0.988	0.937	Korsmeyer-Peppas
IgG-Fab	0.997	0.642	0.996	0.961	0.956	0.966	Korsmeyer-Peppas
IgG	0.998	0.597	0.980	0.996	0.991	0.994	Korsmeyer-Peppas
Catalase	0.992	0.588	0.987	0.932	0.947	0.972	Korsmeyer-Peppas

Table 6.7: Enzymatic activity of lysozyme estimated in the released samples and controls.

Time (days)	Specific enzyme activity (U/mg) x 10³	
	Release samples	Controls
4	61.2 ± 3.4	59.5 ± 1.7
15	53.3 ± 4.2	46.8 ± 4.4
45	35.7 ± 2.1	26.7 ± 2.7
63	26.3 ± 3.6	18.9 ± 1.6

Table 6.8: Enzymatic activity of catalase estimated in the released samples and controls.

Time (days)	Specific enzyme activity (U/mg) x 10³	
	Release samples	Controls
1	10.8 ± 1.2	10.6 ± 0.5
15	5.5 ± 0.1	5.0 ± 0.2
45	3.9 ± 0.2	3.6 ± 0.2
63	3.6 ± 0.2	3.3 ± 0.3

It is anticipated that during NP preparation ($W_1/O/W_2$ double emulsion), PEG may have been located on the aqueous-organic interface facing towards W_1 and W_2 phase. Hence, PEG may have reduced the interaction of lysozyme with the hydrophobic polymer segments (PCL and PLA) as well as with organic solvent (DCM) which may have reduced the denaturation of protein. However, the biological activity for lysozyme was reduced with the respect to time, as were the controls. This may be due to the fact that protein remained in the release medium for a significant time during the release study. Therefore, storage conditions may have affected the stability of proteins, which will not be the situation at *in vivo* conditions. During *in vivo* conditions, proteins released from composite formulation will be immediately absorbed from the vitreous cavity.

According to the results depicted in Table 6.8, enzymatic activity of freshly prepared catalase solution was estimated to be $10.8 \pm 0.2 \times 10^3$. Similar to the lysozyme release samples, enzymatic activity estimated for catalase control samples were relatively lower than the respective release samples. It may be due to the fact that catalase-encapsulated in the formulation may have been protected from hydrolytic degradation. Moreover, the biological activity of the catalase release samples and controls were reduced with the time which may be attributed to the storage conditions. The polymer matrix of NPs and thermosensitive gel may have reduced the exposure of proteins to the water molecules and hence protected the lysozymes/catalase from hydrolytic degradation [178].

Conclusion

We have successfully synthesized and characterized novel PB copolymers with different block ratios and block arrangements of PEG/PCL/PLA or PEG/PCL/PGA. These PB copolymers (PLA-PCL-PEG-PCL-PLA and PGA-PCL-PEG-PCL-PGA) were studied for the

preparation of protein/peptide-encapsulated NPs. NP preparation methods were successfully optimized with respect to polymer hydrophobicity, presence of salt (NaCl), drug to polymer ratio, and phase volumes to achieve maximum possible DL. In addition, effect of hydrodynamic radius of protein/peptides on DL and *in vitro* release behavior were studied. With different arrangement of polymer blocks i.e., PEG-PCL-PLA-PCL-PEG, we have synthesized PB thermosensitive gel which remained in solution phase at room temperature and transformed to gel at body temperature. PB copolymer based composite formulation (PB NPs suspended in PB thermosensitive gel) exhibited constant release for significantly longer duration of time without showing any burst release effect. Moreover, retention of enzymatic activity of lysozyme and catalase in release samples were also confirmed. A biodegradable and biocompatible PB composite formulation comprising protein-encapsulated NPs dispersed in thermosensitive gel can be easily injected intravitreally. This formulation can carry significantly high doses in very limited volume (<100 μ L) and can sustain the release of protein/peptides for significantly longer durations without exhibiting burst release. These results clearly suggest that PB copolymer-based protein-encapsulated, formulations can act as a platform therapy for the treatment of posterior segment chronic diseases such as wet-AMD, DR and DME.

CHAPTER 7

IN VIVO OCULAR TOLERABILITY STUDIES OF VARIOUS PENTABLOCK COPOLYMER BASED FORMULATIONS DELIVERED TOPICALLY OR INTRAVITREALLY

Rationale

Vision-threatening disorders such as age-related macular degeneration (wet-AMD), diabetic retinopathy (DR) and diabetic macular edema (DME) are commonly treated with frequent intravitreal injections of anti-VEGF antibodies or fragments thereof. Intravitreal injections are associated with complications such as secondary infection (endophthalmitis), retinal hemorrhage, retinal detachment and more importantly patient non-compliance. Therefore, sustained release therapeutic formulations for ocular posterior segment diseases that can reduce the frequency of intravitreal injection are highly desirable.

This need for sustained-release of anti VEGF therapy has stimulated research on use of thermosensitive *in situ* hydrogels composed of biodegradable and biocompatible polymers and tissue scaffolds [222-227]. *In situ* gelling systems offer several advantages over current formulations, including minimal invasiveness (no surgery required) and injectability through small (27 gauge) needles. However, thermosensitive gels alone do not extend drug release sufficiently to reduce the need for frequent injections. Nanoparticulate systems (NPs) have been investigated for the long-term controlled release of anti-VEGF medications. However, NPs alone typically exhibit burst release (initial rapid drug release phase) which can result in dose dependent toxicity. This can be overcome by composite formulations of nanoparticles (NPs) dispersed in a hydrogel, which can provide ocular delivery of therapeutic drug molecules over a longer period of time with a reduced burst effect.

In vitro drug release assays provide limited information regarding *in vivo* drug release. Moreover, *in vitro* cell culture based assays only provide toxicity information regarding short-term exposure only. Therefore, *in vivo*, long-term biocompatibility testing is necessary to establish safety of controlled delivery systems.

In this study, we report the development of novel PB copolymers based controlled release systems and the evaluation of their ocular tolerability. This study provides ocular tolerability of thermosensitive PBC gel was evaluated in rabbits after topical instillation and after a single intravitreal injection of gel, NPs and a composite formulation comprising NPs dispersed in gel. PB copolymer based formulations are under development for the sustained release of biologicals (proteins, antibodies/fragments, RNA) and small molecules (hydrophilic and hydrophobic) for the treatment of ocular diseases.

Materials and methods

Materials

PB copolymers, PB-D and PB-E described in chapter 6, were utilized for the preparation of NPs and thermosensitive gel, respectively. Endotoxin-free water was purchased from Fisher Scientific. Endotoxin estimation kit was procured from GenScript USA Inc. Polyvinyl alcohol (PVA) was obtained from Sigma Aldrich.

Methods

Preparation of sterile, low endotoxin PB thermosensitive gel

Thermosensitive gels were prepared in sterile glassware pre-rinsed with endotoxin free water. In order to prepare low endotoxin PB thermosensitive gel, 20 wt% of PB copolymer was dissolved in endotoxin free (EF) water. Once the polymer was solubilized, 20 wt% aqueous solutions was filtered through 0.2 μm (pore size) filter in aseptic conditions under

laminar flow. The filtrate was analyzed for its gelling behavior and endotoxin levels. Gelling behavior of aqueous solution was confirmed by exposing the solution to 37 °C for 5 min.

Preparation of low endotoxin PB NPs

All aqueous solutions utilized during NP preparation were prepared with EF water followed by filter sterilization. NPs were prepared in sterile glassware pre-rinsed with endotoxin free water. PB-D NPs were prepared by $W_1/O/W_2$ double emulsion solvent evaporation method. Briefly, syringe filtered EF water (W_1 phase) was added drop-wise in organic phase (PB-D copolymer dissolved in dichloromethane) under constant sonication. The resulting W_1/O primary emulsion was then added drop-wise in the W_2 phase (2% PVA) under constant sonication. The $W_1/O/W_2$ double emulsion was diluted with a W_3 phase (2% PVA) and vortexed for 5 min. Dichloromethane was then evaporated from multiple emulsions under low pressure. The resulting NPs were centrifuged at 20000 rpm for 30 min at 4 °C. In order to remove residual PVA, NPs were washed two times with EF water followed by centrifugation. Finally, NPs were suspended in 2 mL of EF water and freeze-dried overnight. After freeze-drying, NPs were stored at -20 °C until further analysis. NPs were tested for endotoxin levels. A schematic diagram of NP preparation is illustrated in Figure 7.1.

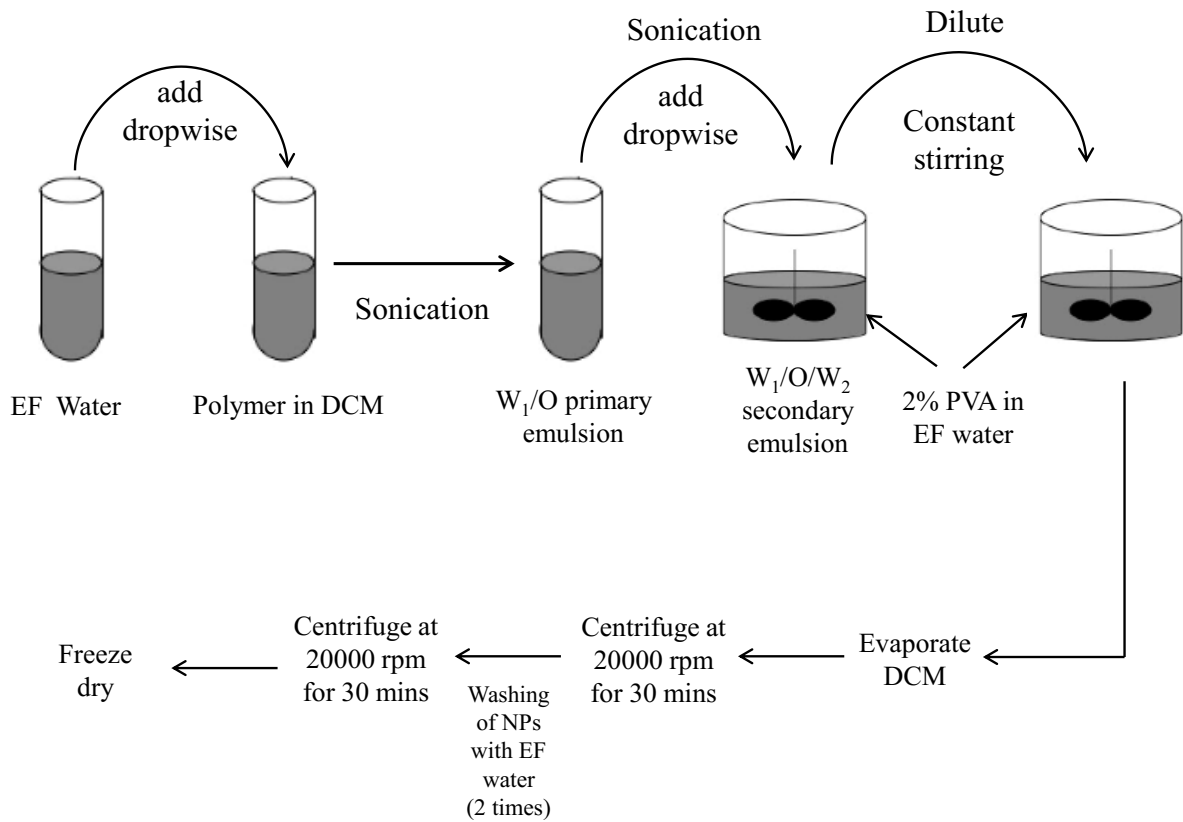


Figure 7.1: Preparation of low endotoxin PB NPs for ocular tolerability studies.

All the aqueous solutions were prepared with EF water followed by filter sterilization. Thermosensitive gel and NPs were prepared in sterile glassware pre-rinsed with endotoxin free water.

Evaluation of endotoxin levels

Levels of endotoxins in various formulations were evaluated utilizing an endotoxin assay kit. Limulus Amebocyte Lysate (LAL) endotoxin assay was performed according to the supplier's protocol under aseptic conditions (laminar flow). Briefly, three test samples were prepared, i.e. thermosensitive gel solution (20 wt%), NP suspension in EF water (5.5 mg/100 μ L) and NP suspension in thermosensitive gel solution (20 wt%). A 100 μ L aliquot of test or standard solution/suspensions were transferred in vials followed by addition of 100 μ L LAL reagent. Mixture was gently stirred for 30 sec, and followed by incubation at 37 °C for 45 min. After incubation, 100 μ L of chromogenic reagent was added and gently stirred for 30 sec followed by 6 min incubation at 37 °C. At the end of incubation, 500 μ L of color-stabilizer 1, 2 and 3 were added in a defined order. In order to remove NPs from the samples, samples containing NPs were syringe-filtered. Absorbance of samples and standards were estimated at 570 nm utilizing 96-well plate reader.

In vivo tolerability studies

Use of animals in this study adhered to the ARVO Statement for the Use of Animals in Ophthalmic and Vision Research and was approved and monitored by the North Carolina State University Institutional Animal Care and Use Committee. Details about animal, housing and environment are described in Table 7.1. Methods along with evaluation parameters for topical drops and intravitreal injections are described below.

Table 7.1: Animals, housing and environmental conditions.

Species/Strain	Rabbit (<i>Oryctolagus cuniculus</i>)/New Zealand White
Sources	Charles River
Age Range at First Dosing	Approximately 8 months
Weight Range at First Dosing	2 - 3 kg
Identification	Ear tattoo and cage card
Physical Examination Time	During acclimation
Caging	Stainless steel; 17 inches wide x 27 inches deep x 15 inches tall or larger, slatted bottoms. No additional bedding.
Number of animal per cage	1
Target Environmental Conditions	Photoperiod: 12 h light/12 h darkness Temperature: 68 ± 2°F

In vivo ocular tolerability studies were performed in New Zealand White Rabbits. Two batches of filter sterilized low endotoxin thermosensitive gel (FS), one batch of filtered sterilized and gamma irradiated gel (FS+G), one batch of PB-D NPs dispersed in PBS (NP-PBS) (5.5 mg/100 μ L) and one batch of PB-D NPs suspended thermosensitive gel (NP-Gel) (5.5 mg/100 μ L) were evaluated for topical and intravitreal toxicity.

Part - I: topical tolerability studies in rabbit eye model

Dosing

Three animals were randomly assigned to each of five study groups (Table 7.2). The left eye (OS) of each animal was treated topically with 35 μ L of saline (Balanced Salt Solution, Alcon Laboratories, Fort Worth, TX) and an aliquot (35 μ L) of each respective test formulation (i.e. PB thermosensitive gel [FS and FS+G], NPs in PBS [NP-PBS] and NPs in gel [NP-Gel]) was administered to the ocular surface of right eye via calibrated pipette. Animals were then allowed to blink several times prior to returning to the cage. Topical tolerability studies were performed by administering 4 doses (each 35 μ L) at 15 min intervals followed by an observation period of 24 h. Microscopic ocular irritation was scored in both eyes using the Hackett-McDonald Ocular scoring system at 15, 30, and 60 minutes and 3, 6, 12 and 24 hours after the last topical dose.

Part - II: tolerability studies after intravitreal injection in rabbit eye model

Dosing

To evaluate ocular biocompatibility of PB copolymer based formulations, 100 μ L of each of the five formulations were injected intravitreally in the normal NZW rabbits. The number of animals assigned per group is described in Table 7.3.

Table 7.2: Animals assigned per group for topical tolerability study.

Group #	No. of rabbits per group	Treatment Topical (4 doses; 35 μL each, 15 min apart)	Concentration of polymer	pH of the formulation	Sterility	Measured Endotoxin Levels (EU/mL)
1	3	OD: PB Gel (FS); OS:BSS	20 wt%	7.4	Filtered sterilized	BLOQ
1A	3	OD:PB Gel (FS + G); OS:BSS	20 wt%	7.4	Filtered sterilized followed by gamma irradiation	BLOQ
2	3	OD: PB Gel (FS); OS:BSS	20 wt%	7.4	Filtered sterilized	BLOQ
3	3	OD: PB NPs in PBS; OS:BSS	5.5 mg of NPs per 100 μ L of PBS	7.4	Non-sterile	0.17 \pm 0.04
4	3	PB NPs in PB Gel (NS); OS:BSS	5.5 mg of NPs per 100 μ L of 20 wt% gel	7.4	Non-sterile	0.21 \pm 0.01

BLOQ: Below limit of quantification

OD: Right eye

OS: Left eye

FS: Filter Sterilized

FS+G: Filter Sterilized + gamma Irradiated

NS: Non-Sterilized

NPs: Nanoparticles

PBS: Phosphate Buffered Saline

PB: PB Copolymer

Table 7.3: Animals assigned per group for tolerability study of intravitreal injection.

Group #	No. of rabbits per group	Treatment Intravitreal (100 μL)
Control	2	Saline
1	4	PB Gel (FS) (20 wt%)
1A	6	PB Gel (FS+G) (20 wt%)
2	6	PB Gel (FS) (20 wt%)
3	5	PB NPs in PBS (NS) (5.5 mg of NPs per 100 μ L of PBS)
4	5	PB NPs in PB Gel (NS) (5.5 mg of NPs per 100 μ L of 20 wt% gel)

FS: Filter Sterilized

FS+G: Filter Sterilized + gamma Irradiated

NS: Non-Sterilized

NPs: Nanoparticles

PBS: Phosphate Buffered Saline

PB: PB Copolymer

Rabbits were tranquilized with ketamine/dexmedetomidine intramuscularly and were prepared by applying 5% betadine solution topically followed by rinsing with sterile saline and application of 0.5% proparacaine HCl. Intravitreal injections (100 µL) of test formulation or saline was done 2 mm posterior to the superior limbus (through the pars plana) using a 25 gauge needle. Special care was taken during the injection to avoid needle contact with the lens. Following the injection, one drop of 0.5% moxifloxacin (Alcon Laboratories, Fort Worth, TX) was instilled topically to the ocular surface.

Parameters to be evaluated

Ocular Examination

Ocular surface morphology, posterior and anterior segment inflammation, retinal changes and cataract formation were evaluated by ocular examination using a slit lamp and indirect ophthalmoscope. Modified Hackett-McDonald ocular scoring (Microscopic Ocular Grading System without fluorescein application) of inflammation was recorded. Parameters such as congestion (0-3), swelling (0-4), discharge (0-3), aqueous flare (0-3), light reflex of iris (0-4), corneal cloudiness affected area (0-4), corneal cloudiness severity (0-4) and pannus and vitreal cells (0-2) were considered to calculate cumulative mean Hackett-McDonald ocular irritation scoring. Ocular examination was carried out for each rabbit to determine pre-dose (pre-study) baseline data, followed by examination during predetermined time intervals. Formulations were evaluated for tolerability studies after topical and intravitreal injections.

Intraocular Pressure

Intraocular pressure (IOP) was measured in both eyes for control and treated groups. IOP was measured at least twice during the acclimation, then immediately following ocular

examination at the time listed above. Briefly, IOP was estimated without use of topical anesthetic. The Tonovet (iCare tonometer, Finland) tip was used to contact the central cornea and record six consecutive measurements. Post-treatment and pre-treatment IOPs were measured during the same time of the day.

Electroretinography (ERG)

Electroretinography was performed prior to injection in all animals, then again at 4 and 16 weeks (in surviving animals). Prior to ERG, all animals were dark adapted for 15 min. A monopolar contact lens electrode (ERG-jet, La Chaux des Fonds, Switzerland) was placed on the cornea to serve as an active electrode and subdermal electrode at the lateral canthus served as the indifferent electrode. A Barraquer eyelid speculum was placed to maintain open eyelids and a subdermal needle electrode was inserted dorsally as the ground electrode. ERGs were elicited by delivering brief flashes at 0.33 Hz with a mini-ganzfeld photostimulator (Roland Instruments, Wiesbaden, Germany) at maximal intensity. For each animal at each testing interval, twenty responses were amplified, filtered, and averaged (Retiport Electrophysiologic Diagnostic Systems, Roland Instruments, Wiesbaden, Germany)

Euthanasia

Rabbits were euthanized at the predefined time intervals. Euthanasia was performed by intravenous injection of an AVMA-approved barbiturate-based agent. Immediately after euthanasia, eyes were enucleated and processed for histopathology. Following eye removal, carcasses were discarded without necropsy.

Ocular Histopathology

Both eyes of each animal were fixed in Davidson's solution for 24 h, followed by alcohol. Central sections of each globe, including the optic nerve were stained with hematoxylin and eosin stain (H&E stain), and examined by light microscopy.

Results and discussion

Estimation of endotoxin levels in PB thermosensitive gel and PB NPs

Levels of endotoxins in various formulations were evaluated utilizing Limulus Amebocyte Lysate (LAL) endotoxin assay kit. Both batches of PB thermosensitive gelling solution depicted negligible endotoxin levels (below the limit of quantification) (Table 7.2). PB NPs alone (Group 3), and PB NPs (Group 3) dispersed in PB thermosensitive gel (Group 2) exhibited endotoxin levels of 0.17 ± 0.04 EU/mL and 0.21 ± 0.01 EU/mL, respectively. However, these levels of endotoxins for Groups 3 and 4 are well within the acceptable limit (2 EU/mL) for ocular applications.

Tolerability study after topical application

Topical ocular tolerability studies were performed on two batches of thermosensitive gel (20 wt%), PB NPs in PBS buffer, and PB NPs dispersed in thermosensitive gel (20 wt% filter sterilized). These formulations were instilled directly on the ocular surface in right eye of each animal, while left eyes were treated with balanced salt solution (BSS).

General ocular observation

No adverse reactions (blepharospasm or evasive action) by the animals were observed during or after the administration of test samples or BSS. Immediately after the application to the left eye, BSS rapidly flowed to the ventral conjunctival cul-de-sacs and disappeared from view.

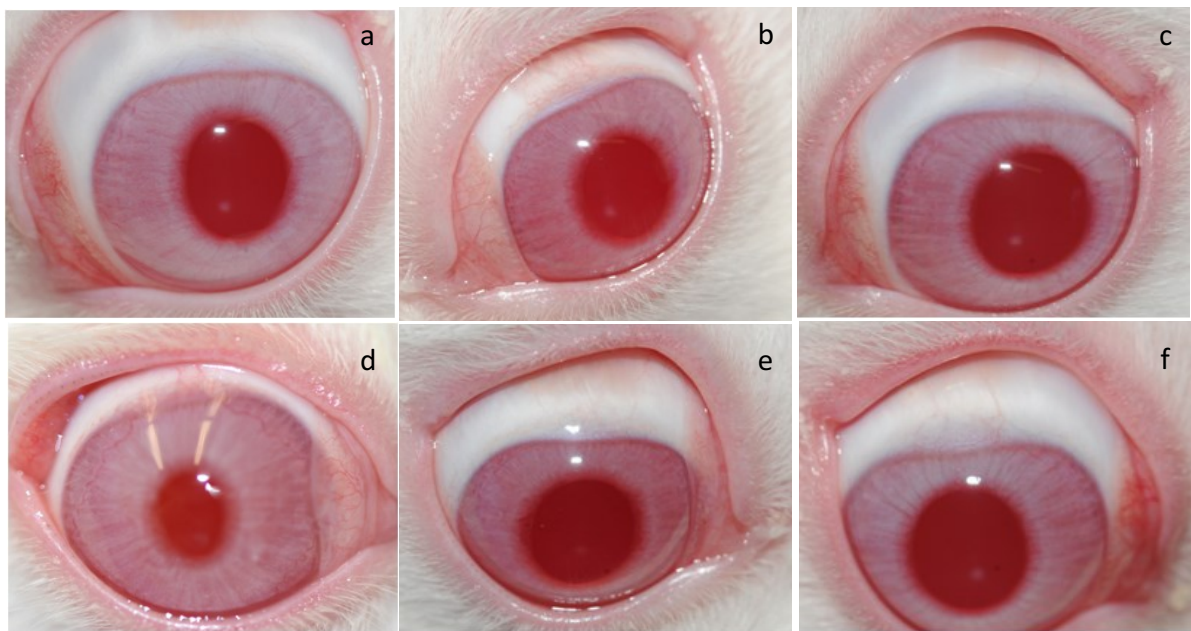


Figure 7.2: Representative images of rabbit eyes, 6 h post-topical application. (a), (b) and (c) are control eyes for the Groups 1, 3 and 4. (d) PB thermosensitive gel treated rabbit eye (Group 1), (e) PB NPs treated rabbit eye (Group 3) and (f) PB NPs dispersed PB thermosensitive gel treated rabbit eye (Group 4).

Table 7.4: Mean cumulative Hackett-McDonald Ocular Irritation Scores after topical treatment.

		Mean Cumulative Microscopic Observation Score \pm SD ^a							
Group Identification (n/group)	Eye	Pre-Dose 0 h	0.25 h	0.5 h	1 h	3 h	6 h	12 h	24 h
1 (3)	Left (OS)	0	0	0.3 \pm 0.6	0	0.3 \pm 0.6	0	0	0
	Right (OD)	0	0.3 \pm 0.6	0.7 \pm 0.6	0.3 \pm 0.6	2.0 \pm 0.0*	0.3 \pm 0.6	0.7 \pm 0.6	0.3 \pm 0.6
1A (3)	Left(OS)	0.3 \pm 0.6	0.3 \pm 0.6	0.3 \pm 0.6	0.3 \pm 0.6	0.3 \pm 0.6	0.3 \pm 0.6	0.3 \pm 0.6	0
	Right (OD)	0.3 \pm 0.6	2.0 \pm 1.0*	2.0 \pm 0.0	1.7 \pm 0.6	1.7 \pm 0.6	1.3 \pm 0.6	1.0 \pm 1.0	1.0 \pm 1.0
2 (3)	Left (OS)	0	0.3 \pm 0.6	0	0	0	0	0	0
	Right (OD)	0.3 \pm 0.6	2.0 \pm 0.0*	1.3 \pm 0.6*	1.3 \pm 0.6*	1.3 \pm 0.6	0.3 \pm 0.6	0.3 \pm 0.6	0.3 \pm 0.6
3 (3)	Left(OS)	0	0.3 \pm 0.6	0.3 \pm 0.6	0.3 \pm 0.6	0	0.3 \pm 0.6	0.3 \pm 0.6	0
	Right (OD)	0	1.0 \pm 1.0	1.3 \pm 0.6	0.7 \pm 1.2	1.0 \pm 1.0	0.3 \pm 0.6	0.3 \pm 0.6	0
4 (3)	Left(OS)	0	0.3 \pm 0.6	0.3 \pm 0.6	0.3 \pm 0.6	0	0	0	0
	Right (OD)	0	1.3 \pm 0.6	1.3 \pm 0.6	1.0 \pm 1.0	0.7 \pm 0.6	1.3 \pm 0.6*	1.0 \pm 1.0	0.7 \pm 0.6

SD = Standard Deviation^a Cumulative Observation Score: Average of severity scores for all observations combined (congestion, swelling, discharge, aqueous flare, light reflex (iris), involvement (iris), corneal cloudiness (severity and affected area), pannus and vitreal cells. However severity scores were zero for aqueous flare, corneal cloudiness, pannus and vitreal cells

* OD: significantly greater than OS (P = 0.033; Wilcoxon test)

PB thermosensitive gel solutions were able to be administered on the corneal surface by pipette where, upon contact with cornea, the solution transformed to clear uniform gel film. Representative images of the control (BSS) and PB formulations treated eyes are depicted in Figure 7.2. PB gel film was observed on the ocular surface through the 1 h examination and a small amount of gel was observed in the conjunctival cul-de-sacs at the 6 h examination. However, application of the PB NPs demonstrated milky opacity on the corneal surface for a few seconds that rapidly dissolved and cleared from the ocular surface.

Ocular Examination (slit lamp and indirect ophthalmoscope) and Irritation Scores

Throughout the 24 h post-treatment observations, both BSS treated left eyes and PB formulation treated right eyes exhibited very minimal mean cumulative Hackett-McDonald ocular irritation scores (≤ 2) (Table 7.4). No statistically significant differences in ocular irritation scores were observed between test articles at any time points post-treatment. We have observed statistically significant elevation of ocular irritation scores at several individual time points relative to control treatment (BSS) i.e., Group 1 at 3 h, Group 1A at 0.25 h, Group 2 at 0.25, 0.5 and 1 h, and Group 4 at 6 h. However, cumulative ocular scores were ≤ 2 , representing mild and transient congestion (swelling) and conjunctival hyperemia (redness). There was no evidence of intraocular or corneal inflammation. No significant difference in ocular irritation scores between the groups were observed at 24 h post-treatment examination suggesting excellent tolerability of the PB copolymer based formulations for topical ocular applications.

Tolerability study after intravitreal injection

Ocular irritation after single intravitreal injection

Mildly elevated mean cumulative Hackett-McDonald ocular irritation scores peaked at ~1 h after intravitreal injection and returned to baseline at 7 days (Figure 7.3). There were no significant differences observed in inflammatory scores between the groups except for the group 3 which exhibited elevated inflammation at 6 and 7 days. Animals treated with PB NPs in PBS buffer (Group 3) demonstrated mild signs of uveitis including iris hyperemia and aqueous flare. Animals injected with composite formulations (PB NPs dispersed in PB thermosensitive gel) exhibited no signs of elevated clinical inflammatory scores relative to saline treated eyes or PB gel treated eyes. No signs of inflammation have been subsequently observed in eyes examined up to 4 months after injection.

Other ocular examination findings

Focal posterior cortical cataract was observed in one of the rabbit (group 1) at day 1 after the injection was observed. However, this lesion was not changed in size over the course of study. It was anticipated that formation of cataract was most likely from the injection procedure and not associated with the PB gel itself. Hence, it was not considered as a sign of toxicity. We have not observed any signs of vitreous inflammation or toxicity, damage of retinal or optic nerve, or lens toxicity (opacity or cataract) (Figures 7.4, 7.5 and 7.6).

Intraocular pressure (IOP)

All rabbits exhibited IOP in acceptable range, and no consistent elevation or decrease of IOP was noted. One exception was in group 3, where rabbits demonstrated significantly ($P = 0.03$) reduced IOP at day 7 after the injection relative to the saline or PB-gel treated animals. This result was consistent with observation of with the clinical inflammation noted slit-lamp examination (Figure 7.7).

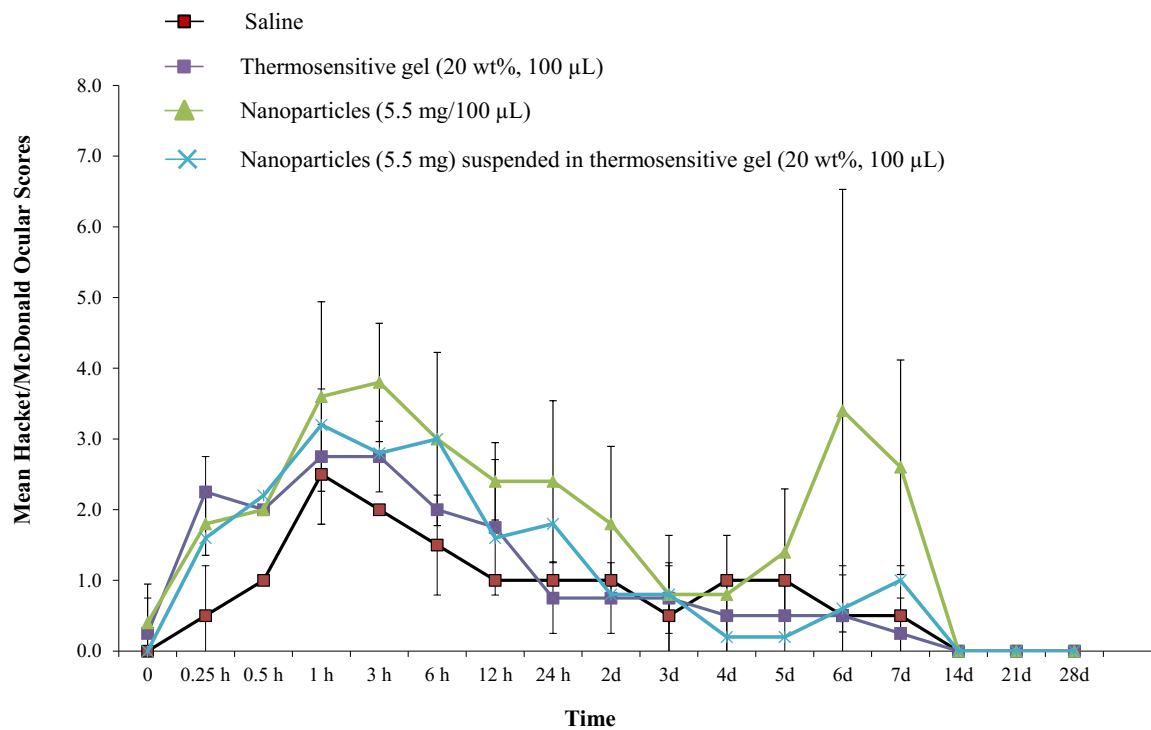


Figure 7.3: Mean +/-SD Cumulative Hackett-McDonald Irritation Scores.

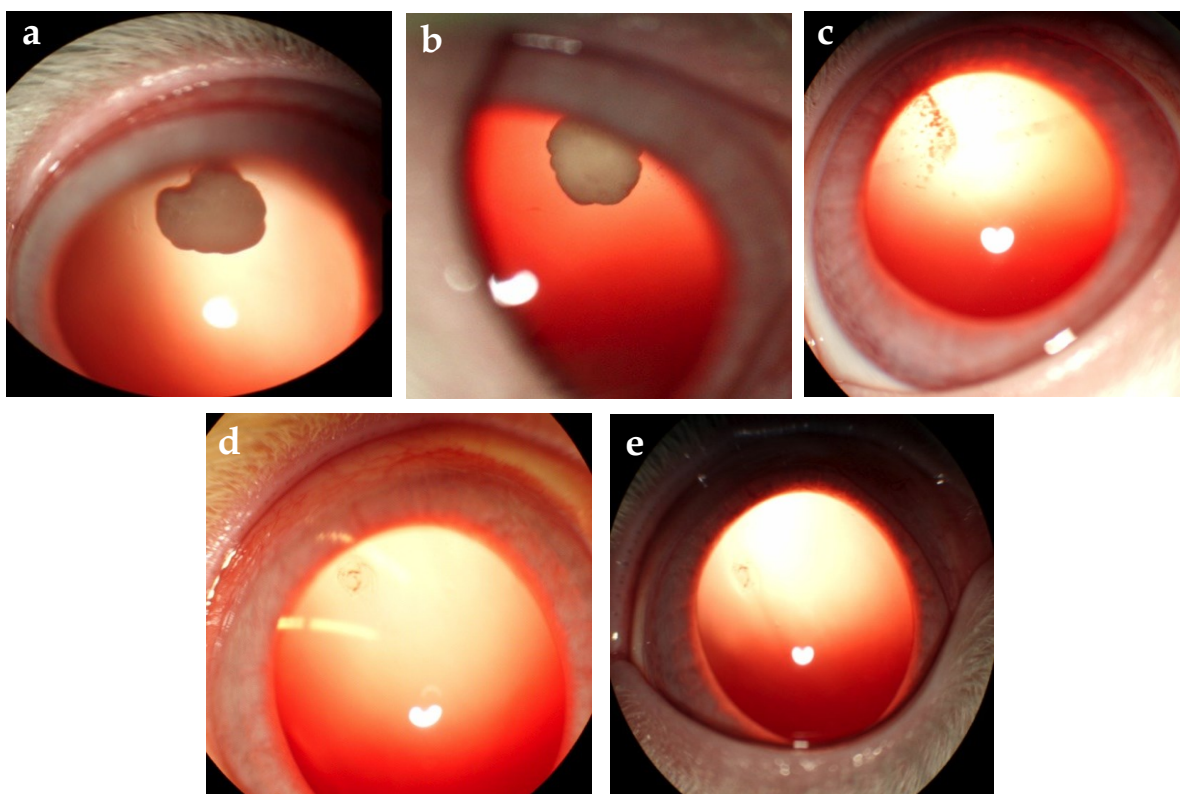


Figure 7.4: Images of rabbit eyes taken after single intravitreal injection (100 μ L) of PB thermosensitive gel, (a) day 1, (b) day 21, (c) day 42, (d) day 49, and (e) day 98.

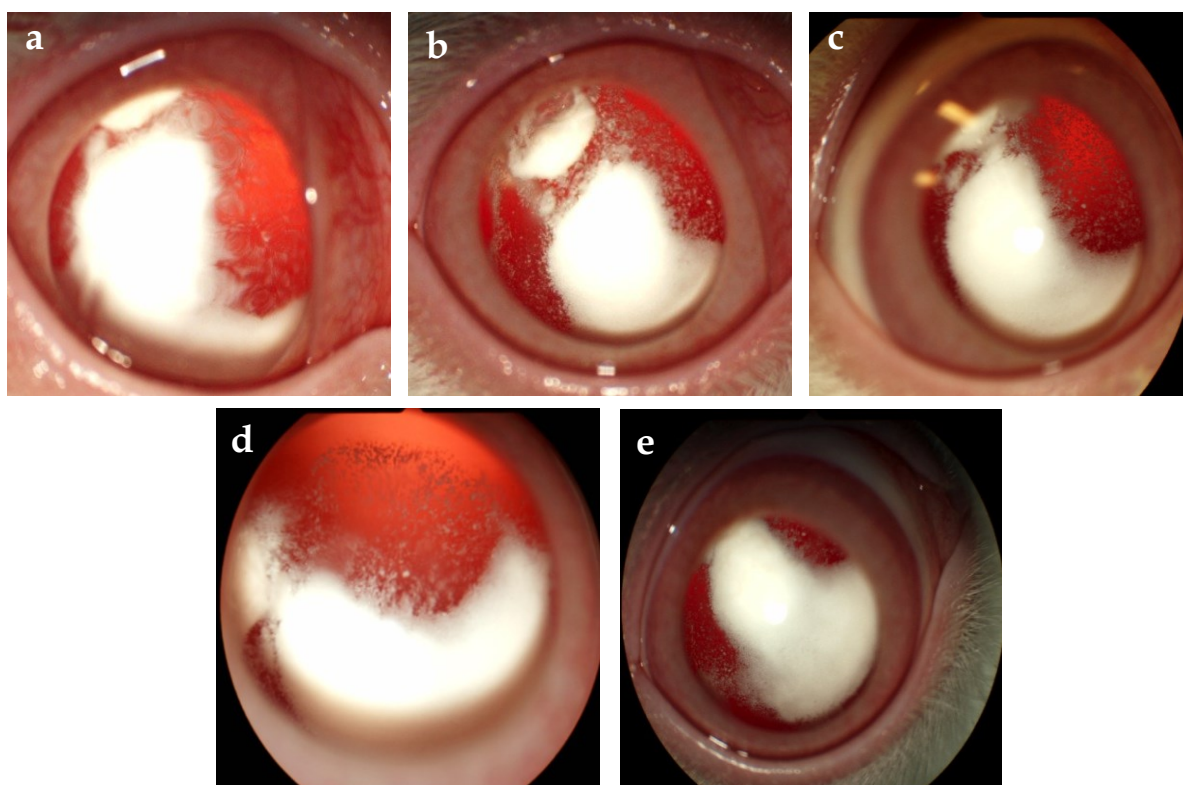


Figure 7.5: Images of rabbit eyes taken after single intravitreal injection (100 μ L) of PB NPs dispersed in PBS, (a) day 1, (b) day 21, (c) day 35, (d) day 42, and (e) day 77.

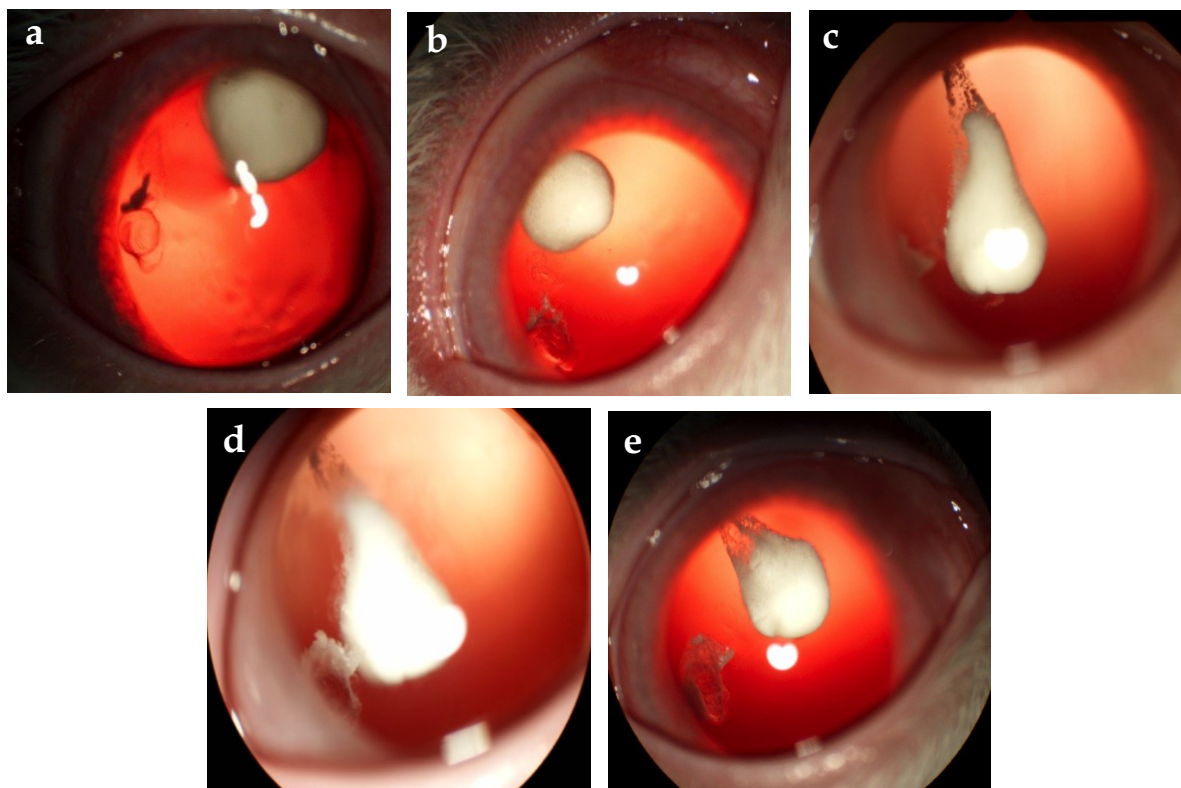


Figure 7.6: Images of rabbit eyes taken after single intravitreal injection (100 μ L) of PB NPs dispersed in PB thermosensitive gel, (a) day 1, (b) day 21, (c) day 35, (d) day 42, and (e) day 77.

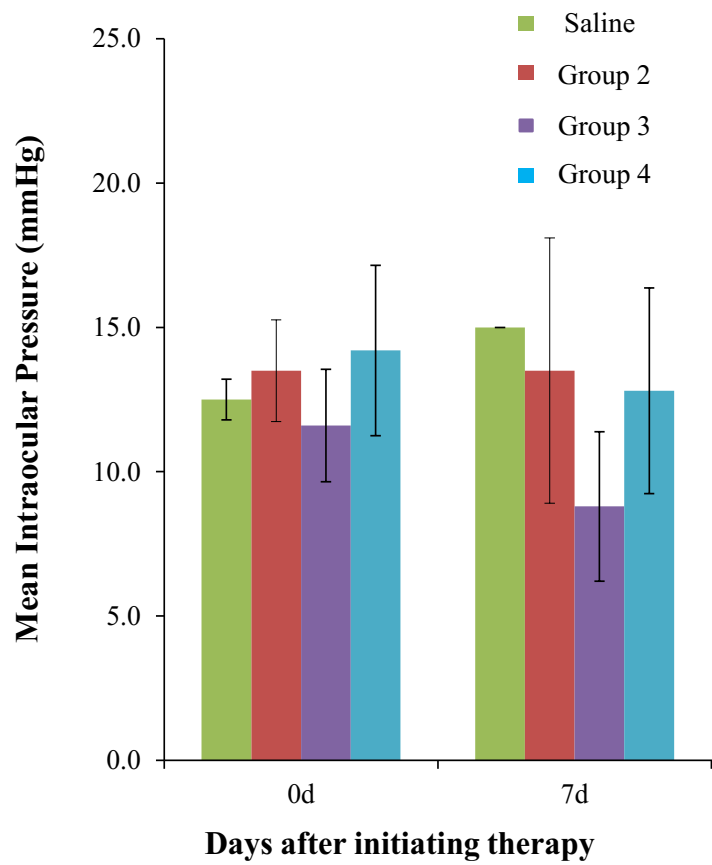


Figure 7.7: Intraocular pressure (IOP) estimated after single intravitreal injection.

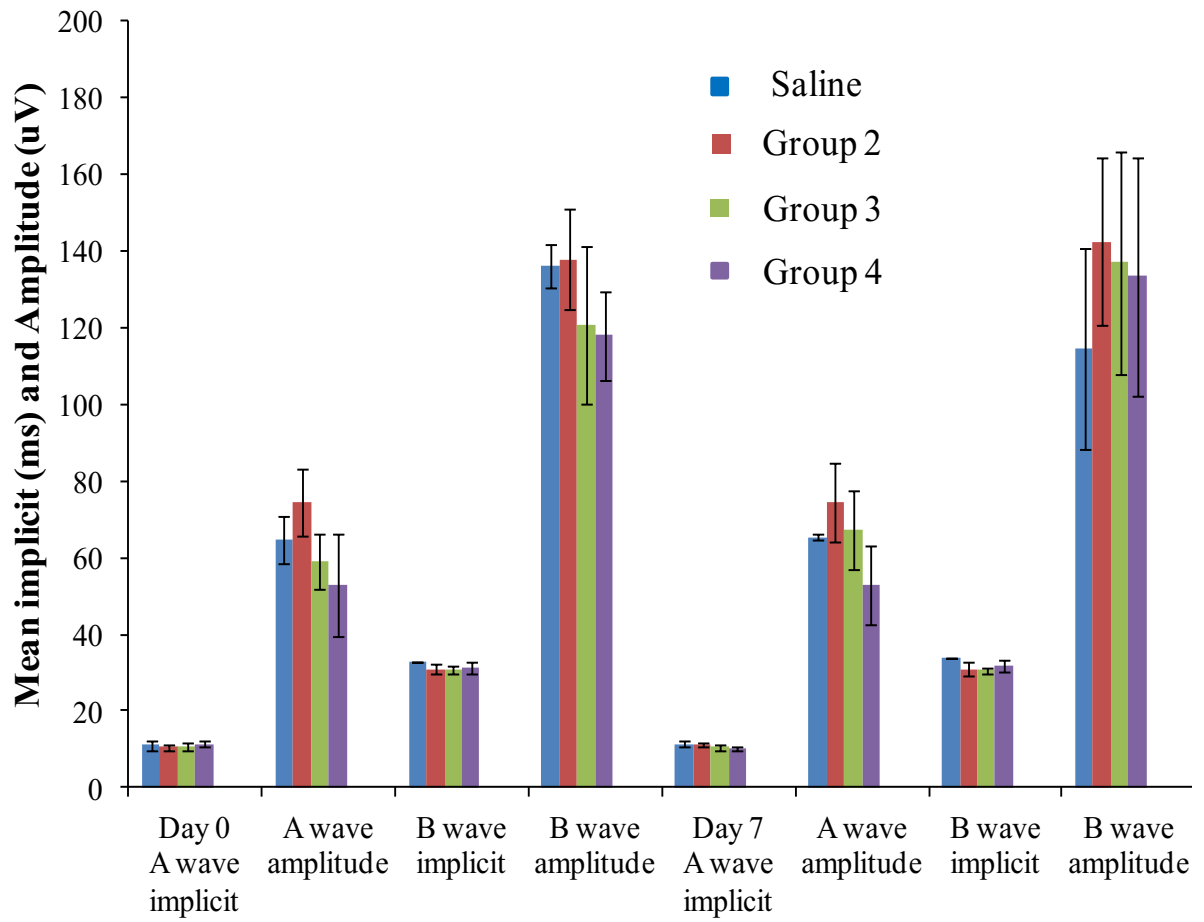


Figure 7.8: Electroretinography performed after single intravitreal injection.

Table 7.5: Ocular histopathology of rabbit eyes after single intravitreal injection of various PB copolymer based formulations.

Group	Weeks after injection	Anterior segment inflammation	Posterior segment inflammation	Lens damage	Retinal damage	Comments
Saline	1	-	-	-	-	-
	4	-	-	-	-	-
Group 1	1	-	-	-	-	-
	1	-	-	-	-	-
	4	-	+	-	-	Few mononuclear cells in vitreous near lens
Group 1A	1	-	+	-	-	Few neutrophils in anterior vitreous
	1	-	-	-	-	-
	1	-	++	++	-	Neutrophils in anterior vitreous, posterior lens rupture
	4	-	-	-	-	-
Group 2	1	-	-	+	-	Focal area of lens capsule rupture and lens fiber change
	1	+	-	-	-	Few neutrophils in anterior chamber and ICA
	4	-	-	+	-	Focal area of lens capsule break and lens fiber change
Group 3	1	-	-	-	-	Nanoparticles visible in anterior vitreous
	1	+	+++	+	+	Epithelial downgrowth, lens rupture, Pyogranulomatous infiltrate
	4	-	-	-	-	-
Group 4	1	-	-	-	-	-
	1	-	-	-	-	-
	4	-	-	-	-	Epithelial downgrowth at injection site

- = none

+ = mild

++ = moderate

+++ = severe

Electroretinography

The pre-study and weeks 1, 4, and 16 post injection ERGs were normal in each rabbit. No significant differences in a-wave and b-wave implicit times or amplitudes before and after treatment (Figure 7.8) were observed, suggesting a lack of retinal toxicity with the injected polymers up to 4 months.

Ocular histopathology

Ocular histopathology was performed at weeks 1, 4 and 16 after intravitreal injection. Results reported in Table 7.5 indicated that in most eyes no evidence of inflammation or toxicity associated with the injection procedure or test articles were observed. Two eyes exhibited mild anterior segment/anterior vitreous inflammation. However, we have observed injection procedure associated damage and inflammation in a few eyes, including lens trauma and wound epithelial downgrowth. These changes appear to be associated with the injection procedure in sensitive rabbit eyes rather than the test articles. Only one animal of group 3 (PB NPs in PBS) exhibited severe posterior segment inflammation at week 1 after injection. These results are consistent with the results of ocular irritation score and reduced IOP observed in the same group of animals. Based on these findings, it appears that the test articles are well tolerated by the rabbit eyes, without evidence of overt inflammation or histopathologic evidence of tissue damage indicating excellent biocompatibility of PB copolymer based formulations. However, changes associated with injection procedure are relatively common and may cause most of the inflammatory and tissue damage observed (both histologic and clinical).

Conclusion

We have prepared endotoxin-free thermogelling polymer solutions and have tested these with topical application to rabbit eyes. In addition we have tested thermogelling solution with and without PB NPs. Topical application of 4 consecutive doses (35 μ L each) at intervals of 15 min produced no signs of irritation. No adverse reactions, such as evasive action or blepharospasm were observed during or after the application suggesting adequate tolerability for topical ocular applications. Minimal mean cumulative Hackett-McDonald ocular irritation scores of ≤ 2 were observed for all the formulations indicating mild and transient conjunctival hyperemia (redness) and congestion (swelling). Low ocular irritation scores up to 4 weeks demonstrate that PB copolymer NPs dispersed in thermogelling solution are well tolerated. No significant difference in IOP was observed between saline treated or PB copolymer formulation treated eyes. ERG results showed no changes in retinal functions in either control or test groups. Moreover, no sign of inflammation or cataract formation during the treatment period was observed. These results indicate that PB copolymer based formulations are biodegradable and biocompatible, and well suited for ocular application, both topically or by intravitreal injection. These polymers can be successfully used for the development of controlled release systems for ocular delivery of therapeutic proteins.

CHAPTER 8

SUMMARY AND RECOMMENDATIONS

Summary

Development of sustained release formulation for the protein therapeutics in the treatment of posterior segment diseases such as wet-AMD, DR and DME, is a very challenging task for the formulation scientists. The ideal formulation for the intravitreal delivery should possess following characteristics, (a) high drug loading in small volume ($\leq 100 \mu\text{L}$) that lasts up to 6 months or more, (b) provide constant release (zero-order release) throughout the release period without any burst effect, (c) easy to administered such as injectable system and not implants, (d) ensure stability of protein/peptide, (e) biodegradable and biocompatible, and (f) the time required for biodegradation of formulation should not be more than 1.5 times the release period.

In order to achieve this goal, we have synthesized novel biodegradable and biocompatible PB copolymers. PB copolymers are composed of various FDA approved polymeric blocks such as PEG, PCL, and PLA/PGA. Each block plays an important role such as presence of PEG helps to improve stability of NPs by reducing NP aggregation, and also helps to escape phagocytosis by macrophages resulting in improved half-life. PCL is a slow degrading semi-crystalline polymer which improves protein loading in NPs and also sustains drug release for longer duration of time. Such a slow degradation is also not advantageous particularly for intravitreal injections. It is important for formulation scientists to synchronize polymer degradation profiles with the drug release profiles in order to avoid accumulation of empty formulation in the limited vitreous cavity. Previous reports suggest that poor degradation of PCL is attributed to its crystalline nature, hence reduction in the crystallinity of PCL may improve its hydrolytic and enzymatic degradation. Covalent conjugation of

PLA/PGA to PCL chains can significantly reduce crystallinity resulting in faster degradation of PCL [203, 219]. PB copolymers were utilized to prepare thermosensitive gel or NPs.

Firstly, we have synthesized and characterized various TB (PCL-PEG-PCL, B-A-B) and PB (PLA-PCL-PEG-PCL-PLA (C-B-A-B-C) and PEG-PCL-PLA-PCL-PEG (A-B-C-B-A)) copolymer based thermosensitive gelling polymers. Arrangement of polymer blocks, molecular weight and presence of PLA exhibited significant effect on sol-gel transition curve and kinematic viscosity of respective aqueous solutions. IgG-loaded PB thermosensitive gels exhibited sustained release up to ~20 days. Results of release kinetics suggested Korsmeyer-Peppas as a best fit model and diffusion exponent values (n value) were ranging from 0.272-0.386 for all gelling polymers indicating diffusion controlled release of IgG. Moreover, secondary stability of released IgG was confirmed by CD spectroscopy. PB copolymers with A-B-C-B-A block arrangements demonstrated noticeably lower kinematic viscosity of aqueous solution at 25 °C than the TB (B-A-B) copolymers and other PB copolymers with C-B-A-B-C block arrangements suggesting easy to handle during injection. Presence of PLA block has significantly reduced crystallinity of PB copolymers (C-B-A-B-C and A-B-C-B-A). Hence, it was anticipated that PB copolymers will have faster rate of degradation relative to PCL-PEG-PCL based TB copolymers. The difference in results of viscosity and sol-gel transition has been explained by two different processes of micellization for A-B-C-B-A and B-A-B or C-B-A-B-C types of copolymers. Cell viability and biocompatibility studies suggested that PCL, PLA and PEG based block copolymers are compatible with various ocular and macrophage cell lines. In our first approach, we were able to develop sustained release, biocompatible and biodegradable polymeric formulation which can be administered with semi-invasive technique. However, thermogelling system exhibited sustained release up to only ~20

days, which was shorter than our target profile (4-6 months). Moreover, it also demonstrated significant burst release.

Therefore in our second approach, we have utilized PB copolymers for the preparation of protein-encapsulated NPs. We have synthesized and evaluated series of PB copolymers with significantly high molecular weights and utilized them for the preparation of NPs. PB copolymers with different block arrangement and molecular weights were successfully synthesized by ring-opening bulk polymerization and characterized by ¹H-NMR, gel permeation chromatography (GPC) and X-ray diffraction (XRD) spectroscopy. We have prepared IgG-loaded (a model protein) PB NPs and studied the effects of molecular weight, polymer composition (PEG/PCL/PLA or PEG/PCL/PGA) and isomerism (PLA with L or DL isomers) on various formulation parameters such as EE, DL and *in vitro* release profile. Results demonstrated that crystallinity of PB copolymers can be easily modulated by altering the ratio of PLA/PCL or PGA/PCL. Moreover, molecular weight, crystallinity and copolymer composition exhibited significant effect on EE, DL and *in vitro* release kinetics. PB copolymers composed of PLA with D,L-lactide demonstrated EE (~63%), and DL (~5.8%) with sustained release up to ~60 days which were significantly higher than PB copolymers comprising PLA (L-lactide) or PGA. Secondary structure of released IgG was confirmed by CD spectroscopy. *In vitro* cytotoxicity, cell viability and inflammatory studies performed on human retinal pigment epithelial cells (ARPE-19) and/or macrophage cell line (RAW-264.7) established biocompatibility of PB copolymers for ocular applications. However, PB NPs exhibited significant burst release within first two days which may be attributed to surface adsorbed protein. Moreover, poor DL was also an issue which was needed to be resolved. In

addition, upon intravitreal injection, NPs may distribute throughout the vitreous (floater effect) and obstruct patient's vision which may eventually leads to patient's non-compliance.

In order to resolve the problem of burst release and floater effect, we designed a composite formulation. The composite formulation was comprised of protein-encapsulated PB NPs suspended in PB thermosensitive gel. A novel approach had successfully diminished burst release effect and exhibited nearly zero-order release throughout the release period. This behavior may be due to the fact that when NPs were suspended in gel matrix, entangled polymer chains of thermosensitive gel may serve as an additional diffusion barrier for the surface adsorbed drug. The polymer matrix might deter the dumping of surface adsorbed dose eliminating burst effect and avoiding any possibility of dose dependent toxicity which may occur due to the initial burst release. Simultaneously, we have also hypothesized that proteins with similar molecular weights behave very identical in same polymer matrix. Hence, we have prepared and characterized PB NPs loaded with BSA (66 kDa), IgG (150 kDa) and bevacizumab (150 kDa). Our results demonstrated not significant difference in EE, DL and *in vitro* release profile of IgG or bevacizumab from PB NPs. However, these results were significantly different than BSA-encapsulated PB NPs. Moreover, cell viability, cytotoxicity and biocompatibility studies performed with PB copolymers revealed non-toxic and biocompatible nature of PB copolymers. Results of CD spectroscopy, cell migration and cell proliferation assays confirmed structural and biological activity of released proteins. *In situ* thermosensitive gelling solution immediately transforms to gel at body temperature entrapping protein-loaded PB NPs that inhibits PB NP dispersion in the vitreous fluid and localizes them in the gel matrix. Hence, by developing a composite formulation, we were able to eliminate burst release, achieved nearly zero-order drug release and also eliminated possibility of the

floaters effect. However, in order to deliver large dose in very limited injection volume, the most important challenge was to improve DL. We were also not able to sustain the release for more than ~60 days. From our previous results we learnt that hydrophobicity of polymer have significant effect on sustaining the release of proteins.

In our last approach we have synthesized most hydrophobic PB copolymers to sustain the release for significantly longer duration and we have optimized NP preparation parameters to achieve maximum possible DL. Most hydrophobic PB copolymers were synthesized with two different block arrangements i.e., PLA/PCL/PEG and PGA/PCL/PEG with very high molecular weight. NP preparation method was successfully optimized with respect to polymer hydrophobicity, presence of salt (NaCl), drug to polymer ratio, and phase volumes to achieve high DL. With optimized NP preparation methods, we were able to achieve more than 15% of loading for IgG-Fab, IgG and catalase, and ~8% of loading for octreotide, insulin and lysozyme in PB NPs. PB NPs encapsulating different proteins were also evaluated for their sustain release behavior. All the NPs depicted negligible or no burst release phase. We have observed significantly rapid release of octreotide (~93% in 63 days) from composite formulation relative to the release of lysozyme (~72% in 63 days). It can be explained due to the fact that octreotide has smaller hydrodynamic diameter than lysozyme which may have facilitated rapid diffusion of octreotide from composite formulation. The similar trend was observed when we compared the release profiles of lysozyme and IgG-Fab (~24% in 65 days). These results clearly suggest that the hydrodynamic radius of protein molecules plays a crucial role in defining of their release profiles from composite formulation. However, we have not observed any significant difference between the release profile of octreotide and insulin (~89% in 63 days). It may possible that difference in molecular weights between octreotide and insulin was not sufficient

enough to exert any difference of diffusivity through formulation which may eventually lead to similar release profiles. This fact may be true with smaller molecular weight proteins. However, we observed no significant difference between the release profiles of IgG-Fab, IgG (~20% in 65 days) and catalase (~13% in 63 days) from PB NPs dispersed in thermosensitive gel. It may possible that IgG-Fab, IgG and catalase have very less diffusivity through polymer matrix (due to large molecular weight) and hence their release was mainly controlled by degradation of polymers. With the projected release profiles for IgG-Fab, IgG and catalase, we can easily achieve sustain release for more than 6 months. We have also confirmed enzymatic activity of lysozyme and catalase in the release samples with their respective enzymatic activity assays.

Finally, we have evaluated *in vivo* tolerability of *in situ* thermosensitive gel alone, PB NPs alone and a composite formulation in rabbit eye model. Intravitreal injection of *in situ* thermosensitive gel and composite formulation demonstrated immediate transformation from solution to hydrogel. All the formulations were easily injectable through a 27 gauge needle without showing any back pressure. Moreover, as anticipated, PB NPs were dispersed throughout the vitreous immediately after intravitreal injection and remained dispersed even after 56 days. However, intravitreal injection of composite formulation formed a depot entrapping PB NPs inhibiting NP dispersion in vitreous fluid. *In situ* thermosensitive gel (alone) disintegrated and dissolved in vitreous fluid within 56 days after intravitreal delivery indicating the biodegradable nature of PB copolymers. Rabbit eyes exhibited no signs of toxicity (inflammation, cataract or change in ocular pressure) against any of the PB copolymer-based formulations. Similar formulations were also investigated for their topical applicability.

Even after 4 doses of topical instillation, no signs of irritation or inflammation were observed in rabbit eyes.

In this project, we were successful to develop novel PB based composite formulation for the intravitreal delivery of protein therapeutics. This formulation exhibited all the desired properties of ideal formulation such as, biodegradability, biocompatibility, ability to carry large dose in limited volume, depicted more than 6 month of release, exhibited nearly zero-order release without burst effect, easy injectability, and also ensured stability of proteins/peptides.


Recommendations

According to our results, proteins with similar molecular weights behave very similarly during NP preparation with same PB copolymers. Hence, they exhibit very similar EE, DL and *in vitro* release profile. Our optimized sustained delivery formulation can be utilized with fine tuning to develop a formulation with same molecular weight proteins. PB copolymers utilized for NP preparation are composed of PLA/PCL/PEG and PGA/PCL/PEG with block arrangements of PLA-PCL-PEG-PCL-PLA and PGA-PCL-PEG-PCL-PGA. These polymers demonstrated very slow release rate of IgG-Fab (2-2.5 $\mu\text{g/day}$). Therefore, these polymers are suitable for very potent drugs or to conditions where a lower rate of release is required for a longer duration of time (about 6-10 months). However, these polymeric systems are not useful where higher release rate with high DL is required. Therefore, there is a need to develop a formulations that can provide higher release rate for 4-6 months. According to results, release of IgG-Fab, IgG and catalase (high molecular weight proteins) from the composite formulation is mainly govern by degradation of polymers. Hence, by improving the hydrolytic degradation of PB copolymers, a higher rate of protein release can be achieved. This goal can be achieved



by changing the order of block copolymers to PCL-PLA-PEG-PLA-PCL or PCL-PGA-PEG-PGA-PCL. PEG is a non-degradable polymer whereas PCL is very slow degrading polymer. PLA and PGA are rapidly degrading polymer blocks. In case of PLA-PCL-PEG-PCL-PLA and PGA-PCL-PEG-PCL-PGA terminals blocks degrades very rapidly leaving slow degrading TB copolymer (PCL-PEG-PCL). However, for the new sequence of PB copolymers (PCL-PLA-PEG-PLA-PCL or PCL-PGA-PEG-PGA-PCL) center blocks (PLA/PGA) degrades rapidly, leaving small fragments of block copolymers comprised of homo polymers (PCL or PEG), diblock copolymers (PCL-PLA or PLA-PEG) or TB copolymers (PLA-PEG-PLA or PCL-PLA-PEG). Resulting diblock or TB copolymers may eventually degrade to homopolymers of PEG or PCL. Moreover, this arrangement of blocks will significantly reduce the crystallinity of PB copolymers which will further enhance the rate of polymer degradation. Rapid disintegration of PB copolymers can improve the rate of protein release from the composite formulation. According to the results observed during *in vivo* studies, the thermosensitive gelling polymer degraded very rapidly relative to PB NPs. Faster degradation of gelling polymer may allow PB NPs to escape from the depot to some extent. Free NPs may interfere with a patient's vision, leading to non-compliance. Uptake of these NPs in retinal epithelial cells could be enhanced by functionalizing the NP surface with targeting agents such as folate or biotin. Surface modified PB NPs might be recognized by folate receptor or sodium-dependent multivitamin transporter (SMVT) located on the apical site of retinal pigment epithelial cells. Hence via surface modification approach, free NPs may be diverted from the vitreous fluid to the target site. The composite formulation approach may serve as a platform technology for the delivery of siRNA, peptides, proteins and antibodies in the treatment of

ocular diseases. This technology may not be limited to ocular applications but may be used for any chronic diseases where sustained delivery of macromolecules is required.

APPENDIX



Welcome, Sulabh
Not you?

Log out |  Cart (0) | Manage Account | Feedback | Help |  Live Help

GET PERMISSION | LICENSE YOUR CONTENT | PRODUCTS AND SOLUTIONS | PARTNERS | EDUCATION | ABOUT US


Get Permission / Find Title

[Advanced Search Options](#)

1 PAYMENT — 2 REVIEW — 3 **CONFIRMATION**

Step 3: Order Confirmation

[Start new search >](#) [View your Order History >](#)

 [Print order information:](#) includes order confirmation, terms and conditions, and citation information ([What's this?](#))

Thank you for your order! A confirmation for your order will be sent to your account email address. If you have questions about your order, you can call us at 978-646-2600, M-F between 8:00 AM and 6:00 PM (Eastern), or write to us at info@copyright.com.

Confirmation Number: 11108201
Order Date: 07/18/2013


If you pay by credit card, your order will be finalized and your card will be charged within 24 hours. If you pay by invoice, you can change or cancel your order until the invoice is generated.

Payment Information

Sulabh Patel
University of Missouri Kansas City
spp2m9@mail.umkc.edu
+1 (816)2352423
Payment Method: n/a

Order Details

RECENT PATENTS ON NANOMEDICINE

Order detail ID: 63853729	Permission Status:  Granted
Order License Id: 3192180877926	Permission type: Republish or display content
ISSN: 1877-9123	Type of use: Republish in a thesis/dissertation
Publication Type: Journal	<input type="checkbox"/> View details
Volume:	
Issue:	
Start page:	
Publisher: Bentham Science Publishers, Ltd	

Note: This item will be invoiced or charged separately through CCC's **RightsLink** service. [More info](#) **\$ 0.00**

Total order items: 1 **Order Total: 0.00 USD**



RightsLink®

Home

Create Account

Help



Title: Novel Strategies for Anterior Segment Ocular Drug Delivery
Author: Kishore Cholkar, Sulabh P. Patel, Aswani Dutt Vadlapudi et al.
Publication: Journal of Ocular Pharmacology and Therapeutics
Publisher: Mary Ann Liebert, Inc.
Date: Mar 1, 2013
Copyright © 2013, Mary Ann Liebert, Inc.

User ID
<input type="text"/>
Password
<input type="text"/>
<input type="checkbox"/> Enable Auto Login
<input type="button" value="LOGIN"/>
Forgot Password/User ID?
If you're a copyright.com user, you can login to RightsLink using your copyright.com credentials. Already a RightsLink user or want to learn more?

Permissions Request

Mary Ann Liebert, Inc. publishers does not require authors of the content being used to obtain a license for their personal reuse of full article, charts/graphs/tables or text excerpt.

**Future Science Ltd LICENSE
TERMS AND CONDITIONS**

Oct 14, 2013

This is a License Agreement between University of Missouri Kansas City ("You") and Future Science Ltd ("Future Science Ltd") provided by Copyright Clearance Center ("CCC"). The license consists of your order details, the terms and conditions provided by Future Science Ltd, and the payment terms and conditions.

All payments must be made in full to CCC. For payment instructions, please see information listed at the bottom of this form.

License Number	3192470839144
License date	Jul 19, 2013
Licensed content publisher	Future Science Ltd
Licensed content title	Therapeutic delivery
Licensed content date	Jul 1, 2010
Type of Use	Thesis/Dissertation
Requestor type	Academic institution
Format	Print, Electronic
Portion	chart/graph/table/figure
Number of charts/graphs/tables/figures	1
Title or numeric reference of the portion(s)	I want to use Figure 2 (Ocular barriers) for my dissertation thesis
Title of the article or chapter the portion is from	Polymeric vectors for ocular gene delivery
Editor of portion(s)	N/A
Author of portion(s)	N/A
Volume of serial or monograph.	2
Issue, if republishing an article from a serial	4
Page range of the portion	20
Publication date of portion	April 1, 2011
Rights for	Main product and any product related to main product
Duration of use	Life of current edition
Creation of copies for the disabled	no
With minor editing privileges	yes
For distribution to	Worldwide
In the following language(s)	Original language of publication
With incidental promotional use	no
The lifetime unit quantity of new product	0 to 499
Made available in the following markets	Education
The requesting person/organization is:	Sulabh Patel, UMKC
Order reference number	
Author/Editor	Sulabh Patel
The standard identifier	Dissertation
Title	Development and evaluation of novel pentablock copolymers as a nanotechnology platform for the sustained ocular delivery of peptides and proteins
Publisher	UMKC
Expected publication date	Dec 2013
Estimated size (pages)	200
Total (may include CCC user fee)	0.00 USD

RE: Reproduction permission



AMBREEN IRSHAD - Bentham [ambreenirshad@benthamsci...]

Monday, July 22, 2013 1:43 AM

To: Patel, Sulabh P. (UMKC-Student)

Cc: m.ahmed@benthamscience.org

Grant of Permission

Dear Dr. Patel:

Thank you for your interest in our copyrighted material, and for requesting permission for its use.

Permission is granted for the following subject to the conditions outlined below:

eBook, titled as "Treatise on Ocular Drug Delivery" and edited by Dr. Ashim K. Mitra.
Chapter 5: Biodegradable polymers for ophthalmic applications

To be used in the following manner:

1. Bentham Science Publishers grants you the right to reproduce the material indicated above on a one-time, non-exclusive basis, solely for the purpose described. Permission must be requested separately for any future or additional use.
2. For an article, the copyright notice must be printed on the first page of article or book chapter. For figures, photographs, covers, or tables, the notice may appear with the material, in a footnote, or in the reference list.

Thank you for your patience while your request was being processed. If you wish to contact us further, please use the address below.

Sincerely,

AMBREEN IRSHAD

Permissions & Rights Manager

Bentham Science Publishers

Email: ambreenirshad@benthamscience.org

URL: www.benthamscience.com

LIST OF REFERENCES

1. S. Patel, and A.K. Mitra, , An Overview of Recent Patents on Nanocarrier Based Ophthalmic Drug Delivery Systems Recent patents on nanomedicine, 2 (2012) 2-16.
2. V. Tamboli, G.P. Mishra, A.K. Mitra, Polymeric vectors for ocular gene delivery, Therapeutic delivery, 2 (2011) 523-536.
3. H. Ananthula, R.D. Vaishya, M. Barot, A.K. Mitra, Bioavailability, in: W. Tasman, E.A. Jaeger (Eds.) Duane's Ophthalmology, Lippincott Williams & Wilkins, Philadelphia, 2009.
4. S.D. Klyce, C.E. Crosson, Transport processes across the rabbit corneal epithelium: a review, Curr Eye Res, 4 (1985) 323-331.
5. B.J. McLaughlin, R.B. Caldwell, Y. Sasaki, T.O. Wood, Freeze-fracture quantitative comparison of rabbit corneal epithelial and endothelial membranes, Curr Eye Res, 4 (1985) 951-961.
6. G. Sunkara, U.B. Kompella, Membrane transport processes in the eye, in: A.K. Mitra (Ed.) Ophthalmic drug delivery systems, Marcel Dekker, Inc, New York, 2003, pp. 13-58.
7. P. Saha, K.J. Kim, V.H. Lee, A primary culture model of rabbit conjunctival epithelial cells exhibiting tight barrier properties, Curr Eye Res, 15 (1996) 1163-1169.
8. D.H. Geroski, H.F. Edelhauser, Transscleral drug delivery for posterior segment disease, Adv Drug Deliv Rev, 52 (2001) 37-48.
9. S.H. Kim, R.J. Lutz, N.S. Wang, M.R. Robinson, Transport barriers in transscleral drug delivery for retinal diseases, Ophthalmic Res, 39 (2007) 244-254.
10. D. Ghate, H.F. Edelhauser, Ocular drug delivery, Expert Opin Drug Deliv, 3 (2006) 275-287.
11. K. Hosseini, D. Matsushima, J. Johnson, G. Widera, K. Nyam, L. Kim, Y. Xu, Y. Yao, M. Cormier, Pharmacokinetic study of dexamethasone disodium phosphate using intravitreal, subconjunctival, and intravenous delivery routes in rabbits, J Ocul Pharmacol Ther, 24 (2008) 301-308.
12. O. Weijtens, E.J. Feron, R.C. Schoemaker, A.F. Cohen, E.G. Lentjes, F.P. Romijn, J.C. van Meurs, High concentration of dexamethasone in aqueous and vitreous after subconjunctival injection, Am J Ophthalmol, 128 (1999) 192-197.
13. A. Urtti, Challenges and obstacles of ocular pharmacokinetics and drug delivery, Adv Drug Deliv Rev, 58 (2006) 1131-1135.
14. M.R. Prausnitz, J.S. Noonan, Permeability of cornea, sclera, and conjunctiva: a literature analysis for drug delivery to the eye, J Pharm Sci, 87 (1998) 1479-1488.
15. A.K. Mitra, B.S. Anand, S. Duvvuri, Drug delivery to the eye, in: J. Fischbarg (Ed.) The biology of the eye, Elsevier Inc, New York, 2006, pp. 307-351.
16. R. Gaudana, J. Jwala, S.H. Boddu, A.K. Mitra, Recent perspectives in ocular drug delivery, Pharm Res, 26 (2009) 1197-1216.
17. E. Mannermaa, K.S. Vellonen, A. Urtti, Drug transport in corneal epithelium and blood-retina barrier: emerging role of transporters in ocular pharmacokinetics, Adv Drug Deliv Rev, 58 (2006) 1136-1163.
18. S. Dey, B.S. Anand, J. Patel, A.K. Mitra, Transporters/receptors in the anterior chamber: pathways to explore ocular drug delivery strategies, Expert Opin Biol Ther, 3 (2003) 23-44.
19. P.A. Constable, J.G. Lawrenson, D.E. Dolman, G.B. Arden, N.J. Abbott, P-Glycoprotein expression in human retinal pigment epithelium cell lines, Exp Eye Res, 83 (2006) 24-30.

20. K.S. Vellonen, E. Mannermaa, H. Turner, M. Hakli, J.M. Wolosin, T. Tervo, P. Honkakoski, A. Urtti, Effluxing ABC transporters in human corneal epithelium, *J Pharm Sci*, 99 (2010) 1087-1098.
21. P. Saha, J.J. Yang, V.H. Lee, Existence of a p-glycoprotein drug efflux pump in cultured rabbit conjunctival epithelial cells, *Invest Ophthalmol Vis Sci*, 39 (1998) 1221-1226.
22. J.J. Yang, K.J. Kim, V.H. Lee, Role of P-glycoprotein in restricting propranolol transport in cultured rabbit conjunctival epithelial cell layers, *Pharm Res*, 17 (2000) 533-538.
23. B.G. Kennedy, N.J. Mangini, P-glycoprotein expression in human retinal pigment epithelium, *Mol Vis*, 8 (2002) 422-430.
24. S. Duvvuri, M.D. Gandhi, A.K. Mitra, Effect of P-glycoprotein on the ocular disposition of a model substrate, quinidine, *Curr Eye Res*, 27 (2003) 345-353.
25. T. Zhang, C.D. Xiang, D. Gale, S. Carreiro, E.Y. Wu, E.Y. Zhang, Drug transporter and cytochrome P450 mRNA expression in human ocular barriers: implications for ocular drug disposition, *Drug Metab Dispos*, 36 (2008) 1300-1307.
26. J.V. Aukunuru, G. Sunkara, N. Bandi, W.B. Thoreson, U.B. Kompella, Expression of multidrug resistance-associated protein (MRP) in human retinal pigment epithelial cells and its interaction with BAPSG, a novel aldose reductase inhibitor, *Pharm Res*, 18 (2001) 565-572.
27. P.K. Karla, R. Earla, S.H. Boddu, T.P. Johnston, D. Pal, A. Mitra, Molecular expression and functional evidence of a drug efflux pump (BCRP) in human corneal epithelial cells, *Curr Eye Res*, 34 (2009) 1-9.
28. B.S. Larsson, Interaction between chemicals and melanin, *Pigment Cell Res*, 6 (1993) 127-133.
29. B. Leblanc, S. Jezequel, T. Davies, G. Hanton, C. Taradach, Binding of drugs to eye melanin is not predictive of ocular toxicity, *Regul Toxicol Pharmacol*, 28 (1998) 124-132.
30. R.D. Schoenwald, V. Tandon, D.E. Wurster, C.F. Barfknecht, Significance of melanin binding and metabolism in the activity of 5-acetoxyacetylmino-4-methyl-delta2-1,3,4,-thiadiazolin e-2-sulfonamide, *Eur J Pharm Biopharm*, 46 (1998) 39-50.
31. L. Pitkanen, V.P. Ranta, H. Moilanen, A. Urtti, Binding of betaxolol, metoprolol and oligonucleotides to synthetic and bovine ocular melanin, and prediction of drug binding to melanin in human choroid-retinal pigment epithelium, *Pharm Res*, 24 (2007) 2063-2070.
32. L. Salminen, G. Imre, R. Huupponen, The effect of ocular pigmentation on intraocular pressure response to timolol, *Acta Ophthalmol Suppl*, 173 (1985) 15-18.
33. L. Pitkanen, V.P. Ranta, H. Moilanen, A. Urtti, Permeability of retinal pigment epithelium: effects of permeant molecular weight and lipophilicity, *Invest Ophthalmol Vis Sci*, 46 (2005) 641-646.
34. S. Wang, B. Lu, S. Girman, T. Holmes, N. Bischoff, R.D. Lund, Morphological and functional rescue in RCS rats after RPE cell line transplantation at a later stage of degeneration, *Invest Ophthalmol Vis Sci*, 49 (2008) 416-421.
35. N.P. Cheruvu, U.B. Kompella, Bovine and porcine transscleral solute transport: influence of lipophilicity and the Choroid-Bruch's layer, *Invest Ophthalmol Vis Sci*, 47 (2006) 4513-4522.
36. K. Cholkar, S.P. Patel, A.D. Vadlapudi, A.K. Mitra, Novel strategies for anterior segment ocular drug delivery, *J Ocul Pharmacol Ther*, 29 (2013) 106-123.

37. G. Meseguer, P. Buri, B. Plazonnet, A. Rozier, R. Gurny, Gamma scintigraphic comparison of eyedrops containing pilocarpine in healthy volunteers, *J Ocul Pharmacol Ther*, 12 (1996) 481-488.
38. L. Lapcik, Jr., L. Lapcik, S. De Smedt, J. Demeester, P. Chabreck, Hyaluronan: Preparation, Structure, Properties, and Applications, *Chemical reviews*, 98 (1998) 2663-2684.
39. I.P. Kaur, R. Smitha, Penetration enhancers and ocular bioadhesives: two new avenues for ophthalmic drug delivery, *Drug development and industrial pharmacy*, 28 (2002) 353-369.
40. B.M. Gebhardt, E.D. Varnell, H.E. Kaufman, Cyclosporine in collagen particles: corneal penetration and suppression of allograft rejection, *J Ocul Pharmacol Ther*, 11 (1995) 509-517.
41. E. Dimitrova, S. Bogdanova, M. Mitcheva, I. Tanev, E. Minkov, Development of model aqueous ophthalmic solution of indomethacin, *Drug development and industrial pharmacy*, 26 (2000) 1297-1301.
42. P. Chetoni, L. Panichi, S. Burgalassi, U. Benelli, M.F. Saettone, Pharmacokinetics and anti-inflammatory activity in rabbits of a novel indomethacin ophthalmic solution, *J Ocul Pharmacol Ther*, 16 (2000) 363-372.
43. N. Vulovic, M. Primorac, M. Stupar, M.W. Brown, J.L. Ford, Some studies on the preservation of indometacin suspensions intended for ophthalmic use, *Die Pharmazie*, 45 (1990) 678-679.
44. C. Bucolo, A. Spadaro, Pharmacological evaluation of anti-inflammatory pyrrole-acetic acid derivative eye drops, *J Ocul Pharmacol Ther*, 13 (1997) 353-361.
45. Y. Gao, Y. Sun, F. Ren, S. Gao, PLGA-PEG-PLGA hydrogel for ocular drug delivery of dexamethasone acetate, *Drug development and industrial pharmacy*, 36 (2010) 1131-1138.
46. X. Chen, X. Li, Y. Zhou, X. Wang, Y. Zhang, Y. Fan, Y. Huang, Y. Liu, Chitosan-based thermosensitive hydrogel as a promising ocular drug delivery system: preparation, characterization, and in vivo evaluation, *Journal of biomaterials applications*, 27 (2012) 391-402.
47. Y. Qian, F. Wang, R. Li, Q. Zhang, Q. Xu, Preparation and evaluation of in situ gelling ophthalmic drug delivery system for methazolamide, *Drug development and industrial pharmacy*, 36 (2010) 1340-1347.
48. S.H. Boddu, J. Jwala, R. Vaishya, R. Earla, P.K. Karla, D. Pal, A.K. Mitra, Novel nanoparticulate gel formulations of steroids for the treatment of macular edema, *J Ocul Pharmacol Ther*, 26 (2010) 37-48.
49. H. Yin, C. Gong, S. Shi, X. Liu, Y. Wei, Z. Qian, Toxicity evaluation of biodegradable and thermosensitive PEG-PCL-PEG hydrogel as a potential in situ sustained ophthalmic drug delivery system, *Journal of biomedical materials research. Part B, Applied biomaterials*, 92 (2010) 129-137.
50. Y. Cao, C. Zhang, W. Shen, Z. Cheng, L.L. Yu, Q. Ping, Poly(N-isopropylacrylamide)-chitosan as thermosensitive in situ gel-forming system for ocular drug delivery, *Journal of controlled release*, 120 (2007) 186-194.
51. T. Gratieri, G.M. Gelfuso, O. de Freitas, E.M. Rocha, R.F. Lopez, Enhancing and sustaining the topical ocular delivery of fluconazole using chitosan solution and poloxamer/chitosan in situ forming gel, *Eur J Pharm Biopharm*, 79 (2011) 320-327.

52. H. Gupta, S. Jain, R. Mathur, P. Mishra, A.K. Mishra, T. Velpandian, Sustained ocular drug delivery from a temperature and pH triggered novel in situ gel system, *Drug delivery*, 14 (2007) 507-515.
53. F. Cao, X. Zhang, Q. Ping, New method for ophthalmic delivery of azithromycin by poloxamer/carbopol-based in situ gelling system, *Drug delivery*, 17 (2010) 500-507.
54. I.P. Kaur, M. Kanwar, Ocular preparations: the formulation approach, *Drug development and industrial pharmacy*, 28 (2002) 473-493.
55. R. Valls, E. Vega, M.L. Garcia, M.A. Egea, J.O. Valls, Transcorneal permeation in a corneal device of non-steroidal anti-inflammatory drugs in drug delivery systems, *The open medicinal chemistry journal*, 2 (2008) 66-71.
56. S.H. Loftsson T, Hreinsdottir D, Konradsdottir F, Stefansson E. , Dexamethasone delivery to posterior segment of the eye, *J InclPhenomMacrocycl Chem*, 57 (2007) 585-589.
57. T. Loftsson, E. Stefansson, Cyclodextrin nanotechnology for ophthalmic drug delivery, US7893040, 2011.
58. T.T. Kararli, R. Bandyopadhyay, S.K. Singh, L.C. Hawlwy, Ophthalmic formulation of a selective cyclooxygenase-2 inhibitory drug, WO02005815, 2002.
59. A.R. Bary, I.G. Tucker, N.M. Davies, Considerations in the use of hydroxypropyl-beta-cyclodextrin in the formulation of aqueous ophthalmic solutions of hydrocortisone, *Eur J Pharm Biopharm*, 50 (2000) 237-244.
60. J.K. Kristinsson, H. Fridriksdottir, S. Thorisdottir, A.M. Sigurdardottir, E. Stefansson, T. Loftsson, Dexamethasone-cyclodextrin-polymer co-complexes in aqueous eye drops. Aqueous humor pharmacokinetics in humans, *Invest Ophthalmol Vis Sci*, 37 (1996) 1199-1203.
61. R.M. Mainardes, M.C. Urban, P.O. Cinto, N.M. Khalil, M.V. Chaud, R.C. Evangelista, M.P. Gremiao, Colloidal carriers for ophthalmic drug delivery, *Curr Drug Targets*, 6 (2005) 363-371.
62. L. Rabinovich-Guilatt, P. Couvreur, G. Lambert, C. Dubernet, Cationic vectors in ocular drug delivery, *J Drug Target*, 12 (2004) 623-633.
63. A.C. Amrite, U.B. Kompella, Size-dependent disposition of nanoparticles and microparticles following subconjunctival administration, *J Pharm Pharmacol*, 57 (2005) 1555-1563.
64. A.C. Amrite, H.F. Edelhauser, S.R. Singh, U.B. Kompella, Effect of circulation on the disposition and ocular tissue distribution of 20 nm nanoparticles after periocular administration, *Mol Vis*, 14 (2008) 150-160.
65. G.P. Mishra, M. Bagui, V. Tamboli, A.K. Mitra, Recent applications of liposomes in ophthalmic drug delivery, *Journal of drug delivery*, 2011 (2011) 863734.
66. I.P. Kaur, A. Garg, A.K. Singla, D. Aggarwal, Vesicular systems in ocular drug delivery: an overview, *International journal of pharmaceutics*, 269 (2004) 1-14.
67. M.K. Kothuri, S. Pinnamaneni, N.G. Das, S.K. Das, Microparticles and nanoparticles in ocular drug delivery, in: A.K. Mitra (Ed.) *Ophthalmic drug delivery systems*, Marcel Dekker Inc, New York, 2003, pp. 437-466.
68. A. Samad, Y. Sultana, M. Aqil, Liposomal drug delivery systems: an update review, *Curr Drug Deliv*, 4 (2007) 297-305.
69. S.M. Ansell, T.O. Harasym, P.G. Tardi, S.S. Buchkowsky, M.B. Bally, P.R. Cullis, Antibody conjugation methods for active targeting of liposomes, *Methods Mol Med*, 25 (2000) 51-68.

70. R.M. Hathout, S. Mansour, N.D. Mortada, A.S. Guinedi, Liposomes as an ocular delivery system for acetazolamide: in vitro and in vivo studies, *AAPS PharmSciTech*, 8 (2007) 1.
71. M.S. Nagarsenker, V.Y. Londhe, G.D. Nadkarni, Preparation and evaluation of liposomal formulations of tropicamide for ocular delivery, *International journal of pharmaceutics*, 190 (1999) 63-71.
72. H.E. Schaeffer, D.L. Krohn, Liposomes in topical drug delivery, *Invest Ophthalmol Vis Sci*, 22 (1982) 220-227.
73. L. Peeters, N.N. Sanders, K. Braeckmans, K. Boussery, J. Van de Voorde, S.C. De Smedt, J. Demeester, Vitreous: a barrier to nonviral ocular gene therapy, *Invest Ophthalmol Vis Sci*, 46 (2005) 3553-3561.
74. C. Hatzifoti, A. Bacon, H. Marriott, P. Laing, A.W. Heath, Liposomal co-entrapment of CD40mAb induces enhanced IgG responses against bacterial polysaccharide and protein, *PLoS One*, 3 (2008) e2368.
75. R. Zeimer, M.F. Goldberg, Novel ophthalmic therapeutic modalities based on noninvasive light-targeted drug delivery to the posterior pole of the eye, *Adv Drug Deliv Rev*, 52 (2001) 49-61.
76. S.K. Dharma, P.H. Fishman, G.A. Peyman, A preliminary study of corneal penetration of 125I-labelled idoxuridine liposome, *Acta ophthalmologica*, 64 (1986) 298-301.
77. O. Felt, P. Furrer, J.M. Mayer, B. Plazonnet, P. Buri, R. Gurny, Topical use of chitosan in ophthalmology: tolerance assessment and evaluation of precorneal retention, *International journal of pharmaceutics*, 180 (1999) 185-193.
78. A.S. Monem, F.M. Ali, M.W. Ismail, Prolonged effect of liposomes encapsulating pilocarpine HCl in normal and glaucomatous rabbits, *International journal of pharmaceutics*, 198 (2000) 29-38.
79. S.L. Law, K.J. Huang, C.H. Chiang, Acyclovir-containing liposomes for potential ocular delivery. Corneal penetration and absorption, *Journal of controlled release*, 63 (2000) 135-140.
80. Y. Shen, J. Tu, Preparation and ocular pharmacokinetics of ganciclovir liposomes, *AAPS J*, 9 (2007) E371-377.
81. K.M. Hosny, Ciprofloxacin as ocular liposomal hydrogel, *AAPS PharmSciTech*, 11 241-246.
82. V.H. Lee, P.T. Urrea, R.E. Smith, D.J. Schanzlin, Ocular drug bioavailability from topically applied liposomes, *Surv Ophthalmol*, 29 (1985) 335-348.
83. K.M. Hosny, Preparation and evaluation of thermosensitive liposomal hydrogel for enhanced transcorneal permeation of ofloxacin, *AAPS PharmSciTech*, 10 (2009) 1336-1342.
84. T.M. Allen, L. McAllister, S. Mausolf, E. Gyorffy, Liposome-cell interactions. A study of the interactions of liposomes containing entrapped anti-cancer drugs with the EMT6, S49 and AE1 (transport-deficient) cell lines, *Biochim Biophys Acta*, 643 (1981) 346-362.
85. P.I. Campbell, Toxicity of some charged lipids used in liposome preparations, *Cytobios*, 37 (1983) 21-26.
86. S.C. Chang, H. Bundgaard, A. Buur, V.H. Lee, Improved corneal penetration of timolol by prodrugs as a means to reduce systemic drug load, *Invest Ophthalmol Vis Sci*, 28 (1987) 487-491.
87. E. Yoshihara, T. Nakae, Cytolytic activity of liposomes containing stearylamine, *Biochim Biophys Acta*, 854 (1986) 93-101.

88. K.G. Janoria, S. Hariharan, C.R. Dasari, A.K. Mitra, Recent patents and advances in ophthalmic drug delivery, *Recent Pat Drug Deliv Formul*, 1 (2007) 161-170.
89. R. Pignatello, C. Bucolo, P. Ferrara, A. Maltese, A. Puleo, G. Puglisi, Eudragit RS100 nanosuspensions for the ophthalmic controlled delivery of ibuprofen, *European journal of pharmaceutical sciences*, 16 (2002) 53-61.
90. R. Pignatello, C. Bucolo, G. Spedalieri, A. Maltese, G. Puglisi, Flurbiprofen-loaded acrylate polymer nanosuspensions for ophthalmic application, *Biomaterials*, 23 (2002) 3247-3255.
91. Y. Rojanasakul, L.Y. Wang, M. Bhat, D.D. Glover, C.J. Malanga, J.K. Ma, The transport barrier of epithelia: a comparative study on membrane permeability and charge selectivity in the rabbit, *Pharm Res*, 9 (1992) 1029-1034.
92. P. Calvo, J.L. Vila-Jato, M.J. Alonso, Comparative in vitro evaluation of several colloidal systems, nanoparticles, nanocapsules, and nanoemulsions, as ocular drug carriers, *J Pharm Sci*, 85 (1996) 530-536.
93. E. Vega, M.A. Egea, O. Valls, M. Espina, M.L. Garcia, Flurbiprofen loaded biodegradable nanoparticles for ophthalmic administration, *J Pharm Sci*, 95 (2006) 2393-2405.
94. A.M. De Campos, A. Sanchez, M.J. Alonso, Chitosan nanoparticles: a new vehicle for the improvement of the delivery of drugs to the ocular surface. Application to cyclosporin A, *International journal of pharmaceuticals*, 224 (2001) 159-168.
95. X.B. Yuan, Li, H., Yuan, Y.B., Preparation of cholesterol-modified chitosan self-aggregated nanoparticles for delivery of drugs to ocular surface, *Carbohydrate Polymers*, 65 (2006) 337-345.
96. X.B. Yuan, Y.B. Yuan, W. Jiang, J. Liu, E.J. Tian, H.M. Shun, D.H. Huang, X.Y. Yuan, H. Li, J. Sheng, Preparation of rapamycin-loaded chitosan/PLA nanoparticles for immunosuppression in corneal transplantation, *International journal of pharmaceuticals*, 349 (2008) 241-248.
97. H.K. Ibrahim, I.S. El-Leithy, A.A. Makky, Mucoadhesive nanoparticles as carrier systems for prolonged ocular delivery of gatifloxacin/prednisolone bitherapy, *Molecular pharmaceuticals*, 7 (2010) 576-585.
98. F.M.J. Alonso, S.P. Calvo, L.C. Remunan, J.J.L. Vila, Stabilization of colloidal systems by the formation of ionic lipid-polysaccharide complexes, EP0771566, 2006.
99. A.K. Mitra, G.P. Mishra, Pentablock Polymers, US0250283, 2011.
100. L. Contreras-Ruiz, M. de la Fuente, J.E. Parraga, A. Lopez-Garcia, I. Fernandez, B. Seijo, A. Sanchez, M. Calonge, Y. Diebold, Intracellular trafficking of hyaluronic acid-chitosan oligomer-based nanoparticles in cultured human ocular surface cells, *Mol Vis*, 17 (2011) 279-290.
101. M. de la Fuente, B. Seijo, M.J. Alonso, Novel hyaluronic acid-chitosan nanoparticles for ocular gene therapy, *Invest Ophthalmol Vis Sci*, 49 (2008) 2016-2024.
102. A. Enriquez de Salamanca, Y. Diebold, M. Calonge, C. Garcia-Vazquez, S. Callejo, A. Vila, M.J. Alonso, Chitosan nanoparticles as a potential drug delivery system for the ocular surface: toxicity, uptake mechanism and in vivo tolerance, *Invest Ophthalmol Vis Sci*, 47 (2006) 1416-1425.
103. U.B. Kompella, S. Sundaram, S. Raghava, E.R. Escobar, Luteinizing hormone-releasing hormone agonist and transferrin functionalizations enhance nanoparticle delivery in a novel bovine ex vivo eye model, *Mol Vis*, 12 (2006) 1185-1198.

104. B.E. Rabinow, Nanosuspensions in drug delivery, *Nat Rev Drug Discov*, 3 (2004) 785-796.
105. D.R. Sanders, B. Goldstick, C. Kraff, R. Hutchins, M.S. Bernstein, M.A. Evans, Aqueous penetration of oral and topical indomethacin in humans, *Archives of ophthalmology*, 101 (1983) 1614-1616.
106. M.A. Kassem, A.A. Abdel Rahman, M.M. Ghorab, M.B. Ahmed, R.M. Khalil, Nanosuspension as an ophthalmic delivery system for certain glucocorticoid drugs, *International journal of pharmaceutics*, 340 (2007) 126-133.
107. J.D. Quintana-Hau, E. Cruz-Olmos, M.I. Lopez-Sanchez, V. Sanchez-Castellanos, L. Baiza-Duran, J.R. Gonzalez, M. Tornero, R. Mondragon-Flores, A. Hernandez-Santoyo, Characterization of the novel ophthalmic drug carrier Sophisen in two of its derivatives: 3A Ofteno and Modusik-A Ofteno, *Drug development and industrial pharmacy*, 31 (2005) 263-269.
108. S. Panmai, L.L. Alani, Ophthalmic nanoparticulate formulation of a cyclooxygenase-2 selective inhibitor, WO2006062875, 2006.
109. V.B. Patravale, A.A. Date, R.M. Kulkarni, Nanosuspensions: a promising drug delivery strategy, *J Pharm Pharmacol*, 56 (2004) 827-840.
110. A.A. Badawi, H.M. El-Laithy, R.K. El Qidra, H. El Mofty, M. El dally, Chitosan based nanocarriers for indomethacin ocular delivery, *Archives of pharmacal research*, 31 (2008) 1040-1049.
111. L. Gan, Y. Gan, C. Zhu, X. Zhang, J. Zhu, Novel microemulsion in situ electrolyte-triggered gelling system for ophthalmic delivery of lipophilic cyclosporine A: in vitro and in vivo results, *International journal of pharmaceutics*, 365 (2009) 143-149.
112. L. Baydoun, C.C. Muller-Goymann, Influence of n-octenylsuccinate starch on in vitro permeation of sodium diclofenac across excised porcine cornea in comparison to Voltaren ophtha, *Eur J Pharm Biopharm*, 56 (2003) 73-79.
113. M. ShaulMughtar, Joseph Frucht-Pery, Simon Benita, , Ex-vivo permeation study of indomethacin from a submicron emulsion through albino rabbit cornea, , *Journal of controlled release*, 44 (1997) 55-64.
114. S. Benita, G. Lambert, Method and composition for dry eye treatment, US0108626, 2003.
115. Y. Gan, L. Gan, J. Shen, C. Zhu, Ophthalmic flurbiprofen ester nano-emulsion in-situ gel formulation and the preparation method there of, WO2010048788, 2010.
116. S.H. Hyon, K. Jamshidi, Y. Ikada, Synthesis of polylactides with different molecular weights, *Biomaterials*, 18 (1997) 1503-1508.
117. J.M. Lu, X. Wang, C. Marin-Muller, H. Wang, P.H. Lin, Q. Yao, C. Chen, Current advances in research and clinical applications of PLGA-based nanotechnology, *Expert Rev Mol Diagn*, 9 (2009) 325-341.
118. V.P. Torchilin, Structure and design of polymeric surfactant-based drug delivery systems, *Journal of controlled release*, 73 (2001) 137-172.
119. C. Civiale, M. Licciardi, G. Cavallaro, G. Giammona, M.G. Mazzone, Polyhydroxyethylaspartamide-based micelles for ocular drug delivery, *International journal of pharmaceutics*, 378 (2009) 177-186.
120. A.K. Mitra, P. Velagaleti, U.M. Grau, Topical drug delivery systems for ophthalmic use, WO2010144194, 2010.
121. A.K. Mitra, P. Velagaleti, N. Subramanian, Ophthalmic compositions comprising calcineurin inhibitors or mtor inhibitors, US0092665, 2009.

122. L. Gan, S. Han, J. Shen, J. Zhu, C. Zhu, X. Zhang, Y. Gan, Self-assembled liquid crystalline nanoparticles as a novel ophthalmic delivery system for dexamethasone: Improving precocular retention and ocular bioavailability, *International journal of pharmaceutics*, 396 (2010) 179-187.
123. J.L. Bourges, C. Bloquel, A. Thomas, F. Froussart, A. Bochot, F. Azan, R. Gurny, D. BenEzra, F. Behar-Cohen, Intraocular implants for extended drug delivery: therapeutic applications, *Adv Drug Deliv Rev*, 58 (2006) 1182-1202.
124. T.J. Smith, P.A. Pearson, D.L. Blandford, J.D. Brown, K.A. Goins, J.L. Hollins, E.T. Schmeisser, P. Glavinos, L.B. Baldwin, P. Ashton, Intravitreal sustained-release ganciclovir, *Archives of ophthalmology*, 110 (1992) 255-258.
125. J.I. Lim, R.A. Wolitz, A.H. Dowling, H.R. Bloom, A.R. Irvine, D.M. Schwartz, Visual and anatomic outcomes associated with posterior segment complications after ganciclovir implant procedures in patients with AIDS and cytomegalovirus retinitis, *Am J Ophthalmol*, 127 (1999) 288-293.
126. G.E. Sanborn, R. Anand, R.E. Torti, S.D. Nightingale, S.X. Cal, B. Yates, P. Ashton, T. Smith, Sustained-release ganciclovir therapy for treatment of cytomegalovirus retinitis. Use of an intravitreal device, *Archives of ophthalmology*, 110 (1992) 188-195.
127. T. Yasukawa, Y. Ogura, H. Kimura, E. Sakurai, Y. Tabata, Drug delivery from ocular implants, *Expert Opin Drug Deliv*, 3 (2006) 261-273.
128. K. Okabe, H. Kimura, J. Okabe, A. Kato, N. Kunou, Y. Ogura, Intraocular tissue distribution of betamethasone after intrascleral administration using a non-biodegradable sustained drug delivery device, *Invest Ophthalmol Vis Sci*, 44 (2003) 2702-2707.
129. G.J. Jaffe, R.M. McCallum, B. Branchaud, C. Skalak, Z. Butuner, P. Ashton, Long-term follow-up results of a pilot trial of a fluocinolone acetonide implant to treat posterior uveitis, *Ophthalmology*, 112 (2005) 1192-1198.
130. P.A. Pearson, G.J. Jaffe, D.F. Martin, G.J. Cordahi, H. Grossniklaus, E.T. Schmeisser, P. Ashton, Evaluation of a delivery system providing long-term release of cyclosporine, *Archives of ophthalmology*, 114 (1996) 311-317.
131. L.B. Enyedi, P.A. Pearson, P. Ashton, G.J. Jaffe, An intravitreal device providing sustained release of cyclosporine and dexamethasone, *Curr Eye Res*, 15 (1996) 549-557.
132. H. Kimura, Y. Ogura, Biodegradable polymers for ocular drug delivery, *Ophthalmologica. Journal international d'ophtalmologie. International journal of ophthalmology*, 215 (2001) 143-155.
133. N. Kunou, Y. Ogura, T. Yasukawa, H. Kimura, H. Miyamoto, Y. Honda, Y. Ikada, Long-term sustained release of ganciclovir from biodegradable scleral implant for the treatment of cytomegalovirus retinitis, *Journal of controlled release*, 68 (2000) 263-271.
134. P.E. Rubsamen, P.A. Davis, E. Hernandez, G.E. O'Grady, S.W. Cousins, Prevention of experimental proliferative vitreoretinopathy with a biodegradable intravitreal implant for the sustained release of fluorouracil, *Archives of ophthalmology*, 112 (1994) 407-413.
135. T. Zhou, H. Lewis, R.E. Foster, S.P. Schwendeman, Development of a multiple-drug delivery implant for intraocular management of proliferative vitreoretinopathy, *Journal of controlled release*, 55 (1998) 281-295.
136. L. Xie, J. Sun, Z. Yao, Heparin drug delivery system for prevention of posterior capsular opacification in rabbit eyes, *Graefes' archive for clinical and experimental ophthalmology*, 241 (2003) 309-313.

137. T. Yasukawa, H. Kimura, Y. Tabata, H. Miyamoto, Y. Honda, Y. Ogura, Sustained release of cis-hydroxyproline in the treatment of experimental proliferative vitreoretinopathy in rabbits, *Graefes archive for clinical and experimental ophthalmology*, 240 (2002) 672-678.
138. C. Koelwel, S. Rothschenk, B. Fuchs-Koelwel, B. Gabler, C. Lohmann, A. Gopferich, Alginate inserts loaded with epidermal growth factor for the treatment of keratoconjunctivitis sicca, *Pharmaceutical development and technology*, 13 (2008) 221-231.
139. C.F. Yang, T. Yasukawa, H. Kimura, H. Miyamoto, Y. Honda, Y. Tabata, Y. Ikada, Y. Ogura, Experimental corneal neovascularization by basic fibroblast growth factor incorporated into gelatin hydrogel, *Ophthalmic Res*, 32 (2000) 19-24.
140. M. Hashizoe, Y. Ogura, T. Takanashi, N. Kunou, Y. Honda, Y. Ikada, Implantable biodegradable polymeric device in the treatment of experimental proliferative vitreoretinopathy, *Curr Eye Res*, 14 (1995) 473-477.
141. M. Hashizoe, Y. Ogura, H. Kimura, T. Moritera, Y. Honda, M. Kyo, S.H. Hyon, Y. Ikada, Scleral plug of biodegradable polymers for controlled drug release in the vitreous, *Archives of ophthalmology*, 112 (1994) 1380-1384.
142. H. Miyamoto, Y. Ogura, M. Hashizoe, N. Kunou, Y. Honda, Y. Ikada, Biodegradable scleral implant for intravitreal controlled release of fluconazole, *Curr Eye Res*, 16 (1997) 930-935.
143. E. Sakurai, M. Nozaki, K. Okabe, N. Kunou, H. Kimura, Y. Ogura, Scleral plug of biodegradable polymers containing tacrolimus (FK506) for experimental uveitis, *Invest Ophthalmol Vis Sci*, 44 (2003) 4845-4852.
144. J. Okabe, H. Kimura, N. Kunou, K. Okabe, A. Kato, Y. Ogura, Biodegradable intrascleral implant for sustained intraocular delivery of betamethasone phosphate, *Invest Ophthalmol Vis Sci*, 44 (2003) 740-744.
145. Y. Morita, A. Ohtori, M. Kimura, K. Tojo, Intravitreal delivery of dexamethasone sodium m-sulfobenzoate from poly(DL-lactic acid) implants, *Biological & pharmaceutical bulletin*, 21 (1998) 188-190.
146. M.R. Prausnitz, Microneedles for transdermal drug delivery, *Adv Drug Deliv Rev*, 56 (2004) 581-587.
147. J. Jiang, H.S. Gill, D. Ghate, B.E. McCarey, S.R. Patel, H.F. Edelhauser, M.R. Prausnitz, Coated microneedles for drug delivery to the eye, *Invest Ophthalmol Vis Sci*, 48 (2007) 4038-4043.
148. J. Jiang, J.S. Moore, H.F. Edelhauser, M.R. Prausnitz, Intrascleral drug delivery to the eye using hollow microneedles, *Pharm Res*, 26 (2009) 395-403.
149. S. Patel, V. Tamboli, G.P. Mishra, A.K. Mitra, Biodegradable Polymers for Ophthalmic Applications, in: A.K. Mitra (Ed.) *Treatise on Ocular Drug Delivery*, Bentham Science, 2013, pp. 96-113.
150. J.L. Arias, M.A. Ruiz, M. Lopez-Viota, A.V. Delgado, Poly(alkylcyanoacrylate) colloidal particles as vehicles for antitumour drug delivery: a comparative study, *Colloids Surf B Biointerfaces*, 62 (2008) 64-70.
151. R.J. Tamargo, J.I. Epstein, C.S. Reinhard, M. Chasin, H. Brem, Brain biocompatibility of a biodegradable, controlled-release polymer in rats, *J Biomed Mater Res*, 23 (1989) 253-266.
152. H. Brem, Polymers to treat brain tumours, *Biomaterials*, 11 (1990) 699-701.

153. N. Kumar, R.S. Langer, A.J. Domb, Polyamides: an overview, *Adv Drug Deliv Rev*, 54 (2002) 889-910.
154. J.C. Middleton, A.J. Tipton, Synthetic biodegradable polymers as orthopedic devices, *Biomaterials*, 21 (2000) 2335-2346.
155. R. Jain, N.H. Shah, A.W. Malick, C.T. Rhodes, Controlled drug delivery by biodegradable poly(ester) devices: different preparative approaches, *Drug development and industrial pharmacy*, 24 (1998) 703-727.
156. R. Tang, R.N. Palumbo, W. Ji, C. Wang, Poly(ortho ester amides): acid-labile temperature-responsive copolymers for potential biomedical applications, *Biomacromolecules*, 10 (2009) 722-727.
157. J. Heller, J. Barr, S.Y. Ng, K.S. Abdellauoi, R. Gurny, Poly(ortho esters): synthesis, characterization, properties and uses, *Adv Drug Deliv Rev*, 54 (2002) 1015-1039.
158. S. Einmahl, S. Capancioni, K. Schwach-Abdellaoui, M. Moeller, F. Behar-Cohen, R. Gurny, Therapeutic applications of viscous and injectable poly(ortho esters), *Adv Drug Deliv Rev*, 53 (2001) 45-73.
159. J.A. Tielsch, Vision problems in the US: a report on blindness and vision impairment in adults age 40 and older, *Prevent Blindness America*, (1994).
160. C.C. Hu, J.D. Ho, H.C. Lin, Neovascular age-related macular degeneration and the risk of stroke: a 5-year population-based follow-up study, *Stroke*, 41 (2010) 613-617.
161. A.D. Kulkarni, B.D. Kuppermann, Wet age-related macular degeneration, *Adv Drug Deliv Rev*, 57 (2005) 1994-2009.
162. T. Inai, M. Mancuso, H. Hashizume, F. Baffert, A. Haskell, P. Baluk, D.D. Hu-Lowe, D.R. Shalinsky, G. Thurston, G.D. Yancopoulos, D.M. McDonald, Inhibition of vascular endothelial growth factor (VEGF) signaling in cancer causes loss of endothelial fenestrations, regression of tumor vessels, and appearance of basement membrane ghosts, *The American journal of pathology*, 165 (2004) 35-52.
163. B.T. Ozturk, H. Kerimoglu, B. Bozkurt, S. Okudan, Comparison of intravitreal bevacizumab and ranibizumab treatment for diabetic macular edema, *J Ocul Pharmacol Ther*, 27 373-377.
164. M.I. Canut, A. Alvarez, J. Nadal, R. Abreu, J.A. Abreu, J.S. Pulido, Anterior segment changes following intravitreal bevacizumab injection for treatment of neovascular glaucoma, *Clin Ophthalmol*, 5 715-719.
165. F. Bock, J. Onderka, T. Dietrich, B. Bachmann, F.E. Kruse, M. Paschke, G. Zahn, C. Cursiefen, Bevacizumab as a potent inhibitor of inflammatory corneal angiogenesis and lymphangiogenesis, *Invest Ophthalmol Vis Sci*, 48 (2007) 2545-2552.
166. M.S. Alforja, N. Sabater, J. Giralt, A. Adan, L. Pelegrin, R. Casaroli-Marano, Intravitreal bevacizumab injection for peripheral exudative hemorrhagic chorioretinopathy, *Japanese journal of ophthalmology*, 55 (2011) 425-427.
167. A. Sayen, I. Hubert, J.P. Berrod, Age related macular degeneration, *La Revue du praticien*, 61 (2011) 159-164.
168. S. Saati, R.N. Agrawal, S. Louie, G.J. Chader, M.S. Humayun, Effect of multiple injections of small divided doses vs single injection of intravitreal bevacizumab on retinal neovascular model in rabbits, *Graefes' archive for clinical and experimental ophthalmology*, 248 457-466.

169. J. Kang, S.P. Schwendeman, Comparison of the effects of Mg(OH)₂ and sucrose on the stability of bovine serum albumin encapsulated in injectable poly(D,L-lactide-co-glycolide) implants, *Biomaterials*, 23 (2002) 239-245.
170. A. Budhian, S.J. Siegel, K.I. Winey, Production of haloperidol-loaded PLGA nanoparticles for extended controlled drug release of haloperidol, *Journal of microencapsulation*, 22 (2005) 773-785.
171. J. Jwala, S.H. Boddu, S. Shah, S. Sirimulla, D. Pal, A.K. Mitra, Ocular sustained release nanoparticles containing stereoisomeric dipeptide prodrugs of acyclovir, *J Ocul Pharmacol Ther*, 27 (2011) 163-172.
172. G.A. Peyman, E.M. Lad, D.M. Moshfeghi, Intravitreal injection of therapeutic agents, *Retina*, 29 (2009) 875-912.
173. R.D. Jager, L.P. Aiello, S.C. Patel, E.T. Cunningham, Jr., Risks of intravitreal injection: a comprehensive review, *Retina*, 24 (2004) 676-698.
174. K.M. Sampat, S.J. Garg, Complications of intravitreal injections, *Curr Opin Ophthalmol*, 21 (2010) 178-183.
175. S.R. Van Tomme, G. Storm, W.E. Hennink, In situ gelling hydrogels for pharmaceutical and biomedical applications, *International journal of pharmaceutics*, 355 (2008) 1-18.
176. M. Gou, C. Gong, J. Zhang, X. Wang, Y. Gu, G. Guo, L. Chen, F. Luo, X. Zhao, Y. Wei, Z. Qian, Polymeric matrix for drug delivery: honokiol-loaded PCL-PEG-PCL nanoparticles in PEG-PCL-PEG thermosensitive hydrogel, *J Biomed Mater Res A*, 93 (2010) 219-226.
177. B. Jeong, Y.H. Bae, S.W. Kim, In situ gelation of PEG-PLGA-PEG triblock copolymer aqueous solutions and degradation thereof, *J Biomed Mater Res*, 50 (2000) 171-177.
178. S. Singh, D.C. Webster, J. Singh, Thermosensitive polymers: synthesis, characterization, and delivery of proteins, *International journal of pharmaceutics*, 341 (2007) 68-77.
179. C.B. Liu, C.Y. Gong, M.J. Huang, J.W. Wang, Y.F. Pan, Y.D. Zhang, G.Z. Li, M.L. Gou, K. Wang, M.J. Tu, Y.Q. Wei, Z.Y. Qian, Thermoreversible gel-sol behavior of biodegradable PCL-PEG-PCL triblock copolymer in aqueous solutions, *J Biomed Mater Res. Part B, Applied biomaterials*, 84 (2008) 165-175.
180. C. Gong, S. Shi, L. Wu, M. Gou, Q. Yin, Q. Guo, P. Dong, F. Zhang, F. Luo, X. Zhao, Y. Wei, Z. Qian, Biodegradable in situ gel-forming controlled drug delivery system based on thermosensitive PCL-PEG-PCL hydrogel. Part 2: sol-gel-sol transition and drug delivery behavior, *Acta Biomater*, 5 (2009) 3358-3370.
181. M.-H. Huang, S. Li, M. Vert, Synthesis and degradation of PLA-PCL-PLA triblock copolymer prepared by successive polymerization of 3-caprolactone and DL-lactide., *Polymer*, 45 (2004) 8675-8681.
182. M.L. Houchin, E.M. Topp, Chemical degradation of peptides and proteins in PLGA: a review of reactions and mechanisms, *J Pharm Sci*, 97 (2008) 2395-2404.
183. Y. Zhang, S.P. Schwendeman, Minimizing acylation of peptides in PLGA microspheres, *Journal of controlled release*, 162 (2012) 119-126.
184. M.J. Hwang, J.M. Suh, Y.H. Bae, S.W. Kim, B. Jeong, Caprolactonic poloxamer analog: PEG-PCL-PEG, *Biomacromolecules*, 6 (2005) 885-890.
185. A. Prabhu, C.E. Shelburne, D.F. Gibbons, Cellular proliferation and cytokine responses of murine macrophage cell line J774A.1 to polymethylmethacrylate and cobalt-chrome alloy particles, *J Biomed Mater Res*, 42 (1998) 655-663.

186. D. Lee, M. Shim, S. Kim, H. Lee, I. Park, T. Chang, Novel thermoreversible gelation of biodegradable PLGA-block-PEOblock-PLGA triblock copolymers in aqueous solution, *Macromolecular rapid communications*, 22 (2001) 587-592.
187. B. Jeong, Y.H. Bae, S.W. Kim, Drug release from biodegradable injectable thermosensitive hydrogel of PEG-PLGA-PEG triblock copolymers, *Journal of controlled release*, 63 (2000) 155-163.
188. S.H. Lee, Z. Zhang, S.S. Feng, Nanoparticles of poly(lactide)-tocopheryl polyethylene glycol succinate (PLA-TPGS) copolymers for protein drug delivery, *Biomaterials*, 28 (2007) 2041-2050.
189. W. Jia, Y. Gu, M. Gou, M. Dai, X. Li, B. Kan, J. Yang, Q. Song, Y. Wei, Z. Qian, Preparation of biodegradable polycaprolactone/poly (ethylene glycol)/polycaprolactone (PCEC) nanoparticles, *Drug delivery*, 15 (2008) 409-416.
190. U. Bilati, E. Allemann, E. Doelker, Poly(D,L-lactide-co-glycolide) protein-loaded nanoparticles prepared by the double emulsion method--processing and formulation issues for enhanced entrapment efficiency, *Journal of microencapsulation*, 22 (2005) 205-214.
191. C. Perez, I.J. Castellanos, H.R. Costantino, W. Al-Azzam, K. Griebenow, Recent trends in stabilizing protein structure upon encapsulation and release from bioerodible polymers, *J Pharm Pharmacol*, 54 (2002) 301-313.
192. S.D. Putney, Encapsulation of proteins for improved delivery, *Curr Opin Chem Biol*, 2 (1998) 548-552.
193. T.R. Kumar, K. Soppimath, S.K. Nachaegari, Novel delivery technologies for protein and peptide therapeutics, *Curr Pharm Biotechnol*, 7 (2006) 261-276.
194. M. van de Weert, W.E. Hennink, W. Jiskoot, Protein instability in poly(lactic-co-glycolic acid) microparticles, *Pharm Res*, 17 (2000) 1159-1167.
195. H. Sah, Stabilization of proteins against methylene chloride/water interface-induced denaturation and aggregation, *Journal of controlled release*, 58 (1999) 143-151.
196. K. Fu, D.W. Pack, A.M. Klibanov, R. Langer, Visual evidence of acidic environment within degrading poly(lactic-co-glycolic acid) (PLGA) microspheres, *Pharm Res*, 17 (2000) 100-106.
197. E. Zablotna, A. Jaskiewicz, A. Legowska, H. Miecznikowska, A. Lesner, K. Rolka, Design of serine proteinase inhibitors by combinatorial chemistry using trypsin inhibitor SFTI-1 as a starting structure, *J Pept Sci*, 13 (2007) 749-755.
198. J. Wang, K.M. Chua, C.H. Wang, Stabilization and encapsulation of human immunoglobulin G into biodegradable microspheres, *J Colloid Interface Sci*, 271 (2004) 92-101.
199. J. Jwala, R.K. Vadlapatla, A.D. Vadlapudi, S.H. Boddu, D. Pal, A.K. Mitra, Differential expression of folate receptor-alpha, sodium-dependent multivitamin transporter, and amino acid transporter (B (0, +)) in human retinoblastoma (Y-79) and retinal pigment epithelial (ARPE-19) cell lines, *J Ocul Pharmacol Ther*, 28 (2012) 237-244.
200. D. Pissuwan, C. Boyer, K. Gunasekaran, T.P. Davis, V. Bulmus, In vitro cytotoxicity of RAFT polymers, *Biomacromolecules*, 11 (2010) 412-420.
201. U. Bilati, E. Allemann, E. Doelker, Sonication parameters for the preparation of biodegradable nanocapsules of controlled size by the double emulsion method, *Pharmaceutical development and technology*, 8 (2003) 1-9.

202. M.I. Sabir, X. Xu, L. Li, A review on biodegradable polymeric materials for bone tissue engineering applications, *Journal of material science*, 44 (2009) 5713-5724.
203. M.H. Huang, S. Li, M. Vert, Synthesis and degradation of PLA-PCL-PLA triblock copolymer prepared by successive polymerization of ϵ -caprolactone and DL-lactide, *Polymer*, 45 (2004) 8675-8681.
204. A. Frank, S.K. Rath, S.S. Venkatraman, Controlled release from bioerodible polymers: effect of drug type and polymer composition, *Journal of controlled release*, 102 (2005) 333-344.
205. M.H. Huang, S. Li, D.W. Hutmacher, J.T. Schantz, C.A. Vacanti, C. Braud, M. Vert, Degradation and cell culture studies on block copolymers prepared by ring opening polymerization of epsilon-caprolactone in the presence of poly(ethylene glycol), *J Biomed Mater Res A*, 69 (2004) 417-427.
206. S. Li, I. Molina, M.B. Martinez, M. Vert, Hydrolytic and enzymatic degradations of physically crosslinked hydrogels prepared from PLA/PEO/PLA triblock copolymers, *J Mater Sci Mater Med*, 13 (2002) 81-86.
207. S. Li, P. Dobrzynski, J. Kasperczyk, M. Bero, C. Braud, M. Vert, Structure-property relationships of copolymers obtained by ring-opening polymerization of glycolide and epsilon-caprolactone. Part 2. Influence of composition and chain microstructure on the hydrolytic degradation, *Biomacromolecules*, 6 (2005) 489-497.
208. T.G. Park, Degradation of poly (D,L-lactic acid) microspheres: Effect of molecular weight, *Journal of Controlled Release*, 30 (1994) 161-173.
209. S. Du, Q. Zhang, S. Zhang, L. Wang, J. Lian, Heat shock protein 70 expression induced by diode laser irradiation on choroid-retinal endothelial cells in vitro, *Mol Vis*, 18 (2012) 2380-2387.
210. V. Bhardwaj, D.D. Ankola, S.C. Gupta, M. Schneider, C.M. Lehr, M.N. Kumar, PLGA nanoparticles stabilized with cationic surfactant: safety studies and application in oral delivery of paclitaxel to treat chemical-induced breast cancer in rat, *Pharm Res*, 26 (2009) 2495-2503.
211. S. Basu, R. Harfouche, S. Soni, G. Chimote, R.A. Mashelkar, S. Sengupta, Nanoparticle-mediated targeting of MAPK signaling predisposes tumor to chemotherapy, *Proc Natl Acad Sci U S A*, 106 (2009) 7957-7961.
212. Q.T. Shubhra, T. Feczko, A.F. Kardos, J. Toth, H. Mackova, D. Horak, G. Dosa, J. Gyenis, Co-encapsulation of human serum albumin and superparamagnetic iron oxide in PLGA nanoparticles: Part II. Effect of process variables on protein model drug encapsulation efficiency, *Journal of microencapsulation*, (2013).
213. H. Mu, R. Ohashi, S. Yan, H. Chai, H. Yang, P. Lin, Q. Yao, C. Chen, Adipokine resistin promotes in vitro angiogenesis of human endothelial cells, *Cardiovasc Res*, 70 (2006) 146-157.
214. A. Kasai, N. Shintani, M. Oda, M. Kakuda, H. Hashimoto, T. Matsuda, S. Hinuma, A. Baba, Apelin is a novel angiogenic factor in retinal endothelial cells, *Biochem Biophys Res Commun*, 325 (2004) 395-400.
215. Y. Xu, H. Zhao, Y. Zheng, Q. Gu, J. Ma, X. Xu, A novel antiangiogenic peptide derived from hepatocyte growth factor inhibits neovascularization in vitro and in vivo, *Mol Vis*, 16 (2010) 1982-1995.

216. W.Z. Yu, H. Zou, X.X. Li, Z. Yan, J.Q. Dong, Effects of the phosphatidylinositol 3-kinase inhibitor in a mouse model of retinal neovascularization, *Ophthalmic Res*, 40 (2008) 19-25.
217. M. Gou, C. Gong, J. Zhang, X. Wang, X. Wang, Y. Gu, G. Guo, L. Chen, F. Luo, X. Zhao, Y. Wei, Z. Qian, Polymeric matrix for drug delivery: honokiol-loaded PCL-PEG-PCL nanoparticles in PEG-PCL-PEG thermosensitive hydrogel, *J Biomed Mater Res A*, 93 (2010) 219-226.
218. Y. Tang, J. Singh, Biodegradable and biocompatible thermosensitive polymer based injectable implant for controlled release of protein, *International journal of pharmaceuticals*, 365 (2009) 34-43.
219. M.H. Huang, S. Li, J. Coudane, M. Vert, Synthesis and Characterization of Block Copolymers of ϵ -Caprolactone and DL-Lactide Initiated by Ethylene Glycol or Poly(ethylene glycol), *Macromolecular chemistry and physics*, 204 (2003) 1994-2001.
220. K.F. Pistel, T. Kissel, Effects of salt addition on the microencapsulation of proteins using W/O/W double emulsion technique, *Journal of microencapsulation*, 17 (2000) 467-483.
221. J.X. Zhang, K.J. Zhu, D. Chen, Preparation of bovine serum albumin loaded poly (D, L-lactic-co-glycolic acid) microspheres by a modified phase separation technique, *Journal of microencapsulation*, 22 (2005) 117-126.
222. H. Tan, C.M. Ramirez, N. Miljkovic, H. Li, J.P. Rubin, K.G. Marra, Thermosensitive injectable hyaluronic acid hydrogel for adipose tissue engineering, *Biomaterials*, 30 (2009) 6844-6853.
223. L. Bian, D.Y. Zhai, E. Tous, R. Rai, R.L. Mauck, J.A. Burdick, Enhanced MSC chondrogenesis following delivery of TGF-beta3 from alginate microspheres within hyaluronic acid hydrogels in vitro and in vivo, *Biomaterials*, 32 (2011) 6425-6434.
224. A.M. Kloxin, M.W. Tibbitt, K.S. Anseth, Synthesis of photodegradable hydrogels as dynamically tunable cell culture platforms, *Nature protocols*, 5 (2010) 1867-1887.
225. N. Bhattarai, J. Gunn, M. Zhang, Chitosan-based hydrogels for controlled, localized drug delivery, *Adv Drug Deliv Rev*, 62 (2010) 83-99.
226. C.H. Wang, Y.S. Hwang, P.R. Chiang, C.R. Shen, W.H. Hong, G.H. Hsiue, Extended release of bevacizumab by thermosensitive biodegradable and biocompatible hydrogel, *Biomacromolecules*, 13 (2012) 40-48.
227. J.J. Kang Derwent, W.F. Mieler, Thermoresponsive hydrogels as a new ocular drug delivery platform to the posterior segment of the eye, *Transactions of the American Ophthalmological Society*, 106 (2008) 206-213; discussion 213-204.

VITA

Sulabh P. Patel was born on 3rd June, 1983, in Ahmedabad, Gujarat, India. He completed his Bachelor of Pharmacy from Hemchandracharya North Gujarat University in 2004 and received his Master of Science degree with the specialization in Pharmaceutical Analysis (2006) from National Institute of Pharmaceutical Education and Research (NIPER), S.A.S. Nagar, Mohali, Punjab, India. After completion of his M.S. degree, he joined the Bioanalytical division of Cadila Pharmaceuticals, India and worked as Research Associate until August, 2007.

To pursue a Ph.D. degree, Sulabh Patel initiated Doctoral study in the Interdisciplinary Ph.D. program at UMKC in January, 2009. He is an active member of American Association of Pharmaceutical Scientists (AAPS), Association of Research in Vision and Ophthalmology (ARVO) and Pharmaceutical Sciences Graduate Student Association (PSGSA). He served as the Secretary of American Association of Pharmaceutical Scientists (AAPS) student chapter, UMKC, for two consecutive academic years (2010-11 and 2011-12). He received the first prize at Interdisciplinary community of scholar poster presentation, April 2011. He completed his doctoral studies in January, 2014 under the guidance of Dr. Ashim K. Mitra. He has authored/co-authored several peer reviewed publications and book chapters, and has also presented his work in several annual national conferences.